

DISSERTATION

**SYNTHESIS OF STEREOCHEMICALLY CONTROLLED FUNCTIONALIZED VINYL  
POLYMERS AND POLYESTERS BY METALLOCENE-BASED CATALYSTS**

Submitted by

Yalan Ning

Department of Chemistry

In partial fulfillment of the requirements

For the Degree of Doctor of Philosophy

Colorado State University

Fort Collins, Colorado

Spring 2009

UMI Number: 3374636

### INFORMATION TO USERS

The quality of this reproduction is dependent upon the quality of the copy submitted. Broken or indistinct print, colored or poor quality illustrations and photographs, print bleed-through, substandard margins, and improper alignment can adversely affect reproduction.

In the unlikely event that the author did not send a complete manuscript and there are missing pages, these will be noted. Also, if unauthorized copyright material had to be removed, a note will indicate the deletion.

UMI<sup>®</sup>

---

UMI Microform 3374636  
Copyright 2009 by ProQuest LLC  
All rights reserved. This microform edition is protected against  
unauthorized copying under Title 17, United States Code.

---

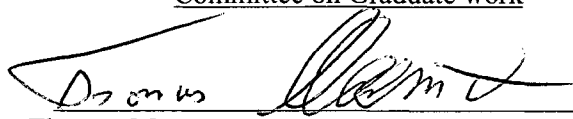
ProQuest LLC  
789 East Eisenhower Parkway  
P.O. Box 1346  
Ann Arbor, MI 48106-1346

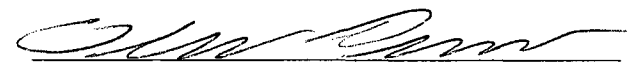
COLORADO STATE UNIVERSITY

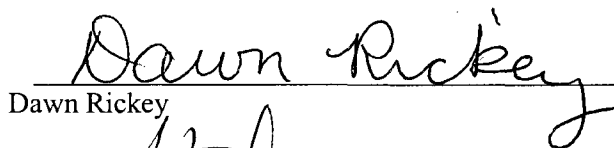
Feb 18, 2009

WE HEREBY RECOMMEND THAT THE THESIS PREPARED UNDER OUR SUPERVISION BY YALAN NING ENTITLED SYNTHESIS OF STEREOCHEMICALLY CONTROLLED FUNCTIONALIZED VINYL POLYMERS AND POLYESTERS BY METALLOCENE-BASED CATALYSTS BE ACCEPTED AS FULFILLING IN PART REQUIREMENTS FOR THE DEGREE OF DOCTOR OF SCIENCE.

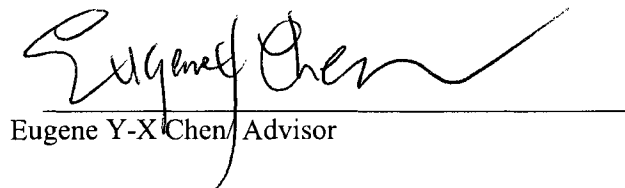
Committee on Graduate work

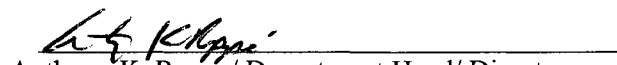
  
Thomas Meersmann

  
Olve B Peersen

  
Dawn Rickey

  
Steven H Strauss

  
Eugene Y-X Chen/ Advisor

  
Anthony K. Rappe/ Department Head/ Director

## ABSTRACT OF DISSERTATION

### Synthesis of Stereochemically Controlled Functionalized Vinyl Polymers and Polyesters by Metallocene-Based Catalysts

The research presented herein studies the polymerization of functionalized alkenes (methacrylates and acrylamides) and cyclic esters (lactide and lactone) catalyzed by group 4 metallocene complexes. Key findings of this study include: (1) development of the novel diastereospecific ion-pairing polymerization effected by a catalyst system comprising a chiral  $C_2$ -zirconocene bis(ester enolate) and two equiv of lewis acid  $Al(C_6F_5)_3$ , producing polymers with isotactic, syndiotactic, and isotactic-*b*-syndiotactic multiblock microstructures, (2) development of the highly syndiospecific polymerization by  $C_s$ -ligated *ansa*-zirconocene bis- and mono(ester enolate) complexes at room temperature, and (3) development of quantitatively isospecific polymerization of L-lactide by  $C_s$ -ligated *ansa*-zirconocene bis- and mono(ester enolate) complexes.

The broad focus of this dissertation concerns the kinetic and mechanistic studies of the polymerization of functionalized alkenes and cyclic esters, which provided several novel and useful polymerization systems.

**Yalan Ning**  
**Chemistry Department**  
**Colorado State University**  
**Fort Collins, CO 80523**  
**Spring 2009**

## TABLE OF CONTENTS

<b>CHAPTER I.....</b>	<b>1</b>
<b>INTRODUCTION.....</b>	<b>1</b>
<b>CHAPTER II.....</b>	<b>4</b>
<b>POLYMERIZATION OF MMA BY OSCILLATING ZIRCONOCENE CATALYSTS.....</b>	<b>4</b>
ABSTRACT.....	4
INTRODUCTION.....	4
EXPERIMENTAL.....	5
RESULTS AND DISCUSSION.....	8
CONCLUSIONS.....	12
REFERENCES.....	13
<b>CHAPTER III.....</b>	<b>16</b>
<b>DIASTEREOSPECIFIC ION-PAIRING POLYMERIZATION OF FUNCTIONALIZED ALKENES BY METALLOCENE/LEWIS ACID HYBRID CATALYSTS.....</b>	<b>16</b>
ABSTRACT.....	16
INTRODUCTION.....	17
EXPERIMENTAL.....	19
RESULTS AND DISCUSSION.....	25
CONCLUSIONS.....	46
REFERENCES.....	48
<b>CHAPTER IV.....</b>	<b>52</b>
<b>REMARKABLE LEWIS ACID EFFECTS ON POLYMERIZATION OF FUNCTIONALIZED ALKENES BY METALLOCENE AND LITHIUM ESTER ENOLATES.....</b>	<b>52</b>
ABSTRACT.....	52
INTRODUCTION.....	53
EXPERIMENTAL.....	55
RESULTS AND DISCUSSION.....	60
CONCLUSIONS.....	72
REFERENCES.....	74
<b>CHAPTER V.....</b>	<b>76</b>
<b>METALLOCENE-CATALYZED POLYMERIZATION OF METHACRYLATES TO HIGHLY SYNDIOTACTIC POLYMERS AT HIGH TEMPERATURES.....</b>	<b>76</b>
ABSTRACT.....	76
INTRODUCTION.....	77
EXPERIMENTAL.....	79
RESULTS AND DISCUSSION.....	86
CONCLUSIONS.....	90
REFERENCES.....	91
<b>CHAPTER VI.....</b>	<b>95</b>

<b>SYNDIOSELECTIVE MMA POLYMERIZATION BY GROUP 4 CONSTRAINED GEOMETRY CATALYSTS: A COMBINED EXPERIMENTAL AND THEORETICAL STUDY .....</b>	<b>95</b>
ABSTRACT.....	95
INTRODUCTION .....	96
EXPERIMENTAL.....	99
RESULTS AND DISCUSSION .....	107
CONCLUSIONS .....	120
REFERENCES .....	122
<b>CHAPTER VII .....</b>	<b>129</b>
<b>NEUTRAL METALLOCENE ESTER ENOLATE COMPLEXES OF ZIRCONIUM FOR CATALYTIC RING-OPENING POLYMERIZATION OF CYCLIC ESTERS.....</b>	<b>129</b>
ABSTRACT.....	129
INTRODUCTION .....	130
EXPERIMENTAL.....	132
RESULTS AND DISCUSSION .....	135
CONCLUSIONS .....	143
REFERENCES .....	145
<b>CHAPTER VIII.....</b>	<b>152</b>
<b>SUMMARY.....</b>	<b>152</b>
<b>CHAPTER IX.....</b>	<b>153</b>
<b>APPENDIX .....</b>	<b>153</b>
LIST OF REFEREED PUBLICATIONS BY YALAN NING.....	153

# CHAPTER I

## INTRODUCTION

This dissertation is written in a “journals-format” style that the graduate school at Colorado State University allows and is based on six separate peer-reviewed publications appearing in American Chemical Society and Elsevier journals, including Journal of the American Chemical Society, Macromolecules, Organometallics and Journal of Organometallic Chemistry. Chapter I is this introduction; chapters II, III, IV concentrated on the diastereospecific polymerization for isotactic-*b*-syndiotactic multiblock microstructures; Chapters V and VI concentrated on the syndiospecific polymerization for highly syndiotactic microstructures; Chapter VII focused on the ring-opening polymerization of cyclic esters for isotactic microstructures; Chapters VIII and chapter IX are summary and appendices, respectively. A concise overview of some important chapter’s contents is presented below.

Chapter II examines characteristics of methyl methacrylate (MMA) polymerization using oscillating zirconocene catalysts. MMA polymerization using the dichloride catalyst precursor activated with a large excess of the modified methyl aluminoxane is sluggish, uncontrolled, and produces atactic PMMA. On the other hand, the polymerization using the dimethyl catalyst precursor activated with 0.5 equiv of  $B(C_6F_5)_3$  or 0.5 equiv of  $Ph_3CB(C_6F_5)_4$  is controlled and produces syndiotactic PMMA.

Chapter III studies the mechanism and application of the novel diastereospecific ion-pairing polymerization (DIPP) effected by a catalyst system comprising chiral zirconocene bis(ester enolate) and 2 equiv of Lewis acid  $Al(C_6F_5)_3$ . The system effectively promotes DIPP of functionalized alkenes such as MMA, producing polymers having various stereoregularities,

including isotactic, syndiotactic, and isotactic-*b*-syndiotactic multiblock microstructures, depending on the [monomer]/[catalyst] ratio employed.

Chapter IV describes drastic effects of Lewis acids  $E(C_6F_5)_3$  ( $E = Al, B$ ) on polymerization of functionalized alkenes such as MMA and *N,N*-dimethyl acrylamide (DMAA) mediated by metallocene and lithium ester enolates. In the case of metallocene bis(ester enolate), when combined with 2 equiv of  $Al(C_6F_5)_3$ , it effects highly active ion-pairing polymerization of MMA and DMAA; the living nature of this polymerization system allows for the synthesis of well-defined diblock and triblock copolymers of MMA with longer-chain alkyl methacrylates.

Chapter V describes synthesis, polymerizations studies of a highly active polymerization system based on  $C_s$ -ligated *ansa*-zirconocene bis(ester enolate) and mono(ester enolate) complexes—which, upon activation with appropriate activators, generate the corresponding chiral cationic catalysts that produce highly syndiotactic PMMA (94% *rr*) at industrially convenient temperatures.

Chapter VI reports a combined experimental (with kinetics and tangible effects on syndioselectivity) and theoretical (with density functional theory) study of (CGC)M [ $M = Ti, Zr$ ; CGC =  $Me_2Si(\eta^5-Me_4C_5)(^iBuN)$ ] catalysts, addressing a need for a fundamental understanding of the stereoselectivity observed for such catalysts in polymerization of MMA and an explanation for the chain-end control nature of the syndioselective MMA polymerization by the chiral (CGC)Ti catalyst.

Chapter VII studies several neutral zirconocene bis(ester enolate) complexes employed for ring-opening polymerizations and chain transfer polymerizations of L-lactide (L-LA) and  $\epsilon$ -caprolactone ( $\epsilon$ -CL). All  $C_{2v}$ -,  $C_2$ -, and  $C_s$ -ligated neutral zirconocene bis(ester enolate) complexes effectively polymerize  $\epsilon$ -CL at 80 °C with high (>90%) initiator efficiencies. The  $C_s$ -ligated complex also promotes highly efficient polymerization of L-LA and is at least 100 times more reactive than the  $C_{2v}$ - and  $C_2$ -ligated analogous. And the L-LA polymerization exhibits

living characteristics, producing PLA with quantitative isotacticity and controlled molecular weight.

The unpublished work still in progress is not described here which includes the highly syndiospecific polymerization by a series of  $C_s$ -ligated complexes at high temperatures, chain-transfer polymerization between different stereospecific precatalysts for isotactic, syndiotactic, and isotactic-*b*-syndiotactic multiblock microstructures, and the material study of the PMMA stereocomplex. For the convenience of the reader, Appendix A lists all publications during the dissertation work.

## CHAPTER II

### Polymerization of MMA by Oscillating Zirconocene Catalysts

#### Abstract

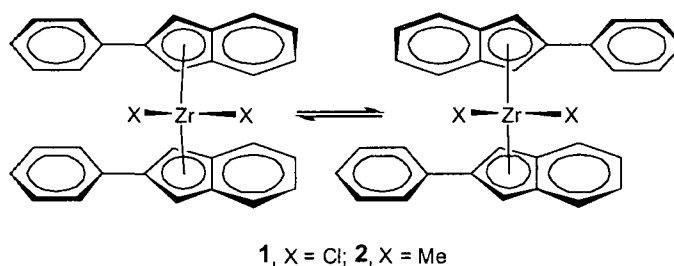
Characteristics of methyl methacrylate (MMA) polymerization using oscillating zirconocene catalysts,  $(2\text{-Ph-Ind})_2\text{ZrX}_2$  ( $\text{X} = \text{Cl}$ , **1**;  $\text{X} = \text{Me}$ , **2**) are reported. MMA polymerization using the chloride catalyst precursor **1** activated with a large excess of the modified methyl aluminoxane is sluggish, uncontrolled, and produces atactic PMMA. On the other hand, the polymerization by a 2/1 ratio of **2**/ $\text{B}(\text{C}_6\text{F}_5)_3$  or **2**/ $\text{Ph}_3\text{CB}(\text{C}_6\text{F}_5)_4$  is controlled and produces syndiotactic PMMA.

#### Introduction

A growing number of publications have been devoted to the investigation of the polymerization of methyl methacrylate (MMA) by group 4 metallocene and related catalysts; such complexes used for these studies have included achiral zirconocenes,<sup>1</sup> chiral *ansa*-zirconocenes,<sup>2</sup> achiral titanocenes,<sup>3</sup> chiral *ansa*-titanocenes,<sup>4</sup> half-sandwich titanium complexes,<sup>5</sup> and constrained geometry titanium and zirconium complexes.<sup>6</sup> Furthermore, this polymerization has been examined theoretically.<sup>7</sup> Three important attributes of this polymerization explain why it has attracted increasing attention. First, there is a paradigm shift in terms of scientific curiosity on utilizing highly active, electro-deficient transition metal complexes for polymerization of polar functionalized alkenes. Second, group 4 metallocene complexes with considerably diverse structural motifs are readily, and in many cases commercially, available, thanks to comprehensive studies of their roles in coordination polymerization of nonpolar olefins. Third, these complexes, when used in a suitable initiating form, typically exhibit a high degree of control over polymerization, especially the stereochemistry of polymerization.

These recent advances,<sup>1-7</sup> enabled by group 4 metallocene complexes, have resulted in the production of poly(methyl methacrylate) (PMMA) having various stereo-microstructures, including atactic, isotactic, syndiotactic, as well as isotactic-*b*-syndiotactic stereo-diblock and -multiblock PMMAs.<sup>5a</sup> We have been especially interested in the production of stereoblock PMMA microstructures using metallocene and related complexes through various unique strategies.<sup>2c,g,5a</sup> In the present study, we became interested in unbridged bis(2-aryl-substituted indenyl) zirconocenes such as (2-Ph-Ind)<sub>2</sub>ZrCl<sub>2</sub>, which can oscillate between achiral (*meso*-like) and chiral (*rac*-like) configurations; when activated with methyl aluminoxane, they have been known to produce atactic-*b*-isotactic stereomultiblock polypropylene.<sup>8</sup> Thus, it is of interest to examine if such oscillating metallocene catalysts can also produce PMMA with stereomultiblock microstructures. To address the fundamentally interesting question, the present contribution investigates the MMA polymerization behavior of the following classes of group 4 metallocenes (Scheme 1): oscillating catalysts **1** and **2**.

Scheme 1



## Experimental

**Materials and Methods.** All syntheses and manipulations of air- and moisture-sensitive materials were carried out in flamed Schlenk-type glassware on a dual-manifold Schlenk line, a high-vacuum line ( $10^{-5}$  to  $10^{-7}$  Torr), or in an argon-filled glovebox (<1.0 ppm oxygen and moisture). NMR-scale reactions (typically in a 0.02 mmol scale) were conducted in Teflon-valve-sealed J. Young-type NMR tubes. HPLC grade organic solvents were first saturated with nitrogen

during filling the solvent reservoir and then dried by passage through activated alumina (for Et<sub>2</sub>O, THF, and CH<sub>2</sub>Cl<sub>2</sub>) followed by passage through Q-5-supported copper catalyst (for toluene and hexanes) stainless steel columns. Benzene-*d*<sub>6</sub>, toluene-*d*<sub>8</sub>, and THF-*d*<sub>8</sub> were dried over sodium/potassium alloy and vacuum-distilled or filtered. NMR spectra were recorded on either a Varian Inova 300 (FT 300 MHz, <sup>1</sup>H; 75 MHz, <sup>13</sup>C; 282 MHz, <sup>19</sup>F) or a Varian Inova 400 spectrometer. Chemical shifts for <sup>1</sup>H and <sup>13</sup>C spectra were referenced to internal solvent resonances and are reported as parts per million relative to tetramethylsilane, whereas <sup>19</sup>F NMR spectra were referenced to external CFCl<sub>3</sub>.

Methyl methacrylate (MMA) was purchased from Aldrich Chemical Co.; MMA was first degassed and dried over CaH<sub>2</sub> overnight, followed by vacuum distillation; final purification involved titration with neat tri(*n*-octyl)aluminum to a yellow end point<sup>9</sup> followed by distillation under reduced pressure. The purified MMA was stored in a -30 °C glovebox freezer.

Tris(pentafluorophenyl)borane, B(C<sub>6</sub>F<sub>5</sub>)<sub>3</sub>, was obtained as a research gift from Boulder Scientific Co. and further purified by recrystallization from hexanes at -35 °C. Triisobutylaluminum-modified methylalumoxanes (MMAO) was purchased from Azko-Nobel, whereas Ph<sub>3</sub>CB(C<sub>6</sub>F<sub>5</sub>)<sub>4</sub> was prepared according to a literature procedure.<sup>10</sup> Tris(pentafluorophenyl)alane, Al(C<sub>6</sub>F<sub>5</sub>)<sub>3</sub>, as a 0.5•toluene adduct based on the elemental analysis for the vacuum-dried sample, was prepared from the exchange reaction of B(C<sub>6</sub>F<sub>5</sub>)<sub>3</sub> and AlMe<sub>3</sub> in a 1:3 toluene/hexanes solvent mixture in quantitative yield according to a literature procedure,<sup>11</sup> which is the modified synthesis of the alane first disclosed by Biagini et al.<sup>12</sup> *Extra caution should be exercised when handling this material because of its thermal and shock sensitivity.*

Literature procedures were employed for the preparation of the following metallocene complexes: (2-Ph-Ind)<sub>2</sub>ZrX<sub>2</sub> (X = Cl, **1**; X = Me, **2**),<sup>13</sup> in situ generation of the cationic species derived from the oscillating metallocene **2** is described as follows.

**Reaction of (2-Ph-Ind)<sub>2</sub>ZrMe<sub>2</sub> and B(C<sub>6</sub>F<sub>5</sub>)<sub>3</sub>.** (2-Ph-Ind)<sub>2</sub>ZrMe<sub>2</sub> (0.02 mmol), B(C<sub>6</sub>F<sub>5</sub>)<sub>3</sub> (0.02 mmol), and ~ 0.7 mL toluene-*d*<sub>8</sub> were mixed in a 4-mL vial, and the resulting orange yellow solution was loaded into a J. Young NMR tube via pipette. The mixture was allowed to react at ambient temperature for 15 min before the NMR spectra were recorded. All spectroscopic data clearly show the formation of the corresponding cationic species: (2-Ph-Ind)<sub>2</sub>ZrMe<sup>+</sup>MeB(C<sub>6</sub>F<sub>5</sub>)<sub>3</sub><sup>-</sup> (**3**). No decomposition was detected when a toluene solution of **3** was left in the NMR tube over a period of 24 h at room temperature.

<sup>1</sup>H NMR (C<sub>7</sub>D<sub>8</sub>, 23°C) for **3**: δ 7.11 (m, 6H), 7.00 (m, 4H), 6.82 (s, br. 2H), 6.68 (s, br. 2H), 6.62 (m, 4H), 6.09 (s, br. 2H), 5.85 (s, br. 2H), -0.37 (s, 3H, Zr-Me), -0.40 (s, br. 3H, B-Me). <sup>19</sup>F NMR (C<sub>7</sub>D<sub>8</sub>, 23°C): δ -132.60 (d, <sup>3</sup>J<sub>F-F</sub> = 22.6 Hz, 6F, *o*-F), -159.78 (t, <sup>3</sup>J<sub>F-F</sub> = 19.7 Hz, 3F, *p*-F), -164.75 (m, 6F, *m*-F).

The above reaction was repeated but with a 2:1 Zr:B ratio. The formation of a small amount of the μ-Me-bridged dinuclear cation, [(2-Ph-Ind)<sub>2</sub>ZrMe(μ-Me)MeZr(2-Ph-Ind)<sub>2</sub>]<sup>+</sup>MeB(C<sub>6</sub>F<sub>5</sub>)<sub>3</sub><sup>-</sup> (**4**), was apparent: -1.14 (s, 6H, Zr-Me), -1.79 (s, 3H, Zr-Me-Zr); other spectral data for **4** are similar to those of the monomeric cation **3**. There were no observable spectral changes between 20 min and 24 h of reaction time, and thus an equilibrium has been reached, resulting in a molar ratio of **3/4** = 10/1 in the mixture still containing excess, unreacted dimethyl precursor **2**.

**General Polymerization Procedures.** Polymerizations were performed either in 30-mL, oven- and flame-dried vacuum flasks inside the glovebox, or in 25-mL oven- and flame-dried Schlenk flasks interfaced to a dual-manifold Schlenk line. In a typical procedure, a metallocene complex (or a complex mixture in a desired ratio) and an activator in a predetermined ratio (see polymerization tables for details) were loaded into the flask in the glovebox. Toluene was added (10 mL total volume) and the mixture was stirred for 10 min to generate the active, cationic catalysts. MMA (1.00 mL, 9.35 mmol) was quickly added via pipette (for polymerizations in the

glovebox) or gastight syringe (for polymerizations on the Schlenk line), and the sealed flask was kept with vigorous stirring at the pre-equilibrated bath temperature. After the measured time interval, the polymerization was quenched by the addition of 5 mL of 5% HCl-acidified methanol. The quenched mixture was precipitated into 100 mL of methanol, stirred for > 1 h, filtered, washed with methanol, and dried in a vacuum oven at 50 °C overnight to a constant weight.

**Polymer Characterizations.** Glass transition temperatures ( $T_g$ ) of the polymers were measured by differential scanning calorimetry (DSC) on a DSC 2920, TA Instrument. Samples were first heated to 180 °C at 20 °C/min, equilibrated at this temperature for 4 min, and cooled to 0 °C at 20 °C/min. After being held at this temperature for 4 min, the samples were then reheated to 200°C at 10 °C/min. All  $T_g$  values were obtained from the second scan, after removing the thermal history. Polymer molecular weights and molecular weight distributions were measured by gel permeation chromatography (GPC) analyses carried out at 40 °C, a flow rate of 1.0 mL/min, and with THF as the eluent, on a Waters University 1500 GPC instrument or a Polymer Laboratory-210 instrument. The instrument was calibrated with 10 PMMA or PS standards, and chromatograms were processed with Waters Empower software.  $^1\text{H}$  NMR spectra for the analysis of PMMA microstructures were recorded in  $\text{CDCl}_3$  and analyzed according to the literature.<sup>14</sup>

## Results and Discussion

**MMA Polymerization Using Oscillating Metallocene Catalysts 1 and 2.** Results of MMA polymerization by **1** and **2** in toluene at 23 °C are summarized in Table 1. As shown in Table 1, polymerizations of MMA by the chloride **1** in a  $[\text{MMA}]/[\text{MMAO}]/[\mathbf{1}]$  ratio of 1000/500/1 are sluggish; the isolated polymer yields were only 6% for a 2-h reaction (run 1) and 17% for a 24-h reaction (run 2). The PMMAs produced have low molecular weights ( $M_n < 10.2$  kg/mol) and broad molecular weight distributions ( $\text{PDI} = M_w/M_n > 1.48$ ), indicative of an

uncontrolled polymerization. More importantly, the polymers produced are atactic with typical methyl triad distributions of  $[mm] = 30.3\%$ ,  $[mr] = 45.8\%$ , and  $[rr] = 23.9\%$  (run 1); this tacticity is also consistent with a measured  $T_g$  value of  $97\text{ }^\circ\text{C}$  for a typical atactic PMMA sample.

**Table 1.** Results of MMA Polymerization by  $(2\text{-Ph-Ind})_2\text{ZrX}_2$  ( $X = \text{Cl}$ , **1**;  $\text{Me}$ , **2**)<sup>a</sup>

run no.	$[\text{Zr}]_0$ (mM)	$[\text{cocatalyst}]_0$ (mM)	time (h)	yield (%)	$[mm]^b$ (%)	$[mr]^b$ (%)	$[rr]^b$ (%)	$T_g^c$ ( $^\circ\text{C}$ )	$10^4 M_n^d$ (g/mol)	PDI <sup>d</sup> ( $M_w/M_n$ )
1	<b>1</b> 1.87	MMAO 935	2	6	30.3	45.8	23.9	97	1.02	1.48
2	<b>1</b> 1.87	MMAO 935	24	17	23.7	41.6	34.7	93	0.74	1.50
3	<b>2</b> 4.68	$\text{B}(\text{C}_6\text{F}_5)_3$ 4.68	2	4	6.2	27.9	65.9		3.24	1.67
4	<b>2</b> 9.36	$\text{B}(\text{C}_6\text{F}_5)_3$ 4.68	24	88	3.2	27.2	69.6	128	3.24	1.13
5	<b>2</b> 4.68	$\text{Ph}_3\text{CB}(\text{C}_6\text{F}_5)_4$ 4.68	2	3	6.8	27.5	65.7		3.12	1.43
6	<b>2</b> 9.36	$\text{Ph}_3\text{CB}(\text{C}_6\text{F}_5)_4$ 4.68	24	69	2.4	23.3	74.3	128	3.19	1.15

<sup>a</sup> All polymerizations were carried out in 5 mL toluene at  $23\text{ }^\circ\text{C}$ ;  $[\text{MMA}] = 1.87\text{ M}$ . <sup>b</sup> Tacticity (methyl triad distributions) determined by  $^1\text{H}$  NMR spectroscopy in  $\text{CDCl}_3$ . <sup>c</sup> Glass transition temperature ( $T_g$ ) determined by DSC from second scans. <sup>d</sup> Number-average molecular weight ( $M_n$ ) and polydispersity index (PDI) determined by GPC relative to PMMA standards.

A large excess of MMAO and related alkyl aluminoxane activators present in MMA polymerizations can complicate the polymerization results, especially with a long reaction time, because alkyl aluminoxanes have been found to slowly polymerize MMA to PMMA with large PDI values.<sup>15</sup> To avoid any potential complications brought about by MMAO, we subsequently employed  $\text{B}(\text{C}_6\text{F}_5)_3$  and  $\text{Ph}_3\text{CB}(\text{C}_6\text{F}_5)_4$  activators for MMA polymerizations by the dimethyl catalyst precursor **2** because neither activator itself is capable of polymerizing MMA. The reaction of **2** and  $\text{B}(\text{C}_6\text{F}_5)_3$  (1:1 ratio) in toluene cleanly and quantitatively generates the corresponding cationic species:  $(2\text{-Ph-Ind})_2\text{ZrMe}^+\text{MeB}(\text{C}_6\text{F}_5)_3^-$  (**3**, see Experimental section). On the other hand, the same reaction but with a  $2/\text{B}(\text{C}_6\text{F}_5)_3$  ratio of 2/1 produces a mixture containing both the monomeric cation **3** and the dinuclear cation  $[(2\text{-Ph-Ind})_2\text{ZrMe}(\mu\text{-Me})\text{MeZr}(2\text{-Ph-Ind})_2]^+\text{MeB}(\text{C}_6\text{F}_5)_3^-$  (**4**). When the equilibrium was reached, the molar ratio of **3/4** in the mixture

was approximately 10/1, and thus the monocation **3** and the neutral dimethyl **2** are predominate species in the mixture.

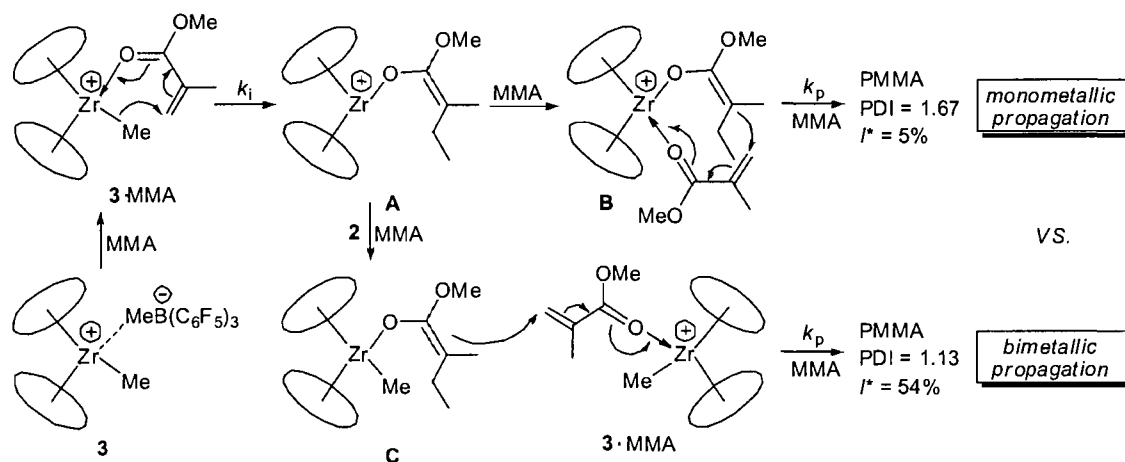
Following the lead of this catalyst activation study, we carried out MMA polymerizations using **2** via in situ activation with  $\text{B}(\text{C}_6\text{F}_5)_3$  (runs 3 and 4) and with  $\text{Ph}_3\text{CB}(\text{C}_6\text{F}_5)_4$  (runs 5 and 6). As can be seen in Table 1, the polymerization of MMA by the dimethyl **2** in a  $[\text{MMA}]/[\mathbf{2}]/[\text{B}(\text{C}_6\text{F}_5)_3]$  ratio of 400/1/1 is as sluggish as the polymerization using **1** via in situ activation with MMAO. The isolated polymer yield was only 4% for a 2-h reaction (run 3), but the PMMA produced has a moderate molecular weight of  $M_n = 32.4$  kg/mol and a broad molecular weight distribution of  $\text{PDI} = 1.67$ , giving a low initiator efficiency  $I^*$  ( $I^* = M_n(\text{calcd})/M_n(\text{exptl})$ , where  $M_n(\text{calcd}) = \text{MW}(\text{MMA}) \times [\text{MMA}]/[\mathbf{2}] \times \text{conversion}\%$ ) of only 5%. All results indicate an uncontrolled polymerization under these conditions; however, the PMMA produced is syndio-rich atactic ( $[rr] = 65.8\%$ ).

The MMA polymerization, using a  $[\text{MMA}]/[\mathbf{2}]/[\text{B}(\text{C}_6\text{F}_5)_3]$  ratio of 400/2/1 (run 2), afforded an 88% polymer yield in a 24 h time period, producing PMMA with a slightly higher syndiotacticity ( $[rr] = 69.6\%$ ); the measured  $T_g$  value of 128 °C is consistent with this tacticity. *Significantly*, the experimentally determined  $M_n$  of 32.4 kg/mol is approximately double what might be expected on the basis of a monomer-to-initiator  $\{[\text{MMA}]/[\mathbf{2}]\}$  ratio of 200 and a monomer conversion value of 88% (i.e., the calculated  $M_n = 17.6$  kg/mol), giving a much improved initiator efficiency of 54%. This evidence, coupled with a low PDI value of 1.13, argues that the polymerization using a 2:1 ratio of  $\mathbf{2}/\text{B}(\text{C}_6\text{F}_5)_3$  occurs via a *bimetallic mechanism*<sup>lj</sup> and is *controlled*. Results of the MMA polymerization by **2** activated with  $\text{Ph}_3\text{CB}(\text{C}_6\text{F}_5)_4$  are similar to those obtained from **2** activated with  $\text{B}(\text{C}_6\text{F}_5)_3$ , with only small variations in polymer yield, as well as in PMMA tacticity, molecular weight, and polydispersity values.

The observed sharply different MMA polymerization behavior between the 1:1  $\mathbf{2}/\text{B}(\text{C}_6\text{F}_5)_3$  and 2:1  $\mathbf{2}/\text{B}(\text{C}_6\text{F}_5)_3$  systems can be explained by the competition between the monometallic and

bimetallic propagation mechanisms shown in Scheme 2. In the MMA polymerization by a 1:1 ratio of **2**/ $\text{B}(\text{C}_6\text{F}_5)_3$ , which clearly generates the cation **3**, a slow initiation step involves methyl transfer to the coordinated MMA in the **3**·MMA adduct, leading to cationic zirconocene enolate **A**.<sup>lj</sup> Subsequent events involve MMA binding to **A** and repeated *intramolecular* Michael additions involved in **B** and its homologues in propagation steps, producing PMMA via a monometallic propagation mechanism. On the other hand, in the MMA polymerization by a 2:1 ratio of **2**/ $\text{B}(\text{C}_6\text{F}_5)_3$ , which affords a mixture containing predominately the monocation **3** and the unreacted neutral dimethyl **2**, a fast methyl transfer reaction between **A** and **2** produces neutral methyl zirconocene enolate **C**<sup>lj</sup> and **3** (which is then trapped by MMA in the form of the **3**·MMA adduct). Subsequent events involve rapidly repeated *intermolecular* Michael additions of **C** and its homologues to **3**·MMA in propagation steps, leading to PMMA via a bimetallic propagation mechanism. For the present unbridged bis(indenyl) zirconocene system, it is clear that the bimetallic pathway is more competitive and controlled than a monometallic one, the result of which is consistent with that obtained from the parent  $[\text{Cp}_2\text{Zr}]$  system.<sup>1a</sup>

Scheme 2



## Conclusions

To probe new strategies for the production of stereoblock PMMA, we have investigated the behavior of the MMA polymerization using three classes of group 4 metallocene catalysts, including oscillating catalysts **1** and **2**. The system was chosen for this study because of their potential for exhibiting catalyst-site isomerization within the timescale of the MMA polymerization.

Although none of the system investigated gave the desired stereoblock microstructures, several findings of this study are significant. First, the MMA polymerization with a 2/1 ratio of **2**/ $B(C_6F_5)_3$  or **2**/ $Ph_3CB(C_6F_5)_4$ —the reaction of which produces a mixture containing predominately the monocation **3** and the unreacted **2**—is controlled and produces syndiotactic PMMA, whereas the MMA polymerization using the monomeric cation alone is sluggish and uncontrolled. These results are consistent with the conclusion that the bimetallic propagating mechanism is more effective and controlled than the monometallic one for the MMA polymerization by the unbridged bis(indenyl) oscillating zirconocene catalysts.

**Acknowledgment.** This work was supported by the National Science Foundation and Colorado State University. We thank Boulder Scientific Co. for the gift of  $B(C_6F_5)_3$ ; Y.N. thank Wesley Mariott for their respective mentorship. E.Y.C. acknowledges an Alfred P. Sloan Research Fellowship.

## References

---

1. (a) G. Stojcevic, H. Kim, N.J. Taylor, T.B. Marder, S. Collins, *Angew. Chem. Int. Ed.* 43 (2004) 5523–5526. (b) B. Lian, L. Toupet, J.-F. Carpentier, *Chem. Eur. J.* 10 (2004) 4301–4307. (c) M. Ferez, F. Bandermann, R. Sustmann, W. Sicking, *Macromol. Chem. Phys.* 205 (2004) 1196–1205. (d) G. Karanikolopoulos, C. Batis, M. Pitsikalis, N. Hadjichristidis, *J. Polym. Sci. Part A: Polym. Chem.* 42 (2004) 3761–3774. (e) J. Wang, G. Odian, H. Haubenstein, *Polym. Prepr. Am. Chem. Soc. Div. Polym. Chem.* 44 (2003) 673–674; J. Wang, H. Haubenstein, G. Odian, *Polym. Prepr. Am. Chem. Soc. Div. Polym. Chem.* 44 (2003) 675–676. (f) F. Bandermann, M. Ferez, R. Sustmann, W. Sicking, *Macromol. Symp.* 174 (2001) 247–253. (g) G. Karanikolopoulos, C. Batis, M. Pitsikalis, N. Hadjichristidis, *Macromolecules* 34 (2001) 4697–4705. (h) F. Bandermann, M. Ferez, R. Sustmann, W. Sicking, *Macromol. Symp.* 161 (2000) 127–134. (i) T. Shiono, T. Saito, N. Saegusa, H. Hagihara, T. Ikeda, H. Deng, K. Soga, *Macromol. Chem. Phys.* 199 (1998) 1573–1579. (j) Y. Li, D.G. Ward, S.S. Reddy, S. Collins, *Macromolecules* 30 (1997) 1875–1883. (k) H. Deng, T. Shiono, K. Soga, *Macromol. Chem. Phys.* 196 (1995) 1971–1980. (l) S. Collins, D.G. Ward, *J. Am. Chem. Soc.* 114 (1992) 5460–5462. (m) W.B. Farnham, W. Hertler, U.S. Pat. (1988) 4,728,706.
2. (a) A.D. Bolig, E.Y.-X. Chen, *J. Am. Chem. Soc.* 126 (2004) 4897–4906. (b) J.W. Strauch, J.-L. Fauré, S. Bredeau, C. Wang, G. Kehr, R. Fröhlich, H. Luftmann, G. Erker, *J. Am. Chem. Soc.* 126 (2004) 2089–2104. (c) E.Y.-X. Chen, M.J. Cooney, *J. Am. Chem. Soc.* 125 (2003) 7150–7151. (d) G. Karanikolopoulos, C. Batis, M. Pitsikalis, N. Hadjichristidis, *Macromol. Chem. Phys.* 204 (2003) 831–840. (e) C. Batis, G. Karanikolopoulos, M. Pitsikalis, N. Hadjichristidis, *Macromolecules* 36 (2003) 9763–9774. (f) See ref 1(e). (g)

- 
- A.D. Bolig, E.Y.-X. Chen, *J. Am. Chem. Soc.* 124 (2002) 5612–5613. (h) H. Frauenrath, H. Keul, H. Höcker, *Macromolecules* 34 (2001) 14–19. (i) A.D. Bolig, E.Y.-X. Chen, *J. Am. Chem. Soc.* 123 (2001) 7943–7944. (j) P.A. Cameron, V. Gibson, A.J. Graham, *Macromolecules* 33 (2000) 4329–4335. (k) T. Stuhldreier, H. Keul, H. Höcker, *Macromol. Rapid Commun.* 21 (2000) 1093–1098. (l) Y.X. Chen, M.V. Metz, L. Li, C.L. Stern, T.J. Marks, *J. Am. Chem. Soc.* 120 (1998) 6287–6305. (m) H. Deng, T. Shiono, K. Soga, *Macromolecules* 28 (1995) 3067–3073. (n) K. Soga, H. Deng, T. Yano, T. Shiono, *Macromolecules* 27 (1994) 7938–7940. (o) S. Collins, D.G. Ward, K.H. Suddaby, *Macromolecules* 27 (1994) 7222–7224.
3. (a) N. Saegusa, T. Shiono, T. Ikeda, K. Mikami, (1998) JP 10330391. (b) See ref 1(m).
  4. (a) J. Jin, W.R. Mariott, E.Y.-X. Chen, *J. Polym. Chem. Part A: Polym. Chem.* 41 (2003) 3132–3142. (b) J. Jin, E.Y.-X. Chen, *Organometallics* 21 (2002) 13–15.
  5. (a) E.Y.-X. Chen, *J. Polym. Sci. Part A: Polym. Chem.* 42 (2004) 3395–3403. (b) T.R. Jensen, S.C. Yoon, A.K. Dash, L. Luo, T.J. Marks, *J. Am. Chem. Soc.* 125 (2003) 14482–14494.
  6. (a) A. Rodriguez-Delgado, W.R. Mariott, E.Y.-X. Chen, *Macromolecules* 37 (2004) 3092–3100. (b) J. Jin, E.Y.-X. Chen, *Macromol. Chem. Phys.* 203 (2002) 2329–2333. (c) J. Jin, D.R. Wilson, E.Y.-X. Chen, *Chem. Comm.* (2002) 708–709. (d) H. Nguyen, A.P. Jarvis, M.J.G. Lesley, W.M. Kelly, S.S. Reddy, N.J. Taylor, S. Collins, *Macromolecules* 33 (2000) 1508–1510.
  7. (a) M. Hölscher, H. Keul, H. Höcker, *Macromolecules* 35 (2002) 8194–8202. (b) M. Hölscher, H. Keul, H. Höcker, *Chem. Eur. J.* 7 (2001) 5419–5426. (c) R. Sustmann, W. Sickling, F. Bandermann, M. Ferenz, *Macromolecules* 32 (1999) 4204–4213.
  8. G.W. Coates, R.M. Waymouth, *Science* 267 (1995) 217–219.

- 
9. R.D. Allen, T.E. Long, J.E. McGrath, *Polym. Bull.* 15 (1986) 127–134.
  - 10 (a) J.C.W. Chien, W.-M. Tsai, M.D. Rausch, *J. Am. Chem. Soc.* 113 (1991) 8570–8571. (b) J.A. Ewen, M.J. Elder, *Eur. Pat. Appl. EP* (1991) 0,426,637.
  11. S. Feng, G.R. Roof, E.Y.-X. Chen, *Organometallics* 21 (2002) 832–839.
  12. (a) P. Biagini, G. Lugli, L. Abis, P. Andreussi, *U.S. Pat.* (1997) 5,602269. (b) C.H. Lee, S.J. Lee, J.W. Park, K.H. Kim, B.Y. Lee, J.S. Oh, *J. Mol. Cat., A: Chem.* 132 (1998) 231–239.
  13. G.W. Coates, R.M. Waymouth, E.M. Hauptman, *U.S. Pat.* (1997) 5,594,080.
  14. (a) F.A. Bovey, P.A. Mirau, *NMR of Polymers*; Academic Press: San Diego, CA, 1996. (b) R.C. Ferguson, D.W. Ovenall, *Polym. Prepr. (Am. Chem. Soc. Div. Polym. Chem.)* 26 (1985) 182–183. (c) R. Subramanian, R.D. Allen, J.E. McGrath, T.C. Ward, *Polym. Prepr. (Am. Chem. Soc. Div. Polym. Chem.)* 26 (1985) 238–240.
  15. B. Wu, R.W. Lenz, B. Hazer, *Macromolecules* 32 (1999) 6856–6859.

---

## CHAPTER III

### Diastereospecific Ion-Pairing Polymerization of Functionalized Alkenes by Metallocene/Lewis Acid Hybrid Catalysts

#### Abstract

This work studies the mechanism and application of the novel diastereospecific ion-pairing polymerization (DIPP) effected by a catalyst system comprising chiral zirconocene bis(ester enolate) *rac*-(EBI)Zr[OC(O<sup>i</sup>Pr)=CMe<sub>2</sub>]<sub>2</sub> [**1**, EBI = C<sub>2</sub>H<sub>4</sub>(Ind)<sub>2</sub>] and 2 equiv of Lewis acid Al(C<sub>6</sub>F<sub>5</sub>)<sub>3</sub>. The 1/2Al(C<sub>6</sub>F<sub>5</sub>)<sub>3</sub> system effectively promotes DIPP of functionalized alkenes such as methyl methacrylate (MMA), producing polymers having various stereoregularities, including isotactic, syndiotactic, and isotactic-*b*-syndiotactic multiblock microstructures, depending on the [monomer]/[catalyst] ratio employed. Our detailed investigations into the polymerization characteristics and kinetics, elementary reactions, characterization and behavior of the isolated key intermediates, as well as temperature and Lewis acid effects have yielded a mechanism for the DIPP of MMA by the 1/2Al(C<sub>6</sub>F<sub>5</sub>)<sub>3</sub> system. This mechanism consists of four manifolds: isospecific, syndiospecific, anion-monomer exchange, and chain-transfer domains, and satisfactorily explains the formation of various polymer stereomicrostructures under given conditions. The most significant part of this overall mechanism is for the production of the isotactic-*b*-syndiotactic stereomultiblock structure, which is made possible by two pathways that can interconvert diastereospecific propagating manifolds: exchange between the coordinated anion and monomer as well as chain transfer. This unique polymerization technique has also been applied to the copolymerization of MMA with methacrylates having longer alkyl chains, leading

to functionalized polymeric materials with tunable properties that are controlled by their stereomicrostructures and nature of the comonomer.

## Introduction

Organometallic and polymer chemistry has recently experienced phenomenal scientific and commercial successes in the production of revolutionary polyolefin materials by (co)polymerization of *nonpolar*  $\alpha$ -olefins with metallocene and related catalysts.<sup>1</sup> An ongoing paradigm shift on utilization of highly active, readily accessible, and highly versatile group 4 metallocene and related complexes for the polymerization of *polar* functionalized alkenes has paid increasing attention to the polymerization of methacrylates<sup>2</sup>, acrylates,<sup>3</sup> and acrylamides;<sup>4</sup> owing to the catalyst structure diversity and tunability, most of these polymerization systems exhibit a high degree of control over polymer structures (microstructure and architecture). This shift, however, is typically accompanied by a switch of the polymerization mechanism, i.e., from migratory insertion polymerization of  $\alpha$ -olefins to coordinative (anionic) addition polymerization of functionalized alkenes.

The resulting functionalized polar vinyl polymers such as poly(methyl methacrylate) P(MMA) have stereogenic centers in the repeating units, and the physical and mechanical properties of these polymers depend largely on their stereochemistry.<sup>5</sup> By virtue of the nature of ligand and metal as well as the stereochemical control mechanism, group 4 metallocene and related complexes have demonstrated their ability to control stereoregulation of the polymerization of methacrylates and acrylamides leading to production of the polymers having diverse tacticities, including atactic (*at-*), isotactic (*it-*), syndiotactic (*st-*), and isotactic-*b*-syndiotactic (*it-b-st*) stereoblock (*sb-*) microstructures.<sup>2,4</sup> Our particular interest in the production of poly(functionalized alkene)s with various stereomultiblock microstructures rests on a common belief that introduction of new stereomicrostructures to functionalized vinyl polymers will lead to new materials properties and thus potentially new applications; a testament of this belief was

nicely demonstrated by past examples such as polypropylene (PP)—both *it*- and *at*-PPs are thermoplastic materials, but *it-b-at sb*-PP is a particularly useful thermoplastic elastomer.<sup>6</sup> In the case of P(MMA), the stereochemistry adds another dimension to its materials properties: a stereocomplex—by definition, a crystalline polymer complex between a pair of diastereomeric macromolecules—can be formed between highly *it*- and *st*-P(MMA) blends in a typical 1:2 ratio either in the solid state, when annealed, or in suitable solvents.<sup>7</sup> This self-assembled, double-stranded helical complex exhibits enhanced physical and mechanical properties when compared to the individual tactic polymers. Therefore, the production of *it-b-st sb*-P(MMA)<sup>8</sup> is of great interest because diastereomeric P(MMA) chains in the stereoblock composite become chemically linked and thus stereocomplex formation of helical structures is expected to be more facile and diverse (e.g., intermolecular vs. intramolecular stereocomplex formation).

To this end, we communicated earlier a novel diastereospecific ion-pairing polymerization (DIPP) that produces multi *it-b-st sb*-P(MMA).<sup>2n</sup> That initial system employed a catalyst mixture containing chiral zirconocenium methyl cations paired with both methyl borate and methyl aluminate anions, e.g., *rac*-(EBI)ZrMe<sup>+</sup>[MeB(C<sub>6</sub>F<sub>5</sub>)<sub>3</sub>]<sup>-</sup><sub>0.5</sub>[MeAl(C<sub>6</sub>F<sub>5</sub>)<sub>3</sub>]<sup>-</sup><sub>0.5</sub>, which is generated by activation of *rac*-(EBI)ZrMe<sub>2</sub> with a 1:1 ratio of Lewis acids E(C<sub>6</sub>F<sub>5</sub>)<sub>3</sub> (E = B, Al). The polymerization of MMA by such a system was proposed to proceed in a diastereospecific ion-pairing fashion, in which the Zr<sup>+</sup>/B<sup>-</sup> ion pair produces the *it*-block via the zirconium ester enolate cation and the Zr<sup>+</sup>/Al<sup>-</sup> ion pair affords the *st*-block via the enolaluminate anion, whereas the exchange of growing diastereomeric polymer chains occurs via a neutral zirconocene bis(ester enolate) intermediate to yield *it-b-st* multiblock P(MMA).

Details of the DIPP mechanism, however, remained unknown before the current work. Additionally, that early system affords only short blocks with an average length of *it*- and *st*-sequences of approximately five. Accordingly, our continued studies of this unique DIPP over the past three years have been focused on mechanistic aspects of the polymerization as well as

development of the DIPP system with higher efficiency and degree of control over diastereomeric blocks. We recognized that the polymerization by the early system employing the chiral zirconocenium methyl cations paired with mixed methyl borate and methyl aluminate anions commences with slow initiation steps that involve transfers of methyl groups to the activated monomers by the Zr cation and by the Al Lewis acid to generate cationic zirconocenium ester enolate and anionic enolaluminate diastereospecific propagating species; these slow initiation steps hampered our mechanistic studies and also resulted in the formation of ill-controlled polymer products. Subsequently, we reasoned that a new system consisting of the preformed propagating intermediate, zirconocene bis(ester enolate) complex *rac*-(EBI)Zr[OC(O<sup>i</sup>Pr)=CMe<sub>2</sub>]<sub>2</sub>,<sup>2f</sup> and 2 equiv of strongly Lewis acidic alane Al(C<sub>6</sub>F<sub>5</sub>)<sub>3</sub>, should form rapidly, in the presence of MMA, the diastereospecific propagating species in a single fast reaction, thus eliminating those slow initiation steps in the earlier system. As a result, the new 1/2Al(C<sub>6</sub>F<sub>5</sub>)<sub>3</sub> catalyst system should lead to a DIPP process with higher efficiency and enhanced control over polymerization characteristics; equally important is the excellent opportunity, offered by this controlled system, to investigate the kinetics and mechanism of DIPP. With these goals in mind, we present here a full account of our efforts to understand the polymerization control, stereoregulation, active species, kinetics, and mechanism of DIPP, using the 1/2Al(C<sub>6</sub>F<sub>5</sub>)<sub>3</sub> system for the polymerization and copolymerization of MMA and other alkyl methacrylates under systematically varied conditions.

## Experimental

**Materials and Methods.** All syntheses and manipulations of air- and moisture-sensitive materials were carried out in flamed Schlenk-type glassware on a dual-manifold Schlenk line, a high-vacuum line (typically 10<sup>-5</sup> to 10<sup>-7</sup> Torr), or in an argon or nitrogen-filled glovebox (typically <1.0 ppm oxygen and moisture). NMR-scale reactions (typically in a 0.02 mmol scale in ~0.7 mL of an NMR solvent) were conducted in Teflon-valve-sealed J. Young-type NMR

tubes. HPLC grade organic solvents were sparged extensively with nitrogen during filling of the 20-L solvent reservoir and then dried by passage through activated alumina (for THF, Et<sub>2</sub>O, and CH<sub>2</sub>Cl<sub>2</sub>) followed by passage through Q-5-supported copper catalyst (for toluene and hexanes) stainless steel columns. Benzene-*d*<sub>6</sub> and toluene-*d*<sub>8</sub> were degassed, dried over sodium/potassium alloy, and filtered before use, whereas CDCl<sub>3</sub> and CD<sub>2</sub>Cl<sub>2</sub> were degassed and dried over activated Davison 4 Å molecular sieves. NMR spectra were recorded on either a Varian Inova 300 (FT 300 MHz, <sup>1</sup>H; 75 MHz, <sup>13</sup>C; 282 MHz, <sup>19</sup>F) or a Varian Inova 400 spectrometer. Chemical shifts for <sup>1</sup>H and <sup>13</sup>C spectra were referenced to internal solvent resonances and are reported as ppm relative to tetramethylsilane, whereas <sup>19</sup>F NMR spectra were referenced to external CFCl<sub>3</sub>. Elemental analyses were performed by Desert Analytics, Tucson, Az.

Methyl methacrylate (MMA), *n*-butyl methacrylate (BMA), and 2-ethylhexyl methacrylate (EHM) were purchased from Aldrich, Alfa Aesar, and TCI America, respectively, and purified by degassing and drying over CaH<sub>2</sub> for two days, followed by vacuum distillation; final purification of MMA involved titration with neat tri(*n*-octyl)aluminum to a yellow end point<sup>9</sup> followed by a second vacuum distillation. The purified monomers were stored in brown glass bottles in a -30 °C freezer inside the glovebox. 2,6-Di-*tert*-butyl-4-methylphenol (butylated hydroxytoluene, BHT-H) was purchased from Aldrich Chemical Co. and recrystallized from hexanes prior to use.

Tris(pentafluorophenyl)borane B(C<sub>6</sub>F<sub>5</sub>)<sub>3</sub> was obtained as a research gift from Boulder Scientific Co. and further purified by recrystallization from hexanes at -30 °C. Tris(pentafluorophenyl)alane Al(C<sub>6</sub>F<sub>5</sub>)<sub>3</sub>, as a 0.5 toluene adduct Al(C<sub>6</sub>F<sub>5</sub>)<sub>3</sub>•(C<sub>7</sub>H<sub>8</sub>)<sub>0.5</sub>, was prepared by the reaction of B(C<sub>6</sub>F<sub>5</sub>)<sub>3</sub> and AlMe<sub>3</sub> in a 1:3 toluene/hexanes solvent mixture in quantitative yield;<sup>10</sup> this is the modified synthesis based on literature procedures.<sup>11</sup> Although we have experienced no incidents when handling this material, *extra caution should be exercised*, especially when dealing with the unsolvated form, because of its thermal and shock sensitivity. The alane employed in this work is the toluene adduct. The Al(C<sub>6</sub>F<sub>5</sub>)<sub>3</sub>•MMA adduct<sup>2w</sup> was

prepared by addition of excess MMA to a toluene solution of the alane followed by removal of the volatiles and drying in vacuo; when no isolation is needed, this adduct can be prepared by direct mixing of  $\text{Al}(\text{C}_6\text{F}_5)_3$  with MMA. Literature procedures were employed for the preparation of the following compounds and metallocene complexes:  $\text{MeAl}(\text{BHT})_2$ ,<sup>12</sup>  $(\text{EBI})\text{H}_2$  [ $\text{EBI} = \text{C}_2\text{H}_4(\text{Ind})_2$ ],<sup>13</sup>  $\text{rac}-(\text{EBI})\text{Zr}(\text{NMe}_2)_2$ ,<sup>14</sup>  $\text{rac}-(\text{EBI})\text{ZrMe}_2$ ,<sup>14</sup> and  $\text{rac}-(\text{EBI})\text{Zr}[\text{OC}(\text{O}^i\text{Pr})=\text{CMe}_2]_2$  (**1**).<sup>2f</sup>

**Isolation of  $[\text{rac}-(\text{EBI})\text{Zr}(\text{OC}(\text{OMe})=\text{C}(\text{Me})\text{CH}_2\text{C}(\text{Me}_2)\text{C}(\text{O}^i\text{Pr})=\text{O})]^+[(\text{C}_6\text{F}_5)_3\text{Al}-\text{OMe}-\text{Al}(\text{C}_6\text{F}_5)_3]^-$  (**2**).** In an argon-filled glovebox, a 30-mL glass reactor was charged with **1** (30.3 mg, 0.05 mmol),  $\text{Al}(\text{C}_6\text{F}_5)_3 \cdot \text{MMA}$  (62.8 mg, 0.10 mmol), and 15 mL of  $\text{CH}_2\text{Cl}_2$ . The resulting yellow solution was stirred for 24 h at ambient temperature, after which the orange-red suspension was filtered. The solvent of the filtrate was removed, and the resulting residue was extensively dried in vacuo affording 63.3 mg (76%) of complex **2** as an orange red solid. The cation portion of **2** is identical to the cyclic ester enolate zirconocenium cation that is paired with the methylborate anion,  $\text{rac}-(\text{EBI})\text{Zr}[\text{OC}(\text{OMe})=\text{C}(\text{Me})\text{CH}_2\text{C}(\text{Me}_2)\text{C}(\text{O}^i\text{Pr})=\text{O}]^+[\text{MeB}(\text{C}_6\text{F}_5)_3]^-$ , which was derived from the single MMA addition to  $\text{rac}-(\text{EBI})\text{Zr}^+(\text{THF})[\text{OC}(\text{O}^i\text{Pr})=\text{CMe}_2][\text{MeB}(\text{C}_6\text{F}_5)_3]^-$  and spectroscopically/analytically (but not structurally) characterized.<sup>2b</sup> Accordingly, single crystals of **2** suitable for X-ray diffraction studies were grown from toluene at  $-30\text{ }^\circ\text{C}$  inside the freezer of the glovebox.

<sup>1</sup>H NMR ( $\text{CD}_2\text{Cl}_2$ ,  $21\text{ }^\circ\text{C}$ ) for **2**:  $\delta$  8.06 (d,  $J = 8.4$  Hz, 1H), 7.95 (d,  $J = 8.4$  Hz, 1H), 7.38–7.23 (m, 6H), 6.31 (d,  $J = 3.3$  Hz, 1H), 6.27 (d,  $J = 3.3$  Hz, 1H), 6.23 (d,  $J = 3.3$  Hz, 1H), 5.95 (d,  $J = 3.0$  Hz, 1H), 4.34 (sept,  $J = 6.4$  Hz, 1H,  $\text{CHMe}_2$ ), 4.12–3.97 (m, 4H,  $\text{CH}_2\text{CH}_2$ ), 4.05 (s, br, 3H,  $\text{AlOMe}$ ), 3.14 (s, 3H,  $\text{OMe}$ ), 2.28 (s, br, 2H,  $\text{CH}_2$ ), 1.52 (s, 3H,  $=\text{CMe}$ ), 1.40 (d,  $J = 6.3$  Hz, 3H,  $\text{CHMe}_2$ ), 1.29 (d,  $J = 6.3$  Hz, 3H,  $\text{CHMe}_2$ ), 1.26–1.16 (m, 6H,  $\text{CMe}_2$ ). <sup>19</sup>F NMR ( $\text{CD}_2\text{Cl}_2$ ,  $21\text{ }^\circ\text{C}$ ):  $\delta$   $-119.36$  (d, 12F, *o*-F),  $-154.19$  (t, 6F, *p*-F),  $-162.17$  (m, 12F, *m*-F).

**Isolation of *rac*-(EBI)Zr[OC(OMe)=C(Me)CH<sub>2</sub>C(Me<sub>2</sub>)C(O<sup>*i*</sup>Pr)=O•Al(C<sub>6</sub>F<sub>5</sub>)<sub>3</sub>]<sub>2</sub> (3).** In an argon-filled glovebox, a 60-mL glass reactor was charged with **1** (12.1 mg, 0.02 mmol), Al(C<sub>6</sub>F<sub>5</sub>)<sub>3</sub>•MMA (25.1 mg, 0.04 mmol), and 25 mL of hexanes. The resulting yellow suspension was stirred for 30 min at ambient temperature, after which the reaction mixture was filtered. The filtrate was concentrated under reduced pressure to ~0.5 mL and subsequently cooled to -30 °C inside the freezer of the glovebox over 2 h. The supernatant was quickly decanted, and the solid collected was extensively dried in vacuo to give 28.0 mg (76%) of complex **3** as a yellow power. Anal. Calcd. for C<sub>80</sub>H<sub>58</sub>Al<sub>2</sub>F<sub>30</sub>O<sub>8</sub>Zr: C, 51.59; H, 3.14. Found: C, 51.42; H, 2.84.

<sup>1</sup>H NMR (C<sub>6</sub>D<sub>6</sub>, 21°C) for **3**: δ 7.28 (d, *J* = 8.4 Hz, 2H), 7.06 (d, *J* = 8.4 Hz, 2H), 6.90–6.85 (m, 4H), 5.99 (d, *J* = 3.0 Hz, 2H), 5.80 (d, *J* = 3.0 Hz, 2H), 5.19 (sept, *J* = 6.4 Hz, 2H, CHMe<sub>2</sub>), 3.23 and 3.10 (m, 4H, CH<sub>2</sub>CH<sub>2</sub>), 2.99 (s, 6H, OMe), 2.31 (q<sub>AB</sub>, 4H, CH<sub>2</sub>), 1.28 (s, 6H, =CMe), 1.12 (d, *J* = 6.0 Hz, 12H, CHMe<sub>2</sub>), 0.86 (m, 12H, CMe<sub>2</sub>). <sup>13</sup>C NMR (C<sub>6</sub>D<sub>6</sub>, 21°C): δ 189.0 [C(O<sup>*i*</sup>Pr)=O], 158.35 (OC(OMe)=), 150.33 (d, <sup>1</sup>J<sub>C-F</sub> = 211.0 Hz, C<sub>6</sub>F<sub>5</sub>), 142.06 (d, <sup>1</sup>J<sub>C-F</sub> = 251.6 Hz, C<sub>6</sub>F<sub>5</sub>), 137.29 (d, <sup>1</sup>J<sub>C-F</sub> = 251.5 Hz, C<sub>6</sub>F<sub>5</sub>), 132.14, 125.78, 124.81, 123.73, 122.71, 122.39, 121.08, 115.18, 103.02 (a total of 9 resonances for the indenyl carbons), 79.91 (=CMe<sub>2</sub>), 78.22 (OCHMe<sub>2</sub>), 54.35 (OCH<sub>3</sub>), 45.90 (CH<sub>2</sub>), 41.79 (CMe<sub>2</sub>), 29.09 (CH<sub>2</sub>CH<sub>2</sub>), 24.45 (OCHMe<sub>2</sub>), 23.56 (OCHMe<sub>2</sub>), 20.65 (CMe<sub>2</sub>), 17.36 (=CMe). <sup>19</sup>F NMR (C<sub>6</sub>D<sub>6</sub>, 21°C): δ -122.90 (d, 12F, *o*-F), -152.07 (t, 6F, *p*-F), -161.20 (m, 12F, *m*-F).

**Generation of *rac*-(EBI)Zr[OC(OMe)=C(Me)CH<sub>2</sub>C(Me<sub>2</sub>)C(O<sup>*i*</sup>Pr)=O•Al(C<sub>6</sub>F<sub>5</sub>)<sub>3</sub>][OC(O<sup>*i*</sup>Pr)=CMe<sub>2</sub>] (4).** In an argon-filled glovebox, a 60-mL glass reactor was charged with **1** (18.2 mg, 0.03 mmol), Al(C<sub>6</sub>F<sub>5</sub>)<sub>3</sub>•MMA (18.8 mg, 0.03 mmol), and 30 mL of hexanes. The resulting yellow suspension was stirred for 10 min at ambient temperature, after which <sup>1</sup>H NMR of an aliquot showed an incomplete consumption of **1**. Accordingly, a second portion of Al(C<sub>6</sub>F<sub>5</sub>)<sub>3</sub>•MMA (0.01 mmol) was added, and the mixture was stirred for another 20 min. The reaction mixture was filtered, and the filtrate was concentrated under reduced pressure to ~2 mL. The concentrated filtrate was left inside a -30 °C freezer of the glovebox. The supernatant was

quickly decanted, and the solid collected was extensively dried in vacuo to give 27.8 mg of the product as a yellow solid. NMR spectra of the product showed formation of the title complex **4**, but accompanied by ~40% of complex **3** (i.e., the 1:2 ratio reaction product); repeated attempts to separate them by recrystallization were unsuccessful.

$^1\text{H}$  NMR ( $\text{C}_6\text{D}_6$ , 21°C) for **4**:  $\delta$  7.35 (m, 2H), 7.25–7.05 (m, 3H), 6.89 (m, 3H), 6.39 (d,  $J$  = 3.0 Hz, 1H), 6.05 (d,  $J$  = 3.0 Hz, 1H), 5.96 (d,  $J$  = 3.0 Hz, 1H), 5.87 (d,  $J$  = 3.0 Hz, 1H), 5.19 (sept,  $J$  = 6.4 Hz, 1H,  $\text{CHMe}_2$ ), 3.65 (sept,  $J$  = 6.4 Hz, 1H,  $\text{CHMe}_2$ ), 3.31 and 3.16 (m, 4H,  $\text{CH}_2\text{CH}_2$ ), 2.97 (s, 3H,  $\text{OMe}$ ), 2.34 (q<sub>AB</sub>, 2H,  $\text{CH}_2$ ), 1.73 and 1.44 (s, 3H,  $=\text{CMe}_2$ ), 1.31 (s, 3H,  $=\text{CMe}$ ), 1.23 (d,  $J$  = 6.3 Hz, 3H,  $\text{CHMe}_2$ ), 1.16 (d,  $J$  = 6.0 Hz, 6H,  $\text{CHMe}_2$ ), 1.07 (d,  $J$  = 6.3 Hz, 3H,  $\text{CHMe}_2$ ), 0.89 (m, 6H,  $\text{CMe}_2$ ).  $^{19}\text{F}$  NMR ( $\text{C}_6\text{D}_6$ , 21°C):  $\delta$  -122.87 (d, 12F, *o*-F), -152.14 (t, 6F, *p*-F), -161.25 (m, 12F, *m*-F).

**Isolation of  $[\text{rac}(\text{EBI})\text{Zr}(\text{OC}(\text{O}^i\text{Pr})=\text{CMe}_2)]^+[\text{O}=\text{C}(\text{O}^i\text{Pr})\text{C}(\text{Me}_2)\text{B}(\text{C}_6\text{F}_5)_3]^-$  (**5**).** In an argon-filled glovebox, a 20-mL glass reactor was charged with **1** (18.2 mg, 0.03 mmol),  $\text{B}(\text{C}_6\text{F}_5)_3$  (15.4 mg, 0.03 mmol), and 2 mL of  $\text{CD}_2\text{Cl}_2$ . The resulting dark red solution was stirred for 30 min at ambient temperature, after which it was filtered. The filtrate was first analyzed by NMR showing the clean formation of **5**, then the solvent of which was removed in vacuo to give 24.9 mg of complex **5** (72%) as a red solid. Anal. Calcd. for  $\text{C}_{52}\text{H}_{42}\text{BF}_{15}\text{O}_4\text{Zr}$ : C, 55.87; H, 3.79. Found: C, 55.85; H, 3.60.

$^1\text{H}$  NMR ( $\text{CD}_2\text{Cl}_2$ , 21°C) for **5**:  $\delta$  8.06 (d,  $J$  = 8.4 Hz, 1H), 7.94 (d,  $J$  = 8.4 Hz, 1H), 7.39–7.22 (m, 6H), 6.29 (d,  $J$  = 3.0 Hz, 3H), 5.97 (d,  $J$  = 3.0 Hz, 1H), 4.33 (sept,  $J$  = 6.4 Hz, 1H,  $\text{CHMe}_2$ ), 4.14–3.95 (m, 4H,  $\text{CH}_2\text{CH}_2$ ), 3.62 (s, br, 1H,  $\text{CHMe}_2$ ), 1.54 (s, 3H,  $=\text{CMe}_2$ ), 1.38 (d,  $J$  = 6.0 Hz, 3H,  $\text{CHMe}_2$ ), 1.27 (d,  $J$  = 6.0 Hz, 6H,  $\text{CHMe}_2$ ), 1.21 [s, br, 9H, *Me*'s for  $=\text{CMe}_2$  (3H),  $\text{CHMe}_2$  (3H), and  $\text{CMe}_2$  (3H)], 1.02 (s, br, 3H,  $\text{CMe}_2$ ).  $^{13}\text{C}$  NMR ( $\text{CD}_2\text{Cl}_2$ , 21°C, only key resonances shown):  $\delta$  192.47 [ $\text{C}(\text{O}^i\text{Pr})=\text{O}$ ], 150.08 [ $\text{OC}(\text{O}^i\text{Pr})=\text{C}$ ], 69.02 ( $\text{OCHMe}_2$ ).  $^{19}\text{F}$  NMR

(CD<sub>2</sub>Cl<sub>2</sub>, 21 °C):  $\delta$  -132.30 (d,  $^3J_{F-F} = 19.5$  Hz, 6F, *o*-F), -163.09 (t,  $^3J_{F-F} = 19.5$  Hz, 3F, *p*-F), -165.94 (m, 6F, *m*-F).

**General Polymerization Procedures.** Polymerizations were performed in 25-mL flame-dried Schlenk flasks interfaced to the dual-manifold Schlenk line. In a typical procedure, a predetermined amount of Al(C<sub>6</sub>F<sub>5</sub>)<sub>3</sub> was first dissolved in MMA (9.35 mmol) inside a glovebox, and the polymerization was started by rapid addition of this *in situ* prepared alane-MMA solution via gastight syringe to a 10-mL CH<sub>2</sub>Cl<sub>2</sub> solution of **1** under vigorous stirring at the pre-equilibrated bath temperature. (The amount of MMA was fixed for all polymerizations, and the amounts of Al(C<sub>6</sub>F<sub>5</sub>)<sub>3</sub> and **1** were adjusted according to the ratios specified in the polymerization tables.) After the measured time interval, the polymerization was quenched by the addition of 5 mL of 5% HCl-acidified methanol. The quenched mixture was precipitated into 100 mL of methanol, stirred for 1 h, filtered, washed with methanol, and dried in a vacuum oven at 50 °C overnight to a constant weight.

**Polymerization Kinetics.** Kinetic experiments were carried out in stirred 25-mL Schlenk flasks at a given temperature using stock solutions of the catalyst. Aliquots (0.2 mL) were taken at appropriate time intervals, treated, and analyzed according to literature procedures.<sup>2b,15</sup>

**Polymer Characterizations.** Glass transition temperatures ( $T_g$ ) of the polymers were measured by differential scanning calorimetry (DSC) on a DSC 2920, TA Instrument. Samples were first heated to 180 °C at 20 °C/min, equilibrated at this temperature for 4 min, and cooled to -60 °C at 20 °C/min. After being held at this temperature for 4 min, the samples were then reheated to 180 °C at 10 °C/min. All  $T_g$  values were obtained from the second scan, after removing the thermal history. Gel permeation chromatography (GPC) analyses of the polymers were carried out at 40 °C and a flow rate of 1.0 mL/min, with CHCl<sub>3</sub> as the eluent, on a Waters University 1500 GPC instrument equipped with four 5  $\mu$ m PL gel columns (Polymer Laboratories) and calibrated using 10 PMMA standards. Chromatograms were processed with

Waters Empower software (version 2002). NMR spectra for the polymers were recorded in CDCl<sub>3</sub> and analyzed according to literature procedures.<sup>16</sup>

**X-Ray Crystallographic Analysis of 2.** Single crystals of complex **2** grown from toluene were quickly covered with a layer of Paratone-N oil (Exxon, dried and degassed at 120 °C/10<sup>-6</sup> Torr for 24 h), after the mother liquors were decanted, and then mounted on a thin glass fiber and transferred into the cold nitrogen stream of a Bruker SMART CCD diffractometer. The structure was solved by direct methods and refined using the Bruker SHELXTL program library by full-matrix least-squares on  $F^2$  for all reflections.<sup>17</sup> All non-hydrogen atoms were refined with anisotropic displacement parameters, whereas hydrogen atoms were included in the structure factor calculations at idealized positions. There is a toluene molecule found in the lattice. Selected crystallographic data for **2**·C<sub>7</sub>H<sub>8</sub>: C<sub>76</sub>H<sub>48</sub>Al<sub>2</sub>F<sub>30</sub>O<sub>5</sub>Zr, triclinic, space group  $P\bar{1}$ ,  $a = 10.3530(6)$  Å,  $b = 16.3085(10)$  Å,  $c = 21.7857(13)$  Å,  $\alpha = 83.8880(10)^\circ$ ,  $\beta = 80.7960(10)^\circ$ ,  $\gamma = 76.1090(10)^\circ$ ,  $V = 3515.9(4)$  Å<sup>3</sup>,  $Z = 2$ ,  $D_{\text{calcd}} = 1.658$  Mg/m<sup>3</sup>,  $R1 = 0.0531$  [ $I > 2\sigma(I)$ ],  $wR2 = 0.1134$ .

## Results and Discussion

**Polymerization Characteristics.** Table 1 summarizes representative results of MMA polymerization by the 1/2Al(C<sub>6</sub>F<sub>5</sub>)<sub>3</sub> system in CH<sub>2</sub>Cl<sub>2</sub> in a [MMA]<sub>0</sub>/[**1**]<sub>0</sub> ratio ranging from 600 to 1500. It must be noted here that the catalyst Al(C<sub>6</sub>F<sub>5</sub>)<sub>3</sub> and the solvent CH<sub>2</sub>Cl<sub>2</sub> are incompatible if directly mixed as CH<sub>2</sub>Cl<sub>2</sub> decomposes Al(C<sub>6</sub>F<sub>5</sub>)<sub>3</sub> via chloride abstraction to form (C<sub>6</sub>F<sub>5</sub>)<sub>2</sub>AlCl that has been structurally characterized as a dimer in the solid state.<sup>18</sup> Conversely, CH<sub>2</sub>Cl<sub>2</sub> presents no problems for reactions using the alane in the form of a base adduct such as Al(C<sub>6</sub>F<sub>5</sub>)<sub>3</sub>·THF and Al(C<sub>6</sub>F<sub>5</sub>)<sub>3</sub>·MMA. Additionally, direct contact of Al(C<sub>6</sub>F<sub>5</sub>)<sub>3</sub> with **1** leads to rapid decomposition as well. Thus, in the present polymerization system, it is critical that Al(C<sub>6</sub>F<sub>5</sub>)<sub>3</sub> be first mixed (dissolved) in large excess MMA (the amount of which depends on the [MMA]<sub>0</sub>/[**1**]<sub>0</sub> ratio employed) followed by addition to a CH<sub>2</sub>Cl<sub>2</sub> solution of **1** to start the polymerization. (All

elementary reactions involving these reagents when mixed in different sequences will be thoroughly discussed later.) As can be seen from the Table, the polymerization at 22 °C with a relatively high concentration of  $[1] = 1.50 \text{ mM}$ , which corresponds to a  $[\text{MMA}]_0/[1]_0$  ratio of 600, is rapid and produces essentially *st*-P(MMA) with nearly constant *st*- ( $[rr] = 68\text{--}71\%$ ) and *ht*- (heterotactic,  $[mr] = 22\text{--}24\%$ ) indices vs. monomer conversion (runs 1 to 10, Table 1). Number average molecular weights ( $M_n$ ) of the resulting polymers at various conversions indicate that approximately two polymer chains were produced per Zr center. For example, at 67% conversion, the measured  $M_n$  was  $2.34 \times 10^4$  compared to the calculated  $M_n$  of  $2.01 \times 10^4$  based on  $2[\text{MMA}]_0/[1]_0 = 600$ , giving an initiator efficiency  $[I^* = M_n(\text{calcd})/M_n(\text{exptl})]$ , where  $M_n(\text{calcd}) = \text{MW}(\text{MMA}) \times [\text{MMA}]_0/[1]_0 \times \text{conversion}\%$  of 86%. Likewise, the  $I^*$  was calculated to be 87% at a conversion of 82%; these  $I^*$  values are typical of those MMA polymerizations by the metallocene system.<sup>2b</sup> All polymers produced exhibit unimodal molecular weight distributions (MWD) with polydispersity indices ( $\text{PDI} = M_w/M_n$ ) ranging from 1.43 to 1.54.

The polymerization in a  $[\text{MMA}]_0/[1]_0$  ratio of 800 at 22 °C is considerably slower and achieves quantitative monomer conversion in 70 min (runs 11 to 23, Table 1), but the  $M_n$  data of the resulting polymers are still consistent with the production of two polymer chains per Zr center. However, the polymerization at this ratio is more controlled in terms of an observed linear increase of the polymer  $M_n$  with monomer conversion, which is coupled with relatively small and nearly constant PDI values (Figure 1). More significantly, the polymers produced exhibit *it-b-st sb*-microstructures,<sup>8</sup> with enriched in both *st* ( $[rr] = 40\text{--}45\%$ ) and *it* ( $[mm] = 43\text{--}39\%$ ) contents as well as reduced *ht*-contents ( $[mr] = 16\text{--}17\%$ ). The polymers produced are unimodal with relatively narrow MWDs as measured by GPC in either THF (stereocomplex solvent) or  $\text{CHCl}_3$  (no complex solvent), exhibit single  $T_g$  values ranging from 93 to 99 °C, and show practically no change in stereomicrostructures (triad distributions) with quantitative recovery yields after they have been extracted by boiling absolute ethanol for >12 h [*it*-P(MMA) of medium molecular weight ( $M_n < 5 \times 10^4$ ) is soluble in hot ethanol<sup>2n</sup>]; the combined above evidence supports the

conclusion that these polymers produced by the  $1/2\text{Al}(\text{C}_6\text{F}_5)_3$  system under these conditions are *it-b-st* multiblock P(MMA), implying that the polymerization occurs in a diastereospecific fashion. Polymerizations at 0 °C (runs 24 to 31, Table 1) behave similarly, except that the resulting polymers have ~20% more *st*-contents than those produced at 22 °C.

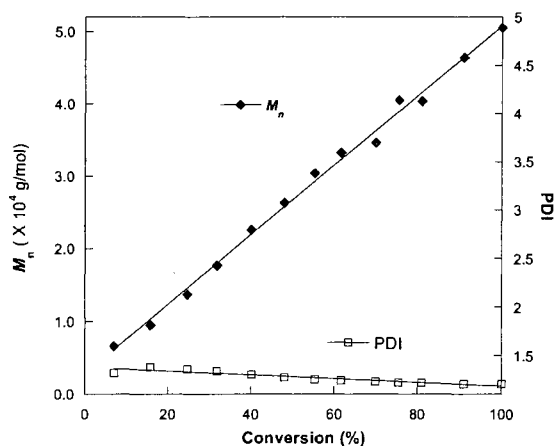


**Figure 1.** Plot of  $M_n$  and PDI of P(MMA) by the  $1/2\text{Al}(\text{C}_6\text{F}_5)_3$  system  $\{[\text{MAA}]_0/[\text{I}]_0 = 800; 22$  °C $\}$  vs. monomer conversion.

**Table 1.** Selected MMA Polymerization Results by the  $1/2\text{Al}(\text{C}_6\text{F}_5)_3$  System<sup>a</sup>

run no.	[I] (mM)	$[\text{MMA}]_0/[\text{I}]_0$	temp (°C)	time (min)	conv. (%)	$10^4 M_n^b$ (g/mol)	PDI <sup>b</sup> ( $M_w/M_n$ )	$[\text{mm}]^c$ (%)	$[\text{mr}]^c$ (%)	$[\text{rr}]^c$ (%)
1	1.56	600	22	1	38	2.08	1.54	6.6	22.1	71.3
2				2	45	2.24	1.50	7.0	23.1	69.9
3				3	52	2.15	1.54	7.2	22.7	70.1
4				4	56	2.37	1.47	7.2	22.6	70.2
5				5	60	2.37	1.48	7.8	23.7	68.5
6				6	67	2.34	1.51	6.9	24.0	69.1
7				7	72	2.50	1.50	8.3	23.7	68.0
8				8	76	2.56	1.49	8.9	22.6	68.5
9				9	82	2.82	1.47	8.7	23.4	67.9
10				10	88	2.92	1.43	8.6	23.7	67.7
11	1.17	800	22	1	7	0.66	1.32	32.5	19.0	48.5
12				5	16	0.95	1.38	36.7	18.2	45.1
13				10	24	1.37	1.36	40.7	17.1	42.2
14				15	32	1.77	1.34	42.4	16.5	41.1
15				20	40	2.26	1.30	42.7	16.7	40.6
16				25	48	2.63	1.27	44.3	16.0	39.7
17				30	55	3.04	1.25	44.7	15.9	39.4
18				35	62	3.32	1.24	44.5	16.2	39.3
19				40	70	3.46	1.23	44.2	16.4	39.4
20				46	75	4.05	1.22	45.0	16.1	38.9
21				50	81	4.04	1.22	44.2	16.3	39.5

22				60	91	4.64	1.20	41.9	16.8	41.3
23				70	100	5.05	1.20	40.0	17.4	42.6
24	1.17	800	0	2	17	0.83	1.61	18.7	19.4	61.9
25				10	25	1.48	1.38	21.7	17.9	60.4
26				20	38	2.21	1.32	21.2	18.0	60.8
27				30	49	2.91	1.27	22.9	18.5	58.6
28				40	57	3.46	1.24	21.5	18.1	60.4
29				55	71	4.18	1.24	21.3	18.0	60.7
30				70	86	4.93	1.24	22.0	18.8	59.2
31				104	95	5.80	1.24	20.7	18.1	61.2
32	0.935	1000	22	5	12	0.90	1.31	38.5	17.6	43.9
33				7	14	1.09	1.33	41.4	18.2	40.4
34				10	23	1.40	1.33	46.2	16.8	37.0
35				15	29	1.85	1.32	45.7	17.1	37.3
36				20	34	2.12	1.35	47.8	16.3	35.9
37				30	46	2.89	1.30	47.5	15.8	36.7
38				45	62	3.91	1.27	50.2	15.5	34.3
39				75	84	5.01	1.34	54.1	14.4	31.5
40				120	94	5.55	1.23	56.0	13.8	30.2
41				180	98	6.10	1.34	60.9	12.6	26.5
42	0.935	1000	0	4	15	0.60	1.31	39.0	18.8	42.2
43				10	21	0.99	1.25	40.6	15.8	43.6
44				20	31	1.52	1.24	42.0	15.7	42.3
45				30	42	2.01	1.24	43.3	15.0	41.7
46				45	45	2.78	1.20	41.0	15.6	43.4
47				60	52	3.36	1.19	43.7	14.9	41.4
48				90	66	4.22	1.18	47.2	14.2	38.6
49				120	77	5.15	1.18	48.8	13.8	37.4
50				181	88	5.73	1.19	52.5	13.0	34.5
51				240	92	5.97	1.20	54.4	12.5	33.1
52	0.78	1200	22	2	12	0.58	1.32	52.9	18.2	28.9
53				6	14	1.40	1.41	64.8	13.7	21.5
54				10	20	2.10	1.43	69.3	12.3	18.4
55				15	24	2.54	1.52	70.1	12.1	17.8
56				20	28	3.21	1.47	71.3	12.2	16.5
57				30	43	4.19	1.43	71.0	12.1	16.9
58				45	58	5.50	1.38	73.9	10.9	15.2
59				60	67	5.98	1.34	73.4	10.8	15.8
60				90	82	6.90	1.34	71.6	11.7	16.7
61				120	89	6.95	1.38	72.5	11.3	16.2
62				150	93	7.87	1.37	74.7	10.6	14.7
63	0.62	1500	22	5	9	2.16	1.17	77.2	12.7	10.1
64				11	18	3.72	1.28	80.1	11.3	8.6
65				20	22	5.24	1.38	84.1	9.1	6.8
66				30	31	6.65	1.41	81.5	10.6	7.9
67				45	43	8.06	1.42	80.3	11.0	8.7
68				60	53	9.46	1.44	81.7	10.4	7.9
69				90	64	9.88	1.54	80.9	10.7	8.4
70				120	72	9.65	1.61	81.2	10.6	8.2

<sup>a</sup> Carried out in Schlenk flasks on a Schlenk line using an external temperature-control bath, 10 mL CH<sub>2</sub>Cl<sub>2</sub>.  
<sup>b</sup> Number average molecular weight ( $M_n$ ) and polydispersity index (PDI) determined by GPC relative to PMMA standards in CHCl<sub>3</sub>. <sup>c</sup> Tacticity (methyl triad distribution) determined by <sup>1</sup>H NMR spectroscopy.

A further decrease in the concentration of **1** to reach a [MMA]<sub>0</sub>/[**1**]<sub>0</sub> ratio of 1000 further slows down the polymerization at 22 °C (runs 32 to 41, Table 1), however, the  $M_n$  data of the resulting polymers are still consistent with the production of two polymer chains per Zr center. Under this condition, there is a gradual increase in *it*-content from [mm] = 39% to 61% as monomer conversion increases from 12% to 98%, and conversely the *st*-content decreases from [rr] = 44% to 27%; in the same conversion window, the *ht*-content remained relatively low ([mr] = 18–13%). The polymerization also shows a linear increase of the polymer  $M_n$  vs. monomer conversion with relatively small, nearly constant PDI values (Figure 2). Using the same analytical procedures employed for the polymers produced at the 800:1 ratio, all polymers produced at the 1000:1 ratio are confirmed to be *it-b-st* multiblock P(MMA), but they have considerably longer *it*-sequences. Polymerizations at 0 °C (runs 42 to 51, Table 1) produce polymers with similar characteristics. Polymerizations under a further reduced catalyst concentration in [MMA]<sub>0</sub>/[**1**]<sub>0</sub> ratio of 1200 (runs 52 to 62) give polymers with increasingly more *it*-contents than *st*-contents in the *it-b-st* *sb*-P(MMA) product, with [mm] reaching ~70%. Lastly, when the catalyst concentration is further reduced to such that the [MMA]<sub>0</sub>/[**1**]<sub>0</sub> ratio = 1500, the resulting polymers are essentially *it*-P(MMA) with nearly constant *it*-content of [mm] ~80%.

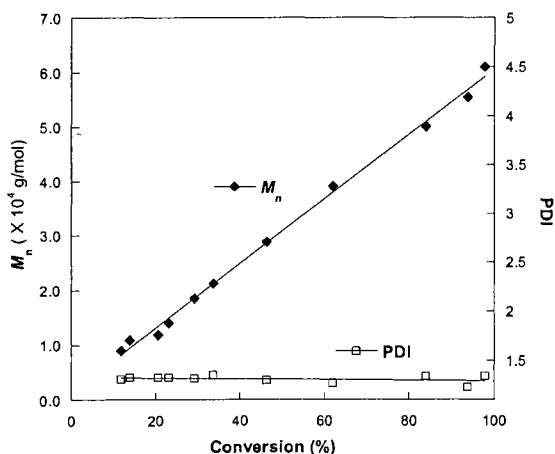


**Figure 2.** Plot of  $M_n$  and PDI of P(MMA) by the  $1/2\text{Al}(\text{C}_6\text{F}_5)_3$  system  $\{[\text{MMA}]_0/[\mathbf{1}]_0 = 1000; 22\text{ }^\circ\text{C}\}$  vs. monomer conversion.

**Polymerization Kinetics.** MMA polymerizations by the  $1/2\text{Al}(\text{C}_6\text{F}_5)_3$  system with relatively high catalyst concentrations of  $[\mathbf{1}] \geq 1.17\text{ mM}$  (i.e.,  $[\text{MMA}]_0/[\mathbf{1}]_0 \leq 800$ ) at  $22\text{ }^\circ\text{C}$  follow zero order kinetics in  $[\text{MMA}]$  (Figure 3); this kinetic behavior holds true for the polymerizations at  $0\text{ }^\circ\text{C}$  despite the expected lower rates. Varying the equivalency of  $\text{Al}(\text{C}_6\text{F}_5)_3$  employed did not alter this kinetic order (Figure 3), and analyses of the resulting polymer by the  $1/x\text{Al}(\text{C}_6\text{F}_5)_3$  system ( $x = 2$  to  $5$ ) showed similar polymer  $M_n$  and PDI values at nearly the same monomer conversions although the *st*-content of the resulting P(MMA) gradually increased from  $\sim 40\%$  to  $\sim 60\%$  when  $x$  was varied from  $2$  to  $5$ . A double logarithm plot (Figure 4) of the apparent rate constants ( $k_{\text{app}}$ ), which were obtained from the slopes of the best-fit lines to the plots of  $[\text{MMA}]_t/[\text{MMA}]_0$  vs time, as a function of  $[\text{Al}(\text{C}_6\text{F}_5)_3]$ , was fit to a straight line of slope =  $1.9(1)$ . Hence, the kinetic order with respect to  $[\text{Al}(\text{C}_6\text{F}_5)_3]$ , given by the slope of  $1.9(1)$ , reveals that propagation is approximately second order in  $[\text{Al}(\text{C}_6\text{F}_5)_3]$  under the concentration regime defined above.

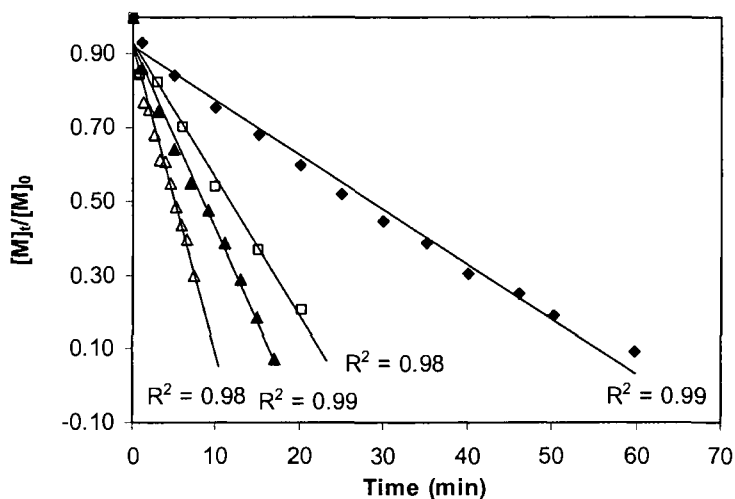


**Figure 3.** Selected zero-order plots of  $[\text{M}]_t/[\text{M}]_0$  vs time for the polymerization of MMA by  $1/x\text{Al}(\text{C}_6\text{F}_5)_3$  in  $\text{CH}_2\text{Cl}_2$  at  $22\text{ }^\circ\text{C}$ . Conditions:  $[\text{MMA}]_0/[\text{Al}]_0/[\text{Zr}]_0 = 800/2/1$  ( $\blacklozenge$ ),  $800/3/1$  ( $\square$ ),  $800/4/1$  ( $\blacktriangle$ ), and  $800/5/1$  ( $\triangle$ ).

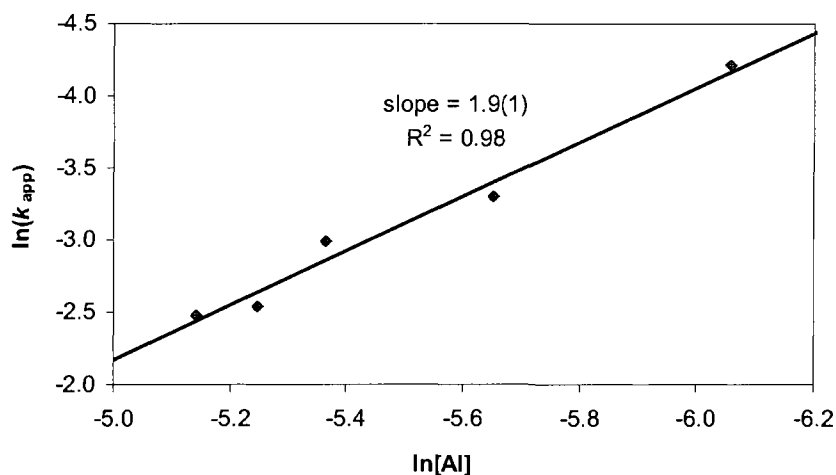


**Figure 4.** Plot of  $\ln(k_{app})$  versus  $\ln[Al]$  for the MMA polymerization by  $1/xAl(C_6F_5)_3$  at 22 °C.

On the other hand, MMA polymerizations by the  $1/2Al(C_6F_5)_3$  system with relatively low zirconocene concentrations of  $[1] \leq 0.935$  mM (i.e.,  $[MMA]_0/[1]_0 \geq 1000$ ) at 22 °C follow strictly first order kinetics in  $[MMA]$  (Figure 5). As can be seen from this Figure, the first order kinetics within this concentration regime is invariant of both the  $1/Al(C_6F_5)_3$  ratio (with two equiv of the alane or greater) and reaction temperature.

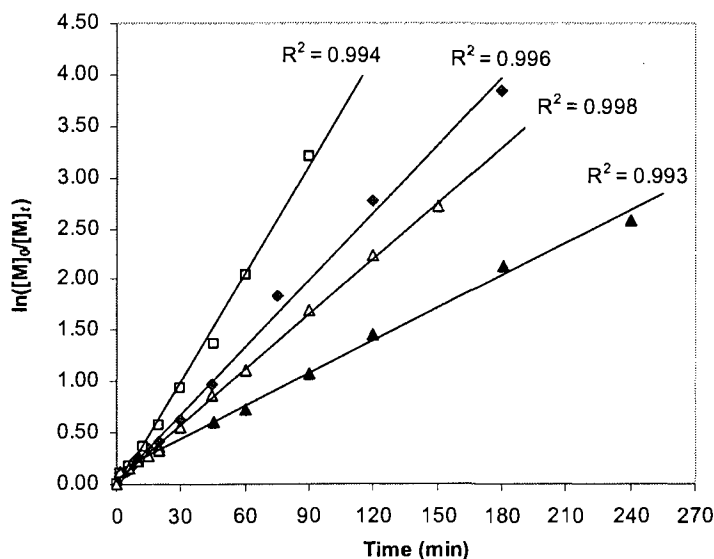
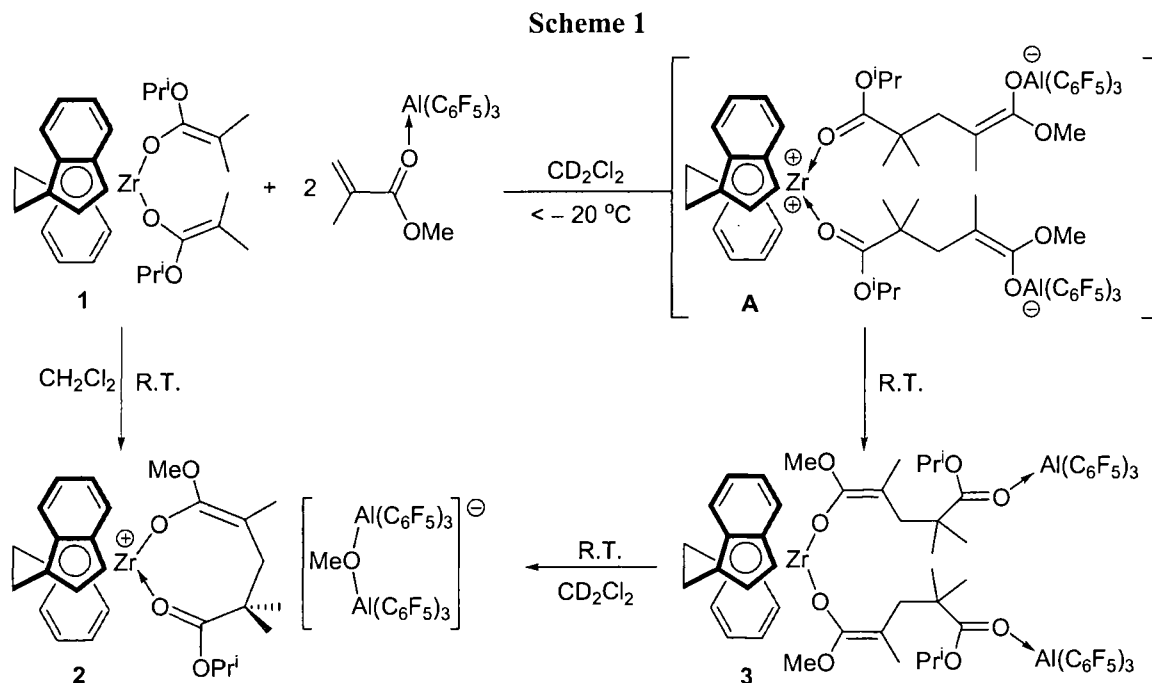


**Figure 5.** Selected first-order plots of  $\ln([M]_0/[M]_t)$  vs time for the polymerization of MMA by  $1/xAl(C_6F_5)_3$  in  $CH_2Cl_2$ . Conditions:  $[MMA]_0/[Al]_0/[Zr]_0 = 1000/3/1$  at 22 °C ( $\square$ ),  $1000/2/1$  at 22 °C ( $\blacklozenge$ ),  $1200/2/1$  at 22 °C ( $\triangle$ ), and  $1000/2/1$  at 0 °C ( $\blacktriangle$ ).

**Elementary Reactions.** There are four possible elementary reactions to consider in the current polymerization system containing the monomer MMA as well as catalysts zirconocene bis(ester enolate) **1** and Lewis acid  $\text{Al}(\text{C}_6\text{F}_5)_3$ . First, there was no reaction between MMA and **1** under the polymerization conditions employed (in  $\text{CH}_2\text{Cl}_2$  at ambient temperature up to several hours). Second, mixing of MMA and  $\text{Al}(\text{C}_6\text{F}_5)_3$  spontaneously forms the adduct  $\text{Al}(\text{C}_6\text{F}_5)_3 \cdot \text{MMA}$ . Third, direct contact of **1** with  $\text{Al}(\text{C}_6\text{F}_5)_3$  in toluene led to the formation of a mixture of unidentified species. Decomposition of the analogous mono-ester enolate complex, *rac*-(EBI)ZrMe[OC(O<sup>*i*</sup>Pr)=CMe<sub>2</sub>], by  $\text{Al}(\text{C}_6\text{F}_5)_3$  was reported to occur via the alane-assisted 1,5-H sigma-tropic shift of  $\beta$ -H of the isopropoxy group to the =CMe<sub>2</sub> carbon followed by elimination of propylene and formation of the carboxylate bridged ion pair.<sup>2f</sup> In the current polymerization system, however, at no time does the free  $\text{Al}(\text{C}_6\text{F}_5)_3$  exist because it is always in the form of an adduct with either MMA or the ester group of the polymer chain. Thus, the fourth elementary reaction consider is the reaction of **1** with the adduct  $\text{Al}(\text{C}_6\text{F}_5)_3 \cdot \text{MMA}$ , which is precisely related to the current polymerization system and identical to our practice (i.e., we premix the alane with excess MMA to form the adduct before addition to a  $\text{CH}_2\text{Cl}_2$  solution of **1** to start the polymerization, *vide supra*). Significantly, unlike the complex decomposition reactions observed upon mixing of **1** and  $\text{Al}(\text{C}_6\text{F}_5)_3$ , the reaction of **1** with  $\text{Al}(\text{C}_6\text{F}_5)_3 \cdot \text{MMA}$  yielded no such complex decomposition products, but clean and characterizable species. Thus, the reaction of **1** with 2 equiv of  $\text{Al}(\text{C}_6\text{F}_5)_3 \cdot \text{MMA}$  in  $\text{CH}_2\text{Cl}_2$  for 24 h (to ensure a complete conversion of **1** and other related species shown in Scheme 1 to **2**) at ambient temperature afforded ion pair **2** as an orange red crystalline solid in 76% isolated yield. The cation portion of **2** is identical to the living, highly isospecific, cyclic ester enolate zirconocenium cation that is paired with the methyl borate anion, *rac*-(EBI)Zr[OC(OMe)=C(Me)CH<sub>2</sub>C(Me)<sub>2</sub>C(O<sup>*i*</sup>Pr)=O]<sup>+</sup>[MeB(C<sub>6</sub>F<sub>5</sub>)<sub>3</sub>]<sup>-</sup>, which was derived from the single MMA addition to *rac*-(EBI)Zr<sup>+</sup>(THF)[OC(O<sup>*i*</sup>Pr)=CMe<sub>2</sub>][MeB(C<sub>6</sub>F<sub>5</sub>)<sub>3</sub>]<sup>-</sup> and previously isolated as well as spectroscopically/analytically (but not structurally) characterized;<sup>2b</sup> the cation

is also an isoelectronic structure of the neutral samarium complex  $(C_5Me_5)_2Sm(MMA)_2H$ , which was isolated from the reaction of the samarium hydride precursor with 2 equiv of MMA and crystallographically characterized.<sup>19</sup>



X-ray diffraction analysis of single crystals of **2** confirmed the molecular structure inferred from spectroscopic and analytical data, featuring unassociated cation and anion pairs (Figure 6). The structural motif of the cation is indeed that of the proposed chiral *ansa*-zirconocenium center incorporating the *rac*-(EBI) ligand and eight-membered-ring cyclic ester enolate moiety,<sup>2b</sup> whereas the anion is a methoxy-bridged dialuminate in which the bridging oxygen adopts a trigonal planar geometry with a sum of the angles around the oxygen of 359.9°. The covalent Zr–enolate oxygen bond [Zr–O(2) = 1.987(3) Å] is noticeably shorter than the dative Zr–carbonyl oxygen bond [Zr–O(1) = 2.117(3) Å] by 0.13 Å, whereas the enolate carbon–oxygen single bond [C(22)–O(2) = 1.361(5) Å] is longer than the C=O double bond [C(29)–O(1) = 1.247(4) Å] by 0.11 Å. The C(22)=C(24) double bond is characterized by a bond distance of 1.322(6) Å and a sum of the angles around C(22) of 360.0° for a trigonal-planar geometry. Interestingly, the O(1)–

Zr–O(2) angle of  $97.4(1)^\circ$  in **2** is identical to that observed in the precursor bis(ester enolate) **1**, despite its formation of the eight-membered-ring cyclic ester enolate moiety that adopts an unusual conformation in which both the enolate oxygen atom O(2) and the methylene carbon atom C(25) are located above the plane defined approximately by the remaining ring atoms. On the other hand, unlike the partial double-bond character for the Zr–O bond in **1** where the oxygen is partly  $sp$ -hybridized due to a  $p\pi$ - $d\pi$  interaction between zirconium and enolate oxygen,<sup>2f</sup> the Zr–enolate oxygen bond in **2** is purely a single bond, as evidenced by its bond length and a small Zr–O(2)–C(22) vector angle of  $125.2(2)^\circ$ , presumably as a consequence of the eight-membered-ring conformation. This unique ring conformation places the C(27) atom, equivalent of the growing polymer chain (which would make the C(26) the chiral penultimate chain end), in the coordination sphere voids of the *rac*-(EBI) ligand structure, facing away from the  $C_6$ -rings of the bridged indenyl ligands and also avoiding the steric congestion with the vinyl methyl C(23) atom with approximately a *trans* arrangement between these two groups. This interplay between the chirality of the  $C_2$ -ligand and the growing penultimate chain end as well as the vinyl methyl group presumably determines how the incoming MMA approaches and ring opens this active resting cyclic enolate intermediate—the rate limiting step of the polymerization,<sup>2b</sup> and thus the isospecificity of this cation.

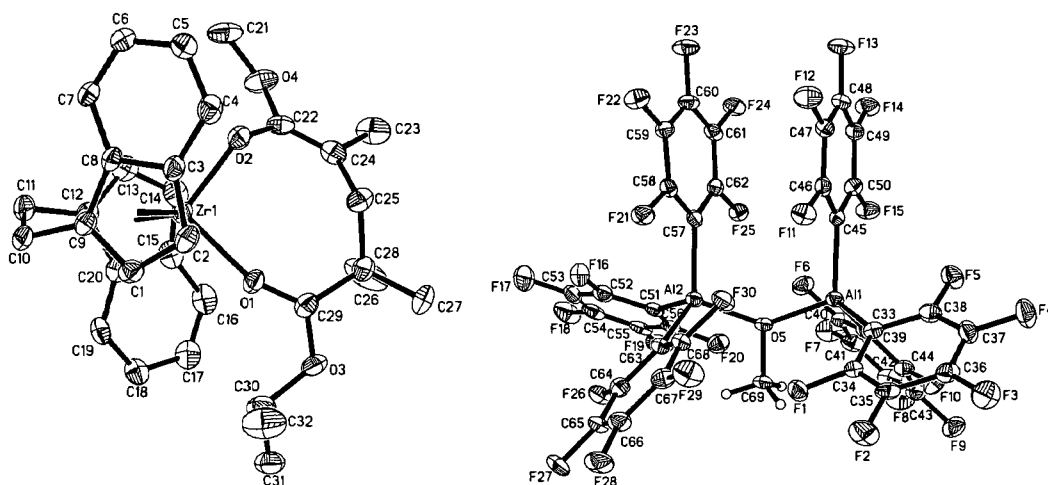


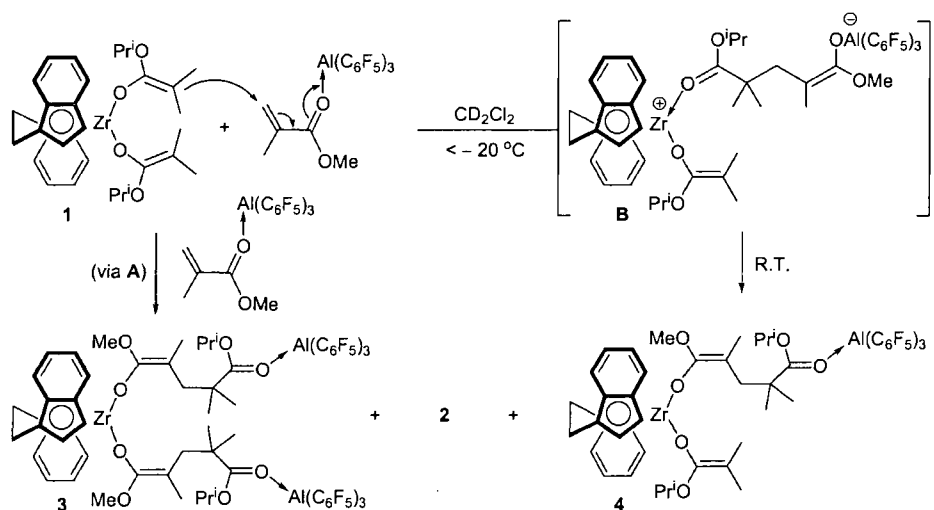
**Figure 6.** Molecular structure of **2**. Selected bond lengths (Å): Zr–O(1) = 2.117(3), Zr–O(2) = 1.987(3), C(29)–O(1) = 1.247(4), C(29)–O(3) = 1.303(4), C(22)–O(2) = 1.361(5), C(22)–O(4) = 1.373(5), C(22)–C(24) = 1.322(6), Al(1)–O(5) = 1.846(3), Al(2)–O(5) = 1.831(3); selected bond angles (°): Zr–O(1)–C(29) = 159.9(3), Zr–O(2)–C(22) = 125.2(2), O(1)–Zr–O(2) = 97.4(1), Al(1)–O(5)–Al(2) = 138.6(2).

Monitoring the reaction of **1** + 2[Al(C<sub>6</sub>F<sub>5</sub>)<sub>3</sub>•MMA] in CD<sub>2</sub>Cl<sub>2</sub> by VT NMR revealed, upon mixing of these two reagents at –78 °C, spontaneous formation of a deep red solution, characteristic of zirconocenium dication formation,<sup>20a,b</sup> spectroscopic data are also consistent with formation of intermediate **A**, shown in Scheme 1, comprising the zirconocenium dication<sup>20a,b</sup> paired with enolaluminate anions.<sup>15</sup> This dicationic intermediate is thermally unstable; on warming to about –20 °C, it begins to undergo ester–enolate isomerization to form yellowish neutral zirconocene bis(ester enolate) complex **3** in which both terminal ester carbonyl oxygen atoms are coordinated to Al(C<sub>6</sub>F<sub>5</sub>)<sub>3</sub>. Further standing of the resulting yellow solution of **3** at ambient temperature induced a gradual transformation of neutral complex **3** to cationic complex **2** as outlined in Scheme 1. These two complexes can be readily distinguished by <sup>1</sup>H and <sup>19</sup>F NMR; while there are 4 sets (doublets) of signals for the four C<sub>5</sub>-ring protons in <sup>1</sup>H NMR of complex **2** (C<sub>1</sub> symmetry), there are only 2 sets of signals for the four C<sub>5</sub>-ring protons in complex **3** as a consequence of C<sub>2</sub> symmetry. The enolate MeO group exhibits similar chemical shifts in both complexes (δ 3.14 ppm in **2** vs. 2.99 ppm in **3**), but the second MeO group in **2** is linked to two Al centers in the anion (δ 4.05 ppm). The coordinated isopropyl ester group [–C(O<sup>*i*</sup>Pr)=O] also gives rise to sharply different chemical shifts, depending on whether the carbonyl oxygen is coordinated to Zr in **2** or Al in **3**; specifically, the <sup>1</sup>H NMR signal for –OCHMe<sub>2</sub> (sept, 4.34 ppm) in **2** is considerably down-field shifted to 5.19 ppm (sept) for –OCHMe<sub>2</sub> in **3**. Lastly, the <sup>19</sup>F NMR chemical shift difference further confirms their structural assignments; a further upfield shift for the *para*- and *meta*-fluorines and a smaller chemical shift difference between the *para*- and *meta*-fluorines in ion pair **2**, as compared to those observed in neutral complex **3**, are

consistent with the anionic nature of the aluminate moiety<sup>20</sup> in **2** vs. the datively coordinated neutral alane moiety in complex **3** that shows a nearly identical <sup>19</sup>F NMR spectrum to Al(C<sub>6</sub>F<sub>5</sub>)<sub>3</sub>•MMA. It is noteworthy that, owing to this transformation in polar solvents such as CH<sub>2</sub>Cl<sub>2</sub> (the conversions of **3** to **2** in CD<sub>2</sub>Cl<sub>2</sub> at 23 °C were 8% and 36% for 20 min and 2 h, respectively), isolation of the yellow neutral complex **3** in pure state was achieved only from the **1** + 2[Al(C<sub>6</sub>F<sub>5</sub>)<sub>3</sub>•MMA] reaction in hexanes at ambient temperature for 30 min, the conditions of which suppressed the formation of **2**.

We also investigated the reaction of **1** with 1 equiv of Al(C<sub>6</sub>F<sub>5</sub>)<sub>3</sub>•MMA in CH<sub>2</sub>Cl<sub>2</sub>, which was found to occur analogously to the 1:2 ratio reaction. Under this ratio, however, both dicationic **A** and monocationic **B** intermediates (plus the remaining unreacted **1**) were generated at low temperatures, which, upon warming to ambient temperature, led to formation of a mixture containing neutral complexes **3** and **4** as well as the cationic complex **2** (Scheme 2), depending on how long the solution mixture was kept at this temperature. Complexes **3** and **4** can be readily distinguished by <sup>1</sup>H NMR (see Experimental), most notably, the splitting pattern of the *rac*-(EBI) moiety due to differences in symmetry (*C*<sub>2</sub> for **3** vs. *C*<sub>1</sub> for **4**) and the type of the O<sup>*i*</sup>Pr group present due to differences in linkage (identical two ester O<sup>*i*</sup>Pr groups in **3** vs. different one ester and one enolate O<sup>*i*</sup>Pr groups in for **4**); however, isolation of complex **4** in pure state by separation of these two complexes in a preparative scale proved unfeasible. When the reaction of **1** with 1.3 equiv of Al(C<sub>6</sub>F<sub>5</sub>)<sub>3</sub>•MMA (to ensure a complete consumption of **1**) was carried out in hexanes (to suppress the formation of **2**), the formation

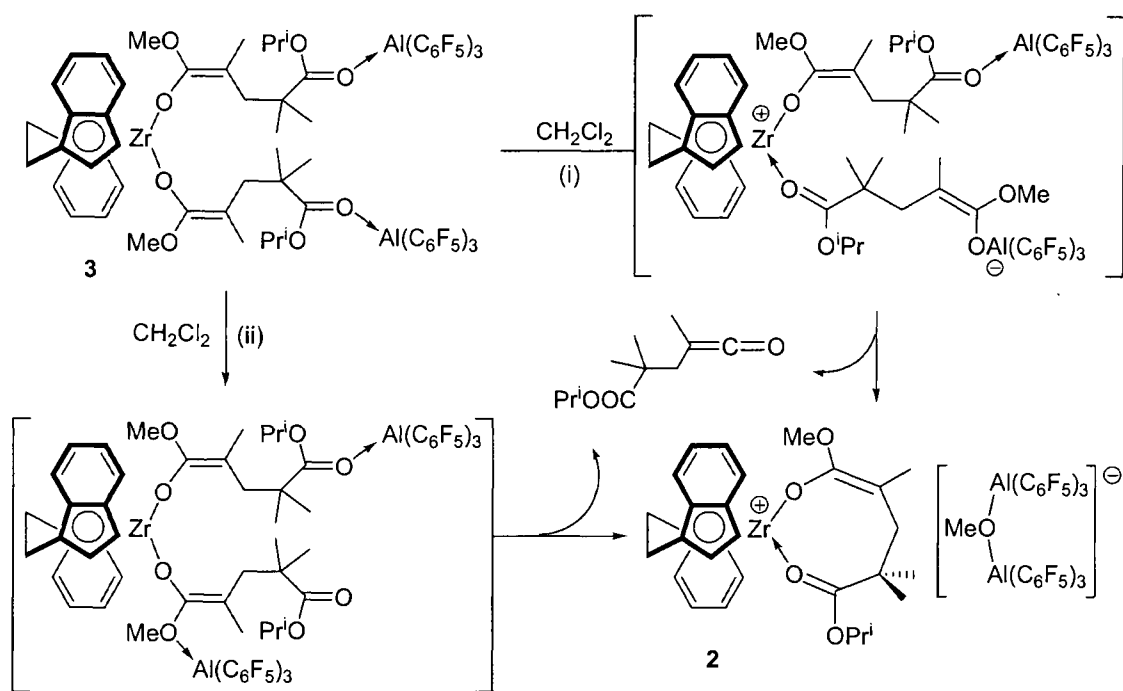
Scheme 2



of **4** was accompanied by ~40% of **3**; attempts to separate them by recrystallization were unsuccessful. Nevertheless, the observation for the formation of intermediate **B** and complex **4** adds additional important pieces to the overall polymerization mechanism described later.

Two possible pathways for converting neutral complex **3** to cationic complex **2** are proposed in Scheme 3. Pathway (i) proceeds via enolate-ester isomerization, formally abstraction of the enolate moiety by the alane, to the cationic ester enolate intermediate analogous to **B** that undergoes methoxide abstraction by the alane followed by elimination of a ketene and ring closure to form complex **2**. On the hand, pathway (ii) proceeds via a non-ionic intermediate derived from migration of the alane from the carbonyl oxygen to the enolate methoxy oxygen to effect methoxide abstraction there followed by the ketene elimination and ring closure to give **2**. The observed significant rate acceleration in noncoordinating polar solvent  $\text{CH}_2\text{Cl}_2$  over toluene and no conversion in nonpolar hexane solvent suggest that pathway (i) is presumably operative.

Scheme 3



**Temperature and Lewis Acid Effects.** When the polymerization temperature decreased from 22 °C to -40 °C at the constant catalyst concentration ( $[\mathbf{1}] = 1.17 \text{ mM}$ ) and ratio ( $[\text{MMA}]_0/[\text{Al}]_0/[\mathbf{1}]_0 = 800/2/1$ ), the time required for achieving quantitative monomer conversion increased gradually from 70 min to 120 min, and the resulting polymer *st*-content and molecular weight increased gradually to afford essentially *st*-P(MMA) at -20 ( $[rrr] = 81\%$ ) and -40 °C ( $[rrr] = 83\%$ ), as shown in Table 2. These results imply that, as the reaction temperature decreases, the bimolecular propagation process brought about by the Al catalyst that produces the *st*-blocks becomes increasingly more competitive than the monometallic propagation process operated by the Zr catalyst that yields the *it*-blocks.

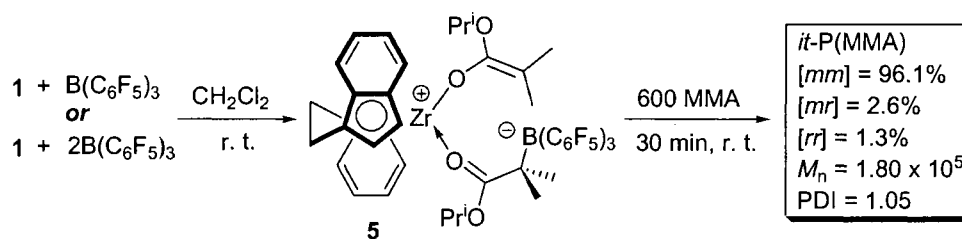
**Table 2.** Comparisons of the P(MMA) at Quantitative Conversions at Varied Temperatures <sup>a</sup>

run no.	temp (°C)	10 <sup>4</sup> M <sub>n</sub> (g/mol)	PDI (M <sub>w</sub> /M <sub>n</sub> )	[ <i>mm</i> ] (%)	[ <i>mr</i> ] (%)	[ <i>rr</i> ] (%)
1	22	5.05	1.20	40.0	17.4	42.6
2	0	5.80	1.26	21.4	18.8	59.8
3	-20	6.37	1.54	2.7	16.2	81.1
4	-40	7.05	1.87	3.1	13.8	83.1

<sup>a</sup> See Table 1 footnotes for explanations of the abbreviations listed in this table; conditions: [1] = 1.17 mM, [MMA]<sub>0</sub>/[Al]<sub>0</sub>/[1]<sub>0</sub> = 800/2/1.

A seemingly analogous system comprising **1** and B(C<sub>6</sub>F<sub>5</sub>)<sub>3</sub> (1 or 2 equiv) gave no formation of the *sb*-polymer but simply highly *it*-P(MMA). To seek for an answer to this observation, we examined the 1:1 ratio reaction of **1** and B(C<sub>6</sub>F<sub>5</sub>)<sub>3</sub> and found that it forms cationic zirconocene ester enolate- $\alpha$ -ester borate ion pair **5** (Scheme 4), as a result of apparent electrophilic addition of the borane to the nucleophilic ester enolate  $\alpha$ -carbon, reminiscent of the reaction of B(C<sub>6</sub>F<sub>5</sub>)<sub>3</sub> with the sterically unprotected bis(2-propenolato)zirconocene reported by Erker et al.<sup>21</sup> The reaction with 2 equiv of B(C<sub>6</sub>F<sub>5</sub>)<sub>3</sub> affords the same product with no indication of the possible bis-adduct formation. The MMA polymerization by the isolated species **5** indeed affords P(MMA) with high isotacticity of [*mm*] = 96% by a site-control mechanism (2[*rr*]/[*mr*] = 1.0) and low polydispersity of PDI = 1.05, showing the similar polymerization behavior to the THF-coordinated cationic *ansa*-zirconocenium ester enolate,<sup>2b</sup> except for somewhat lower activity of **5**. Polymerizations by *in situ* mixing of MMA with 1 or 2 equiv of B(C<sub>6</sub>F<sub>5</sub>)<sub>3</sub> followed by addition of complex **1** (i.e., activated monomer approach), or by *in situ* mixing of complex **1** with B(C<sub>6</sub>F<sub>5</sub>)<sub>3</sub> followed by addition of MMA (i.e., activated complex approach), gave similarly highly *it*-P(MMA). Overall, the Lewis acid in the **1**/B(C<sub>6</sub>F<sub>5</sub>)<sub>3</sub> system functions only as a cation-forming agent, and neither the resulting anion nor the neutral borane participates in the polymer chain formation steps as do Al(C<sub>6</sub>F<sub>5</sub>)<sub>3</sub> and its derived anions in the **1**/Al(C<sub>6</sub>F<sub>5</sub>)<sub>3</sub> system.

### Scheme 4



Replacing  $\text{Al}(\text{C}_6\text{F}_5)_3$  in the highly effective  $1/2\text{Al}(\text{C}_6\text{F}_5)_3$  system with common trialkyl aluminum reagents such as  $\text{AlMe}_3$  (2 and 50 equiv) resulted in a completely inactive system for MMA polymerization, while substituting  $\text{Al}(\text{C}_6\text{F}_5)_3$  with  $\text{MeAl}(\text{BHT})_2$  yielded an active system but with substantially lower activity. Additionally, the  $1/2\text{MeAl}(\text{BHT})_2$  system produce simply *it*-P(MMA) with [mm] ranging from 80% to 87% and the triads conforming to a site-control mechanism, suggesting that only the isospecific zirconocenium site is operative in this polymerization. Furthermore, the polymers produced at monomer conversions  $\geq 50\%$  after 6 h showed bimodal molecular weight distributions with small high-molecular weight tails (Table 3). Increasing the amount of  $\text{MeAl}(\text{BHT})_2$  to 50 equiv with respect to **1** only moderately enhanced the polymerization activity; for example, with a reaction time of 2 h, the conversion reached 38%, which compared to a conversion of 22% with 2 equiv of  $\text{MeAl}(\text{BHT})_2$ , although the resulting polymer exhibits a higher isotacticity ([mm] = 91.7%, [mr] = 5.5%, [rr] = 2.8) again conforming to a site-control mechanism. Lastly, methyl aluminoxane (MAO) behaves similarly to  $\text{MeAl}(\text{BHT})_2$ .

MMA polymerizations by **1** in combination with metallocenium-based Lewis acids, rather than  $\text{Al}(\text{C}_6\text{F}_5)_3$ , were also investigated. Thus, the polymerization of 800 equiv of MMA for 2 h by  $1 + 2 \text{Cp}_2\text{Zr}[\text{OC}(\text{O}^i\text{Pr})=\text{CMe}_2]^+\text{MeB}(\text{C}_6\text{F}_5)_3^-$  (generated by in situ mixing of  $\text{Cp}_2\text{ZrMe}[\text{OC}(\text{O}^i\text{Pr})=\text{CMe}_2]$

**Table 3.** Selected MMA Polymerization Results by the  $1/2\text{MeAl}(\text{BHT})_2$  System <sup>a</sup>

run no.	time (h)	conv. (%)	$10^4 M_n$ (g/mol)	PDI ( $M_w/M_n$ )	[ <i>mm</i> ] (%)	[ <i>mr</i> ] (%)	[ <i>rr</i> ] (%)
1	0.5	10	2.42	1.84	79.7	14.6	5.7
2	1	13	4.07	2.39	88.1	7.9	4.0
3	2	22	7.20	2.39	88.4	7.9	3.7
4	3	30	8.68	2.29	86.5	8.8	4.7
5	4	37	9.37	2.14	84.8	9.7	5.5
6	5	43	15.7	1.54	85.8	9.5	4.7
7	6	50	9.62; 4960 <sup>b</sup>	2.00; 1.27 <sup>b</sup>	85.6	9.6	4.8
8	8	61	9.70; 2725 <sup>b</sup>	1.94; 1.31 <sup>b</sup>	86.6	8.6	4.8
9	10	69	10.9; 1749 <sup>b</sup>	1.92; 1.24 <sup>b</sup>	84.4	10.1	5.5
10	12	78	10.4; 1068 <sup>b</sup>	1.92; 1.28 <sup>b</sup>	82.7	10.5	6.8
11	15	85	9.56; 507 <sup>b</sup>	2.09; 1.24 <sup>b</sup>	85.1	9.6	5.3

<sup>a</sup> See Table 1 footnotes for explanations of the abbreviations listed in this table; conditions:  $[1] = 0.935$  mM,  $[\text{MMA}]_0/[1]_0 = 1000$ , 22 °C. <sup>b</sup> A bimodal distribution with a small high-molecular-weight tail.

with  $\text{B}(\text{C}_6\text{F}_5)_3$  gave P(MMA) in 92% yield with *sb*-like triad distributions:  $[mm] = 45.0\%$ ,  $[mr] = 19.4\%$ , and  $[rr] = 35.6$ ; however, the polymer obtained is not unimodal but exhibits a trimodal MWD (Figure 7), presumably due to a mixture of polymer products derived from the separate isospecific and syndiospecific sites as well as the site exchange process. The polymerization results using the  $1/2\text{Cp}_2\text{ZrMe}^+\text{MeB}(\text{C}_6\text{F}_5)_3^-$  system were nearly identical, and this polymerization behavior was not significantly affected by the mixing sequence of the reagents. These results argue that interconversion between diastereospecific sites is ineffective (none or much slower than the rate of chain formation).

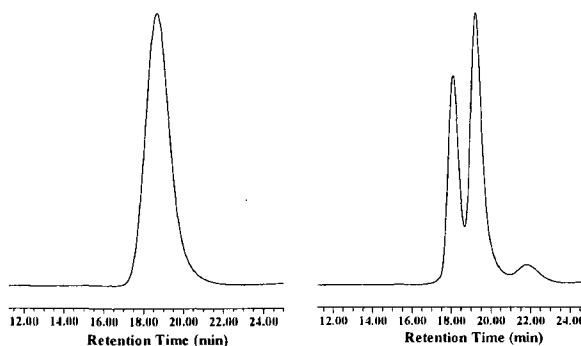
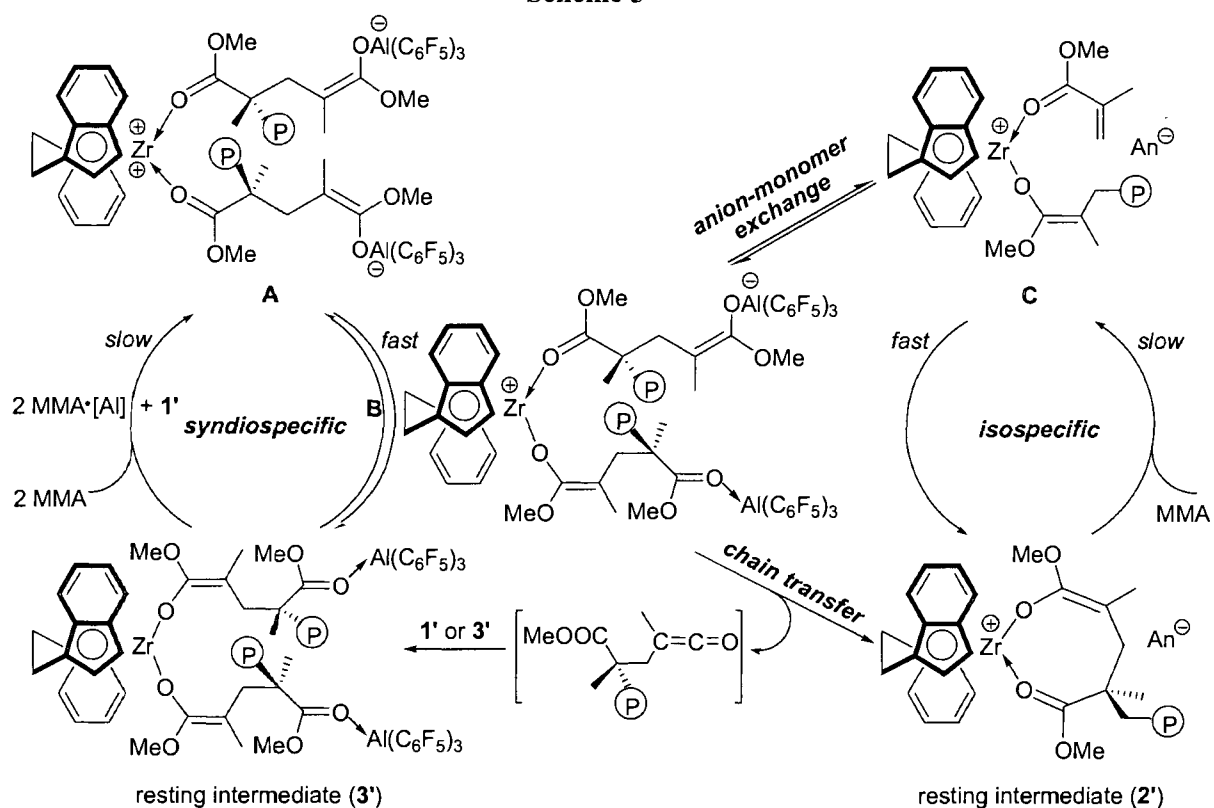


**Figure 7.** Representative GPC traces of P(MMA) by the  $1/2\text{Al}(\text{C}_6\text{F}_5)_3$  system (left; PDI = 1.20 in this example) and by the  $1/2\text{Cp}_2\text{Zr}[\text{OC}(\text{O}^i\text{Pr})=\text{CMe}_2]^+\text{MeB}(\text{C}_6\text{F}_5)_3^-$  system (right, multimodal MWD) both in a  $[\text{MMA}]_0/[1]_0 = 800$  at 22 °C in  $\text{CH}_2\text{Cl}_2$ .

These above results clearly demonstrate that, among the Lewis acids investigated in this study, only  $\text{Al}(\text{C}_6\text{F}_5)_3$  is capable of effecting simultaneous *it*- and *st*-polymer chain formations at the cationic zirconocenium and anionic aluminate sites, respectively, rendering the rate of interconversion between two sites to be faster than the rate of chain formation, and thus producing *it-b-st* multiblock P(MMA) with unimodal MWDs.

**Polymerization Mechanism.** On the basis of the above detailed studies on the polymerization characteristics and kinetics, elementary reactions, characterization and behavior of the isolated key intermediates, as well as temperature and Lewis acid effects, we proposed a mechanism, outlined in Scheme 5, for the DIPP of MMA by the  $1/2\text{Al}(\text{C}_6\text{F}_5)_3$  system. Specifically, this mechanism consists of four manifolds: isospecific, syndiospecific, anion-monomer exchange, and chain-transfer domains. In the *st*-block production manifold, the rate-limiting step of the bimetallic propagation involves intermolecular Michael addition of the bis(ester enolate) ligands in **1'** (**1** and its homologues) to the activated monomer  $\text{MMA}\cdot\text{Al}(\text{C}_6\text{F}_5)_3$ ; the resulting dicationic species **A** rapidly isomerizes to either monocationic species **B** or neutral bis(ester enolate) **3'** (**3** and its homologues) in which the coordinated alane catalyst is released by the incoming monomer to complete a *st*-P(MMA) production cycle, following the kinetics of zero order in [MMA] and second order in [Al] (*c.f.* Schemes 1 and 2). In the isotactic block production manifold, the rate-limiting step is the associative displacement of the coordinated penultimate ester group of the growing chain in the cationic cyclic ester enolate **2'** (**2** and its homologues) by the incoming monomer to regenerate the active species **C** that participates in the fast propagating steps via intramolecular Michael addition, following first-order kinetics in [MMA]; this propagation cycle and kinetics are identical to what have been demonstrated for the MMA polymerization by the same cation but paired with the methyl borate anion.<sup>2b</sup>

Scheme 5



There are two apparent pathways to interconvert two diastereospecific propagating manifolds. The first is the anion-monomer exchange process through monocationic species **B** in which the enolaluminate anion is displaced by MMA to form active species **C**, providing direct interconversion between active species **A** and **C**. The second is the chain transfer going from the resting state **3'** to **2'** also through **B** but with concomitant release of a ketene-terminated polymer chain (*c.f.* Scheme 3) which could be instantaneously trapped by the enolate moieties present in the system (e.g., **1'** or **3'**) to regenerate a (ketone) enolate; the contribution of this chain transfer process may be minimal under the current conditions, but its role cannot be ruled out because of the independently observed conversion of **3** to **2** within the polymerization time scale (*vide supra*). The high catalyst concentration regime, for example,  $[\text{MMA}]_0/[\text{Al}]_0/[\mathbf{1}]_0 = 600/2/1$ , favors the bimetallic, syndiotactic manifold, producing predominately *st*-P(MMA). Conversely, the low catalyst concentration regime, for example,  $[\text{MMA}]_0/[\text{Al}]_0/[\mathbf{1}]_0 = 1500/2/1$ , favors the

monometallic, isotactic manifold, producing predominately *it*-P(MMA). The middle concentration regime with the  $[MMA]_0/[Al]_0/[1]_0$  ratio from 800/2/1 to 1200/2/1 affords *it-b-st* multiblock P(MMA) with various amounts of *it*- and *st*-contents that are a function of relative rates of interconversion vs. propagation of the two diastereospecific propagating species; the rate of interconversion is regulated by the anion-monomer exchange and chain transfer processes.

A check of the kinetic competence of the isolated two key resting intermediates has also been carried out. As expected, the MMA polymerization by **2** alone indeed produces only *it*-P(MMA), and the result of the MMA polymerization by **3** hinges on its concentration and thus the  $[MMA]_0/[3]_0$  ratio; in a low ratio of 400, predominately *st*-P(MMA) was produced with  $[rr] = 70.2\%$ ,  $[mr] = 22.7\%$ , and  $[mm] = 7.1\%$ , but in a higher ratio of 800, *it-b-st* multiblock P(MMA) was produced with  $[mr] = 18.0\%$  and approximately equal amounts of  $[rr]$  and  $[mm]$  tacticities. These results are nearly identical to those derived from the polymerization by the  $1/2Al(C_6F_5)_3$  system. Overall, these experimental observations and those discussed in the previous sections concerning the polymerization by the  $1/2Al(C_6F_5)_3$  system are consistent with the mechanism depicted in Scheme 5.

**Application to Copolymerization.** Homopolymers of MMA are glassy materials with a wide range of the above-ambient-temperature  $T_g$  values as a function of stereomicrostructures: *it*,  $\sim 50$  °C; *it-b-st*,  $\sim 90$  °C; *at*,  $\sim 105$  °C; *st*,  $\sim 130$  °C. To extend the utility of the above demonstrated DIPP process by the  $1/2Al(C_6F_5)_3$  system to the production of functionalized elastomeric materials with low  $T_g$ 's, we also examined its polymerizations of methacrylates with longer alkyl chains, such as *n*-butyl methacrylate (BMA) and 2-ethylhexyl methacrylate (EHM), as well as copolymerizations of MMA with BMA and EHM. Investigation into the ability of the  $1/2Al(C_6F_5)_3$  system to produce *sb*-structures of these longer-chain alkyl methacrylate homopolymers, especially their *sb*-copolymers with MMA, is of great interest as the programmable stereomicrostructures should lead to tunable materials physical and mechanical

properties of these homopolymers and *sb*-copolymers, the latter of which can potentially offer a combination of materials properties unobtainable from homopolymer blends or stereo-random copolymers.

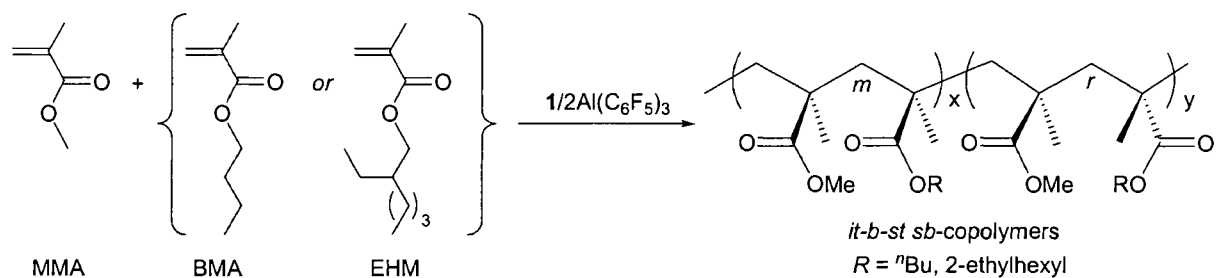
Polymerization of BMA in a  $[BMA]_0/[Al]_0/[1]_0$  ratio of 800/2/1 in  $CH_2Cl_2$  at ambient temperature produces P(BMA) with a  $T_g$  of  $-7$  °C and a triad distribution of  $[rr] = 53.9\%$ ,  $[mr] = 6.6\%$ , and  $[mm] = 39.5\%$  (run 1, Table 4), consistent with the *it-b-st* multiblock microstructure. The considerably lower *ht*-content of only 6.6%, compared to a typical value of  $[mr] = 16\%$  of P(MMA) produced under identical condition, shows much longer diastereo-blocks in the resulting P(BMA), with an average *it*-sequence  $N_m \sim 13$  and *st*-sequence  $N_r \sim 17$ , estimated using  $N_m = 1 + 2[mm]/[mr]$  and  $N_r = 1 + 2[rr]/[mr]$ .<sup>16a</sup> As in the MMA polymerization with this ratio, the  $M_n$  of P(BMA) is consistent with the production of two polymer chains per Zr center, and increasing the ratio to 1200 yields the polymer with predominately *it*-frequency  $[mm] = 88.2\%$  and a  $T_g$  of  $-14$  °C (run 2, Table 4). Copolymerization of BMA with MMA shows the same characteristics, producing *it-b-st sb*-copolymers (Scheme 6) with either nearly equal *it*- and *st*-sequences (runs 3) or predominant *it*-sequences (run 4), depending on the monomer/catalyst ratio employed. The 1:1 molar composition of the two monomer units measured in the copolymers produced is identical to the monomer feed ratio, and the  $T_g$  values of the copolymer are consistent with their stereomicrostructures.

**Table 4.** Alkyl Methacrylate Polymerization and Copolymerization Results by the  $1/2Al(C_6F_5)_3$  System<sup>a</sup>

run no.	monomer (comonomer)	$[M]_0/[1]_0$	time (h)	conv. (%)	$10^4 M_n^b$ (g/mol)	PDI <sup>b</sup> ( $M_w/M_n$ )	$[mm]^c$ (%)	$[mr]$ (%)	$[rr]$ (%)	$T_g$ (°C)
1	BMA	800	2	96	5.25	1.36	39.5	6.6	53.9	-7
2	BMA	1200	3	94	18.9	1.44	88.2	3.9	7.9	-14
3	BMA(MMA)	800	1.3	95	4.72	1.21	44.8	12.8	42.4	37
4	BMA(MMA)	1200	3	95	12.2	1.35	79.1	6.0	15.0	19
5	EHM	800	2	98	9.12	1.59	78.3	5.9	15.8	-26
6	EHM	1200	4	98	20.7	1.37	86.1	0.0	13.9	-29
7	EHM(MMA)	800	1.4	99	5.61	1.31	35.6	13.1	51.3	20
8	EHM(MMA)	1200	3.7	94	11.3	1.42	81.4	8.0	11.6	-3

<sup>a</sup> See Table 1 footnotes for explanations of the abbreviations listed in this table;  $[1] = 1.17$  and  $0.78$  mM for  $[monomer]_0/[1]_0 = 800$  and  $1200$ , respectively; for all copolymerizations, the monomer molar feed ratio = 1:1; 10 mL  $CH_2Cl_2$ , 22 °C.

Scheme 6



Polymerizations of EHM (runs 5 and 6) and its copolymerizations with MMA (runs 7 and 8) are similarly successful, producing *sb*-polymers and copolymers with  $T_g$ 's varying from  $-29$  to  $20$  °C, depending on the stereomicrostructure and comonomer. With these successful polymerization and copolymerization examples using long-chain alkyl methacrylates, it is envisioned that copolymerizations of MMA with methacrylates with even longer alkyl chains, such as octadecyl methacrylate (its homopolymer has a  $T_g$  of about  $-100$  °C), can further lower  $T_g$  of the resulting polymer products for targeted elastomeric applications. Overall, these studies demonstrate the ability of the current DIPP system to extend its application to polymerization and copolymerization of long-chain alkyl methacrylates, thereby providing an access to fine tune the thermal properties of the resulting functionalized polymers by regulating the stereomicrostructure of the polymer and the nature of comonomer.

## Conclusions

We have demonstrated that the catalytic system comprising the readily available chiral zirconocene bis(ester enolate) *rac*-(EBI)Zr[OC(O<sup>*i*</sup>Pr)=CMe<sub>2</sub>]<sub>2</sub> (**1**) and 2 equiv of the Lewis acid Al(C<sub>6</sub>F<sub>5</sub>)<sub>3</sub> effectively promotes the novel diastereospecific ion-pairing polymerization (DIPP) as well as copolymerization of functionalized alkenes such as methacrylates, producing polymers having a range of stereoregularities, including *it*, *st*, and *it-b-st* multiblock microstructures,

depending on the [monomer]/[catalyst] ratio employed. Our detailed investigations into the polymerization characteristics and kinetics, elementary reactions, characterization and behavior of the isolated key intermediates, temperature and Lewis acid effects, as well applications to copolymerization have yielded a mechanism for the DIPP of MMA by the  $1/2\text{Al}(\text{C}_6\text{F}_5)_3$  system, which consists of isospecific, syndiospecific, anion-monomer exchange, and chain-transfer manifolds. This mechanism satisfactorily explains the formation of various polymer stereomicrostructures under given conditions and reveals two pathways to interconvert diastereospecific propagating manifolds—anion-monomer exchange and chain transfer (see Scheme 5)—for the production of the multi *it-b-st sb*-structures. From a broader perspective, this DIPP system presents unique cation-anion cooperativity in ion-pairing catalysis that involves participation from both the cation and the anion as catalysts for the same reaction, with each bringing different reactivity and stereoselectivity to the products.

The current DIPP system also presents at least two potentially significant advantages over other polymerization systems from a practical, industrial point of view. *First*, there is practically no need to remove inhibitors typically present in the functionalized vinyl monomers by distillation or other techniques, as required for processes such as radical polymerization. (Although the results reported in the current study were derived from the experiments employing stringently purified monomers for obvious reasons of eliminating any possible effects of other reagents on our system, selected separate experiments using the commercial-grade MMA, i.e., simple storage over molecular sieves without removal of the inhibitor, showed that the polymerization activity was not noticeably affected.) *Second*, the DIPP system is a simple process, but it can offer diverse polymer products having various stereomicrostructures, namely the industrially desirable approach—one catalyst system, multiple materials.

**Acknowledgements.** Funding for this work was provided by the National Science Foundation and Colorado State University. We thank Boulder Scientific Co. for the gift of B(C<sub>6</sub>F<sub>5</sub>)<sub>3</sub>.

## References

- 
- (1) For selected recent examples and reviews, see: (a) Arriola, D. J.; Carnahan, E. M.; Hustad, P. D.; Kuhlman, R. L.; Wenzel, T. T. *Science* **2006**, *312*, 714–719. (b) Gibson, V. C.; Spitzmesser, S. K. *Chem. Rev.* **2003**, *103*, 283–315. (c) Coates, G. W.; Hustad, P. D.; Reinartz, S. *Angew. Chem. Int. Ed. Engl.* **2002**, *41*, 2236–2257. (d) Chum, P. S.; Kruper, W. J.; Guest, M. J. *Adv. Mater.* **2000**, *12*, 1759–1767. (e) Gladysz, J. A., Ed. *Chem. Rev.* **2000**, *100*, 1167–1681 (special issue on Frontiers in Metal-Catalyzed Polymerization).
- (2) (a) Rodriguez-Delgado, A.; Mariott, W. R.; Chen, E. Y.-X. *J. Organomet. Chem.* **2006**, *691*, 3490–3497. (b) Rodriguez-Delgado, A.; Chen, E. Y.-X. *Macromolecules* **2005**, *38*, 2587–2594. (c) Kostakis, K.; Mourmouris, S.; Kotakis, K.; Nikogeorgos, N.; Pitsikalis, M.; Hadjichristidis, N. *J. Polym. Sci. Part A: Polym. Chem.* **2005**, *43*, 3305–3314. (d) Ning, Y.; Cooney, M. J.; Chen, E. Y.-X. *J. Organomet. Chem.* **2005**, *690*, 6263–6270. (e) Lian, B.; Lehmann, C. W.; Navarro, C.; Carpentier, J.-F. *Organometallics* **2005**, *24*, 2466–2472. (f) Bolig, A. D.; Chen, E. Y.-X. *J. Am. Chem. Soc.* **2004**, *126*, 4897–4906. (g) Stojcevic, G.; Kim, H.; Taylor, N. J.; Marder, T. B.; Collins, S. *Angew. Chem. Int. Ed.* **2004**, *43*, 5523–5526. (h) Strauch, J. W.; Fauré, J.-L.; Bredeau, S.; Wang, C.; Kehr, G.; Fröhlich, R.; Luftmann, H.; Erker, G. *J. Am. Chem. Soc.* **2004**, *126*, 2089–2104. (i) Chen, E. Y.-X. *J. Polym. Sci. Part A: Polym. Chem.* **2004**, *42*, 3395–3403. (j) Karanikolopoulos, G.; Batis, C.; Pitsikalis, M.; Hadjichristidis, N. *J. Polym. Sci. Part A: Polym. Chem.* **2004**, *42*, 3761–3774. (k) Ferez, M.; Bandermann, F.; Sustmann, R.; Sicking, W. *Macromol. Chem. Phys.* **2004**, *205*, 1196–1205. (l) Rodriguez-Delgado, A.; Mariott, W. R.; Chen, E. Y.-X.

---

*Macromolecules* **2004**, *37*, 3092–3100. (m) Jensen, T. R.; Yoon, S. C.; Dash, A. K.; Luo, L.; Marks, T. J. *J. Am. Chem. Soc.* **2003**, *125*, 14482–14494. (n) Chen, E. Y.-X.; Cooney, M. J. *J. Am. Chem. Soc.* **2003**, *125*, 7150–7151. (o) Mariott, W. R.; Chen, E. Y.-X. *J. Am. Chem. Soc.* **2003**, *125*, 15726–15727. (p) Jin, J.; Mariott, W. R.; Chen, E. Y.-X. *J. Polym. Chem. Part A: Polym. Chem.* **2003**, *41*, 3132–3142. (q) Batis, C.; Karanikolopoulos, G.; Batis, C.; Pitsikalis, M.; Hadjichristidis, N. *Macromolecules* **2003**, *36*, 9763–9774. (r) Karanikolopoulos, G.; Batis, C.; Pitsikalis, M.; Hadjichristidis, N. *Macromol. Chem. Phys.* **2003**, *204*, 831–840. (s) Bolig, A. D.; Chen, E. Y.-X. *J. Am. Chem. Soc.* **2002**, *124*, 5612–5613. (t) Jin, J.; Chen, E. Y.-X. *Organometallics* **2002**, *21*, 13–15 (u) Bandermann, F.; Ferez, M.; Sustmann, R.; Sicking, W. *Macromol. Symp.* **2001**, *174*, 247–253. (v) Karanikolopoulos, G.; Batis, C.; Pitsikalis, M.; Hadjichristidis, N. *Macromolecules* **2001**, *34*, 4697–4705. (w) Bolig, A. D.; Chen, E. Y.-X. *J. Am. Chem. Soc.* **2001**, *123*, 7943–7944. (x) Frauenrath, H.; Keul, H.; Höcker, H. *Macromolecules* **2001**, *34*, 14–19. (y) Nguyen, H.; Jarvis, A. P.; Lesley, M. J. G.; Kelly, W. M.; Reddy, S. S.; Taylor, N. J.; Collins, S. *Macromolecules* **2000**, *33*, 1508–1510. (z) Bandermann, F.; Ferez, M.; Sustmann, R.; Sicking, W. *Macromol. Symp.* **2000**, *161*, 127–134. (aa) Cameron, P. A.; Gibson, V.; Graham, A. J. *Macromolecules* **2000**, *33*, 4329–4335. (bb) Stuhldreier, T.; Keul, H.; Höcker, H. *Macromol. Rapid Commun.* **2000**, *21*, 1093–1098. (cc) Chen, Y.-X.; Metz, M. V.; Li, L.; Stern, C. L.; Marks, T. J. *J. Am. Chem. Soc.* **1998**, *120*, 6287–6305. (dd) Shiono, T.; Saito, T.; Saegusa, N.; Hagihara, H.; Ikeda, T.; Deng, H.; Soga, K. *Macromol. Chem. Phys.* **1998**, *199*, 1573–1579. (ee) Li, Y.; Ward, D. G.; Reddy, S. S.; Collins, S. *Macromolecules* **1997**, *30*, 1875–1883. (ff) Deng, H.; Shiono, T.; Soga, K. *Macromol. Chem. Phys.* **1995**, *196*, 1971–1980. (gg) Deng, H.; Shiono, T.; Soga, K. *Macromolecules* **1995**, *28*, 3067–3073. (hh) Soga, K.; Deng, H.; Yano, T.; Shiono, T.

- 
- Macromolecules* **1994**, *27*, 7938–7940. (ii) Collins, S.; Ward, D. G.; Suddaby, K. H. *Macromolecules* **1994**, *27*, 7222–7224. (jj) Collins, S.; Ward, S. G. *J. Am. Chem. Soc.* **1992**, *114*, 5460–5462. (kk) Farnham, W. B.; Hertler, W. U.S. Pat. 4,728,706, 1988.
- (3) (a) Mariott, W. R.; Rodriguez-Delgado, A.; Chen, E. Y.-X. *Macromolecules* **2006**, *39*, 1318–1327. (b) Kostakis, K.; Mourmouris, S.; Pitsikalis, M.; Hadjichristidis, N. *J. Polym. Sci. Part A: Polym. Chem.* **2005**, *43*, 3337–3348. (c) see ref. 2ee. (d) Deng, H.; Soga, K. *Macromolecules* **1996**, *29*, 1847–1848.
- (4) (a) Mariott, W. R.; Chen, E. Y.-X. *Macromolecules* **2005**, *38*, 6822–6832. (b) Mariott, W. R.; Chen, E. Y.-X. *Macromolecules* **2004**, *37*, 4741–4743.
- (5) Hatada, K.; Kitayama, T.; Ute, K. *Prog. Polym. Sci.* **1988**, *13*, 189–276.
- (6) (a) Harney, M. B.; Zhang, Y.; Sita, L. R. *Angew. Chem. Int. Ed.* **2006**, *45*, 1–5. (b) Coates, G. W.; Waymouth, R. M. *Science* **1995**, *267*, 217–219. (c) Llinas, G. L.; Dong, S.-H.; Mallin, D. T.; Rausch, M. D.; Lin, G.-Y.; Winter, H. H.; Chien, J. C. W. *Macromolecules* **1992**, *25*, 1242–1253.
- (7) (a) Serizawa, T.; Hamada, K.-I.; Akashi, M. *Nature* **2004**, *429*, 52–55. (b) Serizawa, T.; Hamada, K.; Kitayama, T.; Fujimoto, N.; Hatada, K.; Akashi, M. *J. Am. Chem. Soc.* **2000**, *122*, 1891–1899. (c) Hatada, K.; Kitayama, T.; Ute, K.; Nishiura, T. *Macromol. Symp.* **1998**, *132*, 221–230. (d) Spevacek, J.; Schneider, B. *Adv. Colloid Interface Sci.* **1987**, *27*, 81–150.
- (8) (a) see refs 2 n and 2s. (b) Knjazhanski, S. Y.; Elizalde, L.; Cadenas, G.; Bulychev, B. M. *J. Polym. Sci. Part A: Polym. Chem.* **1998**, *36*, 1599–1606. (c) Kitayama, T.; Fujimoto, N.; Yanagida, T.; Hatada, K. *Polym. Int.* **1994**, *33*, 165–170.
- (9) Allen, R. D.; Long, T. E.; McGrath, J. E. *Polym. Bull.* **1986**, *15*, 127–134.
- (10) Feng, S.; Roof, G. R.; Chen, E. Y.-X. *Organometallics* **2002**, *21*, 832–839.

- 
- (11) (a) Lee, C. H.; Lee, S. J.; Park, J. W.; Kim, K. H.; Lee, B. Y.; Oh, J. S. *J. Mol. Cat., A: Chem.* **1998**, *132*, 231–239. (b) Biagini, P.; Lugli, G.; Abis, L.; Andreussi, P. U.S. Pat. 5,602269, 1997.
- (12) Shreve, A. P.; Mulhaupt, R.; Fultz, W.; Calabrese, J.; Robbins, W.; Ittel, S. *Organometallics* **1988**, *7*, 409–416.
- (13) (a) Grossman, R. B.; Doyle, R. A.; Buchwald, S. L. *Organometallics* **1991**, *10*, 1501–1505. (b) Collins, S.; Kuntz, B. A.; Taylor, N. J.; Ward, D. G. *J. Organomet. Chem.* **1988**, *342*, 21–29.
- (14) Diamond, G. M.; Jordan, R. F.; Petersen, J. L. *J. Am. Chem. Soc.* **1996**, *118*, 8024–8033.
- (15) Rodriguez-Delgado, A.; Chen, E. Y.-X. *J. Am. Chem. Soc.* **2005**, *127*, 961–974.
- (16) (a) Bovey, F. A.; Mirau, P. A. *NMR of Polymers*; Academic Press: San Diego, CA, 1996. (a) Bulai, A.; Jimeno, M. L.; de Queiroz, A.-A. A.; Gallardo, A.; Roman, J. S. *Macromolecules* **1996**, *29*, 3240–3246. (c) Ferguson, R. C.; Ovenall, D. W. *Macromolecules* **1987**, *20*, 1245–1248. (d) Subramanian, R.; Allen, R. D.; McGrath, J. E.; Ward, T. C. *Polym. Prepr.* **1985**, *26*, 238–240.
- (17) *SHELXTL*, Version 6.12; Bruker Analytical X-ray Solutions: Madison, WI, 2001.
- (18) Chakraborty, D.; Chen, E. Y.-X. *Inorg. Chem. Commun.* **2002**, *5*, 698–701.
- (19) (a) Yasuda, H.; Yamamoto, H.; Yamashita, M.; Yokota, K.; Nakamura, A.; Miyake, S.; Kai, Y.; Kanehisa, N. *Macromolecules* **1993**, *26*, 7134–7143. (b) Yasuda, H.; Yamamoto, H.; Yokota, K.; Miyake, S.; Nakamura, A. *J. Am. Chem. Soc.* **1992**, *114*, 4908–4909.
- (20) (a) Stahl, N. G.; Salata, M. R.; Marks, T. J. *J. Am. Chem. Soc.* **2005**, *127*, 10898–10909. (b) Chen, E. Y.-X.; Kruper, W. J.; Roof, G.; Wilson, D. R. *J. Am. Chem. Soc.* **2001**, *123*, 745–746. (c) Liu, Z.; Somsook, E.; Landis, C. R. *J. Am. Chem. Soc.* **2001**, *123*, 2915–2916.
- (21) Spaether, W.; Klaub, K.; Erker, G.; Zippel, F.; Fröhlich, R. *Chem. Eur. J.* **1998**, *4*, 1411–1417.

---

## CHAPTER IV

### Remarkable Lewis Acid Effects on Polymerization of Functionalized Alkenes by Metallocene and Lithium Ester Enolates

#### Abstract

Drastic effects of Lewis acids  $E(C_6F_5)_3$  ( $E = Al, B$ ) on polymerization of functionalized alkenes such as methyl methacrylate (MMA) and *N,N*-dimethyl acrylamide (DMAA) mediated by metallocene and lithium ester enolates,  $Cp_2Zr[OC(O^iPr)=CMe_2]_2$  (**1**) and  $Me_2C=C(O^iPr)OLi$ , are documented as well as elucidated. In the case of metallocene bis(ester enolate) **1**, when combined with 2 equiv of  $Al(C_6F_5)_3$ , it effects highly active ion-pairing polymerization of MMA and DMAA; the living nature of this polymerization system allows for the synthesis of well-defined diblock and triblock copolymers of MMA with longer-chain alkyl methacrylates. In sharp contrast, the **1**/ $2B(C_6F_5)_3$  combination exhibits low to negligible polymerization activity due to the formation of ineffective adduct  $Cp_2Zr[OC(O^iPr)=CMe_2]^+[O=C(O^iPr)CMe_2B(C_6F_5)_3]^-$  (**2**). Such a profound Al vs. B Lewis acid effect has also been observed for the lithium ester enolate; while the  $Me_2C=C(O^iPr)OLi/2Al(C_6F_5)_3$  system is *highly active* for MMA polymerization, the seemingly analogous  $Me_2C=C(O^iPr)OLi/2B(C_6F_5)_3$  system is *inactive*. Structure analyses of the resulting lithium enolaluminate and enolborate adducts,  $Li^+[Me_2C=C(O^iPr)OAl(C_6F_5)_3]^-$  (**3**) and  $Li^+[Me_2C=C(O^iPr)OB(C_6F_5)_3]^-$  (**4**), coupled with polymerization studies, show that the remarkable differences observed for Al vs. B are due to the inability of the lithium enolborate/borane pair to effect the bimolecular, activated-monomer anionic polymerization as does the lithium enolaluminate/alane pair.

## Introduction

Erker and co-workers [1] first reported facile electrophilic addition of the strongly Lewis acidic  $B(C_6F_5)_3$  to nucleophilic group 4 metallocene *ketone enolates*,  $Cp_2M[OC(Me)=CH_2]_2$  ( $M = Ti, Zr, Hf$ ), affording the corresponding mono-adduct  $Cp_2M[OC(Me)=CH_2]^+[OC(Me)CH_2B(C_6F_5)_3]^-$  or bis-adduct  $Cp_2M^{++}[OC(Me)CH_2B(C_6F_5)_3]_2^-$ , depending on the molar equivalents of the added  $B(C_6F_5)_3$ . Remarkably, this type of adduct formation does not annihilate nucleophilic and electrophilic properties of the adduct constituents. Thus, a combination of  $Cp_2M[OC(Me)=CH_2]_2$  with  $B(C_6F_5)_3$  is active for polymerization of methyl vinyl ketone with activity of the mixture increasing as the molar equivalent of  $B(C_6F_5)_3$  is increased from 1 to 4.

We observed the reaction of chiral *ansa*-zirconocene *ester enolates*, *rac*-(EBI)ZrMe[OC(O<sup>i</sup>Pr)=CMe<sub>2</sub>] and *rac*-(EBI)Zr[OC(O<sup>i</sup>Pr)=CMe<sub>2</sub>]<sub>2</sub> [EBI = C<sub>2</sub>H<sub>4</sub>(Ind)<sub>2</sub>], with strong Lewis acids  $E(C_6F_5)_3$  ( $E = Al, B$ ) is highly sensitive to both the *ansa*-zirconocene precursor and E; for the methyl zirconocene mono-ester enolate, its reaction with  $Al(C_6F_5)_3$  proceeds through a Lewis-acid-assisted intramolecular proton transfer process to afford the carboxylate-bridged ion pair *rac*-(EBI)ZrMe<sup>+</sup>OC(<sup>i</sup>Pr)OAl(C<sub>6</sub>F<sub>5</sub>)<sub>3</sub><sup>-</sup> after elimination of propylene, whereas its reaction with  $B(C_6F_5)_3$  (in the presence of 1 equiv of THF as stabilizing reagent) proceeds through a methide abstraction route to give the cationic ester enolate complex *rac*-(EBI)Zr<sup>+</sup>(THF)[OC(O<sup>i</sup>Pr)=CMe<sub>2</sub>][MeB(C<sub>6</sub>F<sub>5</sub>)<sub>3</sub>]<sup>-</sup> [ 2 ]. Likewise, the reaction involving the bis(ester enolate) critically hinges on E; although its direct contact with  $Al(C_6F_5)_3$  leads to a mixture of products due to decomposition, in the presence of the methyl methacrylate (MMA) monomer the reaction cleanly generates active species that promotes rapid diastereospecific ion-pairing polymerization (DIPP) of MMA producing P(MMA) with unique isotactic-*b*-syndiotactic stereomultiblock microstructures [3]. On the other hand, the reaction of the bis(ester enolate) with 1 or 2 equiv of  $B(C_6F_5)_3$  follows Erker's electrophilic addition pathway generating the cationic zirconocene ester enolate- $\alpha$ -ester borate ion pair *rac*-

(EBI)Zr[OC(O<sup>i</sup>Pr)=CMe<sub>2</sub>]<sup>+</sup>[O=C(O<sup>i</sup>Pr)CMe<sub>2</sub>B(C<sub>6</sub>F<sub>5</sub>)<sub>3</sub>]<sup>-</sup>, which is an active catalyst for the production of the structurally controlled P(MMA) having a high isotacticity of  $[mm] = 96\%$  and a narrow molecular weight distribution (MWD) of  $M_w/M_n = 1.05$  [3].

We and others have been studying the *controlled* polymerization of functionalized alkenes such as MMA and *N,N*-dimethylacrylamide (DMAA) using group 4 metallocene *ester or amide enolate* catalysts incorporating achiral  $C_{2v}$  [4], chiral  $C_2$  [2,5] and  $C_1$  [6], as well as prochiral  $C_s$  [7] ligand symmetries. Some of these polymerization systems are living and stereospecific, thereby allowing for a high degree of control over the polymer MW, MWD, and stereomicrostructure (tacticity), as well as for the synthesis of well-defined block and stereoblock copolymers. In a closely related work, Erker and co-workers [8] carried out a detailed comparative study of MMA polymerization using a series of *ansa*-zirconocene *dimethyl* and *ansa*-zirconocene *butadiene* precursors varying steric bulk of alkyl substituents at one of the *ansa*-Cp rings, both activated by B(C<sub>6</sub>F<sub>5</sub>)<sub>3</sub> leading to the catalysts having the same cations but different anion structures; this work is significant because it provided direct evidence for the anion effect on the stereoselectivity in the metallocene-catalyzed polymerization of MMA.

Within the ester enolate family, simple lithium ester enolates can also initiate polymerization of MMA, producing, however, ill-defined, multimodal polymers [9]. Significantly, a combination of the lithium ester enolate with 2 equiv of suitable aluminum Lewis acids, especially Al(C<sub>6</sub>F<sub>5</sub>)<sub>3</sub>, promotes *highly active* MMA polymerization and, more importantly, produces P(MMA) with controlled MW and narrow MWD ( $M_w/M_n = 1.04$ ) even at room temperature [9,10]. Unexpectedly, addition of 1 or 2 equiv of the seemingly analogous B(C<sub>6</sub>F<sub>5</sub>)<sub>3</sub> to the lithium ester enolate *completely halted* the polymerization [9]! Similar observations were also seen for the MMA polymerization mediated by zirconocene imido complexes [6b] as well as aluminum and zinc alkyl complexes [11].

The current contribution examines two unaddressed issues: (a) Lewis acid effects on the MMA polymerization by achiral  $C_{2v}$ -metallocene ester enolate Cp<sub>2</sub>Zr[OC(O<sup>i</sup>Pr)=CMe<sub>2</sub>]<sub>2</sub> and (b)

explanations for the already observed extreme Lewis acid effects on the MMA polymerization by lithium ester enolate  $\text{Me}_2\text{C}=\text{C}(\text{OR})\text{OLi}$ . We found that there exhibit drastic A1 vs. B Lewis acid effects on the polymerization activity for both ester enolate systems and subsequently elucidated these effects.

## Experimental

### 2.1. Materials and Methods

All syntheses and manipulations of air- and moisture-sensitive materials were carried out in flamed Schlenk-type glassware on a dual-manifold Schlenk line, a high-vacuum line, or in an argon or nitrogen-filled glovebox. NMR-scale reactions (typically in a 0.02 mmol scale) were conducted in Teflon-valve-sealed J. Young-type NMR tubes. HPLC grade organic solvents were sparged extensively with nitrogen during filling of the solvent reservoir and then dried by passage through activated alumina (for THF,  $\text{Et}_2\text{O}$ , and  $\text{CH}_2\text{Cl}_2$ ) followed by passage through Q-5-supported copper catalyst (for toluene and hexanes) stainless steel columns. Benzene- $d_6$  and toluene- $d_8$  were degassed, dried over sodium/potassium alloy, and filtered before use, whereas  $\text{CD}_2\text{Cl}_2$  was degassed and dried over activated Davison 4 Å molecular sieves. NMR spectra were recorded on a Varian Inova 300 (FT 300 MHz,  $^1\text{H}$ ; 75 MHz,  $^{13}\text{C}$ ; 282 MHz,  $^{19}\text{F}$ ), a Varian Inova 400, or a Varian Inova 500 spectrometer. Chemical shifts for  $^1\text{H}$  and  $^{13}\text{C}$  spectra were referenced to internal solvent resonances and are reported as parts per million relative to tetramethylsilane, whereas  $^{19}\text{F}$  NMR spectra were referenced to external  $\text{CFCl}_3$ . Elemental analyses were performed by Desert Analytics, Tucson, AZ.

All common reagents were purchased from Aldrich and used as received unless otherwise indicated. Commercially purchased monomers methyl methacrylate (MMA), *n*-butyl methacrylate (BMA) from Alfa Aesar, 2-ethylhexyl methacrylate (EHM) from TCI America, and *N,N*-dimethylacrylamide (DMAA) from TCI America were purified by first degassing and drying over  $\text{CaH}_2$  overnight, followed by vacuum distillation. Further purification of MMA involved

titration with neat tri(*n*-octyl)aluminum to a yellow end point [12] followed by distillation under reduced pressure. The purified monomers were stored in brown bottles over activated Davison 4-Å molecular sieves (for DMAA) in a -30 °C freezer inside the glovebox. Butylated hydroxytoluene (BHT-H, 2,6-Di-*tert*-butyl-4-methylphenol) was recrystallized from hexanes prior to use.

Tris(pentafluorophenyl)borane B(C<sub>6</sub>F<sub>5</sub>)<sub>3</sub> was obtained as a research gift from Boulder Scientific Co. and further purified by recrystallization from hexanes at -30 °C. Tris(pentafluorophenyl)alane Al(C<sub>6</sub>F<sub>5</sub>)<sub>3</sub>, as a 0.5 toluene adduct Al(C<sub>6</sub>F<sub>5</sub>)<sub>3</sub>·(C<sub>7</sub>H<sub>8</sub>)<sub>0.5</sub>, was prepared by the reaction of B(C<sub>6</sub>F<sub>5</sub>)<sub>3</sub> and AlMe<sub>3</sub> in a 1:3 toluene/hexanes solvent mixture in quantitative yield [13]; this is a modified preparation based on literature procedures [14]. Although we have experienced no incidents when handling this material, *extra caution should be exercised*, especially when dealing with the unsolvated form, because of its thermal and shock sensitivity. Lithium isopropyl isobutyrate Me<sub>2</sub>C=C(O<sup>*i*</sup>Pr)OLi was prepared according to modified literature procedures [15]; the isolated lithium ester enolate was stored in a freezer at -30 °C inside the glovebox.

## 2.2. Preparation of Cp<sub>2</sub>Zr[OC(O<sup>*i*</sup>Pr)=CMe<sub>2</sub>]<sub>2</sub> (1)

The literature procedure for the preparation of the methyl derivative, Cp<sub>2</sub>Zr[OC(OMe)=CMe<sub>2</sub>]<sub>2</sub> [4g], was modified for the preparation of precursor 1. To a stirred solution of Cp<sub>2</sub>ZrCl<sub>2</sub> (0.10 g, 0.34 mmol) in 15 mL of THF at -78 °C was added a solution of Me<sub>2</sub>C=C(O<sup>*i*</sup>Pr)OLi (0.093 g, 0.68 mmol) in 7 mL of THF at -78 °C by cannula. The resulting mixture was gradually warmed to room temperature and stirred for 6 h. The solvent was removed in vacuo, and the resulting suspension was extracted with 20 mL of hexanes inside a glovebox, followed by filtration through a pad of Celite. The yellow filtrate was dried in vacuo to give 0.11 g (67%) of the title product as a yellow oil. <sup>1</sup>H NMR (C<sub>6</sub>D<sub>6</sub>, 21 °C) for Cp<sub>2</sub>Zr[OC(O<sup>*i*</sup>Pr)=CMe<sub>2</sub>]<sub>2</sub>

(1):  $\delta$  6.12 (s, 10H,  $C_5H_5$ ), 4.27 (sept,  $J = 6.3$  Hz, 2H,  $CHMe_2$ ), 1.93 (s, 6H,  $=CMe_2$ ), 1.78 (s, 6H,  $=CMe_2$ ), 1.21 (d,  $J = 6.3$  Hz, 12H,  $CHMe_2$ ).

### 2.3. Isolation of $Cp_2Zr[OC(O^iPr)=CMe_2]^+[O=C(O^iPr)CMe_2B(C_6F_5)_3]^-$ (2)

In an argon-filled glovebox, a 20 mL glass reactor was charged with  $Cp_2Zr[OC(O^iPr)=CMe_2]_2$  (0.048 g, 0.10 mmol),  $B(C_6F_5)_3$  (0.051 g, 0.10 mmol), and 5 mL of  $CH_2Cl_2$ . The resulting orange solution was stirred for 15 min at ambient temperature, after which it was left overnight at  $-30$  °C inside the freezer of the glovebox. The orange red solution was filtrated, and the filtrate was dried in vacuo to give 0.08 g of the title complex (82%) as a red oil; this oily product was not crystallized upon treatment with various types of common crystallization solvents. Anal. Calcd. for  $C_{42}H_{36}BO_4F_{15}Zr$ : C, 50.87; H, 3.66. Found: C, 49.99; H, 3.27.

$^1H$  NMR ( $CD_2Cl_2$ , 21 °C) for  $Cp_2Zr[OC(O^iPr)=CMe_2]^+[O=C(O^iPr)CMe_2B(C_6F_5)_3]^-$  (2):  $\delta$  6.60 (s, 10H,  $C_5H_5$ ), 5.00 (sept,  $J = 6.3$  Hz, 1H,  $CHMe_2$ ), 4.12 (sept,  $J = 6.3$  Hz, 1H,  $CHMe_2$ ), 1.70 (s, 3H,  $=CMe_2$ ), 1.47 (d,  $J = 6.3$  Hz, 6H,  $OCHMe_2$ ), 1.42 (br, 6H,  $CMe_2$ ), 1.35 (s, 3H,  $=CMe_2$ ), 1.24 (d,  $J = 6.3$  Hz, 6H,  $OCHMe_2$ ).  $^{19}F$  NMR ( $CD_2Cl_2$ , 21 °C):  $\delta$   $-132.3$  (d,  $^3J_{F-F} = 18.3$  Hz, 6F, *o*-F),  $-163.0$  (t,  $^3J_{F-F} = 19.7$  Hz, 3F, *p*-F),  $-165.9$  (m, 6F, *m*-F).

### 2.4. Isolation and Structure Analysis of $Li^+[Me_2C=C(O^iPr)OAl(C_6F_5)_3]^-$ (3) and $Li^+[Me_2C=C(O^iPr)OB(C_6F_5)_3]^-$ (4)

In an argon-filled glovebox, a 30 mL glass reactor was charged with  $Me_2C=C(O^iPr)OLi$  (0.041 g, 0.30 mmol) and 10 mL of toluene. A solution of  $E(C_6F_5)_3$  (0.30 mmol) in 10 mL of toluene was carefully layered on top of the lithium ester enolate solution, and the resulting solution mixture was kept at ambient temperature inside the glove box for 1 week, affording complexes **3** or **4** (85%) as colorless crystals which are suitable for X-ray diffraction analysis. Both complexes are insoluble in common NMR solvents, precluding their NMR analysis in

solution; however, they were structurally characterized by X-ray diffraction. Anal. Calcd. for  $C_{50}H_{26}Al_2F_{30}Li_2O_4$  (**3**): C, 45.20; H, 1.97. Found: C, 45.34; H, 2.41.

The crystals were quickly covered with a layer of Paratone-N oil (Exxon, dried and degassed at 120 °C/10<sup>-6</sup> Torr for 24 h) after the mother liquors were decanted and then mounted on a thin glass fiber and transferred into the cold nitrogen stream of a Bruker SMART CCD diffractometer. The structures were solved by direct methods and refined using the Bruker SHELXTL program library by full-matrix least-squares on  $F^2$  for all reflections [16]. All non-hydrogen atoms were located by difference Fourier synthesis and refined anisotropically, whereas hydrogen atoms were included geometrically with  $U_{iso}$  tied to the  $U_{iso}$  of the parent atoms and refined isotropically. Selected crystal data and structural refinement parameters are collected in Table 1. Crystallographic data for the two structures reported in this paper have been deposited with the Cambridge Crystallographic Data Centre as supplementary numbers CCDC-639263 (**3**) and 639264 (**4**). These data can be obtained free of charge from CCDC, 12 Union Road, Cambridge CB21EZ, UK. (fax: (+44) 1223-336-033; e-mail: deposit@ccdc.cam.ac.uk).

**Table 1.** Crystal Data and Structure Refinements for **3** (A) and **4** (B) <sup>a</sup>

	<b>3</b>	<b>4</b>
formula	$C_{50}H_{26}Al_2F_{30}Li_2O_4$	$C_{50}H_{26}B_2F_{30}Li_2O_4$
formula weight	1328.55	1296.21
color, habit	colorless, plate	colorless, cube
crystal system	monoclinic	monoclinic
space group	$P2(1)/n$	$P2(1)/n$
$a/\text{Å}$	13.1937(10)	12.9476(3)
$b/\text{Å}$	13.3605(12)	13.2024(3)
$c/\text{Å}$	15.1332(14)	14.7488(4)
$\beta/\text{deg}$	95.346(3)	97.851(1)
$V/\text{Å}^3$	2656.0(4)	2497.5(1)
$Z$	2	2
$\rho_{\text{calcd}}/\text{g}\cdot\text{cm}^{-3}$	1.661	1.721
$\mu/\text{mm}^{-1}$	0.205	0.183
$F(000)$	1320	1288
crystal size/ $\text{mm}^3$	$0.48 \times 0.23 \times 0.12$	$0.27 \times 0.18 \times 0.16$
$\theta$ range/deg	1.96 - 27.48	1.96 - 32.58
index ranges	$-17 \leq h \leq 17$ $-17 \leq k \leq 17$ $-19 \leq l \leq 19$	$-19 \leq h \leq 12$ $-17 \leq k \leq 20$ $-22 \leq l \leq 22$

collected data	29575	30325
unique data	6053 ( $R_{\text{int}} = 0.0506$ )	9073 ( $R_{\text{int}} = 0.0606$ )
completeness to $\theta$	99.3%	100.0%
data/restraints/parameters	6053 / 0 / 401	9073 / 0 / 401
GOF on $F^2$	1.012	1.036
final R indices [ $I > 2\sigma(I)$ ]	$R_1 = 0.0454$ , $wR_2 = 0.1067$	$R_1 = 0.0617$ , $wR_2 = 0.1384$
R indices (all data)	$R_1 = 0.0879$ , $wR_2 = 0.1236$	$R_1 = 0.1205$ , $wR_2 = 0.1641$
largest diff. peak and hole/ $e \cdot \text{\AA}^{-3}$	0.334 / -0.246	0.521 / -0.313

<sup>a</sup> All data were collected at 100(2) K using Mo  $K\alpha$  ( $\lambda = 0.71073 \text{ \AA}$ ) radiation;  $R_1 = \sum(|F_o| - |F_c|) / \sum|F_o|$ ,  $wR_2 = \{\sum[w(F_o^2 - F_c^2)^2 / \sum[w(F_o^2)^2]]\}^{1/2}$ ; GOF =  $\{\sum[w(F_o^2 - F_c^2)^2] / (N_o - N_p)\}^{1/2}$ .

#### 2.4. General Polymerization Procedures and Polymer Characterizations

Polymerizations were performed either in 25-mL flame-dried Schlenk flasks interfaced to the dual-manifold Schlenk line for runs using external temperature bath, or in 20-mL glass reactors inside the glovebox for ambient temperature ( $\sim 25 \text{ }^\circ\text{C}$ ) runs. In a typical procedure, a predetermined amount of  $\text{E}(\text{C}_6\text{F}_5)_3$  was first dissolved in MMA (9.35 mmol) inside a glovebox, and the polymerization was started by rapid addition of the  $\text{E}(\text{C}_6\text{F}_5)_3$ -MMA solution via gastight syringe to a solution of **1** in 10 mL of  $\text{CH}_2\text{Cl}_2$  under vigorous stirring at the pre-equilibrated bath temperature. (The amount of MMA was fixed for all polymerizations, whereas the amounts of  $\text{E}(\text{C}_6\text{F}_5)_3$  and **1** were adjusted according to the ratios specified in the polymerization tables.) For block copolymerizations, a second quantity of a different monomer was added after the completion of the first block (with the required time indicated in the polymerization table), and the polymerization was continued. After the measured time interval, a 0.2 mL aliquot was taken from the reaction mixture via syringe and quickly quenched into a 4 mL vial containing 0.6 mL of undried “wet”  $\text{CDCl}_3$  stabilized by 250 ppm of BHT-H; the quenched aliquots were later analyzed by  $^1\text{H}$  NMR to obtain monomer conversion data. The polymerization was immediately quenched after the removal of the aliquot by the addition of 5 mL 5% HCl-acidified methanol. For MMA and other methacrylate polymerizations, the quenched mixture was precipitated into 100 mL of methanol, stirred for 1 h, filtered, washed with methanol, and dried in a vacuum oven at  $50 \text{ }^\circ\text{C}$  overnight to a constant weight. For DMAA polymerization, the quenched mixture was precipitated into 100 mL of diethyl ether, stirred for 30 min, and the solvent was decanted off. An

additional 75 mL of diethyl ether was used to wash the polymer and then decanted; the P(DMAA) product was dried in a vacuum oven at 50 °C to a constant weight.

Glass transition temperatures ( $T_g$ ) of the polymers were measured by differential scanning calorimetry (DSC) on a DSC 2920, TA Instrument. Samples were first heated to 180 °C at 20 °C/min, equilibrated at this temperature for 4 min, then cooled to -60 °C at 10 °C/min, held at this temperature for 4 min, and reheated to 180°C at 10 °C/min. All  $T_g$  values were obtained from the second scan, after removing the thermal history. Gel permeation chromatography (GPC) analyses of the polymers were carried out at 40 °C and a flow rate of 1.0 mL/min, with  $\text{CHCl}_3$  as the eluent, on a Waters University 1500 GPC instrument equipped with four 5  $\mu\text{m}$  PL gel columns (Polymer Laboratories) and calibrated using 10 P(MMA) standards. Chromatograms were processed with Waters Empower software (2002); number average molecular weight ( $M_n$ ) and MWD ( $M_w/M_n$ ) of polymers are given relative to P(MMA) standards.  $^1\text{H}$  NMR (300 MHz) spectra of the poly(methacrylate)s and block copolymers were recorded in  $\text{CDCl}_3$  at room temperature and analyzed according to literature procedures [2,7c,17], whereas  $^{13}\text{C}$  NMR (125 MHz) spectra of P(DMAA) were recorded in  $\text{D}_2\text{O}$  at 80 °C and analyzed using literature procedures [5a,18].

## Results and Discussion

### 3.1. MMA Polymerization by $\text{Cp}_2\text{Zr}[\text{OC}(\text{O}^i\text{Pr})=\text{CMe}_2]_2$ (**1**)/ $\text{E}(\text{C}_6\text{F}_5)_3$ ( $\text{E} = \text{Al}, \text{B}$ )

Control runs using either **1** or  $\text{E}(\text{C}_6\text{F}_5)_3$  separately showed no activity for MMA polymerization under the conditions employed in the current study. However, the combination of **1** with 2 equiv of  $\text{Al}(\text{C}_6\text{F}_5)_3$  is highly active for MMA polymerization, achieving a quantitative monomer conversion within just 1 min for the reaction in a  $[\text{MMA}]_0/[\mathbf{1}]_0$  ratio of 200 (run 1, Table 2). When using  $\text{CH}_2\text{Cl}_2$  as solvent, it is critical that one follow the polymerization procedures previously established for the *rac*-(EBI)Zr[OC(O<sup>*i*</sup>Pr)=CMe<sub>2</sub>]<sub>2</sub>/2Al(C<sub>6</sub>F<sub>5</sub>)<sub>3</sub> system in

which  $\text{Al}(\text{C}_6\text{F}_5)_3$  is first mixed (dissolved) in large excess MMA (the amount of which depends on the initial  $[\text{MMA}]_0/[\mathbf{1}]_0$  ratio employed), followed by addition to a  $\text{CH}_2\text{Cl}_2$  solution of the zirconocene bis(ester enolate) to start the polymerization [3]. The P(MMA) produced has a syndiotacticity of  $[rr] = 73\%$ , a  $M_n$  of  $1.50 \times 10^4$ , and a  $M_w/M_n$  of 1.24. As compared to the  $M_n(\text{calcd})$  of  $1.00 \times 10^4$  based on  $2[\text{MMA}]_0/[\mathbf{1}]_0 = 200$ , the measured  $M_n$  gave an initiator efficiency  $[I^* = M_n(\text{calcd})/M_n(\text{exptl})]$ , where  $M_n(\text{calcd}) = \text{MW}(\text{MMA}) \times [\text{MMA}]_0/[\mathbf{1}]_0 \times \text{conversion}\%$  of 67%. This calculation assumed the current system follows the same polymerization mechanism as the *rac*-(EBI)Zr[OC(O<sup>i</sup>Pr)=CMe<sub>2</sub>]<sub>2</sub>/2Al(C<sub>6</sub>F<sub>5</sub>)<sub>3</sub> system in which approximately two polymer chains are produced per Zr center (i.e., both ester enolate groups initiate the polymerization) [3].

**Table 2.** Selected MMA Polymerization Results by  $1/\text{xE}(\text{C}_6\text{F}_5)_3$  <sup>a</sup>

run no.	[Zr] (mM)	$[\text{MMA}]_0/[\text{Zr}]_0$	cocat. (xE)	time (min)	conv. <sup>b</sup> (%)	$M_n^c$ (kg/mol)	MWD <sup>c</sup> ( $M_w/M_n$ )	$[mm]^d$ (%)	$[mr]^d$ (%)	$[rr]^d$ (%)
1	4.68	200	2Al	1	100	15.0	1.24	2.1	24.9	73.0
2	2.34	400	2Al	1.5	100	28.8	1.23	2.7	25.2	72.1
3	1.17	800	2Al	150	100	50.4	1.14	2.0	24.3	73.7
4	1.17	800	Al	240	100	52.2	1.14	1.9	24.5	73.6
5	0.78	1200	2Al	690	100	96.6	1.12	1.9	24.7	73.3
6	1.17	800	B	240	9.5	99.1	1.55	4.0	28.0	68.0
7	1.17	800	2B	240	6.4	93.1	1.49	5.1	29.8	65.1

<sup>a</sup> Carried out in a glovebox in 10 mL  $\text{CH}_2\text{Cl}_2$  at ambient temperature, except for runs 1 and 2 which were performed on a Schlenk line with an external bath set at 25 °C due large exotherm. <sup>b</sup> Monomer conversions measured by <sup>1</sup>H NMR. <sup>c</sup>  $M_n$  and MWD determined by GPC relative to P(MMA) standards in  $\text{CHCl}_3$ . <sup>d</sup> Tacticity (methyl triad distribution) determined by <sup>1</sup>H NMR.

Reducing the amount of [Zr] and [Al] employed by one half while maintaining the [MMA] constant (i.e.,  $[\text{MMA}]_0/[\mathbf{1}]_0 = 400$ ) still afforded highly active polymerization, achieving a quantitative monomer conversion in 1.5 min (run 2, Table 2). Further increasing the  $[\text{MMA}]_0/[\mathbf{1}]_0$  ratio required much longer reaction times to achieve the quantitative monomer conversion and, more importantly, effected a nearly linear increase of the resulting polymer  $M_n$ , coupled with narrow MWD (Fig. 1). The [Al] concentration also affects polymerization activity (run 3 vs. 4) but *not* the resulting polymer characteristics. All the polymers produced (runs 1–5) have nearly identical syndiotacticity of  $[rr] = 73\%$ , whereas MWD becomes narrower as the polymer  $M_n$  gets

higher; however, all of them are unimodal, as shown by Fig. 2 which depicts a representative GPC trace of the P(MMA) with  $M_n = 9.66 \times 10^4$  and  $M_w/M_n = 1.12$  (run 5). Collectively, the evidence discussed above demonstrated the controlled/living characteristics of the polymerization by the  $1/2\text{Al}(\text{C}_6\text{F}_5)_3$  system.

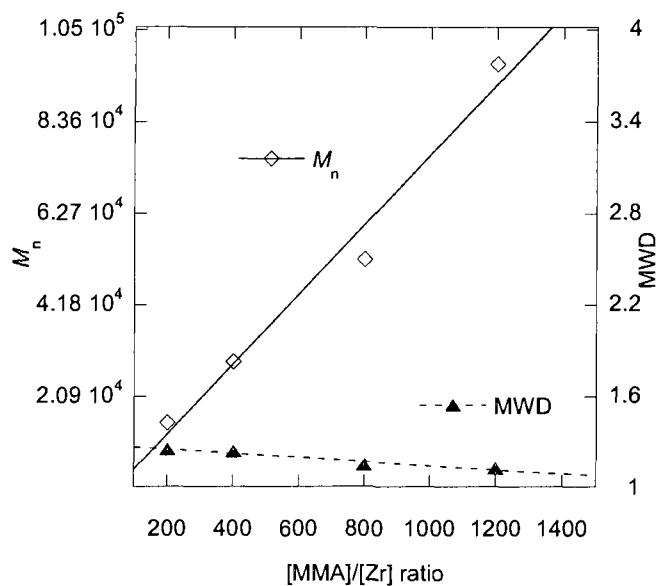


**Fig.1.** Plots of  $M_n$  and MWD of P(MMA) by  $1/2\text{Al}(\text{C}_6\text{F}_5)_3$  vs. the  $[\text{MMA}]_0/[\text{I}]_0$  ratio.

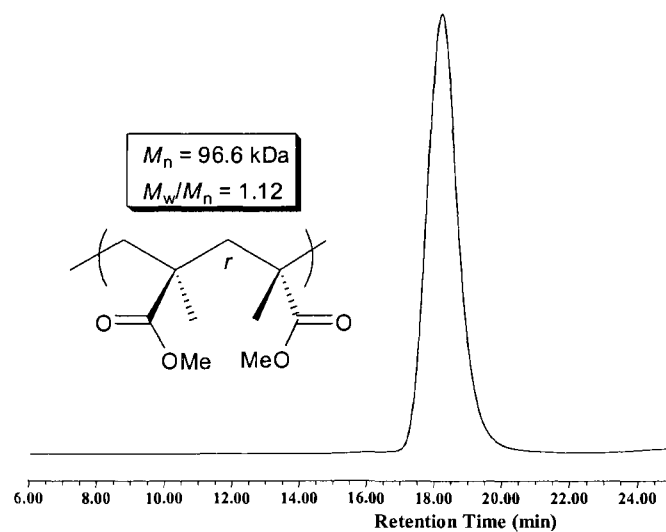


**Fig.2.** Representative GPC trace of P(MMA) by  $1/2\text{Al}(\text{C}_6\text{F}_5)_3$  (this example is for run 5, Table 2).

Switching the alane Lewis acid to analogous  $B(C_6F_5)_3$  brought about a drastic change in the MMA polymerization behavior. Thus, the  $1/xB(C_6F_5)_3$  system, regardless of the borane amount ( $x = 1$ , run 6 vs.  $x = 2$ , run 7) and the reagent mixing sequence (premixing **1** and the borane followed by addition of MMA vs. premixing the borane and MMA followed by addition to **1**), exhibits low to negligible activity as compared to the  $1/xAl(C_6F_5)_3$  system. The polymerization achieved only  $< 10\%$  monomer conversions in 4 h and gave high  $M_n$  P(MMA), resulting in low  $I^*$  of  $< 8\%$  even with a consideration of the production of one polymer chain per Zr center; the polymers have considerably broader MWD and somewhat lower syndiotacticity than those produced by the  $1/xAl(C_6F_5)_3$  system. The sharp contrast observed for different Lewis acids  $E(C_6F_5)_3$  is attributed to their differences in the activation of the zirconocene bis(ester enolate) and polymerization mechanism (vide infra).

### 3.2. *Methacrylate and Acrylamide Polymerizations and Copolymerizations by $1/2Al(C_6F_5)_3$*

As the  $1/2Al(C_6F_5)_3$  system shows high activity and also living characteristics in the MMA polymerization, we further employed this superior system for polymerization of other methacrylates (BMA, *n*-butyl methacrylate; EHM, 2-ethylhexyl methacrylate) and an acrylamide (DMAA, *N,N*-dimethyl acrylamide), as well as block copolymerization of MMA with BMA and EHM. The purposes of this study are to further explore the utilities of this polymerization system in the production of unique block copolymers and confirm the livingness of the  $1/2Al(C_6F_5)_3$  system. Table 3 summarizes the results of this study.

**Table 3.** (Co)Polymerization of Methacrylate and Acrylamide Monomers by  $1/2\text{Al}(\text{C}_6\text{F}_5)_3$ <sup>a</sup>

run no.	$10^2[\text{M}]_0/[\text{Zr}]_0$ monomer	time (min)	$M_n$ (kg/mol)	MWD ( $M_w/M_n$ )	$[mm]$ (%) <sup>b</sup>	$[mr]$ (%) <sup>b</sup>	$[rr]$ (%) <sup>b</sup>
1	4BMA	10	36.8	1.19	3.1	11.8	85.1
2	4MMA/4BMA	1.5/18.5	59.9	1.37	3.0	12.6	84.4
3	4DMAA	3	36.3	1.16	11.2	26.5	62.3
4	4EHM	60	36.3	1.12	0	11.2	88.8
5	4MMA/4EHM	1.5/18.5	50.0	1.15	0	22.1	77.9
6	4MMA/4EHM/4MMA	1.5/18.5/25	74.0	1.19	0	20.2	79.8

<sup>a</sup> Carried out in 10 mL  $\text{CH}_2\text{Cl}_2$  at ambient temperature in water bath set at 25 °C;  $[\text{Zr}]_0 = 2.34$  mM; 100% monomer conversion (by NMR) was achieved for all runs at the indicated reaction time; runs 2, 5, and 6 were sequential diblock, diblock, and triblock copolymerizations, respectively; <sup>b</sup> Triad distributions in the methyl region for poly(methacrylate)s and in the C=O region for P(DMAA) were determined by <sup>1</sup>H NMR (300 MHz) in  $\text{CDCl}_3$  at RT and <sup>13</sup>C NMR (125 MHz) in  $\text{D}_2\text{O}$  at 80 °C, respectively.

As can be seen from the Table, polymerization of BMA proceeds rapidly, achieving a quantitative monomer conversion in 10 min for the reaction using a  $[\text{BMA}]_0/[\text{I}]_0$  ratio of 400 (run 1, Table 3). The P(BMA) produced has a syndiotacticity of  $[rr] = 85\%$ , a  $M_n$  of  $3.68 \times 10^4$ , and a MWD of  $M_w/M_n = 1.19$ ; the calculated  $I^*$  is 77% for the production of two polymer chains per Zr center. Sequential copolymerization of MMA and BMA starting from polymerization of MMA afforded diblock copolymer P(MMA)-*b*-P(BMA), with the final  $M_n$  nearing the sum of two homopolymers (run 2, Table 3). The  $1/2\text{Al}(\text{C}_6\text{F}_5)_3$  system is also highly active for DMAA polymerization, converting all 400 equiv of DMAA to the well-defined P(DMAA) ( $M_w/M_n = 1.16$ ) in 3 min (run 3, Table 3). The  $T_g$  of P(DMAA) is 122 °C, consistent with its syndio-rich atactic stereomicrostructure [18a].

Long-chain alkyl methacrylate EHM was also effectively polymerized by  $1/2\text{Al}(\text{C}_6\text{F}_5)_3$  to the unimodal, syndiotactic P(EHM) with  $M_w/M_n = 1.12$  and  $[rr] = 89\%$  (run 4, Table 3). Sequential copolymerizations of MMA and EHM afforded well-defined diblock copolymer P(MMA)-*b*-P(EHM) (run 5) and triblock copolymer P(MMA)-*b*-P(EHM)-*b*-P(MMA) (run 6). The block copolymers produced are unimodal and exhibit narrow MWD with the final  $M_n$  increased approximately according to the sum of the block components (Fig. 3). The diblock copolymer exhibits two distinct  $T_g$ 's characteristic of each of the component segments [i.e.,  $T_g(1)$

= 133 °C for the syndiotactic P(MMA) block and  $T_g(2) = -4$  °C for the syndiotactic P(EHM) block].

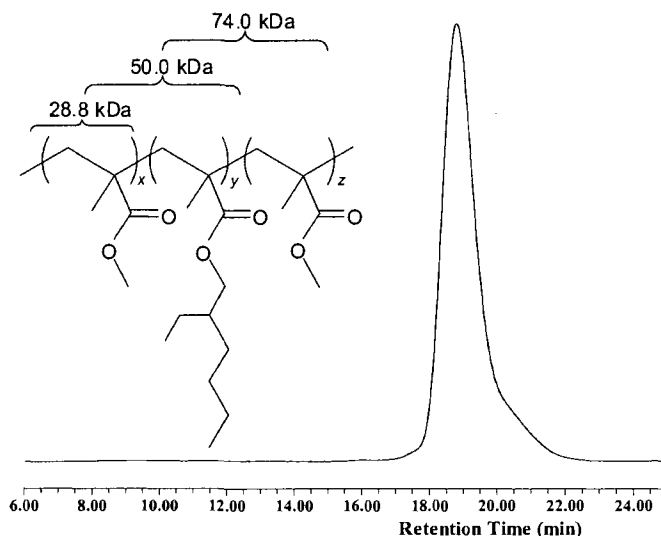


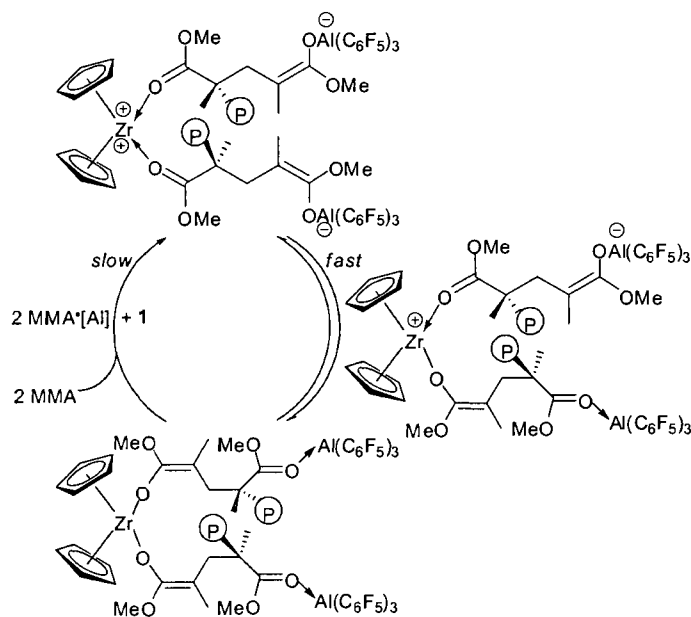
**Fig.3.** GPC trace of triblock copolymer P(MMA)-*b*-P(EHM)-*b*-P(MMA) produced by the  $1/2\text{Al}(\text{C}_6\text{F}_5)_3$  system ( $M_n = 7.40 \times 10^4$ ,  $M_w/M_n = 1.19$  for run 6 in Table 3).

### 3.3. Activation of Zirconocene Bis(ester enolate) **1** by $E(\text{C}_6\text{F}_5)_3$

We have previously examined in detail all the possible elementary reactions involved in the MMA polymerization by *rac*-(EBI)Zr[OC(O<sup>*i*</sup>Pr)=CMe<sub>2</sub>]<sub>2</sub>/2Al(C<sub>6</sub>F<sub>5</sub>)<sub>3</sub> [3]. Direct contact of the zirconocene bis(enolate) with Al(C<sub>6</sub>F<sub>5</sub>)<sub>3</sub> leads to a mixture of products due to decomposition. However, in the polymerization procedure we employed (*vide supra*) at no time does the free Al(C<sub>6</sub>F<sub>5</sub>)<sub>3</sub> exist because it is always in the form of an adduct with either MMA or the ester group of the polymer chain. Thus, the relevant reaction to consider is the reaction of the zirconocene bis(enolate) with the adduct Al(C<sub>6</sub>F<sub>5</sub>)<sub>3</sub>·MMA. In short, that comprehensive study concluded that the polymerization by *rac*-(EBI)Zr[OC(O<sup>*i*</sup>Pr)=CMe<sub>2</sub>]<sub>2</sub>/2Al(C<sub>6</sub>F<sub>5</sub>)<sub>3</sub> produces P(MMA) with isotactic-*b*-syndiotactic stereo-multiblock microstructures, proceeding through a unique diastereospecific ion-pairing polymerization mechanism which consists of four manifolds—an isospecific cycle by the chiral zirconocene cation, a syndiospecific cycle by the enolaluminate anion, anion-monomer exchange, and then chain transfer, the latter two serving to interconvert

diastereospecific propagating manifolds [3]. It is assumed that the current, analogous  $\text{Cp}_2\text{Zr}[\text{OC}(\text{O}^i\text{Pr})=\text{CMe}_2]_2/2\text{Al}(\text{C}_6\text{F}_5)_3$  system follows the same activation and MMA polymerization pathways as the *rac*-(EBI)Zr[OC(O<sup>i</sup>Pr)=CMe<sub>2</sub>]<sub>2</sub>/2Al(C<sub>6</sub>F<sub>5</sub>)<sub>3</sub> system, involving ion-pairing active propagating species consisting of  $\text{Cp}_2\text{Zr}[\text{OC}(\text{OMe})=\text{C}(\text{Me})\text{P}]^+$  and  $[\text{P}(\text{Me})\text{C}=\text{C}(\text{OMe})\text{OAl}(\text{C}_6\text{F}_5)_3]^-$  (Scheme 1, where P denotes a growing polymer chain and only the bimetallic propagation manifold is shown). Because the current system employs the achiral C<sub>2v</sub>-symmetric zirconocene ester enolate, both cationic zirconocene ester enolate and anionic enolaluminate sites are syndiospecific by a chain-end control mechanism in the ion-pairing polymerization of MMA, thereby producing P(MMA) with predominately syndiotactic microstructures.

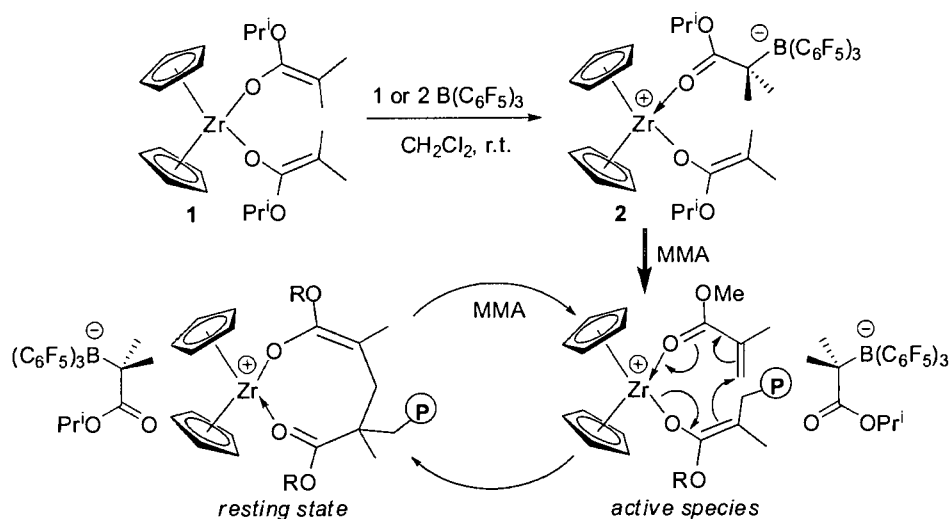
**Scheme 1.**



The substantial A1 vs. B differences observed in the MMA polymerization by the  $1/x\text{E}(\text{C}_6\text{F}_5)_3$  system were also seen for the chiral *rac*-(EBI)Zr[OC(O<sup>i</sup>Pr)=CMe<sub>2</sub>]<sub>2</sub>/x $\text{E}(\text{C}_6\text{F}_5)_3$  system [3]. As in the latter chiral system, the reaction of achiral **1** with 1 equiv of B(C<sub>6</sub>F<sub>5</sub>)<sub>3</sub> forms cationic zirconocene ester enolate- $\alpha$ -ester borate ion pair

$\text{Cp}_2\text{Zr}[\text{OC}(\text{O}^i\text{Pr})=\text{CMe}_2]^+[\text{O}=\text{C}(\text{O}^i\text{Pr})\text{CMe}_2\text{B}(\text{C}_6\text{F}_5)_3]^-$  (**2**, Scheme 2), derived from apparent electrophilic addition of the borane to the nucleophilic ester enolate  $\alpha$ -carbon, reminiscent of the reaction of  $\text{B}(\text{C}_6\text{F}_5)_3$  with the sterically unprotected bis(2-propenolato)zirconocene reported by Erker et al. [1]. The  $^{19}\text{F}$  NMR ( $\text{CD}_2\text{Cl}_2$ ) chemical shifts of  $-132.3$  (d,  $^3J_{\text{F-F}} = 18.3$  Hz, 6F, *o*-F),  $-163.0$  (t,  $^3J_{\text{F-F}} = 19.7$  Hz, 3F, *p*-F),  $-165.9$  (m, 6F, *m*-F) for the  $\alpha$ -ester borate anion in **2** are identical to those observed for the same anion but paired with the chiral cation *rac*-(EBI)Zr[OC(O<sup>*i*</sup>Pr)=CMe<sub>2</sub>]<sup>+</sup>. Consistent with the transformation of one ester enolate ligand in **1** to the ester group in **2** upon treatment with  $\text{B}(\text{C}_6\text{F}_5)_3$ , the  $^1\text{H}$  NMR signal for the methine proton in  $-\text{CHMe}_2$  (sept, 4.27 ppm) attached to the *enolate ligand* in **1** is substantially downfield shifted to 5.00 ppm (sept) for  $-\text{CHMe}_2$  now attached to the *ester group* in **2** [5b], whereas the  $^1\text{H}$  NMR signal for  $-\text{CHMe}_2$  in the other enolate ligand experienced only a minor shift to 4.12 ppm accounting for the neutral to cationic structural change. The reaction with 2 equiv of  $\text{B}(\text{C}_6\text{F}_5)_3$  affords the same product with no indication for the formation of the possible bis-adduct. Hence, the species derived from the borane activation is active only at the cationic site, while the ester borate anion is inactive for the MMA polymerization.

Scheme 2.



The observed little activity for the cation portion of **2** is consistent with prior findings that the cationic zirconocene species incorporating non-bridged bis-Cp ligands exhibit low activity in a monometallic polymerization system [4]. Polymerizations by *in situ* mixing of MMA with 1 or 2 equiv of B(C<sub>6</sub>F<sub>5</sub>)<sub>3</sub> followed by addition of complex **1** (i.e., activated monomer approach), or by *in situ* mixing of complex **1** with B(C<sub>6</sub>F<sub>5</sub>)<sub>3</sub> followed by addition of MMA (i.e., activated complex approach), afforded similar polymerization results. Overall, the Lewis acid in the **1**/B(C<sub>6</sub>F<sub>5</sub>)<sub>3</sub> system functions only as a cation-forming agent, and neither the resulting anion nor the neutral borane participates in the polymer chain formation steps (Scheme 2) as do Al(C<sub>6</sub>F<sub>5</sub>)<sub>3</sub> and its derived anions in the **1**/Al(C<sub>6</sub>F<sub>5</sub>)<sub>3</sub> system (Scheme 1).

### 3.4. Structures of Lithium Ester Enolate and E(C<sub>6</sub>F<sub>5</sub>)<sub>3</sub> Adducts

As we showed earlier, addition of 1 or 2 equiv of B(C<sub>6</sub>F<sub>5</sub>)<sub>3</sub> to the lithium ester enolate *completely halted* MMA polymerization [9], whereas the combination of the lithium ester enolate with 2 equiv of Al(C<sub>6</sub>F<sub>5</sub>)<sub>3</sub> promotes *highly active* MMA polymerization and, more importantly, produces P(MMA) with controlled MW and narrow MWD [9,10]. To seek for a solution to this puzzle, we investigated the reactions of the lithium ester enolate Me<sub>2</sub>C=C(O<sup>*i*</sup>Pr)OLi with E(C<sub>6</sub>F<sub>5</sub>)<sub>3</sub> and structurally characterized the resulting lithium enolaluminate Li<sup>+</sup>[Me<sub>2</sub>C=C(O<sup>*i*</sup>Pr)OAl(C<sub>6</sub>F<sub>5</sub>)<sub>3</sub>]<sup>-</sup> (**3**) and enolborate Li<sup>+</sup>[Me<sub>2</sub>C=C(O<sup>*i*</sup>Pr)OB(C<sub>6</sub>F<sub>5</sub>)<sub>3</sub>]<sup>-</sup> (**4**).

The molecular structure of **3** was determined by X-ray diffraction (Fig. 4), featuring a centrosymmetric dimeric structure in the solid state. The two unique lithium enolaluminate Li<sup>+</sup>[Me<sub>2</sub>C=C(O<sup>*i*</sup>Pr)OAl(C<sub>6</sub>F<sub>5</sub>)<sub>3</sub>]<sup>-</sup> molecules in the dimer are connected by two ionic Li–O<sub>alkoxy</sub> bonds, presenting a Li<sub>2</sub>O<sub>4</sub>C<sub>2</sub> crown-type eight-membered-ring core linkage where the Li–O<sub>alkoxy</sub> bond is only slightly shorter than the Li–O<sub>enolate</sub> bond and the C–O<sub>alkoxy</sub> bond is slightly longer than the C–O<sub>enolate</sub> bond, both by ~0.03 Å. The Al(C<sub>6</sub>F<sub>5</sub>)<sub>3</sub> moiety is directly bonded to the enolate oxygen, and the Al center adopts a distorted tetrahedral geometry with a sum of the C–Al–C angles of 336.8°. The Al–O distance [1.784(2) Å] in **3** is noticeably shorter than that [1.820(3) Å]

in the only other structurally characterized lithium enolaluminate  $\text{Li}^+[\text{Me}_2\text{C}=\text{C}(\text{O}^i\text{Pr})\text{OAlMe}(\text{BHT})_2]^-$  [10], coupled with the smaller Al–O–C vector angle, indicative of a stronger Al–O  $\sigma$  bond in **3**. The coordination sphere of  $\text{Li}^+$  is completed by one enolate O, one centrosymmetrically operated alkoxy O, and two *ortho*-F atoms from two different  $\text{C}_6\text{F}_5$  rings. The C(1)–O(1) [1.367(3) Å], C(1)–O(2) [1.393(3) Å], and C(1)–C(2) [1.322(3) Å] bond lengths evidence a structural feature of the enolate  $\text{Me}_2\text{C}=\text{C}(\text{O}^i\text{Pr})\text{O}$  moiety where  $\pi$  electron conjugation over these bonds is implied. The enolate and isopropoxy oxygens adopt nearly planar and planar geometries, with the sums of the angles around O(1) and O(2) being  $358.9^\circ$  and  $360.0^\circ$ , respectively. Owing to ionic Li–F interactions with separations of 1.942(4) and 1.992(4) Å, the two Al–C(pentafluoroaryl) bond distances [2.005(2) and 2.003(3) Å] appear slightly (by  $\sim 0.02$  Å) longer than the third one without such interactions [1.988(2) Å].

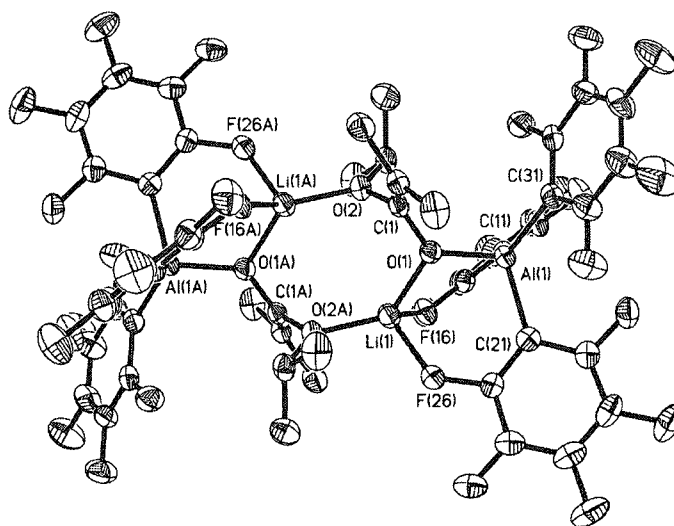


**Fig.4.** X-ray crystal structure of **3** with thermal ellipsoids drawn at the 50% probability. Selected bond lengths [Å] and angles [°]: Al(1)–O(1) 1.784(2), Al(1)–C(11) 2.005(2), Al(1)–C(21) 2.003(2), Al(1)–C(31) 1.988(2), Li(1)–O(1) 1.900(4), Li(1)–O(2A) 1.875(4), Li(1)–F(16) 1.992(4), Li(1)–F(26) 1.942(4); C(11)–Al(1)–C(21) 105.0(1), C(11)–Al(1)–C(31) 117.8(1), C(21)–Al(1)–C(31) 114.0(1), Al(1)–O(1)–C(1) 130.4(1), Al(1)–O(1)–Li(1) 111.8(1), C(1)–O(1)–Li(1) 116.6(2).

The overall structure of lithium enolborate **4** shown in Fig. 5 is remarkably similar to that of lithium enolaluminate **3**. While stronger ionic Li–F interactions are observed in **4**, as evidenced by noticeably shorter Li–F separations in **4** than those observed in **3** (by  $\sim 0.05$  Å), other metric differences can be accounted by the differences in Al/B covalent radii. The overlay plot of the unique molecules of **3** and **4** depicted in Fig. 6 further shows the striking similarities between these two structures.

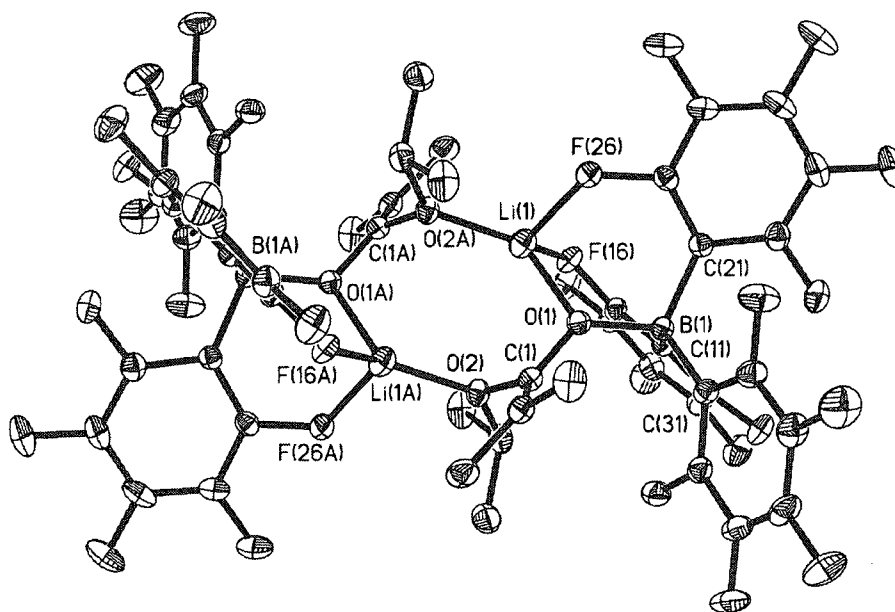


**Fig.5.** X-ray crystal structure of **4** with thermal ellipsoids drawn at the 50% probability. Selected bond lengths [Å] and angles [°]: B(1)–O(1) 1.541(3), B(1)–C(11) 1.666(3), B(1)–C(21) 1.650(3), B(1)–C(31) 1.640(3), Li(1)–O(1) 1.880(4), Li(1)–O(2A) 1.886(4), Li(1)–F(16) 1.941(4), Li(1)–F(26) 1.904(4); C(11)–B(1)–C(21) 104.3(2), C(11)–B(1)–C(31) 115.8(2), C(21)–B(1)–C(31) 112.0(2), B(1)–O(1)–C(1) 128.3(2), B(1)–O(1)–Li(1) 118.4(2), C(1)–O(1)–Li(1) 109.2(2).

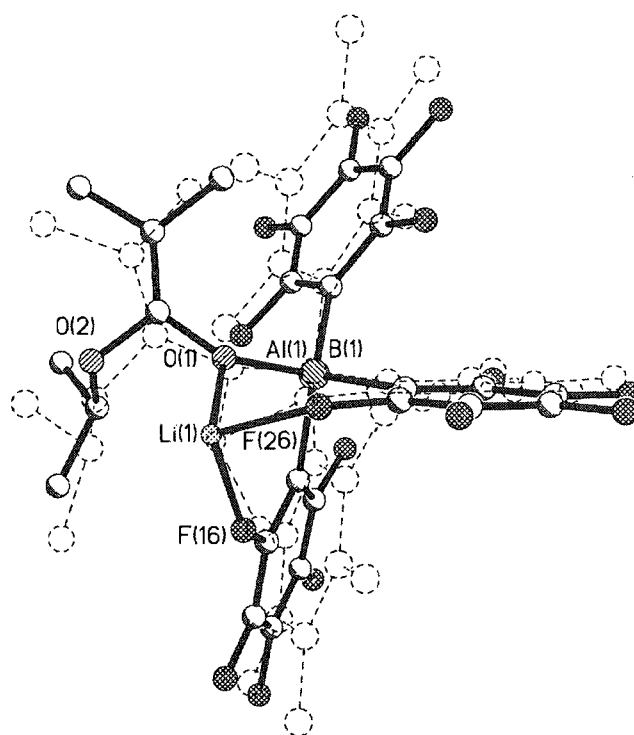
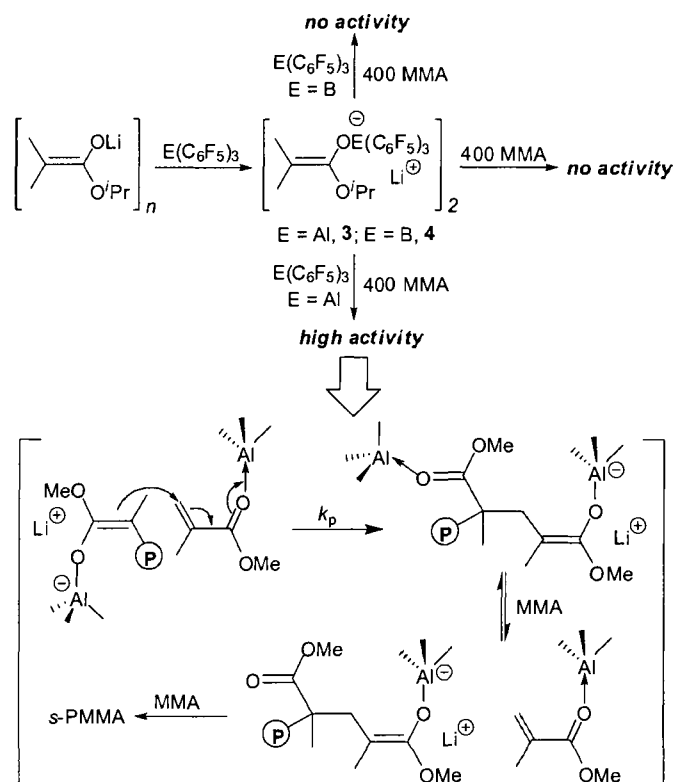


**Fig.6.** Overlay plot of the unique molecules of **3** (solid lines) and **4** (dash lines).

Subsequently, we examined the polymerization activity of the isolated lithium enolaluminate **3** and enolborate **4** under identical conditions and found that neither of them showed any activity for MMA polymerization. A striking difference arises when a second equiv of  $E(C_6F_5)_3$  is added: while the  $3/Al(C_6F_5)_3$  combination [which can also be conveniently generated by in situ mixing of  $Me_2C=C(O^iPr)OLi$  with 2 equiv of  $Al(C_6F_5)_3$ ] is *highly active* for MMA polymerization, the  $4/B(C_6F_5)_3$  system [or  $Me_2C=C(O^iPr)OLi/2B(C_6F_5)_3$ ] is *inactive* (Scheme 3). Collectively, the above structural analysis and polymerization study clearly indicate that the remarkable differences observed for Al vs. B are due to the inability of the lithium enolborate/borane pair to effect the bimolecular, activated-monomer anionic polymerization as does the lithium enolaluminate/alane pair (Scheme 3) [9,10].

**Scheme 3.**



## Conclusions

We presented here two extreme cases of Lewis acid effects on the polymerization of methacrylate and acrylamide monomers by the combination of  $E(\text{C}_6\text{F}_5)_3$  with metallocene and lithium ester enolates,  $\text{Cp}_2\text{Zr}[\text{OC}(\text{O}^i\text{Pr})=\text{CMe}_2]_2$  (**1**) and  $\text{Me}_2\text{C}=\text{C}(\text{O}^i\text{Pr})\text{OLi}$ . In sharp contrast to the low to negligible polymerization activity and ill-behaved polymerization observed for the  $1/x\text{B}(\text{C}_6\text{F}_5)_3$  ( $x = 1, 2$ ) system, the  $1/x\text{Al}(\text{C}_6\text{F}_5)_3$  system is not only highly active but also living in the polymerization of MMA, thereby enabling the synthesis of the well-defined diblock and triblock copolymers including  $\text{P}(\text{MMA})\text{-}b\text{-P}(\text{BMA})$ ,  $\text{P}(\text{MMA})\text{-}b\text{-P}(\text{EHM})$ , and  $\text{P}(\text{MMA})\text{-}b\text{-P}(\text{EHM})\text{-}b\text{-P}(\text{MMA})$ . The striking Al vs. B differences observed for the  $1/2E(\text{C}_6\text{F}_5)_3$  systems are attributed to the facile ion-pairing polymerization via active propagating species consisting of  $\text{Cp}_2\text{Zr}[\text{OC}(\text{OMe})=\text{C}(\text{Me})\text{P}]^+$  and  $[\text{P}(\text{Me})\text{C}=\text{C}(\text{OMe})\text{OAl}(\text{C}_6\text{F}_5)_3]^-$  enabled by  $1/2\text{Al}(\text{C}_6\text{F}_5)_3$  and

the formation of the ineffective cationic zirconocene ester enolate- $\alpha$ -ester borate ion pair  $\text{Cp}_2\text{Zr}[\text{OC}(\text{O}^i\text{Pr})=\text{CMe}_2]^+[\text{O}=\text{C}(\text{O}^i\text{Pr})\text{CMe}_2\text{B}(\text{C}_6\text{F}_5)_3]^-$  (**2**) derived from  $\mathbf{1}/x\text{B}(\text{C}_6\text{F}_5)_3$ .

An additional example of such a profound Al vs. B effect in the polymerization of MMA has also been observed for the combination of the lithium ester enolate initiator with Lewis acids  $\text{E}(\text{C}_6\text{F}_5)_3$ . Again,  $\text{Al}(\text{C}_6\text{F}_5)_3$  in the  $\text{Me}_2\text{C}=\text{C}(\text{O}^i\text{Pr})\text{OLi}/2\text{Al}(\text{C}_6\text{F}_5)_3$  system promotes highly active MMA polymerization, whereas the seemingly analogous  $\text{Me}_2\text{C}=\text{C}(\text{O}^i\text{Pr})\text{OLi}/2\text{B}(\text{C}_6\text{F}_5)_3$  system is inactive. We structurally characterized the resulting adducts, lithium enolaluminate  $\text{Li}^+[\text{Me}_2\text{C}=\text{C}(\text{O}^i\text{Pr})\text{OAl}(\text{C}_6\text{F}_5)_3]^-$  (**3**) and enolborate  $\text{Li}^+[\text{Me}_2\text{C}=\text{C}(\text{O}^i\text{Pr})\text{OB}(\text{C}_6\text{F}_5)_3]^-$  (**4**), and found that they have remarkably similar solid state structures. Overall, the combined structural analyses and the polymerization studies indicate that the extreme differences observed for Al vs. B are due to the inability of the lithium enolborate/borane pair to effect the bimolecular, activated-monomer anionic polymerization as does the lithium enolaluminate/alane pair.

## Acknowledgements

Funding for this work was provided by the National Science Foundation. We thank Hongping Zhu for the development of the crystal of  $^+[\text{Me}_2\text{C}=\text{C}(\text{O}^i\text{Pr})\text{OAl}(\text{C}_6\text{F}_5)_3]^-$  (**3**), Susie Miller for the X-ray diffraction data collections and Boulder Scientific Co. for the gift of  $\text{B}(\text{C}_6\text{F}_5)_3$ .

## References

- 
- [1] W.Spaether, K.Klaß, G. Erker, F.Zippel, R.Fröhlich, *Chem. Eur. J.* 4 (1998), 1411–1417.
- [2] A.D. Bolig, E.Y.-X. Chen, *J. Am. Chem. Soc.* 126 (2004) 4897–4906.
- [3] Y.Ning, E.Y.-X. Chen, *Macromolecules* 39 (2006) 7204–7215.
- [4] (a) B. Lian, C.W. Lehmann, C. Navarro, J.-F. Carpentier, *Organometallics* 24 (2005), 2466–2472. (b) G. Stojcevic, H. Kim, N.J. Taylor, T.B. Marder, S. Collins, S. *Angew. Chem. Int. Ed.* 43 (2004) 5523–5526. (c) M. Ferez, F. Bandermann, R. Sustmann, W. Sicking, *Macromol. Chem. Phys.* 205 (2004) 1196–1205. (d) B. Lian, L. Toupet, J.-F. Carpentier, *Chem. Eur. J.* 10 (2004), 4301–4307. (e) A.D. Bolig, E.Y.-X. Chen, *J. Am. Chem. Soc.* 124 (2002) 5612–5613. (f) F. Bandermann, M. Ferez, R. Sustmann, W. Sicking, *Macromol. Symp.* 174 (2001) 247–253. (g) Y. Li, D.G. Ward, S.S. Reddy, S. Collins, *Macromolecules* 30 (1997) 1875–1883.
- [5] (a) W.R. Mariott, E.Y.-X. Chen, *Macromolecules* 38 (2005) 6822–6832. (b) A. Rodriguez-Delgado, E.Y.-X. Chen, *Macromolecules* 38 (2005) 2587–2594.
- [6] (a) J. Jin, W.R. Mariott, E.Y.-X. Chen, *J. Polym. Chem. Part A: Polym. Chem.* 41 (2003) 3132–3142. (b) J. Jin, E.Y.-X. Chen, *Organometallics* 21 (2002) 13–15.
- [7] (a) B. Lian, C.M. Thomas, C. Navarro, J.-F. Carpentier, *Organometallics* 26 (2007), 187–195. (b) A. Rodriguez-Delgado, W.R. Mariott, E.Y.-X. Chen, *J. Organomet. Chem.* 691 (2006) 3490–3497. (c) A. Rodriguez-Delgado, W.R. Mariott, E.Y.-X. Chen, *Macromolecules* 37 (2004) 3092–3100. (d) H. Nguyen, A.P. Jarvis, M.J.G. Lesley, W.M. Kelly, S.S. Reddy, N.J. Taylor, S. Collins, *Macromolecules* 33 (2000) 1508–1510.
- [8] J.W. Strauch, J.-L. Fauré, S. Bredeau, C. Wang, G. Kehr, R. Fröhlich, H. Luftmann, G. Erker, *J. Am. Chem. Soc.* 126 (2004) 2089–2104.
- [9] A.D. Bolig, E.Y.-X. Chen, *J. Am. Chem. Soc.* 123 (2001) 7943–7944.

- 
- [10] A. Rodriguez-Delgado, E.Y.-X. Chen, *J. Am. Chem. Soc.* 127 (2005) 961–974.
- [11] D. Chakraborty, E.Y.-X. Chen, *Organometallics* 22 (2003) 769–774.
- [12] R.D. Allen, T.E. Long, J.E. McGrath, *Polym. Bull.* 15 (1986) 127–134.
- [13] S. Feng, G.R. Roof, E.Y.-X. Chen, *Organometallics* 21 (2002), 832–839.
- [14] (a) C.H. Lee, S.J. Lee, J.W. Park, K.H. Kim, B.Y. Lee, J.S. Oh, *J. Mol. Cat., A: Chem.* 132 (1998), 231–239. (b) P. Biagini, G. Lugli, L. Abis, P. Andreussi, U.S. Pat. 5,602269, 1997.
- [15] Y.-J. Kim, M.P. Bernstein, A.S. Galiano Roth, F.E. Romesberg, P.G. Williard, D.J. Fuller, A.T. Harrison, D.B. Collum, *J. Org. Chem.* 56 (1991) 4435–4439.
- [16] *SHELXTL*, Version 6.12; Bruker Analytical X-ray Solutions: Madison, WI, 2001.
- [17] R.C. Ferguson, D.W. Ovenall, *Macromolecules* 20 (1987) 1245–1248.
- [18] (a) W.R. Mariott, E.Y.-X. Chen, *Macromolecules* 37 (2004) 4741–4743. (b) M. Kobayashi, S. Okuyama, T. Ishizone, S. Nakahama, *Macromolecules* 32 (1999) 6466–6477. (c) X. Xie, T.E. Hogen-Esch, *Macromolecules* 29 (1996) 1746–1752. (d) A. Bulai, M.L. Jimeno, A.-A.A. de Queiroz, A. Gallardo, J.S. Roman, *Macromolecules* 29 (1996) 3240–3246.

## CHAPTER V

### **Metallocene-Catalyzed Polymerization of Methacrylates to Highly Syndiotactic Polymers at High Temperatures**

#### **Abstract**

This contribution describes synthesis, polymerizations studies of a highly active polymerization system based on  $C_s$ -ligated *ansa*-zirconocene bis(ester enolate) **1** and mono(ester enolate) **2**—which, upon activation with appropriate activators, generate the corresponding chiral cationic catalysts **3** and **4**—that produces highly syndiotactic PMMA(94% *rr*) at industrially convenient temperatures. Kinetic profiling of the MMA polymerization in a [MMA]/[**2**] gives a first-order rate dependence in [MMA] and a linear increase of  $M_n$  vs.  $\rho$  and small PDI values in the range of 1.09–1.23. Preliminary site-control mechanism study is discussed besides the characterization, kinetic studies.

## Introduction

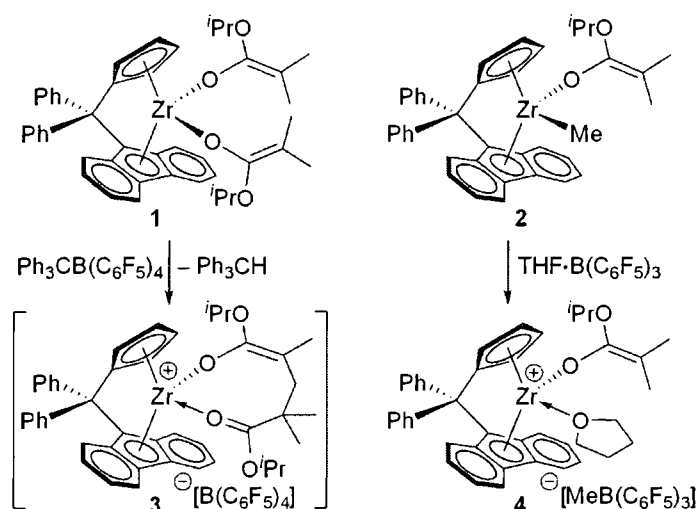
Technologically important, readily accessible, and remarkably tunable chiral metallocene catalysts, especially those of cationic group 4 complexes,<sup>1</sup> have been widely employed to precisely control the stereomicrostructure (tacticity) of polyolefins through their catalyzed homogeneous, single-site, stereospecific polymerization of *nonpolar*  $\alpha$ -olefins.<sup>2</sup> In comparison, the polymerization of *polar* functionalized alkenes with such highly electron-deficient group 4 metallocene and related complexes has been investigated to a much less extent.<sup>3</sup> Nonetheless, there is increasing interest in the latter area,<sup>4</sup> already achieving the synthesis of highly isotactic poly(methacrylate)s ( $\geq 95\%$  *mm*)<sup>5</sup> and poly(acrylamide)s ( $>99\%$  *mm*)<sup>6</sup> using chiral  $C_2$ -ligated zirconocenium complexes at ambient temperature. This initial success seemed to indicate that the catalyst symmetry–polymer stereomicrostructure relationship already established for the polymerization of nonpolar  $\alpha$ -olefins may be readily applied to the polymerization of polar functionalized alkenes, despite their differences in the chain-growth mechanism (i.e., migratory insertion<sup>2</sup> vs. conjugate addition<sup>3</sup>). To further test this hypothesis, over the past decade five research groups<sup>7</sup> have attempted the synthesis of syndiotactic poly(methyl methacrylate), PMMA, using a  $C_s$ -ligated cationic zirconocene methyl complex,  $[\text{Me}_2\text{C}(\text{Cp})(\text{Flu})\text{ZrMe}]^+$  ( $\text{Cp} = \eta^5$ -cyclopentadienyl;  $\text{Flu} = \eta^5$ -fluorenyl)—which is known for its ability to catalyze syndiospecific polymerization of propylene<sup>8</sup>—but none observed any activity for polymerization of methyl methacrylate (MMA). Although we<sup>9</sup> recently solved this inactivity issue using an ester enolate derivative,  $\{\text{Me}_2\text{C}(\text{Cp})(\text{Flu})\text{Zr}(\text{THF})[\text{OC}(\text{O}^i\text{Pr})=\text{CMe}_2]\}^+$ , the resulting PMMA is essentially a syndio-biased atactic polymer (64% *rr*, 32% *mr*, 4.0% *mm*) via a chain-end control mechanism. Another  $C_s$ -ligated zirconium ester enolate complex  $\text{CGCZr}(\text{L})[\text{OC}(\text{O}^i\text{Bu})=\text{CMe}_2]^+$  [ $\text{L} =$  neutral donor ligand,  $\text{CGC} = \text{Me}_2\text{Si}(\eta^5\text{-}\{\text{Me}_4\text{C}_5\})^+(\text{BuN})$ ] affords highly isotactic PMMA via a site-control mechanism at low temperatures,<sup>10</sup> whereas the isostructural titanium CGC complex produces syndiotactic PMMA (up to 82% *rr*) by a chain-end control mechanism.<sup>11</sup> Isoelectronic neutral

lanthanocenes supported by  $C_s$ -symmetric,  $Me_2C<$  and  $Ph_2C<$  bridged (Cp)(Flu) ligands also produce syndio-rich atactic ( $rr \sim 60\%$ ) PMMA.<sup>12</sup> In short, there exhibited no strict analogy between olefin insertion and MMA addition polymerizations catalyzed by  $C_s$ -ligated complexes because of their significant differences revealed in stereoselection<sup>4d</sup> and fundamental chain-growth events<sup>10,11</sup> between those two processes, and the synthesis of highly syndiotactic PMMA by a site-control mechanism remained a challenge.

Intense research efforts have been directed at development of a polymerization system that can lead to the efficient production of highly syndiotactic PMMA, due to the fact that the glass-transition temperature ( $T_g$ )—an important materials property parameter—of PMMA rises as an increase in the polymer syndiotacticity. It has been shown that PMMA exhibits a wide range of the  $T_g$  values as a function of its stereomicrostructure: *ca.* 55 °C,<sup>13</sup> 87 °C,<sup>13</sup> 110 °C,<sup>13</sup> 130 °C,<sup>11b</sup> and 140 °C<sup>7a</sup> for highly isotactic (96% *mm*), isotactic-*b*-syndiotactic (46% *mm*, 46% *rr*), syndio-biased atactic (60% *rr*), syndiotactic (81% *rr*), and highly syndiotactic (95% *rr*) PMMA, respectively. Several initiator systems have been developed to produce highly syndiotactic PMMA, *but all require low to extremely low polymerization temperatures ( $T_p$ )*, Table 1. The syndioselectivity of such non-site-control systems typically erodes to a moderate to low level of  $rr \leq 80\%$  when  $T_p$  reaches 25 °C. Our work communicated herein describes a highly active polymerization system based on  $C_s$ -ligated *ansa*-zirconocene bis(ester enolate) **1** and mono(ester enolate) **2**—which, upon activation with appropriate activators, generate the corresponding chiral cationic catalysts **3** and **4** (Scheme 1)—that produces highly syndiotactic PMMA at ambient or higher temperatures (Table 1).

**Table 1.** Polymerization Systems Producing Highly Syndiotactic PMMA

catalyst or initiator	$T_p$ (°C)	$rr$ (%)	$T_g$ (°C)	ref. no.
$m$ -(CH <sub>2</sub> =CH)C <sub>6</sub> H <sub>4</sub> CH <sub>2</sub> MgCl/THF	-98	94		14
[Cp <sub>2</sub> SmH] <sub>2</sub>	-95	95		15
<sup>t</sup> BuLi/3Al( <sup>n</sup> Oct) <sub>3</sub>	-93	96		16
Ph <sub>3</sub> P/AlEt <sub>3</sub>	-93	95	135	17
Me <sub>2</sub> C=C(OMe)OLi/2Al(C <sub>6</sub> F <sub>5</sub> ) <sub>3</sub>	-78	94	138	7a
Cp <sub>2</sub> YbAlH <sub>3</sub> ·NEt <sub>3</sub>	-40	93		18
[HC(C(Me)=N-2,6- <sup>t</sup> Pr <sub>2</sub> C <sub>6</sub> H <sub>3</sub> ) <sub>2</sub> Mg(μ-OC(=CH <sub>2</sub> )-2,4,6-Me <sub>3</sub> C <sub>6</sub> H <sub>2</sub> ) <sub>2</sub> ]	-30	92	135	19
1/ Ph <sub>3</sub> CB(C <sub>6</sub> F <sub>5</sub> ) <sub>4</sub> (i.e., <b>3</b> )	25	94	139	this work
2/ THF·B(C <sub>6</sub> F <sub>5</sub> ) <sub>3</sub> (i.e., <b>4</b> )	25	95	139	this work
1/ Ph <sub>3</sub> CB(C <sub>6</sub> F <sub>5</sub> ) <sub>4</sub> (i.e., <b>3</b> )	50	93	136	this work

**Scheme 1**

## Experimental

**Materials, Reagents, and Methods.** All syntheses and manipulations of air- and moisture-sensitive materials were carried out in flamed Schlenk-type glassware on a dual-manifold Schlenk line, on a high-vacuum line (typically from  $10^{-5}$  to  $10^{-7}$  Torr), or in an argon-filled glovebox (typically  $<1.0$  ppm oxygen). NMR-scale reactions were conducted in Teflon-valve-sealed J. Young-type NMR tubes. HPLC grade organic solvents were first sparged extensively with nitrogen during filling of the 20-L solvent reservoir and then dried by passage through activated alumina (for THF, Et<sub>2</sub>O, and CH<sub>2</sub>Cl<sub>2</sub>) followed by passage through activated Q-5-supported

copper catalyst (for toluene and hexanes) stainless steel columns. Benzene- $d_6$  and toluene- $d_8$  were dried over sodium/potassium alloy and filtered, whereas  $\text{CDCl}_3$  and  $\text{CD}_2\text{Cl}_2$  were degassed and dried over activated Davison 4 Å molecular sieves. NMR spectra were recorded on Varian Inova 300 (FT 300 MHz,  $^1\text{H}$ ; 75 MHz,  $^{13}\text{C}$ ; 282 MHz,  $^{19}\text{F}$ ), 400 MHz, and 500 MHz spectrometers. Chemical shifts for  $^1\text{H}$  and  $^{13}\text{C}$  spectra were referenced to internal solvent resonances and are reported as parts per million relative to  $\text{SiMe}_4$ ;  $^{19}\text{F}$  NMR spectra were referenced to external  $\text{CFCl}_3$ .

Methyl methacrylate (MMA), *n*-butyl methacrylate (BMA), butylated hydroxytoluene (BHT-H, 2,6-Di-*tert*-butyl-4-methylphenol), isopropyl isobutyrate, methyl magnesium bromide (3.0 M in diethyl ether), and *n*-butyllithium (1.6 M in hexanes) were purchased from Aldrich Chemical Co and used as received unless otherwise specified as follows. The MMA and BMA monomers were first degassed and dried over  $\text{CaH}_2$  overnight, followed by vacuum distillation, titration with neat tri(*n*-octyl)aluminum (Strem Chemical. Co.) to a yellow end point<sup>20</sup> and finally distillation under reduced pressure. The purified monomers were stored in brown bottles inside a glovebox freezer at  $-30\text{ }^\circ\text{C}$ . BHT-H was recrystallized from hexanes prior to use. Tris(pentafluorophenyl)borane  $\text{B}(\text{C}_6\text{F}_5)_3$ , trityl tetrakis(pentafluorophenyl) borate  $\text{Ph}_3\text{CB}(\text{C}_6\text{F}_5)_4$ , and diphenylmethylidene(cyclopentadienyl)(9-fluorenyl)zirconium dichloride  $\text{Ph}_2\text{C}(\text{Cp})(\text{Flu})\text{ZrCl}_2$  were obtained as research gifts from Boulder Scientific Co.;  $\text{B}(\text{C}_6\text{F}_5)_3$  was further purified by recrystallization from hexanes at  $-30\text{ }^\circ\text{C}$ , whereas  $\text{Ph}_3\text{CB}(\text{C}_6\text{F}_5)_4$  and  $\text{Ph}_2\text{C}(\text{Cp})(\text{Flu})\text{ZrCl}_2$  were used as received. The THF-borane adduct  $\text{THF}\cdot\text{B}(\text{C}_6\text{F}_5)_3$  was prepared by addition of THF to a toluene solution of the borane at ambient temperature, followed by removal of the volatiles and drying in vacuo. Trimethylsilyl trifluoromethanesulfonate (TMSOTf) was purchased from Alfa Aesar and redistilled under nitrogen atmosphere prior to use. A literature procedure<sup>21</sup> reported for the general synthesis of unsolvated ketone and ester enolates using the in situ generated lithium diisopropylamide in hexanes was employed and modified for

the preparation of lithium isopropyl isobutyrate  $\text{Me}_2\text{C}=\text{C}(\text{O}^i\text{Pr})\text{OLi}$ , which was isolated in the solid state and stored in a glovebox freezer at  $-30\text{ }^\circ\text{C}$ .

**Synthesis of  $\text{Ph}_2\text{C}(\text{Cp})(\text{Flu})\text{Zr}[\text{OC}(\text{O}^i\text{Pr})=\text{CMe}_2]_2$  (1).** In a nitrogen-filled glovebox, a 100-mL Schlenk flask was equipped with a magnetic stir bar and charged with  $\text{Ph}_2\text{C}(\text{Cp})(\text{Flu})\text{ZrCl}_2$  (0.310 g, 0.552 mmol) and 15 mL of diethyl ether. The flask was sealed with a septum, interfaced to a Schlenk line, and suspended in a dry ice-acetone bath at  $-78\text{ }^\circ\text{C}$ . A solution of  $\text{Me}_2\text{C}=\text{C}(\text{O}^i\text{Pr})\text{OLi}$  (0.194 g, 1.425 mmol) in 25 mL diethyl ether contained in a Schlenk flask was added to the above stirred solution via a cannular. The resulting mixture was allowed to warm gradually to ambient temperature and stirred overnight, after which all volatiles were removed in vacuo to give a yellow solid. The flask was brought back into the glovebox, and the solid was extracted with 50 mL of toluene. The extract was filtered through a pad of Celite, and the filtrate was dried in vacuo to give a residue which was extracted again with toluene and filtered through Celite. Removal of the solvent of the second extract afforded 0.40 g (92.1%) of the spectroscopically pure product **1** as an orange yellow solid. Recrystallization of this product from hexanes at  $-30\text{ }^\circ\text{C}$  inside the glovebox gave 0.31 g of yellow crystals not suitable for X-ray diffraction analysis, and subsequent numerous attempts to grow single crystals of this complex under various crystallization conditions were unsuccessful. This complex is somewhat thermally unstable in the solid state at ambient temperature, thus not suitable for shipping out for elemental analysis.

$^1\text{H}$  NMR ( $\text{C}_6\text{D}_6$ ,  $23\text{ }^\circ\text{C}$ ) for  $\text{Ph}_2\text{C}(\text{Cp})(\text{Flu})\text{Zr}[\text{OC}(\text{O}^i\text{Pr})=\text{CMe}_2]_2$  (**1**):  $\delta$  8.10 (d,  $J = 8.1\text{ Hz}$ , 2H, Flu), 7.87 (d,  $J = 5.4\text{ Hz}$ , 2H, Ph), 7.64 (d,  $J = 12.3\text{ Hz}$ , 2H, Ph), 7.16–6.79 (m, 12H, Flu, Ph), 6.33 (t,  $J = 2.4\text{ Hz}$ , 2H, Cp), 6.11 (t,  $J = 2.4\text{ Hz}$ , 2H, Cp), 3.67 (sept,  $J = 6.0\text{ Hz}$ , 2H,  $\text{CHMe}_2$ ), 1.66 (s, 6H,  $=\text{CMe}_2$ ), 1.47 (s, 6H,  $=\text{CMe}_2$ ), 1.05 (d,  $J = 6.0\text{ Hz}$ , 6H,  $\text{CHMe}_2$ ), 0.94 (d,  $J = 6.0\text{ Hz}$ , 6H,  $\text{CHMe}_2$ ).  $^{13}\text{C}$  NMR ( $\text{C}_6\text{D}_6$ ,  $23\text{ }^\circ\text{C}$ ):  $\delta$  154.7 [ $\text{C}(\text{O}^i\text{Pr})=\text{O}$ ], 146.8, 130.4, 129.4, 129.3, 127.4, 127.3, 123.6, 123.3, 123.2, 122.8, 121.9, 121.6, 115.8, 104.9, 86.56 (a total of 15 resonances

observed for the Flu, Ph, and Cp carbons), 86.23 (=CMe), 68.78 (CHMe<sub>2</sub>), 59.53 (CPh<sub>2</sub>), 22.59, 22.03 (CHMe<sub>2</sub>), 18.44, 18.21 (=CMe).

**Synthesis of Ph<sub>2</sub>C(Cp)(Flu)ZrMe[OC(O<sup>i</sup>Pr)=CMe<sub>2</sub>] (2).** This synthesis consists of the following three steps. First, in a nitrogen-filled glovebox, a 250-mL glass reactor was equipped with a magnetic stir bar, charged with Ph<sub>2</sub>C(Cp)(Flu)ZrCl<sub>2</sub> (1.37 g, 2.46 mmol) and 100 mL of THF, and cooled to -30 °C inside the freezer. A solution of MeMgBr (1.8 mL, 3.0 M in diethyl ether, 5.4 mmol) was added via syringe to the above precooled, vigorously stirred reactor. The resulting orange solution was stirred overnight at ambient temperature, after which all volatiles were removed under reduced pressure and the resulting yellow powder was heated at *ca.* 75 °C on a high-vacuum line for ≥ 8 h for removing the THF coordinated to the salt products. The orange powder obtained after the heat-vacuum treatment was extracted with toluene and filtered through a pad of Celite; the filtrate was dried in vacuo and extracted and filtered again through Celite. Drying of the filtrate gave 1.22 g (96.3%) of the spectroscopically pure dimethyl intermediate as a yellow solid. <sup>1</sup>H NMR (CDCl<sub>3</sub>, 23 °C) for Ph<sub>2</sub>C(Cp)(Flu)ZrMe<sub>2</sub>: δ 8.25 (d, *J* = 8.1 Hz, 2H, Flu), 7.92 (d, *J* = 8.1 Hz, 2H, Ph), 7.83 (d, *J* = 7.8 Hz, 2H, Ph), 7.45–6.88 (m, 10H, Flu, Ph), 6.25–6.40 (m, 4H, Cp, Flu), 5.59 (t, *J* = 2.7 Hz, 2H, Cp), -1.66 (s, 6H, Zr-Me).

Next, a 120-mL glass reactor was equipped with a magnetic stir bar, charged with Ph<sub>2</sub>C(Cp)(Flu)ZrMe<sub>2</sub> (1.22 g, 2.37 mmol) and 70 mL of toluene, and cooled to -30 °C inside the glovebox freezer. TMSOTf (0.61 g, 2.74 mmol) was added via syringe to the precooled reactor while vigorous stirring. The resulting red suspension was stirred for 24 h at ambient temperature. The NMR analysis of an aliquot taken from the reaction mixture revealed the presence of the unconverted Ph<sub>2</sub>C(Cp)(Flu)ZrMe<sub>2</sub>; accordingly, an additional amount of TMSOTf (0.12 g, 0.54 mmol) was added. After the mixture being stirred for another 24 h, an aliquot showed complete conversion of Ph<sub>2</sub>C(Cp)(Flu)ZrMe<sub>2</sub> to the product. All volatiles, including the excess TMSOTf, were removed in vacuo for 6 h, affording 1.32 g (100%) of the spectroscopically pure methyl

triflate intermediate as a red solid.  $^1\text{H}$  NMR ( $\text{CDCl}_3$ , 23 °C) for  $\text{Ph}_2\text{C}(\text{Cp})(\text{Flu})\text{ZrMe}(\text{OTf})$ :  $\delta$  8.26 (dd,  $J = 8.1$  Hz, 2H, Flu), 7.99–7.78 (m, 4H, Ph), 7.64–6.90 (m, 10H, Flu, Ph), 6.62 (q,  $J = 2.1$  Hz, 1H, Cp), 6.46 (d,  $J = 8.7$  Hz, 1H, Flu), 6.30 (d,  $J = 8.7$  Hz, 1H, Flu), 6.22 (q,  $J = 2.7$  Hz, 1H, Cp), 6.00 (q,  $J = 2.7$  Hz, 1H, Cp), 5.52 (q,  $J = 2.7$  Hz, 1H, Cp),  $-1.07$  (s, 3H, Zr–Me).

Third, a 60-mL glass reactor was equipped with a magnetic stir bar, charged with  $\text{Ph}_2\text{C}(\text{Cp})(\text{Flu})\text{ZrMe}(\text{OTf})$  (0.60 g, 1.07 mmol) and 40 mL toluene, and cooled to  $-30$  °C inside the glovebox freezer.  $\text{Me}_2\text{C}=\text{C}(\text{O}^i\text{Pr})\text{OLi}$  (0.15 g, 1.10 mmol) was added to the precooled, stirred reactor. The resulting orange red suspension was stirred for 24 h at ambient temperature, after which an aliquot of the reaction mixture revealed completion of the reaction by NMR. The reaction mixture was filtered through a pad of Celite, and the filtrate was dried in vacuo. The resulting residue was extracted with toluene and filtered again through Celite. Drying of the filtrate afforded 0.51 g (75.4%) of the spectroscopically pure product **2** as an orange solid. Recrystallization of this product from hexanes or toluene at  $-30$  °C inside the glovebox gave 0.36 g of orange crystals not suitable for X-ray diffraction analysis, and subsequent numerous attempts to grow single crystals of this complex under various crystallization conditions were unsuccessful. This complex is somewhat thermally unstable in the solid state at ambient temperature, thus not suitable for shipping out for elemental analysis.

$^1\text{H}$  NMR ( $\text{C}_6\text{D}_6$ , 23 °C) for  $\text{Ph}_2\text{C}(\text{Cp})(\text{Flu})\text{ZrMe}[\text{OC}(\text{O}^i\text{Pr})=\text{CMe}_2]$  (**2**):  $\delta$  7.99 (qt, 2H, Flu), 7.90 (dt, 1H, Ph), 7.71 (qt, 2H, Ph), 7.57 (dt, 1H, Ph), 7.30–6.70 (m, 11H, Flu, Ph), 6.42 (d,  $J = 9.0$  Hz, 1H, Flu), 6.20 (q,  $J = 2.7$  Hz, 1H, Cp), 6.04 (q,  $J = 2.7$  Hz, 1H, Cp), 5.82 (q,  $J = 2.7$  Hz, 1H, Cp), 5.47 (q,  $J = 2.7$  Hz, 1H, Cp), 3.66 (sept,  $J = 6.0$  Hz, 1H,  $\text{CHMe}_2$ ), 1.69 (s, 3H,  $=\text{CMe}$ ), 1.36 (s, 3H,  $=\text{CMe}$ ), 1.09 (d,  $J = 6.0$  Hz, 3H,  $\text{CHMe}_2$ ), 0.98 (d,  $J = 6.0$  Hz, 3H,  $\text{CHMe}_2$ ),  $-0.96$  (s, 3H, Zr–Me).  $^{13}\text{C}$  NMR ( $\text{C}_6\text{D}_6$ , 23 °C):  $\delta$  153.2 [ $\text{C}(\text{O}^i\text{Pr})=\text{O}$ ], 146.9, 146.7, 130.3, 130.2, 129.4, 129.3, 129.3, 129.2, 127.7, 127.4, 127.3, 127.2, 127.1, 126.4, 125.2, 124.1, 123.7, 123.5, 123.4, 122.6, 121.7, 121.6, 120.8, 119.7, 116.0, 115.5, 111.8, 104.9, 102.4, 84.8 (a total of 30

resonances observed for the Flu, Ph, and Cp carbons), 82.55 (=CMe), 68.04 (CHMe<sub>2</sub>), 59.39(CPh<sub>2</sub>), 28.08 (Zr-Me), 22.63, 22.20 (CHMe<sub>2</sub>), 22.20 (CHMe<sub>2</sub>), 17.70, 17.57 (=CMe).

**In Situ Generation of {Ph<sub>2</sub>C(Cp)(Flu)Zr(THF)[OC(O<sup>i</sup>Pr)=CMe<sub>2</sub>]}<sup>+</sup>[MeB(C<sub>6</sub>F<sub>5</sub>)<sub>3</sub>]<sup>-</sup> (4).**

In an argon-filled glovebox, a 4-mL glass vial was charged with complex **2** (18.9 mg, 0.030 mmol) and 0.4 mL CD<sub>2</sub>Cl<sub>2</sub>, while another vial was charged with THF·B(C<sub>6</sub>F<sub>5</sub>)<sub>3</sub> (17.5 mg, 0.030 mmol) and 0.4 mL CD<sub>2</sub>Cl<sub>2</sub>. The two vials were mixed via pipette at ambient temperature to give instantaneously a red solution; subsequent analysis of this red solution by NMR showed the clean and quantitative formation of ion pair **4**.

<sup>1</sup>H NMR (CD<sub>2</sub>Cl<sub>2</sub>, 23°C) for **4**: δ 8.41 (qt, *J* = 8.1 Hz, 2H, Flu), 7.93 (dd, *J* = 8.1 Hz, 2H, Ph), 7.83 (dt, 2H, Ph), 7.55–7.15 (m, 11H, Flu, Ph), 6.68–6.62 (m, 3H, Cp, Flu), 6.08 (m, 1H, Cp), 5.95 (q, *J* = 5.4 Hz, 1H, Cp), 4.02 (br, s, 1H, CHMe<sub>2</sub>), 3.52–3.40 (m, 4 H, α-CH<sub>2</sub>, THF), 2.04–1.62 (m, 4H, β-CH<sub>2</sub>, THF), 1.35 (s, 3H, =CMe), 1.30 (s, 3H, =CMe), 1.07 (d, *J* = 6.0 Hz, 3H, CHMe<sub>2</sub>), 0.95 (d, *J* = 6.0 Hz, 3H, CHMe<sub>2</sub>), 0.47 (br, s, 3H, B-Me). <sup>19</sup>F NMR (CD<sub>2</sub>Cl<sub>2</sub>, 23°C): δ -131.64 (d, *J*<sub>F-F</sub> = 19.8 Hz, 6F, *o*-F), -163.53 (t, *J*<sub>F-F</sub> = 6.6 Hz, 3F, *p*-F), -166.19 (m, 6F, *m*-F). <sup>13</sup>C NMR (CD<sub>2</sub>Cl<sub>2</sub>, 23°C): δ 154.25 [C(O<sup>i</sup>Pr)=O], 144.5, 144.4, 130.1, 130.0, 129.89, 129.58, 129.50, 129.45, 129.4, 128.7, 128.4, 128.3, 127.0, 126.9, 126.2, 125.7, 124.7, 124.3, 123.8, 123.6, 123.1, 122.9, 122.8, 121.6, 118.1, 118.0, 117.7, 108.6, 105.6, 91.14 (a total of 30 resonances observed for the Flu, Ph, and Cp carbons; broad resonances for the C<sub>6</sub>F<sub>5</sub> groups due to C-F coupling omitted), 85.11 (=CMe), 79.46 (α-CH<sub>2</sub>, THF), 72.20 (CHMe<sub>2</sub>), 59.70 (CPh<sub>2</sub>), 26.59 (β-CH<sub>2</sub>, THF), 22.37, 21.54 (CHMe<sub>2</sub>), 18.52, 17.42 (=CMe). The resonance for B-Me, typically a broad singlet at ~ 10 ppm for the Me group in the unassociated anion [MeB(C<sub>6</sub>F<sub>5</sub>)<sub>3</sub>]<sup>-</sup> in CD<sub>2</sub>Cl<sub>2</sub>,<sup>22</sup> was not assigned with confidence for this complex. <sup>19</sup>F NMR (CD<sub>2</sub>Cl<sub>2</sub>, 23°C): δ -131.5 (d, <sup>3</sup>*J*<sub>F-F</sub> = 19.7 Hz, 6F, *o*-F), -163.6 (t, <sup>3</sup>*J*<sub>F-F</sub> = 19.7 Hz, 3F, *p*-F), -166.2 (m, 6F, *m*-F).

**General Polymerization Procedures.** Polymerizations were performed either in 25-mL flame-dried Schlenk flasks interfaced to the dual-manifold Schlenk line for runs using external

temperature bath, or in 20-mL glass reactors inside the glovebox for ambient temperature (*ca.* 25 °C) runs. Two different activation procedures were employed for comparative studies. In a *in-reactor activation* procedure, a predetermined amount of activator [ $\text{Ph}_3\text{CB}(\text{C}_6\text{F}_5)_4$ ,  $\text{THF}\cdot\text{B}(\text{C}_6\text{F}_5)_3$ , or  $\text{B}(\text{C}_6\text{F}_5)_3$ ], which is equal to the amount of complex **1** or **2** employed, first dissolved in MMA (1.00 mL, 9.35 mmol) inside a glovebox, and the polymerization was started by rapid addition of the above activator + MMA solution via gastight syringe to a solution of **1** or **2** (23.4  $\mu\text{mol}$ ) in 10 mL of solvent ( $\text{CH}_2\text{Cl}_2$  or toluene) under vigorous stirring at the pre-equilibrated bath temperature. The amount of the Zr catalyst was fixed for all polymerizations, whereas the amount of MMA was adjusted according to the  $[\text{MMA}]/[\text{Zr}]$  ratio specified in the text. In a *pre-activation procedure*, complex **1** or **2** was premixed with an appropriate activator in solution for 10 min to generate the corresponding activated species, followed by rapid addition of MMA to start the polymerization. In both procedures, after the measured time interval, a 0.2 mL aliquot was taken from the reaction mixture via syringe and quickly quenched into a 4-mL vial containing 0.6 mL of undried “wet”  $\text{CDCl}_3$  stabilized by 250 ppm of BHT-H; the quenched aliquots were later analyzed by  $^1\text{H}$  NMR to obtain the percent monomer conversion data. The polymerization was immediately quenched after the removal of the aliquot by addition of 5 mL 5% HCl-acidified methanol. The quenched mixture was precipitated into 100 mL of methanol, stirred for 1 h, filtered, washed with methanol, and dried in a vacuum oven at 50 °C overnight to a constant weight.

**Polymerization Kinetics.** Kinetic experiments were carried out in a stirred glass reactor at ambient temperature (*ca.* 25 °C) inside an argon-filled glovebox using the *in-reactor activation* procedure already described above and with a  $[\text{MMA}]_0/[\text{Zr}]_0$  ratio of 100:  $[\text{MMA}]_0 = 0.468 \text{ M}$ ,  $[\text{Zr}]_0 = [\text{activator}]_0 = 4.68 \text{ mM}$  in 5 mL of  $\text{CH}_2\text{Cl}_2$ . The procedures for obtaining the monomer conversion data vs. reaction time were described in literature.<sup>23</sup> Specifically, at appropriate time intervals, 0.2 mL aliquots were withdrawn from the reaction mixture using syringe and quickly

quenched into 1 mL vials containing 0.6 mL of undried “wet” CDCl<sub>3</sub> mixed with 250 ppm of BHT-H. The quenched aliquots were analyzed by <sup>1</sup>H NMR. The ratio of [MMA]<sub>0</sub> to [MMA]<sub>t</sub> at a given time *t*, [MMA]<sub>0</sub>/[MMA]<sub>t</sub>, was determined by integration of the peaks for MMA (5.2 and 6.1 ppm for the vinyl signals; 3.4 ppm for the *OMe* signal) and PMMA (centered at 3.4 ppm for the *OMe* signals) according to [MMA]<sub>0</sub>/[MMA]<sub>t</sub> = 2A<sub>3,4</sub>/3A<sub>5,2+6,1</sub>, where A<sub>3,4</sub> is the total integrals for the peaks centered at 3.4 ppm (typically in the region 3.2–3.6 ppm) and A<sub>5,2+6,1</sub> is the total integrals for both peaks at 5.2 and 6.1 ppm. Apparent rate constants (*k*<sub>app</sub>) were extracted by linearly fitting a line to the plot of ln([MMA]<sub>0</sub>/[MMA]<sub>t</sub>) vs. time.

**Polymer Characterizations.** Glass transition temperatures (*T*<sub>g</sub>) of the polymers were measured by differential scanning calorimetry (DSC) on a DSC 2920, TA Instrument. Samples, weighted (typically in a 7–10 mg range) and sealed in hermetic aluminum pans using a DSC press, were first heated to 180 °C at 10 °C/min, equilibrated at this temperature for 4 min, then cooled to 0°C at 10 °C/min, held at this temperature for 4 min, and finally reheated to 180°C at 10 °C/min. All *T*<sub>g</sub> values were obtained from the second scan after removing the thermal history. Polymer number-average molecular weights (*M*<sub>n</sub>) and molecular weight distributions (*M*<sub>w</sub>/*M*<sub>n</sub>) were measured by gel permeation chromatography (GPC) analyses carried out at 40 °C and a flow rate of 1.0 mL/min, with CHCl<sub>3</sub> as the eluent on a Waters University 1500 GPC instrument equipped with one PLgel 5 μm guard and three PLgel 5 μm mixed-C columns (Polymer Laboratories; linear range of molecular weight = 200–2,000,000). The instrument was calibrated with 10 PMMA standards, and chromatograms were processed with Waters Empower software (version 2002). <sup>1</sup>H NMR and <sup>13</sup>C NMR spectra for the analysis of PMMA and PBMA microstructures were recorded in CDCl<sub>3</sub> and analyzed according to the literature methods.<sup>35,24</sup>

## Results and Discussion

Zirconocene bis(ester enolate) **1** was conveniently synthesized by the reaction of the corresponding dichloride precursor<sup>25</sup> with Me<sub>2</sub>C=C(O<sup>*i*</sup>Pr)OLi in 92% yield. The synthesis of

mono(ester enolate) **2** involved three steps: methylation of the dichloride precursor with MeMgBr to yield the dimethyl derivative (96% yield), treatment of the dimethyl with Me<sub>3</sub>SiOTf to give the methyl triflate complex (>99% yield), and reaction of the triflate with Me<sub>2</sub>C=C(O<sup>i</sup>Pr)OLi to afford **2** in 75% yield. Activation of the methyl ester enolate complex **2** with THF•B(C<sub>6</sub>F<sub>5</sub>)<sub>3</sub> in CH<sub>2</sub>Cl<sub>2</sub> at room temperature generated cleanly the corresponding chiral cationic species **4**; the same activation approach has been well established for C<sub>2</sub>- and C<sub>s</sub>-ligated zirconocene methyl ester enolate complexes.<sup>5a,b,9</sup> For the activation of the bis(ester enolate) complex **1**, we employed a unique activation process that we recently developed for oxidative activation of the silyl ketene acetal initiator Me<sub>2</sub>C=C(OMe)OSiMe<sub>3</sub> with a catalytic amount of Ph<sub>3</sub>CB(C<sub>6</sub>F<sub>5</sub>)<sub>4</sub> to a highly active propagating species structure containing both nucleophilic [R(Me)C=C(OMe)OSiMe<sub>3</sub>] and electrophilic (Me<sub>3</sub>Si<sup>+</sup>) catalyst sites.<sup>26</sup> Accordingly, we reasoned that the reaction of **1** with 1 equiv of Ph<sub>3</sub>CB(C<sub>6</sub>F<sub>5</sub>)<sub>4</sub> should occur in the similar fashion: H<sup>-</sup> abstraction from the methyl group within the enolate [OC(O<sup>i</sup>Pr)=CMe<sub>2</sub>] moiety<sup>27</sup> by Ph<sub>3</sub>C<sup>+</sup> forms Ph<sub>3</sub>CH and the resulting isopropyl methacrylate coordinated to Zr, and subsequent nucleophilic addition of another enolate ligand to this activated methacrylate monomer gives the cationic eight-membered-ring chelate **3** (a catalyst resting state).<sup>28</sup> Indeed, the formation of Ph<sub>3</sub>CH was observed at temperature as low as -60 °C (5.55 ppm, CH, CD<sub>2</sub>Cl<sub>2</sub>); however, unlike **4**, complex **3** is unstable in the absence of monomer.

Significantly, the activated species promote rapid and controlled MMA polymerizations with high syndiospecificity at ambient temperature (*ca.* 25 °C). The polymerization by the bis(ester enolate) **1** was carried out in a in-reactor activation mode, that is, addition of a premixed solution of 100 equiv of MMA with 1 equiv of Ph<sub>3</sub>CB(C<sub>6</sub>F<sub>5</sub>)<sub>4</sub> to a CH<sub>2</sub>Cl<sub>2</sub> solution of **1**. A 92% monomer conversion ( $\rho$ ) was reached within 14 min of the reaction, and a linear increase of  $M_n$  (number-average molecular weight) vs.  $\rho$  was observed with PDI (polydispersity index) ranging from 1.10 at low  $\rho$  ( $M_n = 4.51 \times 10^3$ ) to 1.37 at high  $\rho$  ( $M_n = 2.09 \times 10^4$ ). *Most remarkably, the resulting polymer shows  $rr = 94.4\%$  and  $T_g = 139$  °C!* The triad-level stereomicrostructure of the PMMA ( $mr = 4.0\%$ ,  $mm = 1.6\%$ ) is more characteristic of site control than chain-end control, but

the test result of  $2[mm]/[mr] = 0.8$  somewhat deviates from unity which may suggest that it not conform to a pure site-control mechanism. Furthermore, this high level of syndiotacticity is not markedly altered by changing the  $[MMA]/[1]$  ratio (400,  $rr = 93.5\%$ ; 800,  $rr = 93.2\%$ ), solvent (400 MMA, toluene,  $rr = 93.7\%$ ), temperature (400 MMA,  $T_p = 50\text{ }^\circ\text{C}$  in toluene,  $rr = 92.8\%$ ,  $T_g = 136\text{ }^\circ\text{C}$ ; 400 MMA,  $T_p = 0\text{ }^\circ\text{C}$  in  $\text{CH}_2\text{Cl}_2$ ,  $rr = 96.0\%$ ,  $T_g = 140\text{ }^\circ\text{C}$ ), and addition sequence (pre-activation mode, i.e., premixing **1** with  $\text{Ph}_3\text{CB}(\text{C}_6\text{F}_5)_4$  for 10 min before addition of 400 MMA,  $rr = 94.5\%$ ,  $mr = 3.7\%$ ,  $mm = 1.8\%$ ,  $T_g = 139\text{ }^\circ\text{C}$ ). However, the use of the borane  $\text{B}(\text{C}_6\text{F}_5)_3$  as activator for bis(ester enolate) **1** resulted in the formation of PMMA with substantially lower syndiotacticity ( $rr = 76.4\%$ ,  $mr = 20.6\%$ ,  $mm = 3.0\%$ ); this observation is attributable to a combination of a different activation pathway involving  $\text{B}(\text{C}_6\text{F}_5)_3$  (which undergoes electrophilic addition to the ester enolate  $\alpha$ -carbon forming an adduct analogous to the structure previously characterized for the  $C_2$ -symmetric metallocene derivative<sup>28</sup>) with a competing bimetallic pathway as a result of the slow and reversible activation process using  $\text{B}(\text{C}_6\text{F}_5)_3$  (i.e., coexistence of both neutral and cationic species under this activation condition).

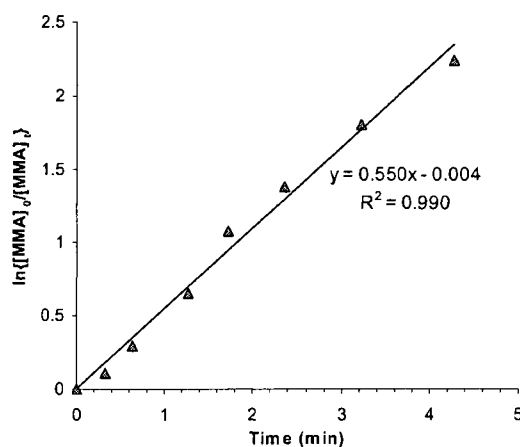


**Figure 1.** First-order kinetic plot of  $\ln\{[MMA]_0/[MMA]_t\}$  vs. time for the MMA polymerization in  $\text{CH}_2\text{Cl}_2$  at  $25\text{ }^\circ\text{C}$ :  $[MMA]_0 = 0.468\text{ M}$ ,  $[2]_0 = [\text{B}(\text{C}_6\text{F}_5)_3]_0 = 4.68\text{ mM}$ .

The mono(ester enolate) **2** is instantaneously activated using  $\text{THF}\cdot\text{B}(\text{C}_6\text{F}_5)_3$  (*in situ* mixing or isolation of **4**),  $\text{B}(\text{C}_6\text{F}_5)_3$  (in-reactor activation), or  $\text{Ph}_3\text{CB}(\text{C}_6\text{F}_5)_4$ , all leading to highly active (a

95% monomer conversion is typically achieved in 7 min) and highly syndiospecific (94% *rr*) polymerization of MMA at ambient temperature. Kinetic profiling of the MMA polymerization in a [MMA]/[**2**] ratio of 100 at 25 °C in CH<sub>2</sub>Cl<sub>2</sub> gives a first-order rate dependence in [MMA] (Figure 1) and a linear increase of  $M_n$  vs.  $\rho$  with a non-zero intercept and small PDI values in the range of 1.09–1.23 (Figure 2). The PMMA produced by **4** derived from **2** + THF•B(C<sub>6</sub>F<sub>5</sub>)<sub>3</sub> + 400 MMA exhibits *rr* = 94.9% (<sup>1</sup>H NMR, 500 MHz), *rrrr* = 93.1% (<sup>13</sup>C NMR, 125 MHz, Figure 3), and  $T_g$  = 139 °C. Polymerization of 200 equiv of *n*-butyl methacrylate by this system also affords highly syndiotactic poly(*n*-butyl methacrylate):  $\rho$  = 90% (1 h),  $M_n$  =  $3.47 \times 10^4$ , PDI = 1.30, *rr* = 94.1%, *mr* = 3.9%, *mm* = 2.0%.

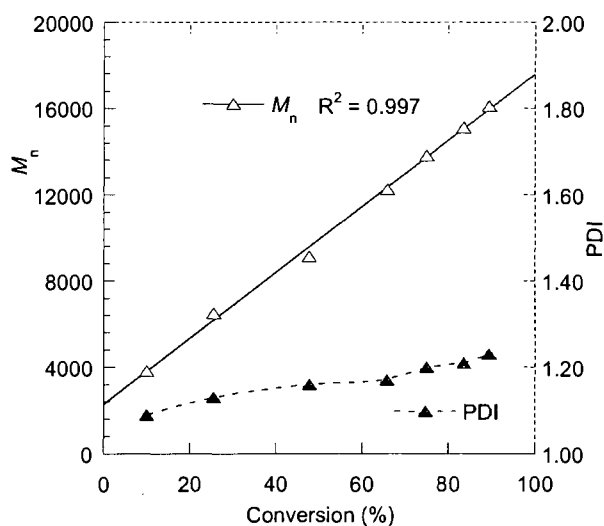
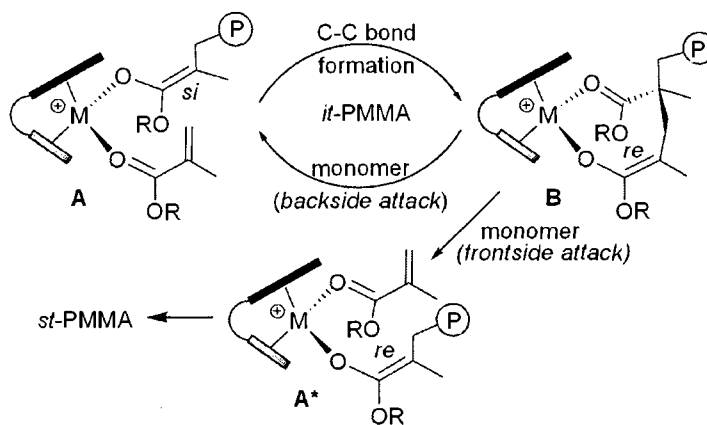


**Figure 2.** Plots of  $M_n$  and PDI of PMMA vs. MMA conversion: [MMA]<sub>0</sub> = 0.468 M, [**2**]<sub>0</sub> = [B(C<sub>6</sub>F<sub>5</sub>)<sub>3</sub>]<sub>0</sub> = 4.68 mM.

*C*<sub>s</sub>-ligated catalyst structure **A** (Scheme 2) is chiral at metal and exhibits two enantiotopic lateral coordination sites. Isotactic PMMA is formed by a site-control mechanism when the reaction follows a **A**→**B**→**A** cycle in which stereoselective C–C bond formation occurs predominantly through the same, preserved structure **A** and the lateral coordination site for MMA is also the same due to monomer *backside* attack (relative to the coordinated ester leaving group) following each bond formation step.<sup>10</sup> On the other hand, syndiotactic PMMA is formed by a site-

control mechanism if both lateral sites are alternately utilized for stereoselective monomer enchainment via a  $A \rightarrow B \rightarrow A^*$  cycle (\* denotes an enantiomer) requiring *frontside* attack of the incoming monomer at the resting cyclic intermediate **B** following each C–C bond formation step. For both site-control cases, the rate of MMA-assisted site epimerization must be slow relative to Michael addition. No site epimerization was observed for **3** and **4** in  $CD_2Cl_2$  or in the presence of 10 or 20 equiv of THF. Consistently, addition of 10 or 20 equiv of THF decreased the syndiotacticity of the PMMA produced by **3** or **4** in  $CH_2Cl_2$  by only ~1.0%, suggesting little to none site epimerization during polymerization by displacement of the coordinated chain end from the metal prior to monomer coordination. Hence, the observed differences in reactivity and stereoselectivity between the  $Me_2C<$  and  $Ph_2C<$  bridged Zr systems may be explained by their different Thorpe–Ingold effect<sup>29</sup> in terms of relative rates of ring-closing (Michael addition step) and ring-opening as compared to the rate of MMA-assisted site epimerization. In the event of fast site epimerization relative to propagation, syndiotactic PMMA would not be formed by a site-control mechanism using  $C_s$ -ligated catalysts.

**Scheme 2**



## Conclusions

In summary, we have developed a highly active catalyst system based on the  $C_s$ -ligated *ansa*-zirconocene bis- and mono(ester enolate) complexes **1** and **2** leading to the production of

highly syndiotactic poly(methacrylate)s at industrially convenient temperatures, thus accomplishing a long-standing scientific goal of the field. However, a fundamental understanding of the unique features that the current system possesses and further development of possibly even better systems based on this understanding require much further work, which will be a focus of our on-going studies.

**Acknowledgment.** This work was supported by the National Science Foundation (NSF-0718061). We thank Boulder Scientific Co. for the research gifts of  $\text{Ph}_2\text{C}(\text{Cp})(\text{Flu})\text{ZrCl}_2$ ,  $\text{Ph}_3\text{CB}(\text{C}_6\text{F}_5)_4$ , and  $\text{B}(\text{C}_6\text{F}_5)_3$ , Prof. Cavallo for discussions, as well as the reviewers for the valuable comments.

## References

- 
- (1) Selected reviews: (a) Bochmann, M. *J. Chem. Soc. Dalton Trans.* **1996**, 255–270. (b) Jordan, R. F. *Adv. Organomet. Chem.* **1991**, 32, 325–387.
  - (2) Selected reviews: (a) Coates, G. W. *Chem. Rev.* **2000**, 100, 1223–1252. (b) Resconi, L.; Cavallo, L.; Fait, A.; Piemontesi, F. *Chem. Rev.* **2000**, 100, 1253–1345. (c) Brintzinger, H. H.; Fischer, D.; Mülhaupt, R.; Rieger, B.; Waymouth, R. M. *Angew. Chem. Int. Ed.* **1995**, 34, 1143–1170.
  - (3) A short review: Chen, E. Y.-X. *J. Polym. Sci. Part A: Polym. Chem.* **2004**, 42, 3395–3403.
  - (4) Recent examples: (a) Miyake, G. M.; Mariott, W. R.; Chen, E. Y.-X. *J. Am. Chem. Soc.* **2007**, 129, 6724–6725. (b) Lian, B.; Thomas, C. M.; Navarro, C.; Carpentier, J.-F. *Macromolecules* **2007**, 40, 2293–2294. (c) Tomasi, S.; Weiss, H.; Ziegler, T. *Organometallics* **2007**, 26, 2157–2166. (d) Caporaso, L.; Gracia-Budría, J.; Cavallo, L. *J. Am. Chem. Soc.* **2006**, 128, 16649–16654. (e) Kostakis, K.; Mourmouris, S.; Kotakis, K.; Nikogeorgos, N.; Pitsikalis, M.; Hadjichristidis, N. *J. Polym. Sci. Part A: Polym. Chem.* **2005**, 43, 3305–3314. (f) Stojcevic,

- 
- G.; Kim, H.; Taylor, N. J.; Marder, T. B.; Collins, S. *Angew. Chem. Int. Ed.* **2004**, *43*, 5523–5526. (g) Strauch, J. W.; Fauré, J.-L.; Bredeau, S.; Wang, C.; Kehr, G.; Fröhlich, R.; Luftmann, H.; Erker, G. *J. Am. Chem. Soc.* **2004**, *126*, 2089–2104. (h) Ferenz, M.; Bandermann, F.; Sustmann, R.; Sicking, W. *Macromol. Chem. Phys.* **2004**, *205*, 1196–1205. (i) Jensen, T. R.; Yoon, S. C.; Dash, A. K.; Luo, L.; Marks, T. J. *J. Am. Chem. Soc.* **2003**, *125*, 14482–14494. (j) Hölscher, M.; Keul, H.; Höcker, H. *Macromolecules* **2002**, *35*, 8194–8202.
- (5) (a) Rodriguez-Delgado, A.; Chen, E. Y.-X. *Macromolecules* **2005**, *38*, 2587–2594. (b) Bolig, A. D.; Chen, E. Y.-X. *J. Am. Chem. Soc.* **2004**, *126*, 4897–4906. (c) Cameron, P. A.; Gibson, V.; Graham, A. J. *Macromolecules* **2000**, *33*, 4329–4335. (d) Deng, H.; Shiono, T.; Soga, K. *Macromolecules* **1995**, *28*, 3067–3073. (e) Collins, S.; Ward, D. G.; Suddaby, K. H. *Macromolecules* **1994**, *27*, 7222–7224.
- (6) Mariott, W. R.; Chen, E. Y.-X. *Macromolecules* **2005**, *38*, 6822–6832; **2004**, *37*, 4741–4743.
- (7) (a) Bolig, A. D.; Chen, E. Y.-X. *J. Am. Chem. Soc.* **2001**, *123*, 7943–7944. (b) Frauenrath, H.; Keul, H.; Höcker, H. *Macromolecules* **2001**, *34*, 14–19. (c) ref. 5c. (d) Chen, Y.-X.; Metz, M. V.; Li, L.; Stern, C. L.; Marks, T. J. *J. Am. Chem. Soc.* **1998**, *120*, 6287–6305. (e) Soga, K.; Deng, H.; Yano, T.; Shiono, T. *Macromolecules* **1994**, *27*, 7938–7940.
- (8) (a) Razavi, A.; Thewalt, U. *J. Organomet. Chem.* **1993**, *445*, 111–114. (b) Razavi, A.; Ferrara, J. *J. Organomet. Chem.* **1992**, *435*, 299–310. (c) Ewen, J. A.; Jones, R. L.; Razavi, A.; Ferrara, J. D. *J. Am. Chem. Soc.* **1988**, *110*, 6255–6256.
- (9) Rodriguez-Delgado, A.; Mariott, W. R.; Chen, E. Y.-X. *J. Organomet. Chem.* **2006**, *691*, 3490–3497.
- (10) Nguyen, H.; Jarvis, A. P.; Lesley, M. J. G.; Kelly, W. M.; Reddy, S. S.; Taylor, N. J.; Collins, S. *Macromolecules* **2000**, *33*, 1508–1510.

- 
- (11) (a) Lian, B.; Thomas, C. M.; Navarro, C.; Carpentier, J.-F. *Organometallics* **2007**, *26*, 187–195. (b) Rodriguez-Delgado, A.; Mariott, W. R.; Chen, E. Y.-X. *Macromolecules* **2004**, *37*, 3092–3100.
- (12) (a) Kirillov, E.; Lehmann, C. W.; Razavi, A.; Carpentier, J.-F. *Organometallics* **2004**, *23*, 2768–2777. (b) Qian, C.; Nie, W.; Chen, Y.; Sun, J. *J. Organomet. Chem.* **2002**, *645*, 82–86.
- (13) Bolig, A. D.; Chen, E. Y.-X. *J. Am. Chem. Soc.* **2002**, *124*, 5612–5613.
- (14) Hatada, K.; Nakanishi, H.; Ute, K.; Kitayama, T. *Polym. J.* **1986**, *18*, 581–591.
- (15) Yasuda, H.; Yamamoto, H.; Yokota, K.; Miyake, S.; Nakamura, A. *J. Am. Chem. Soc.* **1992**, *114*, 4908–4909.
- (16) Kitayama, T.; Shinozaki, T.; Masuda, E.; Yamamoto, M.; Hatada, K. *Polym. Bull.* **1988**, *20*, 505–510.
- (17) Kitayama, T.; Masuda, E.; Yamaguchi, M.; Nishiura, T.; Hatada, K. *Polym. J.* **1992**, *24*, 817–827.
- (18) Knjazhanski, S. Y.; Elizalde, L.; Cadenas, G.; Bulychev, B. M. *J. Organomet. Chem.* **1998**, *568*, 33–40.
- (19) Dove, A. P.; Gibson, V. C.; Marshall, E. L.; White, A. J. P.; Williams, D. J. *Chem. Commun.* **2002**, 1208–1209.
- (20) Allen, R. D.; Long, T. E.; McGrath, J. E. *Polym. Bull.* **1986**, *15*, 127–134.
- (21) Kim, Y.-J.; Bernstein, M. P.; Galiano Roth, A. S.; Romesberg, F. E.; Williard, P. G.; Fuller, D. J.; Harrison, A. T.; Collum, D. B. *J. Org. Chem.* **1991**, *56*, 4435–4439.
- (22) (a) Mariott, W. R.; Chen, E. Y.-X. *Macromolecules* **2005**, *38*, 6822–6832. (b) Bolig, A. D.; Chen, E. Y.-X. *J. Am. Chem. Soc.* **2004**, *126*, 4897–4906. (c) Klosin, J.; Roof, G.; Chen, E. Y.-X.; Abboud, K. A. *Organometallics* **2000**, *19*, 4684–4686.

- 
- (23) (a) Rodriguez-Delgado, A.; Chen, E. Y.-X. *J. Am. Chem. Soc.* **2005**, *127*, 961–974. (b) Rodriguez-Delgado, A.; Mariott, W. R.; Chen, E. Y.-X. *Macromolecules* **2004**, *37*, 3092–3100.
- (24) (a) Bovey, F. A.; Mirau, P. A. *NMR of Polymers*; Academic Press: San Diego, CA, 1996. (b) Kawamura, T.; Toshima, N.; Matsuzaki, K. *Makromol. Chem., Rapid Commun.* **1993**, *14*, 719–724. (c) Chujo, R.; Hatada, K.; Kitamaru, R.; Kitayama, T.; Sato, H.; Tanaka, Y. *Polym. J.* **1987**, *19*, 413–424. (d) Ferguson, R. C.; Ovenall, D. W. *Polym. Prepr.* **1985**, *26*, 182–183. (e) Subramanian, R.; Allen, R. D.; McGrath, J. E.; Ward, T. C. *Polym. Prepr.* **1985**, *26*, 238–240.
- (25) Razavi, A.; Atwood, J. L. *J. Organomet. Chem.* **1993**, *459*, 117–123.
- (26) Zhang, Y.; Chen, E. Y.-X. *Macromolecules* **2008**, *41*, 36–42.
- (27) Hydride abstraction from an enolate methyl group of  $\text{Cp}_2\text{ZrMe}[\text{OC}(\text{O}^t\text{Bu})=\text{CMe}_2]$  by the trityl cation led to the formation of a zirconium-carboxylate dication, after subsequent elimination of methane and isobutene: Lian, B.; Toupet, L.; Carpentier, J.-F. *Chem. Eur. J.* **2004**, *10*, 4301–4307.
- (28) The X-ray crystal structure of the similar complex bearing a  $C_2$ -symmetric ligand has been reported: Ning, Y.; Chen, E. Y.-X. *Macromolecules* **2006**, *39*, 7204–7215.
- (29) (a) Jung, M. E.; Piizzi, G. *Chem. Rev.* **2005**, *105*, 1735–1766. (b) Beesley, R. M.; Ingold, C. K.; Thorpe, J. F. *J. Chem. Soc.* **1915**, *107*, 1080–1106.

---

## CHAPTER VI

### Syndioselective MMA Polymerization by Group 4 Constrained Geometry Catalysts: A Combined Experimental and Theoretical Study

#### Abstract

This contribution reports a combined experimental (with kinetics and tangible effects on syndioselectivity) and theoretical (with density functional theory) study of (CGC)M catalysts [M = Ti, Zr; CGC = Me<sub>2</sub>Si(η<sup>5</sup>-Me<sub>4</sub>C<sub>5</sub>)(<sup>t</sup>BuN)], addressing a need for a fundamental understanding of the stereoselectivity observed for such catalysts in polymerization of methyl methacrylate (MMA) and an explanation for the chain-end control nature of the syndioselective MMA polymerization by the chiral (CGC)Ti catalyst. The living/controlled MMA polymerization by (CGC)TiMe<sup>+</sup>MeB(C<sub>6</sub>F<sub>5</sub>)<sub>3</sub><sup>-</sup> (**1**) follows the zero-order kinetics in [MMA], implying a faster ring-opening process of the cyclic chelate relative to MMA addition within the catalyst-monomer complex in a unimetallic propagation cycle. The syndioselectivity of **1** is insensitive to monomer and catalyst concentrations as well as to ion-pairing strength varied with counterion structure and solvent polarity. Comparative studies using identical (CGC)M bis(isopropyl ester enolate) structures show that the (CGC)Ti system exhibits noticeably higher syndioselectivity than the isostructural Zr system at ambient temperature. Density functional calculations rationalize the higher syndioselectivity observed for the (CGC)Ti catalyst and lend a theoretical support for the mechanism of MMA- or counterion-assisted catalyst site-epimerization after a stereomistake, which accounts for the formation of the predominately isolated *m* stereoerrors.

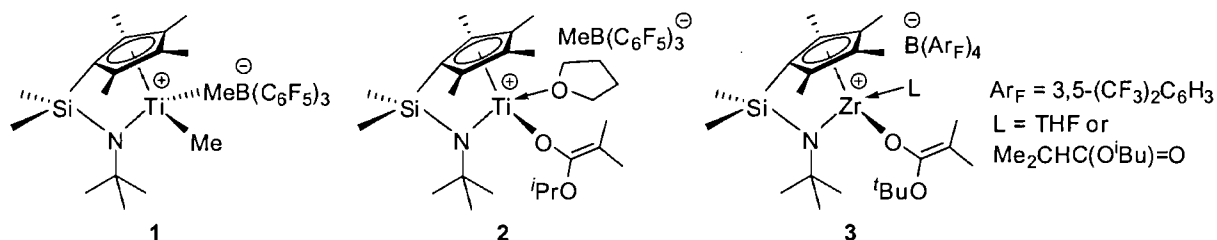
## Introduction

Metallocene complexes, especially those of cationic group 4 complexes,<sup>1</sup> are technologically important, readily accessible, and remarkably tunable catalysts that have been extensively investigated and successfully employed for the production of polyolefins through their catalyzed homogeneous, single-site, (co)polymerization of *nonpolar* vinyl monomers ( $\alpha$ -olefins in particular).<sup>2</sup> In comparison, the polymerization of *polar* vinyl monomers with such highly electron-deficient group 4 metallocene and related complexes has been investigated to a much less extent.<sup>3</sup> Nonetheless, there is increasing interest in the latter area, with several types of group 4 metallocene complexes being examined for polymerizations of methacrylates,<sup>4-46</sup> acrylates,<sup>41, 47-50</sup> acrylamides,<sup>51-54</sup> and methyl vinyl ketone.<sup>55</sup> The polymerization of (meth)acrylates has also been studied computationally.<sup>56-62</sup> Overall, these studies have been focused on the following four major aspects of polymerization: activity/efficiency (catalyst turnover frequency and initiator efficiency), stereospecificity (polymer tacticity and stereocontrol mechanism), control (polymer molecular weight, MW, and molecular weight distribution, MWD, as well as livingness and block copolymer production), and mechanism (kinetics and elementary reactions). Specifically on polymerization stereospecificity, the site-control mechanism enabled the synthesis of highly isotactic poly(methacrylate)s ( $\geq 95\%$  *mm*)<sup>9,13,36,44,45</sup> and poly(acrylamide)s ( $>99\%$  *mm*)<sup>11-54</sup> using chiral  $C_2$ -ligated zirconocenium complexes as well as highly syndiotactic poly(methacrylate)s ( $\geq 94\%$  *rr*)<sup>10</sup> using chiral  $C_s$ -ligated zirconocenium complexes, both at *ambient-temperature*. Furthermore, computational studies gained important insights into the stereocontrol mechanism in the polymerization of MMA by  $C_2$ ,  $C_s$ , and  $C_1$ -ligated chiral *ansa*-zirconocenium complexes.<sup>56,57</sup>

Half-sandwich metal complexes bearing linked (e.g., by the dimethylsilyl group)  $\eta^5$ -cyclopentadienyl (e.g., tetramethyl-substituted Cp)- $\eta^1$ -amido (e.g., <sup>t</sup>BuN) ligands<sup>63</sup> are termed “constrained geometry catalysts”, attributing to the phenomenal commercial successes in the

production of revolutionary polyolefin materials via (co)polymerization of  $\alpha$ -olefins using such group 4 metal catalysts.<sup>64</sup> The  $C_s$ -ligated cationic (CGC)Ti alkyl complex, (CGC)TiMe<sup>+</sup>MeB(C<sub>6</sub>F<sub>5</sub>)<sub>3</sub><sup>-</sup> (**1**) [CGC = Me<sub>2</sub>Si( $\eta^5$ -Me<sub>4</sub>C<sub>5</sub>)(<sup>t</sup>BuN), Scheme 1], effects *living and syndioselective* polymerization of methacrylates at ambient<sup>18,28</sup> or higher (up to 100 °C)<sup>6</sup> temperatures via an apparent *chain-end control* mechanism. The living and syndioselective features of this catalyst system allowed for the highly efficient (>80% initiator efficiency) synthesis of syndiotactic poly(methacrylate)s at ambient temperature [poly(methyl methacrylate), PMMA, up to 80% *rr*; poly(butyl methacrylate), up to 89% *rr*] with controlled MW and narrow MWD (PDI =  $M_w/M_n$  = 1.09) as well as the well-defined, syndiotactic block or random copolymers of methacrylates.<sup>18</sup> The robust (CGC)TiMe<sub>2</sub>/B(C<sub>6</sub>F<sub>5</sub>)<sub>3</sub> system (which generates **1** instantaneously) also effectively promotes the polymerization of *n*-butyl acrylate.<sup>47</sup> The corresponding chiral cationic (CGC)Ti ester enolate complex, {(CGC)Ti(THF)[OC(O<sup>t</sup>Pr)=CMe<sub>2</sub>]}<sup>+</sup>[MeB(C<sub>6</sub>F<sub>5</sub>)<sub>3</sub>]<sup>-</sup> (**2**, Scheme 1), which simulates the structure of the active propagating species, behaves similarly to that of the (CGC)Ti alkyl complex,<sup>18</sup> producing syndiotactic PMMA (80% *rr*, 18% *mr*, 2.0% *mm*) at ambient temperature with *predominately isolated m stereoerrors* (confirmed by the stereomicrostructure analysis at the pentad level<sup>18</sup>) and again pointing to the apparent chain-end control nature of the polymerization.

Scheme 1



In contrast, the isostructural, cationic Zr alkyl complex, (CGC)ZrMe<sup>+</sup>MeB(C<sub>6</sub>F<sub>5</sub>)<sub>3</sub><sup>-</sup>, is inactive for polymerization of MMA at high or low temperature of polymerization ( $T_p$ ). However, the cationic (CGC)Zr ester enolate complex, (CGC)Zr(L)[OC(O<sup>t</sup>Bu)=CMe<sub>2</sub>]}<sup>+</sup>[B(Ar<sub>F</sub>)<sub>4</sub>]<sup>-</sup> [**3**, Ar<sub>F</sub>

= 3,5-(CF<sub>3</sub>)<sub>2</sub>C<sub>6</sub>H<sub>3</sub>, L = neutral donor ligand such as THF or isobutyrate, Scheme 1], is moderately active and affords, unexpectedly (on the basis of its C<sub>s</sub> ligation), highly isotactic PMMA via a site-control mechanism at low T<sub>p</sub>: 95.5% *mm* at -60 °C and -40 °C.<sup>34</sup> Further increasing T<sub>p</sub> to -20 °C gave PMMA with a considerably lower isotacticity of 80.5% *mm*. Ambient temperature polymerization results were not given as this cationic (CGC)Zr complex is thermal unstable at T ≥ -20 °C. A key element in the proposed stereocontrol mechanism for the observed isospecificity of complex **3** is that stereoselective MMA addition occurs predominately at only one of the two enantiotopic lateral sites (i.e., MMA is coordinated to the same lateral Zr site for a site-retention mechanism); this is possible provided that intramolecular 1,4-conjugate Michael addition within the catalyst-monomer complex is fast relative to racemization at Zr by exchange of free and bound MMA and that dissociation of the terminal ester group in the cyclic ester enolate resting intermediate is slow relative to associative displacement (backside attack) by MMA.<sup>34</sup> Apparently, such conditions were met with the polymerization by the in situ-generated **3** in terms of a combination of the low T<sub>p</sub> condition (≤-40 °C) and the use of the oxonium acid activator H<sup>+</sup>(OEt)<sub>2</sub>[B(Ar<sub>F</sub>)<sub>4</sub>] with concomitant delivery of coordinating ligands (diethyl ether and isobutyrate) for the resulting cation upon activation, thereby leading to the production of isotactic PMMA.

As overviewed above, the (CGC)Ti alkyl and ester enolate catalysts **1** and **2** produce syndiotactic PMMA by an apparent chain-end control mechanism at ambient temperature, while the (CGC)Zr ester enolate catalyst **3** affords isotactic PMMA by a site-control mechanism under the low temperature and oxonium acid activation conditions (*vide supra*). The central objective of the current study is to seek for a fundamental understanding of the stereoselectivity observed for such group 4 catalysts and an explanation for the chain-end control nature of the syndiospecific MMA polymerization by the (CGC)Ti catalyst. To this end, we embarked a combined experimental and theoretical study. Experimentally, we investigated the kinetics of the

polymerization by catalyst 1, examined monomer and catalyst concentration, anion and solvent effects on syndioselectivity, as well as synthesized the identical (CGC)Ti and Zr bis(ester enolate) complexes and carried out their comparative studies in MMA polymerization upon activation with three different types of activators at ambient temperature. On the theoretical front, we computed transition states with DFT for MMA additions using both (CGC)Ti and (CGC)Zr catalysts and examined MMA- and anion-assisted site epimerization processes with the (CGC)Ti catalyst.

## Experimental

**Materials, Reagents, and Methods.** All syntheses and manipulations of air- and moisture-sensitive materials were carried out in flamed Schlenk-type glassware on a dual-manifold Schlenk line, on a high-vacuum line, or in an argon-filled glovebox. NMR-scale reactions (typically in a 0.02 mmol scale) were conducted in Teflon-valve-sealed J. Young-type NMR tubes. HPLC-grade organic solvents were first sparged extensively with nitrogen during filling 20 L solvent reservoirs and then dried by passage through activated alumina (for Et<sub>2</sub>O, THF, and CH<sub>2</sub>Cl<sub>2</sub>) followed by passage through Q-5 supported copper catalyst (for toluene and hexanes) stainless steel columns. Benzene-*d*<sub>6</sub> and toluene-*d*<sub>8</sub> were dried over sodium/potassium alloy and vacuum-distilled or filtered, whereas CD<sub>2</sub>Cl<sub>2</sub>, and CDCl<sub>3</sub> were dried over activated Davison 4 Å molecular sieves. NMR spectra were recorded on either a Varian Inova 300 (FT 300 MHz, <sup>1</sup>H; 75 MHz, <sup>13</sup>C; 282 MHz, <sup>19</sup>F) or a Varian Inova 400 spectrometer. Chemical shifts for <sup>1</sup>H and <sup>13</sup>C spectra were referenced to internal solvent resonances and are reported as parts per million relative to SiMe<sub>4</sub>, whereas <sup>19</sup>F NMR spectra were referenced to external CFCl<sub>3</sub>. Elemental analyses were performed by Desert Analytics, Tucson, AZ.

MMA, butylated hydroxytoluene (BHT-H, 2,6-Di-*tert*-butyl-4-methylphenol), diisopropylamine, isopropyl isobutyrate, *n*-butyl lithium (1.6 M in hexanes), and methyl magnesium bromide (3.0 M in diethyl ether) were purchased from Aldrich Chemical Co and used

as received unless otherwise specified as follows. MMA was first degassed and dried over  $\text{CaH}_2$  overnight, followed by vacuum distillation, titration with neat tri(*n*-octyl)aluminum (Strem Chemical) to a yellow end point<sup>65</sup> and finally distillation under reduced pressure; the purified MMA was stored in a brown bottle inside a glovebox freezer at  $-30\text{ }^\circ\text{C}$ . Diisopropylamine and isopropyl isobutyrate were dried over  $\text{CaH}_2$ , followed by vacuum distillation. BHT-H was recrystallized from hexanes prior to use. Triflic acid was purchased from Alfa Aesar and redistilled under nitrogen atmosphere. Tris(pentafluorophenyl)borane,  $\text{B}(\text{C}_6\text{F}_5)_3$ , trityl tetrakis(pentafluorophenyl)borate,  $[\text{Ph}_3\text{C}][\text{B}(\text{C}_6\text{F}_5)_4]$ , and dimethylanilinium tetrakis(pentafluorophenyl)borate,  $[\text{HNMe}_2\text{Ph}][\text{B}(\text{C}_6\text{F}_5)_4]$ , were obtained as research gifts from Boulder Scientific Co.;  $\text{B}(\text{C}_6\text{F}_5)_3$  was further purified by recrystallization from hexanes at  $-30\text{ }^\circ\text{C}$ , whereas  $[\text{Ph}_3\text{C}][\text{B}(\text{C}_6\text{F}_5)_4]$  and  $[\text{HNMe}_2\text{Ph}][\text{B}(\text{C}_6\text{F}_5)_4]$  were used as received. Tris(pentafluorophenyl)alane,  $\text{Al}(\text{C}_6\text{F}_5)_3$ , as a 0.5 toluene adduct  $\text{Al}(\text{C}_6\text{F}_5)_3 \cdot (\text{C}_7\text{H}_8)_{0.5}$ , was prepared by the reaction of  $\text{B}(\text{C}_6\text{F}_5)_3$  and  $\text{AlMe}_3$  in a 1:3 toluene/hexanes solvent mixture in quantitative yield;<sup>66</sup> this is the modified synthesis based on literature procedures.<sup>67</sup> Although we have experienced no incidents when handling this material, *extra caution should be exercised*, especially when dealing with the unsolvated form, because of its thermal and shock sensitivity. Literature procedures were employed and modified for the preparation of the following complexes:  $(\text{CGC})\text{MCl}_2$  ( $\text{M} = \text{Ti}, \text{Zr}$ ),<sup>64h</sup>  $(\text{CGC})\text{TiMe}_2$ ,<sup>64h,68</sup> and  $(\text{CGC})\text{TiMe}^+\text{MeB}(\text{C}_6\text{F}_5)_3^-$  (**1**).<sup>69</sup>

**Preparation of Lithium Isopropyl Isobutyrate  $\text{Me}_2\text{C}=\text{C}(\text{O}^i\text{Pr})\text{OLi}$ .** A literature procedure<sup>70</sup> for the general synthesis of unsolvated ketone and ester enolates using the in situ generated lithium diisopropylamide (LDA) in hexanes was modified for the preparation of  $\text{Me}_2\text{C}=\text{C}(\text{O}^i\text{Pr})\text{OLi}$ . In an argon-filled glovebox, a 200 mL Schlenk flask was equipped with a magnetic stir bar and charged with 50 mL of hexanes. This flask was sealed with a rubber septum, removed from the glovebox, interfaced to a Schlenk line, and placed in a  $0\text{ }^\circ\text{C}$  ice-water bath. Diisopropylamine (6.63 g, 65.6 mmol, predried) was added to this flask via syringe, followed by addition of  $n\text{BuLi}$  (42 mL, 1.6 M in hexanes, 67.2 mmol) dropwise via syringe. The

mixture was stirred for 30 min at 0 °C to generate LDA in situ, after which isopropyl isobutyrate (10 mL, 8.47 g, 65.1 mmol, predried) was added via syringe. The reaction mixture was warmed gradually to room temperature and stirred for another 2 h. All volatiles were removed in vacuo and the residue was thoroughly dried in vacuo to give 8.1 g (91%) of the spectroscopically pure product as a white powder. When needed, further purification can be carried out by recrystallization from hexanes at -30 °C to give crystals. <sup>1</sup>H NMR (C<sub>6</sub>D<sub>6</sub>, 23 °C): δ 4.28 (sept, 1H, -OCHMe<sub>2</sub>), 1.86 (s, 3H, =CMe<sub>2</sub>), 1.76 (s, 3H, =CMe<sub>2</sub>), 1.24 (d, 6H, -CHMe<sub>2</sub>). <sup>13</sup>C NMR (C<sub>6</sub>D<sub>6</sub>, 23 °C): δ 156.2 [C=O(O<sup>i</sup>Pr)], 78.01 (=CMe<sub>2</sub>), 72.21 (OCHMe<sub>2</sub>), 22.27 (OCHMe<sub>2</sub>), 18.07 (=CMe<sub>2</sub>), 17.71 (=CMe<sub>2</sub>). We have previously characterized the molecular structure of the unsolvated Me<sub>2</sub>C=C(O<sup>i</sup>Pr)OLi by single-crystal X-ray diffraction analysis.<sup>71</sup>

**Synthesis of (CGC)Ti[OC(O<sup>i</sup>Pr)=CMe<sub>2</sub>]<sub>2</sub> (4).** This synthesis consists of the following three steps involving the use of the intermediates (CGC)TiMe<sub>2</sub> and (CGC)Ti(OTf)<sub>2</sub>. First, in a nitrogen-filled glovebox, a 250 mL glass reactor was equipped with a magnetic stir bar, charged with (CGC)TiCl<sub>2</sub> (1.00 g, 2.72 mmol) and 80 mL of Et<sub>2</sub>O, and subsequently cooled to -30 °C inside the glovebox freezer. A solution of MeMgBr (2.0 mL, 3.0 M in diethyl ether, 6.0 mmol) was added via syringe to the above pre-chilled, vigorously stirred reactor. The resulting green yellow mixture was stirred overnight at ambient temperature, after which all volatiles were removed under reduced pressure. The pure product as a yellow-green solid was obtained after sublimation at *ca.* 75 °C on a high-vacuum line for ≥ 6 h, and the yield was 0.65 g (73%). <sup>1</sup>H NMR (CD<sub>2</sub>Cl<sub>2</sub>, 23 °C) for (CGC)TiMe<sub>2</sub>: δ 2.14 (s, 6H, C<sub>5</sub>Me<sub>4</sub>), 1.88 (s, 6H, C<sub>5</sub>Me<sub>4</sub>), 1.54 (s, 9H, NCM<sub>3</sub>), 0.45 (s, 6H, TiMe<sub>2</sub>), 0.13 (s, 6H, SiMe<sub>2</sub>). <sup>1</sup>H NMR (C<sub>6</sub>D<sub>6</sub>, 23 °C) for CGCTiMe<sub>2</sub>: δ 1.96 (s, 6H, C<sub>5</sub>Me<sub>4</sub>), 1.85 (s, 6H, C<sub>5</sub>Me<sub>4</sub>), 1.57 (s, 9H, NCM<sub>3</sub>), 0.51 (s, 6H, TiMe<sub>2</sub>), 0.43 (s, 6H, SiMe<sub>2</sub>).

Next, in an argon-filled glovebox, a 50 mL Schlenk flask was equipped with a stir bar and charged with 30 mL of toluene and 0.27 g (0.82 mmol) of (CGC)TiMe<sub>2</sub>. The flask was sealed

with a rubber septum, removed from the glovebox, and interfaced to a Schlenk line. The yellow solution was cooled to  $-78\text{ }^{\circ}\text{C}$ , and to this solution was quickly added triflic acid (0.15 mL, 0.25 g, 1.7 mmol) via glass syringe. The flask was warmed gradually to room temperature over 1 h, and the resulting dark red mixture was stirred overnight. The flask was taken into the glovebox after all volatiles were removed in vacuo. The solid residue was extracted with toluene to colorless and the extract was filtered through a pad of Celite. The dark red filtrate was concentrated and left inside a  $-30\text{ }^{\circ}\text{C}$  freezer overnight, yielding 0.13 g (27%) of the pure product (CGC)Ti(OTf)<sub>2</sub> as red needle-like crystals. <sup>1</sup>H NMR (CD<sub>2</sub>Cl<sub>2</sub>, 23 °C) for (CGC)Ti(OTf)<sub>2</sub>:  $\delta$  1.94 (s, 6H, C<sub>5</sub>Me<sub>4</sub>), 1.88 (s, 6H, C<sub>5</sub>Me<sub>4</sub>), 1.13 (s, 9H, NCM<sub>3</sub>), 0.28 (s, 6H, SiMe<sub>2</sub>). <sup>19</sup>F NMR (CD<sub>2</sub>Cl<sub>2</sub>, 23 °C):  $\delta$  -156.85 (s).

Third, in a nitrogen-filled glovebox, a 30 mL glass reactor was equipped with a magnetic stir bar, charged with 15 mL of toluene, and cooled to  $-30\text{ }^{\circ}\text{C}$  inside a glovebox freezer. To this pre-chilled reactor, with vigorous stirring, was added (CGC)Ti(OTf)<sub>2</sub> (35.4 mg, 0.060 mmol) followed by addition of lithium isopropyl isobutyrate (23.0 mg, 0.17 mmol). The resulting suspension was stirred overnight at ambient temperature, after which it was filtered through a pad of Celite. The solvent of the filtrate was removed in vacuo, yielding 28.0 mg (85%) of the spectroscopically pure final product **4** as a red oily product which can be crystallized at low temperatures but the obtained crystals melt immediately on warming to ambient temperature. The isolated complex is somewhat unstable at ambient temperature for an extended time period (several hours), thus not suitable for shipping out for elemental analysis, but it can be readily characterized by NMR. <sup>1</sup>H NMR (C<sub>6</sub>D<sub>6</sub>, 23 °C) for (CGC)Ti[OC(O<sup>*i*</sup>Pr)=CMe<sub>2</sub>]<sub>2</sub> (**4**):  $\delta$  4.41 (sept,  $J = 6.3$  Hz, 2H, CHMe<sub>2</sub>), 2.23 (s, 6H, C<sub>5</sub>Me<sub>4</sub>), 1.99 (s, 6H, C<sub>5</sub>Me<sub>4</sub>), 1.84 (s, 6H, =CMe<sub>2</sub>), 1.83 (s, 6H, =CMe<sub>2</sub>), 1.38 (s, 9H, NCM<sub>3</sub>), 1.20 (d,  $J = 6.3$  Hz, 6H, CHMe<sub>2</sub>), 1.18 (d,  $J = 6.3$  Hz, 6H, CHMe<sub>2</sub>), 0.63 (s, 6H, SiMe<sub>2</sub>). <sup>13</sup>C NMR (C<sub>6</sub>D<sub>6</sub>, 23°C):  $\delta$  156.8 [C(O<sup>*i*</sup>Pr)=O], 133.6 (C<sub>5</sub>Me<sub>4</sub>), 132.7 (C<sub>5</sub>Me<sub>4</sub>), 105.4 (C<sub>5</sub>Me<sub>4</sub>), 90.03 (=CMe), 69.20 (CHMe<sub>2</sub>), 59.40 (CM<sub>3</sub>), 33.61 (CM<sub>3</sub>), 22.50

(CHMe<sub>2</sub>), 22.23 (CHMe<sub>2</sub>), 19.52 (=CMe), 18.48 (=CMe), 14.69 (C<sub>5</sub>Me<sub>4</sub>), 11.16 (C<sub>5</sub>Me<sub>4</sub>), 7.08 (SiMe<sub>2</sub>).

**Synthesis of (CGC)Zr[OC(O<sup>i</sup>Pr)=CMe<sub>2</sub>]<sub>2</sub> (5).** The same approach for the synthesis of analogous (CGC)Zr[OC(O<sup>i</sup>Bu)=CMe<sub>2</sub>]<sub>2</sub><sup>34</sup> was utilized for the synthesis of **3** with a detailed and modified procedure given below. In a nitrogen-filled glovebox, a 100 mL Schlenk flask was equipped with a magnetic stir bar and charged with (CGC)ZrCl<sub>2</sub> (0.50 g, 1.2 mmol) and 20 mL of THF. The flask was sealed with a rubber septum, interfaced to a Schlenk line, and suspended in a dry ice-acetone bath at -78 °C. A solution of Me<sub>2</sub>C=C(O<sup>i</sup>Pr)OLi (0.34 g, 2.5 mmol) in 20 mL THF contained in a Schlenk flask was added to the above stirred solution via a cannular. The resulting mixture was allowed to warm gradually to ambient temperature and stirred overnight, after which all volatiles were removed in vacuo to give a light yellow solid. The flask was brought back into the glovebox, and the solid was extracted with 40 mL of hexanes. The extract was filtered through a pad of Celite, and the filtrate was dried in vacuo to give 0.68 g (93%) of the crude product as a light yellow oil. The oil was dissolved in 2 to 3 mL of hexanes and cooled down to -30 °C. Precipitates (impurities) formed was removed by filtration, and the solvent of the filtrate was removed to give 0.49 g (67%) of the spectroscopically pure product **3** as a yellow solid. <sup>1</sup>H NMR (C<sub>6</sub>D<sub>6</sub>, 23 °C) for (CGC)Zr[OC(O<sup>i</sup>Pr)=CMe<sub>2</sub>]<sub>2</sub> (**5**): δ 4.41 (sept, *J* = 6.3 Hz, 2H, CHMe<sub>2</sub>), 2.22 (s, 6H, C<sub>5</sub>Me<sub>4</sub>), 2.00 (s, 6H, C<sub>5</sub>Me<sub>4</sub>), 1.84 (s, 6H, =CMe<sub>2</sub>), 1.80 (s, 6H, =CMe<sub>2</sub>), 1.34 (s, 9H, NCM<sub>3</sub>), 1.19 (d, *J* = 6.3 Hz, 12H, CHMe<sub>2</sub>), 0.62 (s, 6H, SiMe<sub>2</sub>).

**Isolation of Active Species (CGC)Zr<sup>+</sup>[OC(O<sup>i</sup>Pr)=C(Me)CH<sub>2</sub>C(Me<sub>2</sub>)C(O<sup>i</sup>Pr)=O][B(C<sub>6</sub>F<sub>5</sub>)<sub>4</sub>]<sup>-</sup> (6).** In an argon-filled glovebox, a 4 mL glass vial was charged with complex **3** (12.0 mg, 0.020 mmol) and 0.4 mL of CH<sub>2</sub>Cl<sub>2</sub>, while another vial was charged with [Ph<sub>3</sub>C][B(C<sub>6</sub>F<sub>5</sub>)<sub>4</sub>] (18.4 mg, 0.020 mmol) and 0.4 mL of CH<sub>2</sub>Cl<sub>2</sub>. The two vials were mixed via pipette at ambient temperature to give instantaneously a yellow/green solution. The solvent was removed in vacuo, and the residue was

washed with 5 mL of hexanes to give a yellow/green oily product; subsequent analysis by NMR showed the clean and quantitative formation of the titled ion pair **6**. Anal. Calcd. for  $C_{53}H_{52}BO_4F_{20}NSiZr$ : C, 49.84; H, 4.11. Found: C, 49.57; H, 4.63.  $^1H$  NMR ( $CD_2Cl_2$ , 23°C) for **6**:  $\delta$  5.24 (sept,  $J = 6.0$  Hz, 1H,  $CHMe_2$ ), 4.30 (sept,  $J = 6.3$  Hz, 1H,  $CHMe_2$ ), 2.24 (s, 3H,  $C_5Me_4$ ), 2.22 (s, 3H,  $C_5Me_4$ ), 2.11 (s, 3H,  $C_5Me_4$ ), 1.99 (s, 3H,  $C_5Me_4$ ), 1.63 (s, br, 2H,  $CH_2$ ), 1.47 (d,  $J = 6.0$  Hz, 3H,  $CHMe_2$ ), 1.43 (d,  $J = 6.0$  Hz, 3H,  $CHMe_2$ ), 1.42 (s, 3H,  $=CMe$ ), 1.34 (s, 3H,  $CMe_2$ ), 1.28 (d,  $J = 6.3$  Hz, 3H,  $CHMe_2$ ), 1.27 (s, 3H,  $CMe_2$ ), 1.22 (d,  $J = 6.3$  Hz, 3H,  $CHMe_2$ ), 1.17 (s, 9H,  $NCMe_3$ ), 0.73 (s, 3H,  $SiMe_2$ ), 0.66 (s, 3H,  $SiMe_2$ ).  $^{19}F$  NMR ( $CD_2Cl_2$ , 23°C):  $\delta$  -131.5 (d,  $^3J_{F-F} = 13.6$  Hz, 8F, *o*-F), -162.0 (t,  $^3J_{F-F} = 22.2$  Hz, 4F, *p*-F), -165.9 (m, 8F, *m*-F).

**In Situ Generation of  $(CGC)Zr[OC(O^iPr)=CMe_2]^+[O=C(O^iPr)CMe_2B(C_6F_5)_3]^-$  (**7**).** In an argon-filled glovebox, a 4 mL glass vial was charged with complex **3** (12.0 mg, 0.020 mmol) and 0.4 mL of  $CD_2Cl_2$ , while another vial was charged with  $B(C_6F_5)_3$  (10.2 mg, 0.020 mmol) and 0.4 mL of  $CD_2Cl_2$ . The two vials were mixed via pipette at ambient temperature to give instantaneously a red solution; subsequent analysis of this red solution by NMR showed the clean and quantitative formation of ion pair **5**. The isolated complex is somewhat unstable at ambient temperature for an extended time period (several hours), thus not suitable for shipping out for elemental analysis.  $^1H$  NMR ( $CD_2Cl_2$ , 23°C) for **7**:  $\delta$  5.24 (sept,  $J = 6.3$  Hz, 1H,  $CHMe_2$ ), 4.30 (sept,  $J = 6.0$  Hz, 1H,  $CHMe_2$ ), 2.23 (s, 3H,  $C_5Me_4$ ), 2.22 (s, 3H,  $C_5Me_4$ ), 2.10 (s, 3H,  $C_5Me_4$ ), 1.99 (s, 3H,  $C_5Me_4$ ), 1.62 (s, 3H,  $=CMe_2$ ), 1.47 (d,  $J = 6.0$  Hz, 6H,  $CHMe_2$ ), 1.41 (s, 3H,  $=CMe_2$ ), 1.34 (s, 3H,  $CMe_2$ ), 1.29 (s, 3H,  $CMe_2$ ), 1.23 (d,  $J = 6.3$  Hz, 6H,  $CHMe_2$ ), 1.17 (s, 9H,  $NCMe_3$ ), 0.73 (s, 3H,  $SiMe_2$ ), 0.66 (s, 3H,  $SiMe_2$ ).  $^{19}F$  NMR ( $CD_2Cl_2$ , 23°C):  $\delta$  -132.3 (br, 6F, *o*-F), -163.2 (br, 3F, *p*-F), -165.9 (br, 6F, *m*-F).

**General Polymerization Procedures.** Polymerizations were performed either in 25-mL flame-dried Schlenk flasks interfaced to the dual-manifold Schlenk line for runs using external

temperature bath, or in 30-mL glass reactors inside the glovebox for ambient temperature (*ca.* 25 °C) runs. Catalyst precursors (CGC)TiMe<sub>2</sub>, (CGC)Ti[OC(O<sup>i</sup>Pr)=CMe<sub>2</sub>]<sub>2</sub>, and (CGC)Zr[OC(O<sup>i</sup>Pr)=CMe<sub>2</sub>]<sub>2</sub> were premixed with an equimolar amount of an appropriate activator B(C<sub>6</sub>F<sub>5</sub>)<sub>3</sub>, Al(C<sub>6</sub>F<sub>5</sub>)<sub>3</sub>, [Ph<sub>3</sub>C][B(C<sub>6</sub>F<sub>5</sub>)<sub>4</sub>], or [HNMe<sub>2</sub>Ph][B(C<sub>6</sub>F<sub>5</sub>)<sub>4</sub>] as indicated, in a toluene or CH<sub>2</sub>Cl<sub>2</sub> solution for *ca.* 30 min [when activated with B(C<sub>6</sub>F<sub>5</sub>)<sub>3</sub>] or 10 min (for all other activators) to generate the corresponding activated species. The polymerization was started by rapid addition of MMA (typically 1.00 mL, 9.35 mmol, or a different amount according to the [MMA]<sub>0</sub>/[(CGC)M]<sub>0</sub> ratio specified in the text) under vigorous stirring at the pre-equilibrated bath temperature. After the measured time interval, a 0.2 mL aliquot was taken from the reaction mixture via syringe and quickly quenched into a 4-mL vial containing 0.6 mL of undried “wet” CDCl<sub>3</sub> stabilized by 250 ppm of BHT-H; the quenched aliquots were analyzed by <sup>1</sup>H NMR to obtain the percent monomer conversion data. The polymerization was immediately quenched after the removal of the aliquot by addition of 5 mL 5% HCl-acidified methanol. The quenched mixture was precipitated into 100 mL of methanol, stirred for 1 h, filtered, washed with methanol, and dried in a vacuum oven at 50 °C overnight to a constant weight.

**Polymerization Kinetics.** Kinetic experiments (conditions: [MMA]<sub>0</sub>/[**1**]<sub>0</sub> = 200, 9.35 mmol MMA, 46.8 μmol (CGC)TiMe<sub>2</sub> and B(C<sub>6</sub>F<sub>5</sub>)<sub>3</sub>, 10 mL of CH<sub>2</sub>Cl<sub>2</sub> or toluene, *ca.* 25 °C) were carried out in a stirred glass reactor inside the glovebox. The procedures for obtaining the monomer conversion vs. reaction time data were described in literature.<sup>9,71</sup> Specifically, at appropriate time intervals, 0.2 mL aliquots were withdrawn from the reaction mixture using syringe and quickly quenched into 1 mL vials containing 0.6 mL of undried “wet” CDCl<sub>3</sub> mixed with 250 ppm of BHT-H. The quenched aliquots were analyzed by <sup>1</sup>H NMR. The ratio of [MMA]<sub>0</sub> to [MMA]<sub>*t*</sub> at a given time *t*, [MMA]<sub>0</sub>/[MMA]<sub>*t*</sub>, was determined by integration of the peaks for MMA (5.2 and 6.1 ppm for the vinyl signals; 3.4 ppm for the *OMe* signal) and PMMA (centered at 3.4 ppm for the *OMe* signals) according to [MMA]<sub>0</sub>/[MMA]<sub>*t*</sub> = 2A<sub>3,4</sub>/3A<sub>5.2+6.1</sub>, where

$A_{3,4}$  is the total integrals for the peaks centered at 3.4 ppm (typically in the region 3.2–3.6 ppm) and  $A_{5,2+6,1}$  is the total integrals for both peaks at 5.2 and 6.1 ppm. The obtained conversion vs. time data were plotted in two ways:  $[MMA]_t/[MMA]_0$  vs. time plot for the zero-order kinetics in  $[MMA]$ , or  $\ln([MMA]_0/[MMA]_t)$  vs. time plot for the first-order kinetics in  $[MMA]$ . The best linearly fit plots will decide the kinetic order and the apparent rate constant ( $k_{app}$ ) for each run will be obtained from the slope of the best-fit line.

**Polymer Characterizations.** Polymer number-average molecular weights ( $M_n$ ) and molecular weight distributions ( $PDI = M_w/M_n$ ) were measured by gel permeation chromatography (GPC) analyses carried out at 40 °C and a flow rate of 1.0 mL/min, with THF as the eluent on a Waters University 1500 GPC instrument equipped with one PLgel 5  $\mu$ m guard and three PLgel 5  $\mu$ m mixed-C columns (Polymer Laboratories; linear range of molecular weight = 200–2,000,000). The instrument was calibrated with 10 PMMA standards, and chromatograms were processed with Waters Empower software (version 2002).  $^1H$  NMR spectra for the analysis of PMMA microstructures were recorded in  $CDCl_3$  and analyzed according to the literature methods.<sup>13,18,72</sup>

**Models and Computational Details.** The Amsterdam Density Functional (ADF) program was used to obtain all the results concerned with the mechanism of stereoselectivity.<sup>73</sup> The electronic configuration of the molecular systems was described by a triple- $\zeta$  STO basis set on Ti and Zr (ADF basis set TZV).<sup>73a</sup> Triple- $\zeta$  STO basis sets, augmented by one polarization function, were used for main group atoms (ADF basis sets TZVP).<sup>73a</sup> The inner shells on Ti and Zr (including 2p and 3d, respectively), Si (including 2p), C, N and O (1s), were treated within the frozen core approximation. Energies and geometries were evaluated using the local exchange-correlation potential by Vosko et al.,<sup>74</sup> augmented in a self-consistent manner with Becke's<sup>75</sup> exchange gradient correction and Perdew's<sup>76</sup> correlation gradient correction (BP86 functional). All geometries were localized in the gas phase. However, since MMA polymerization is usually performed in a rather polar solvent, such as  $CH_2Cl_2$ , we performed single point energy

calculations on the final geometries to take into account solvent effects. The ADF implementation of the conductor-like screening model (COSMO)<sup>77</sup> was used. A dielectric constant of 8.9, and a solvent radius of 2.94 Å were used to represent CH<sub>2</sub>Cl<sub>2</sub> as the solvent. The following radii, in Å, were used for the atoms: H 1.16, C 2.00, N 1.40, O 1.50, Si 2.20, Ti 2.30 and Zr 2.40. All the reported energies include solvent effects.

The Turbomole (TM) package<sup>78</sup> was used to obtain all the results concerned with the mechanism of site-epimerization. The electronic configuration of the molecular systems was described by a triple- $\zeta$  basis set on Ti (TM basis set def-TZVP).<sup>79</sup> A double- $\zeta$  basis set, augmented by one polarization function were used for main group atoms (TM basis sets def-SVP).<sup>79</sup> Core electrons of Zr (up to 3d) were treated with the Stuttgart-Dresden pseudopotential.<sup>80</sup> Energies and geometries were evaluated with the BP86 functional. Solvent effects (both CH<sub>2</sub>Cl<sub>2</sub> and toluene, with a dielectric constant of 8.9 and 2.38, respectively) were evaluated with the COSMO model through single point energy calculations on the final gas-phase geometries. The following radii, in Å, were used for the atoms: H 1.404, C 1.989, N 1.813, O 1.778, Si 2.457, Ti 2.223. All the reported energies include solvent effects.

## Results and Discussion

**Kinetics of Polymerization by the (CGC)Ti Catalyst.** MMA polymerization by the cationic alkyl complex **1** was detailed in several publications.<sup>6,18,28</sup> The living and high-efficiency polymerization by the thermally stable alkyl complex **1** implies that  $k_i$  (rate of initiation) by the Ti-*Me* ligand is  $\geq k_p$  (rate of propagation) by the Ti-*ester enolate* ligand, derived from the initiation step involving nucleophilic attack of the Ti methyl group at the MMA coordinated to the cationic Ti center, and that this polymerization is largely devoid of chain termination or transfer side reactions. This feature renders **1** ideal for investigation of its polymerization kinetics. However, there is no report on such a study, and consequently a fundamental question of whether

this polymerization by the  $C_5$ -ligated complex **1** follows the same kinetics as that by the  $C_2$ -ligated unimetallic complex,<sup>9</sup> or not, remained unaddressed. This information is also needed for elucidating the mechanisms of the polymerization and stereocontrol (*vide infra*). To this end, we set out to examine the kinetics of the MMA polymerization by **1**, the results of which were summarized in Figure 1.

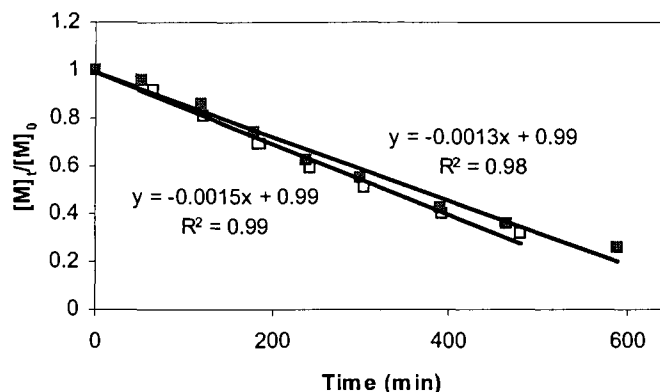
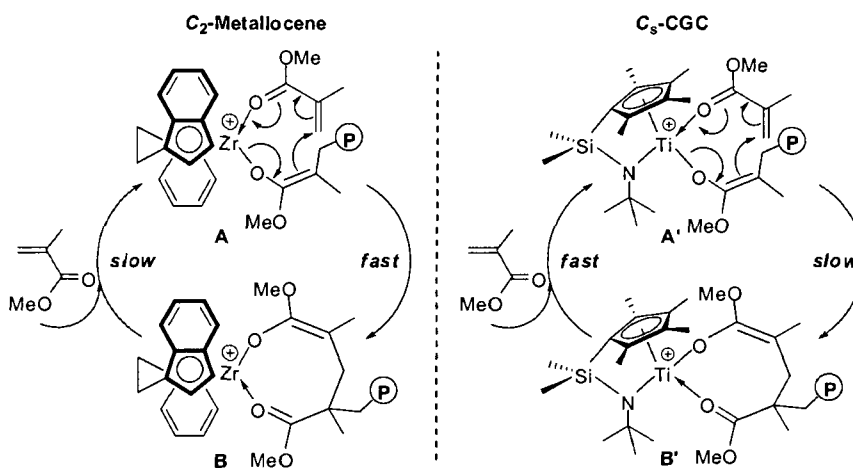


**Figure 1.** Zero-order plots of  $[MMA]_t/[MMA]_0$  vs. time for the polymerization of MMA by **1** in toluene (■) and  $CH_2Cl_2$  (□) at 25 °C. Conditions: 9.35 mmol MMA, 46.8  $\mu$ mol (CGC)TiMe<sub>2</sub> and B(C<sub>6</sub>F<sub>5</sub>)<sub>3</sub> in 10 mL of a solvent for a  $[MMA]_0/[1]_0$  ratio of 200.

Intriguingly, the MMA polymerization by **1** in either toluene or  $CH_2Cl_2$  follows zero-order kinetics with respect to MMA concentration (Figure 1). This result is in sharp contrast to the first-order kinetics observed for the *ansa*- $C_2$ -ligated catalyst in which propagation “catalysis” cycle intramolecular conjugate Michael addition in catalyst-monomer complex **A** leading to the eight-membered-ring cyclic ester enolate chelate (resting active intermediate **B**) is *fast* relative to associative displacement of the coordinated ester group in **B** by the incoming monomer (i.e., the rate-limiting ring-opening of the chelate) to regenerate **A** (Scheme 2).<sup>9</sup> Conversely, the zero-order kinetics in  $[MMA]$  observed for the (CGC)Ti catalyst **1** suggests a different scenario: Michael addition in catalyst-monomer complex **A'** leading to the cyclic chelate **B'** is *slow* relative to associative displacement of the coordinated ester group in **B'** by the incoming monomer (Scheme 2). The observed similar rates of polymerization ( $k_{app} = 1.3 \times 10^{-3}$  mol/L·s<sup>-1</sup> in toluene and  $1.5 \times 10^{-3}$  mol/L·s<sup>-1</sup> in  $CH_2Cl_2$ , Figure 1) are consistent with the MMA addition being the rate-determining

step. This unique observation for the unimetallic MMA propagation system **1**<sup>18</sup> that exhibits a relatively faster ring-opening process provides a kinetic basis for feasible pathways leading to MMA- or anion-assisted epimerization at Ti before MMA additions (*vide infra*).

Scheme 2



**Effects of Monomer and Catalyst Concentrations, Anion Structure, and Solvent Polarity on Syndiotacticity.** To ascertain if the monomer concentration would affect the resulting PMMA syndiotacticity, we kept  $[1]_0$  constant (4.67 mM in toluene) and varied  $[MMA]_0$  by 12-fold (i.e., from 2.81 M to 0.234 M). The polymerizations were carried out at  $T_p$  of 25 °C for 12 h, achieving high MMA conversions (93–99%) for all of the  $[MMA]_0/[1]_0$  ratios employed. Interestingly, the syndiotacticity  $[rr]$  was kept within a 77% – 74% range over a 12-fold  $[MMA]$  change and is thus largely  $[MMA]$ -invariant considering typical errors associated with the tacticity measurement being  $\leq 2\%$ . The  $mr$  (in a 19% – 22% range) and  $mm$  (in a 3% – 4% range) stereoerrors are also insensitive to monomer concentration. Likewise, the same polymerization carried out in  $CH_2Cl_2$  gave similar results (runs 1–4, Table 1). Lastly, a 4-fold reduction of the catalyst concentration while keeping  $[MMA]$  the same yielded identical tacticities (run 5 vs. run 3). Overall, the syndiotacticity of the C<sub>5</sub>-ligated (CGC)Ti catalyst **1** is insensitive to both concentrations of monomer and catalyst as well as to solvent polarity (more on this point is

described below), and the resulting syndiotactic PMMA contains predominately isolated *m* stereoerrors. This observation can be explained by a scenario in which the syndioselectivity of the polymerization is regulated by the chiral catalyst site and catalyst site-epimerization after a stereomistake is responsible for the isolated *m* stereoerrors (vide infra).

**Table 1.** Selected MMA Polymerization Results by (CGC)TiMe<sup>+</sup>MeB(C<sub>6</sub>F<sub>5</sub>)<sub>3</sub><sup>-</sup> (**1**)<sup>a</sup>

run no.	[ <b>1</b> ] (mM)	[MMA] (M)	[MMA] <sub>0</sub> /[ <b>1</b> ] <sub>0</sub>	[ <i>rr</i> ] <sup>b</sup> (%)	[ <i>mr</i> ] <sup>b</sup> (%)	[ <i>mm</i> ] <sup>b</sup> (%)
1	4.67	1.87	400	78	19	3
2	4.67	0.935	200	79	19	2
3	4.67	0.467	100	79	19	2
4	4.67	0.234	50	76	21	3
5	1.17	0.467	400	79	19	2

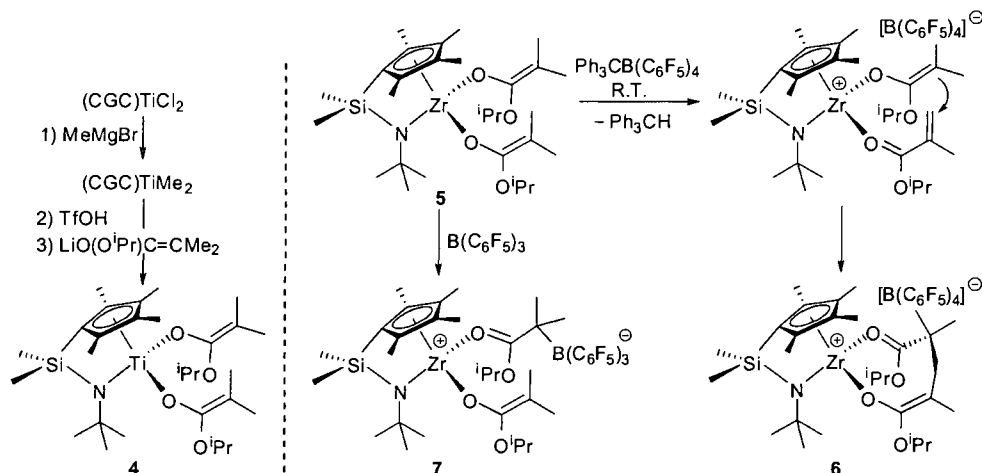
<sup>a</sup> Carried out in an argon-filled glovebox at ambient temperature (~25 °C) in CH<sub>2</sub>Cl<sub>2</sub> for 12 h. <sup>b</sup> Tacticity measured by <sup>1</sup>H NMR.

Next, we examined potential effects of ion-pairing strength, varied with anion structure and solvent polarity, on the syndioselectivity of the polymerization by the (CGC)Ti catalyst. Under identical conditions (9.35 mmol MMA, 46.8 μmol (CGC)TiMe<sub>2</sub> and activator, [MMA]<sub>0</sub>/[Ti]<sub>0</sub> = 200, 10 mL toluene, 25 °C), the catalyst systems derived from activation of (CGC)TiMe<sub>2</sub> with B(C<sub>6</sub>F<sub>5</sub>)<sub>3</sub>, [Ph<sub>3</sub>C][B(C<sub>6</sub>F<sub>5</sub>)<sub>4</sub>], and [HNMe<sub>2</sub>Ph][B(C<sub>6</sub>F<sub>5</sub>)<sub>4</sub>] gave syndiotactic PMMA with the syndiotacticity kept within a 77% *rr* – 80% *rr* range, showing negligible anion effect. Additionally, for all of the above three systems investigated there is no noticeable syndiotacticity change (< 2% *rr*) by switching the solvent from toluene to polar, essentially non-coordinating CH<sub>2</sub>Cl<sub>2</sub>. In short, these results indicate that, *in marked contrast* to the propylene polymerization by C<sub>s</sub>-symmetric metallocene catalysts,<sup>81</sup> ion-pairing has little to negligible effects on the syndioselectivity of the MMA polymerization by the C<sub>s</sub>-symmetric (CGC)Ti catalyst.

**Effects of Metal (Zr vs. Ti) on Syndioselectivity.** Unlike the (CGC)Ti complex **1**, the isostructural Zr alkyl complex (CGC)ZrMe<sup>+</sup>MeB(C<sub>6</sub>F<sub>5</sub>)<sub>3</sub><sup>-</sup> is inactive for the polymerization of MMA, prohibiting us from making a direct comparison using these (CGC)M alkyl complexes. Accordingly, we set out the synthesis of their identical bis(ester enolate) complexes **4** and **5**

(Scheme 3) because the cationic (CGC)Zr *tert*-butyl ester enolate complex **3** has been shown to be active for MMA polymerization at low  $T_p$ .<sup>34</sup>

Scheme 3



We elected to synthesize their *isopropyl* isobutyrate complexes because neutral metallocene *methyl* isobutyrate complexes and cationic *tert*-butyl isobutyrate complexes are not stable at room temperature due to ketene formation and isobutylene elimination,<sup>19,34</sup> respectively, whereas both neutral and cationic metallocene *isopropyl* isobutyrate complexes are stable at room temperature.<sup>13</sup> Indeed, both neutral (CGC)Ti and Zr bis(*isopropyl* ester enolate) complexes **4** and **5** as well as the cationic ester enolate (CGC)Zr complex **6** were successfully isolated (Scheme 3 and Experimental). The (CGC)Zr bis(ester enolate) complex **5** was obtained in a straightforward fashion, that is, one-step reaction of (CGC)ZrCl<sub>2</sub> with Me<sub>2</sub>C=C(O<sup>i</sup>Pr)OLi. The same route failed to give the isostructural (CGC)Ti bis(ester enolate) complex **4**; however, its synthesis was accomplished by a three-step route: methylation of (CGC)TiCl<sub>2</sub> to give (CGC)TiMe<sub>2</sub>, protonolysis with triflic acid to yield (CGC)Ti(OTf)<sub>2</sub>, and nucleophilic ligand substitution with Me<sub>2</sub>C=C(O<sup>i</sup>Pr)OLi to afford **4**. The cationic (CGC)Zr ester enolate complex **6** was generated by oxidative activation of **5** using [Ph<sub>3</sub>C][B(C<sub>6</sub>F<sub>5</sub>)<sub>4</sub>] via a pathway that has already been demonstrated for another C<sub>s</sub>-ligated zirconocene bis(ester enolate) catalyst precursor with a

different ligand framework;<sup>10</sup> the entire activation process involves hydride abstraction from the methyl group within the enolate [OC(O<sup>i</sup>Pr)=CMe<sub>2</sub>] moiety by [Ph<sub>3</sub>C]<sup>+</sup>, followed by nucleophilic addition of another enolate ligand to the resulting isopropyl methacrylate coordinated to the metal center, finally affording the cationic eight-membered-ring active species **6**.

Results of the MMA polymerization at ambient temperature by the bis(ester enolate) complexes **4** and **5** activated with three different types of activators were summarized in Table 2. The B(C<sub>6</sub>F<sub>5</sub>)<sub>3</sub>-activation of the Zr complex **5** generates the tight ion-pairing complex **7**, which exhibits low activity, but nonetheless affords syndiotactic PMMA at 25 °C (70% *rr*, PDI = 1.15, run 1). Addition of another equiv of B(C<sub>6</sub>F<sub>5</sub>)<sub>3</sub> slightly increased MMA conversion from 20% to 26% but left the syndiotacticity and PDI values unchanged (runs 2 vs 1); this experiment ruled out the possible bimetallic pathway contributing to the observed syndiotacticity (the *rr* is 64% when 0.5 equiv of B(C<sub>6</sub>F<sub>5</sub>)<sub>3</sub> relative to **5** or Cp<sub>2</sub>Zr[OC(O<sup>i</sup>Pr)=CMe<sub>2</sub>]<sub>2</sub> was used for the bimetallic system). Similar B(C<sub>6</sub>F<sub>5</sub>)<sub>3</sub>-activation products of C<sub>2</sub>- and C<sub>2v</sub>-ligated Zr analogues and their polymerization characteristics have been observed previously<sup>7,82</sup> On the other hand, the **5** + 2Al(C<sub>6</sub>F<sub>5</sub>)<sub>3</sub> system gave quantitative MMA conversion, while the **5** + Al(C<sub>6</sub>F<sub>5</sub>)<sub>3</sub> system achieved only 66% under the same conditions, although the syndiotacticity (72% *rr*) of the resulting PMMA is identical (runs 4 vs 3); this observation can be attributed to the propagation onto the enolaluminate intermediate for the metallocene + Al(C<sub>6</sub>F<sub>5</sub>)<sub>3</sub> system.<sup>7,23,32,82</sup>

**Table 2.** Selected MMA Polymerization Results by (CGC)M[bis(ester enolate)] Complexes **4** and **5**<sup>a</sup>

run no.	metal (mM)	activator (x equiv)	[MMA]/[metal]	solvent <sup>b</sup>	temp (°C)	time (h)	conv. (%)	[ <i>rr</i> ] (%)
1	<b>5</b> (2.13)	B(C <sub>6</sub> F <sub>5</sub> ) <sub>3</sub>	400	DCM	25	21	20	70
2	<b>5</b> (2.13)	B(C <sub>6</sub> F <sub>5</sub> ) <sub>3</sub> (2)	400	DCM	25	21	26	70
3	<b>5</b> (2.13)	Al(C <sub>6</sub> F <sub>5</sub> ) <sub>3</sub>	400	DCM	25	3	66	72
4	<b>5</b> (2.13)	Al(C <sub>6</sub> F <sub>5</sub> ) <sub>3</sub> (2)	400	DCM	25	3	100	72
5	<b>5</b> (38)	[HNMe <sub>2</sub> Ph][B(C <sub>6</sub> F <sub>5</sub> ) <sub>4</sub> ]	187.5	DCM + T	25	24	67	43
6	<b>4</b> (38)	[HNMe <sub>2</sub> Ph][B(C <sub>6</sub> F <sub>5</sub> ) <sub>4</sub> ]	187.5	DCM + T	25	24	100	74

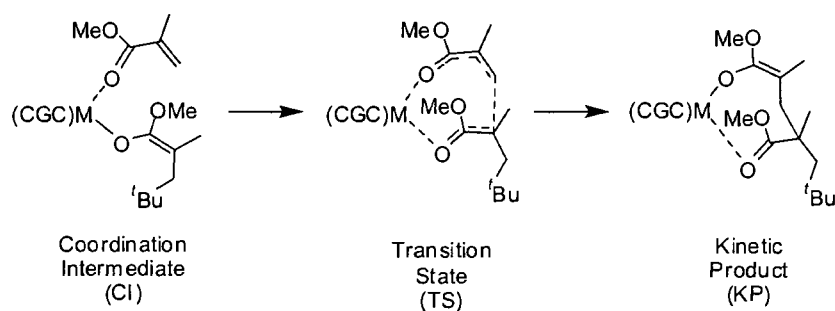
<sup>a</sup> Monomer conversion (%) and syndiotacticity (% *rr*) determined by <sup>1</sup>H NMR; T<sub>p</sub> = ~ 25 °C. <sup>b</sup> 10 mL of dichloromethane (DCM) when DCM used alone, or 0.25 mL DCM (activator solution) plus 0.25 mL T (toluene solution of the metal complex) when DCM and T mixed together (DCM + T).

The MMA polymerization of **5** activated with the protonolysis activator [HNMe<sub>2</sub>Ph][B(C<sub>6</sub>F<sub>5</sub>)<sub>4</sub>], an increased catalyst concentration, and the use of a CH<sub>2</sub>Cl<sub>2</sub>/toluene mixture produced syndio-enriched atactic PMMA (43% *rr*, run 5). Switching to the (CGC)Ti complex **4** with the same [HNMe<sub>2</sub>Ph][B(C<sub>6</sub>F<sub>5</sub>)<sub>4</sub>] activator significantly increased the PMMA syndiotacticity to 74% *rr* (run 6). The above results show that both (CGC)Ti and Zr isopropyl ester enolate catalyst systems derived from the activators currently employed are syndioselective at ambient temperature and the (CGC)Ti system exhibits higher syndioselectivity.

### Computational Insights into the Mechanism of MMA Polymerization

In this section we provide a computational rationalization of the chemical scenario resulting from the experiments. Specifically, we focused on the Michael-addition step (Scheme 4). Since the experimental results indicate that the counterion has negligible effects on the syndioselectivity of the polymerization, the models we used to investigate the chain growth step did not include the counterion, and we started from the coordination intermediate (CI). The reaction follows with MMA-addition through the transition state (TS) for the Michael addition and collapses to a species we called the kinetic product (KP). We calculated these steps for both Ti and Zr systems and considered the two enantiofaces of the ester enolate growing chain, which means we focused on the enantioselectivity of the MMA addition. In all cases we considered an *S* chirality at the metal. Finally, based on our previous theoretical results, we only focused on transition states presenting a relative *trans* disposition of the methoxy groups of both the growing chain and the monomer.<sup>56,57</sup>

#### Scheme 4



As shown in Figure 2, for both the Ti and Zr systems the *re*-face of the enolate growing chain reacts preferentially in the case of an *S*-chirality at the metal. In both systems there is a selection of the *re*-face of the chain even at the coordination intermediate, although enantioselectivity is determined by the energy difference at the transition state. Within this framework the  $\Delta E_{\text{Stereo}}$  is 2.3 and 1.9 kcal/mol for the Ti and Zr systems, respectively. This result means that both systems are enantioselective, although the Ti system is somewhat more enantioselective than the Zr analogue, which is in qualitative agreement with our experimental findings. Finally, there is a non-negligible energy difference also in the kinetic products that correspond to the 8-membered cycles that are obtained from collapsing the two transition states on the products side. The exothermicity of the chain growth step from the coordination intermediate to the products is  $\sim 5$  kcal/mol, which is remarkably smaller than that of ethene or propene polymerization ( $\sim 20$  kcal/mol).<sup>83</sup>

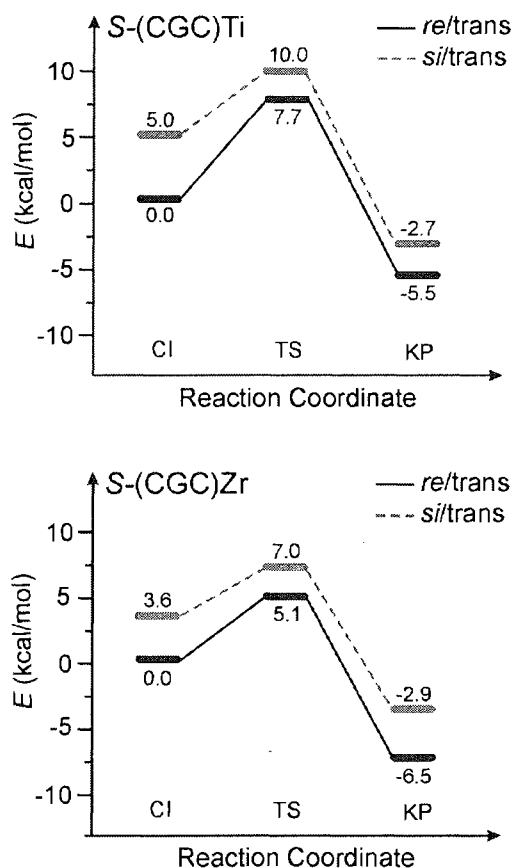


**Figure 2.** Energy diagrams for MMA addition to the *S*-metal center (energies in kcal/mol).

The geometries of the two competing transition states of the (CGC)Ti system are shown in Figure 3. It is clear that the opposite enantiofaces of the enolate chain result in rather different orientation of the growing chain with respect to the bulky Cp' ( $\eta^5$ -Me<sub>4</sub>C<sub>5</sub>) ligand. In the favored transition state (*re*-chain with an *S*-metal) the bulky <sup>t</sup>Bu group of the growing chain is oriented towards the N-group and away from the Cp' ligand, whereas in the unfavored transition state (*si*-chain with an *S*-metal) the bulky <sup>t</sup>Bu group of the growing chain sterically interacts with the Cp' ligand. This steric interaction is more relevant at the level of 8-membered products, when the new C–C bond is completely formed and the back-bonding of the chain pulls the <sup>t</sup>Bu group in close proximity of the Cp' ligand.

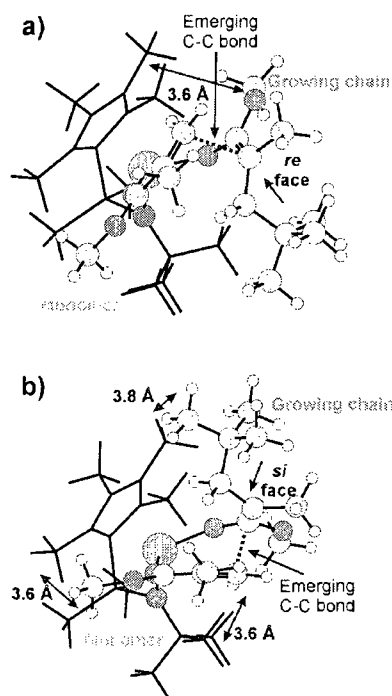


**Figure 3.** Transition states for MMA addition with the (CGC)Ti system with an *S* configuration at the Ti atom. Atoms depicted in spheres are Ti in orange, O in red, N in blue, C in gray, and H in white.

The 8-membered product corresponding to the favored transition state (*S*-metal/*re*-chain) is 2.8 and 3.6 kcal/mol lower in energy than the product corresponding to a stereomistake (*S*-metal/*si*-chain) for the Ti and Zr systems, respectively. This result suggests that there might be a rearrangement of the kinetic product corresponding to the stereomistake toward a more stable resting state. This rearrangement involves a site-epimerization reaction, as shown in Scheme 5. Owing to this site-epimerization reaction, the higher energy kinetic product corresponding to a stereomistake (*S*-metal/*si*-chain) evolves into the *R*-metal/*si*-chain resting state that, by symmetry, is isoenergetic with the thermodynamic *S*-metal/*re*-chain product that is obtained from the favored transition state. To check whether this site-epimerization reaction is possible, we started to break the back-bonding of the last C=O (ester) unit. However, in the gas-phase or even in the presence of solvent effects dissociation of the last C=O unit from the metal is energetically quite



after a stereomistake (**8** in both Scheme 5 and Figure 4) is disfavored by 1.7 and 3.2 kcal/mol respectively in CH<sub>2</sub>Cl<sub>2</sub>, and by 1.6 and 2.9 kcal/mol in toluene, with respect to the *S*-metal/*re*-chain product after a correct enantiofacial addition or, equivalently, to the *R*-metal/*si*-chain thermodynamic product (**11** in both Scheme 5 and Figure 4) that can be reached after site epimerization. The energy difference of 3.2 kcal/mol in the presence of the counterion in CH<sub>2</sub>Cl<sub>2</sub> substantially replicates the energy difference we calculated in its absence of the (CGC)Ti system (see Figure 2). The assistance of the counterion or a MMA molecule results in a very smooth energy profile for the site epimerization reaction, since the two intermediates without a back-bonded C=O group (**9** and **10** in both Scheme 5 and Figure 4) are remarkably stabilized by a tightly bound counterion or a temporarily coordinated MMA molecule. Further, substitution of the coordinated C=O of the last unit of the chain from the C=O of a MMA molecule results in a rather flat energy profile, whereas displacement by the counterion is less favored, which suggests that the C=O group coordinates better to the metal than the counterion. Further evidence of the preferential coordination of the C=O group to the metal with respect to coordination of the counterion is obtained by a comparison between **8** and **9** in the counterion assisted site-epimerization pathway. Both in toluene and in CH<sub>2</sub>Cl<sub>2</sub> the preferred situation is an outer-sphere ion pair with a back-bonding of the last C=O group, structure **8**, rather than an inner-sphere ion pair with no back-bonding from C=O groups of the PMMA chain, structure **9**. This preference is higher in the more polar CH<sub>2</sub>Cl<sub>2</sub> solvent, 9.4 in CH<sub>2</sub>Cl<sub>2</sub> vs 7.1 kcal/mol in toluene, since the counterion/cation interaction is mainly electrostatic in nature, and is thus reduced in more polar solvents.

To investigate in more details the relative strength of the C=O⋯Ti and [MeB(C<sub>6</sub>F<sub>5</sub>)<sub>3</sub>]<sup>-</sup>⋯Ti interactions as well as their dependence on solvent effects, we calculated the coordination energy of a MMA molecule and of the MeB(C<sub>6</sub>F<sub>5</sub>)<sub>3</sub><sup>-</sup> counterion to the (CGC)Ti-OMe<sup>+</sup> system. The presence of a simple methoxy group bonded to the metal avoids any complicity connected to the removal of a back-bonded C=O and/or to the different steric hindrance of the MMA molecule and

of the  $\text{MeB}(\text{C}_6\text{F}_5)_3^-$  counterion. Our calculations indicate that in the low polar toluene solvent the  $\text{MeB}(\text{C}_6\text{F}_5)_3^-$  counterion is bound to the metal quite more strongly than MMA (45.7 vs. 30.1 kcal/mol). Increasing the polarity of the solvent results in a sharp decrease of the binding energy of the  $\text{MeB}(\text{C}_6\text{F}_5)_3^-$  counterion (from 45.7 to 23.4 kcal/mol on going from toluene to  $\text{CH}_2\text{Cl}_2$ ), which is reasonable considering that the interaction between the counterion and the catalyst, as previously indicated, is mainly electrostatic in nature. The binding energy of the MMA molecule, instead, is substantially independent from the polarity of the medium (from 30.1 to 27.3 kcal/mol on going from toluene to  $\text{CH}_2\text{Cl}_2$ ).

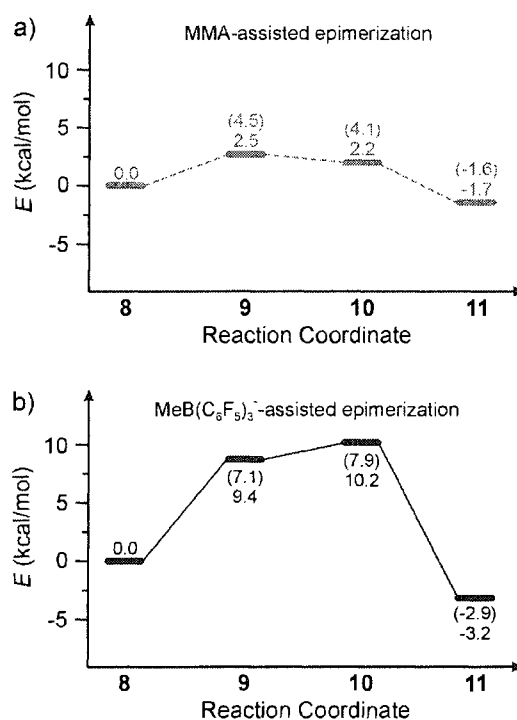


**Figure 4.** Energy profiles for the site-epimerization reaction from the kinetic product after a stereomistake (**8**), to the thermodynamic resting state **11**. Energies are in kcal/mol, and results are reported for both MMA and counterion assisted epimerizations in  $\text{CH}_2\text{Cl}_2$  and toluene (numbers in parenthesis).

These findings support the main mechanistic scenario which emerged from the experiments. That is, the presence of the isolated *m* stereomistakes can be reasonably explained with catalyst site-epimerization *after a stereomistake*, which converts a higher-energy kinetic

product to a thermodynamically more stable resting state. The driving force for the site-epimerization reaction originates from steric interaction between the growing chain after a stereomistake and the Cp' ligand. As an additional remark, we note that higher stability of the 8-membered cycle after correct enantiofacial additions is also a key to rationalize the formation of highly stereoregular syndiotactic PMMA. In fact, there is no tendency for these systems to undergo catalyst site-epimerization after correct enantiofacial addition, which would decrease stereoregularity. This observation highlights another remarkable difference between MMA and propene polymerizations using metallocene-based catalysts.

## Conclusions

In summary, the experimental work on the MMA polymerization by the (CGC)M catalysts has revealed additional important features about this polymerization. First, the MMA polymerization by the living/controlled cationic (CGC)Ti alkyl complex **1** follows the zero-order kinetics in MMA concentration; this implies that, in a unimetallic propagation “catalysis” cycle, displacement of the coordinated ester group in the cyclic intermediate by the incoming monomer (ring-opening of the chelate) is fast relative to intramolecular conjugate MMA addition within the catalyst-monomer complex. This observation provides a kinetic basis for pathways leading to catalyst-site epimerization at Ti before MMA additions. Second, there exhibits negligible effects on the syndiotacticity of the polymerization by monomer and catalyst concentrations as well as ion-pairing strength varied with anion structure and solvent polarity. Third, we have synthesized two neutral (CGC)Ti and Zr bis(isopropyl ester enolate) complexes as well as two cationic complexes derived therefrom for the comparative study that required the use of the same bis(ester enolate) complexes. The MMA polymerization results show that both the present (CGC)Ti and Zr ester enolate catalysts are syndioselective at ambient temperature and the (CGC)Ti system exhibits higher syndioselectivity at this temperature.

On the theoretical side, density functional calculations rationalized the higher syndioselectivity exhibited by the (CGC)Ti catalysts but, more importantly, provided a theoretical support to the catalyst site-epimerization mechanism accounting for the formation of the predominately isolated *m* stereoerrors and indicated the driving force for an almost regular site-epimerization reaction after a stereomistake being in the higher energy of the 8-membered cycle formed after a stereomistake. This MMA- or anion-assisted catalyst site-epimerization reaction converts the kinetic product after a stereomistake into a thermodynamically more stable resting state.

**Acknowledgment.** This experimental work was supported by the National Science Foundation (NSF-0718061) for the work carried out at Colorado State University and the theoretical work was supported by Lyondell-Basell Polyolefins and INSTM (Cineca Grant) for the work carried out at the University of Salerno. We thank Boulder Scientific Co. for the research gifts of  $B(C_6F_5)_3$ ,  $[Ph_3C][B(C_6F_5)_4]$ , and  $[HNMe_2Ph][B(C_6F_5)_4]$ .

## References

---

- (1) Selected reviews: (a) Chen, E. Y.-X.; Rodriguez-Delgado, A. in *Comprehensive Organometallic Chemistry III*; Bochmann, M. Vol. Ed.; Mingos, M. P.; Crabtree, R. H. Chief Eds.; Elsevier: Oxford, **2007**; Vol. 4, pp 759–1004. (b) Cuenca, T. in *Comprehensive Organometallic Chemistry III*; Bochmann, M. Vol. Ed.; Mingos, M. P.; Crabtree, R. H. Chief Eds.; Elsevier: Oxford, **2007**; Vol. 4, pp 323–696. (c) Bochmann, M. *J. Chem. Soc. Dalton Trans.* **1996**, 255–270. (d) Jordan, R. F. *Adv. Organomet. Chem.* **1991**, *32*, 325–387.
- (2) Selected books, book chapters, or special journal issues: (a) *Stereoselective Polymerization with Single-Site Catalysts*, Baugh, L. S.; Canich, J. A. M., Eds.; CRC Press: Boca Raton, FL, **2008**. (b) Resconi, L.; Chadwick, J. C.; Cavallo, L. in *Comprehensive Organometallic Chemistry III*; Bochmann, M. Vol. Ed.; Mingos, M. P.; Crabtree, R. H. Chief Eds.; Elsevier: Oxford, **2007**; Vol. 4, pp 1005–1166. (c) Marks, T. J. Ed. *Proc. Natl. Acad. Sci. U.S.A.* **2006**, *103*, 15288–15354 and contributions therein (issue on “*Polymerization Special Feature*”). (d) Gladysz, J. A., Ed. *Chem. Rev.* **2000**, *100*, 1167–1681 and contributions therein (issue on *Frontiers in Metal-Catalyzed Polymerization*). (e) Marks, T. J.; Stevens, J. C.; Eds. *Top. Catal.* **1999**, *7*, 1–208 and contributions therein (issue on *Advances in Polymerization Catalysis. Catalysts and Processes*). (f) *Metalorganic Catalysts for Synthesis and Polymerization: Recent Results by Ziegler-Natta and Metallocene Investigations*; Kaminsky, W.; Ed. Springer-Verlag: Berlin, **1999**. (g) Jordan, R. F. Ed. *J. Mol. Catal. A: Chem.* **1998**, *128*, 1–337 and contributions therein (issue on *Metallocene and Single-Site Olefin Catalysts*). (h) *Metallocenes: Synthesis – Reactivity – Applications*, Togni A., Halterman, R. L., Eds.; Wiley-VCH: Weinheim, **1998**. (i) *Ziegler Catalysts*; Mülhaupt, R.; Brintzinger, H.-H.; Eds. Springer-Verlag: Berlin, **1995**. (j) Soga,

- 
- K.; Terano, M.; Eds. *Stud. Sur. Sci. Catal.* **1994**, *89*, 1–410 and contributions therein (issue on *Catalyst Design for Tailor-Made Polyolefins*).
- (3) Selected reviews: (a) Chen, E. Y.-X. *J. Polym. Sci. Part A: Polym. Chem.* **2004**, *42*, 3395–3403. (b) Boffa, L. S.; Novak, B. M. *Chem. Rev.* **2000**, *100*, 1479–1493.
- (4) Ning, Y.; Chen, E. Y.-X. *J. Am. Chem. Soc.* **2008**, *130*, 2463–2465.
- (5) Mariott, W. R.; Escudé, N. C.; Chen, E. Y.-X. *J. Polym. Sci. Part A: Polym. Chem.* **2007**, *45*, 2581–2592.
- (6) Lian, B.; Thomas, C. M.; Navarro, C.; Carpentier, J.-F. *Organometallics* **2007**, *26*, 187–195.
- (7) Ning, Y.; Chen, E. Y.-X. *Macromolecules* **2006**, *39*, 7204–7215.
- (8) Rodriguez-Delgado, A.; Mariott, W. R.; Chen, E. Y.-X. *J. Organomet. Chem.* **2006**, *691*, 3490–3497.
- (9) Rodriguez-Delgado, A.; Chen, E. Y.-X. *Macromolecules* **2005**, *38*, 2587–2594.
- (10) Kostakis, K.; Mourmouris, S.; Kotakis, K.; Nikogeorgos, N.; Pitsikalis, M.; Hadjichristidis, N. *J. Polym. Sci. Part A: Polym. Chem.* **2005**, *43*, 3305–3314.
- (11) Ning, Y.; Cooney, M. J.; Chen, E. Y.-X. *J. Organomet. Chem.* **2005**, *690*, 6263–6270.
- (12) Lian, B.; Lehmann, C. W.; Navarro, C.; Carpentier, J.-F. *Organometallics* **2005**, *24*, 2466–2472.
- (13) Bolig, A. D.; Chen, E. Y.-X. *J. Am. Chem. Soc.* **2004**, *126*, 4897–4906.
- (14) Stojcevic, G.; Kim, H.; Taylor, N. J.; Marder, T. B.; Collins, S. *Angew. Chem. Int. Ed.* **2004**, *43*, 5523–5526.
- (15) Strauch, J. W.; Fauré, J.-L.; Bredeau, S.; Wang, C.; Kehr, G.; Fröhlich, R.; Luftmann, H.; Erker, G. *J. Am. Chem. Soc.* **2004**, *126*, 2089–2104.
- (16) Karanikolopoulos, G.; Batis, C.; Pitsikalis, M.; Hadjichristidis, N. *J. Polym. Sci. Part A: Polym. Chem.* **2004**, *42*, 3761–3774.

- 
- (17) Ferenz, M.; Bandermann, F.; Sustmann, R.; Sicking, W. *Macromol. Chem. Phys.* **2004**, *205*, 1196–1205.
- (18) Rodriguez-Delgado, A.; Mariott, W. R.; Chen, E. Y.-X. *Macromolecules* **2004**, *37*, 3092–3100.
- (19) Lian, B.; Toupet, L.; Carpentier, J.-F. *Chem. Eur. J.* **2004**, *10*, 4301–4307.
- (20) Jensen, T. R.; Yoon, S. C.; Dash, A. K.; Luo, L.; Marks, T. J. *J. Am. Chem. Soc.* **2003**, *125*, 14482–14494.
- (21) Chen, E. Y.-X.; Cooney, M. J. *J. Am. Chem. Soc.* **2003**, *125*, 7150–7151.
- (22) Mariott, W. R.; Chen, E. Y.-X. *J. Am. Chem. Soc.* **2003**, *125*, 15726–15727.
- (23) Jin, J.; Mariott, W. R.; Chen, E. Y.-X. *J. Polym. Chem. Part A: Polym. Chem.* **2003**, *41*, 3132–3142.
- (24) Batis, C.; Karanikolopoulos, G.; Batis, C.; Pitsikalis, M.; Hadjichristidis, N. *Macromolecules* **2003**, *36*, 9763–9774.
- (25) Karanikolopoulos, G.; Batis, C.; Pitsikalis, M.; Hadjichristidis, N. *Macromol. Chem. Phys.* **2003**, *204*, 831–840.
- (26) Bolig, A. D.; Chen, E. Y.-X. *J. Am. Chem. Soc.* **2002**, *124*, 5612–5613.
- (27) Jin, J.; Chen, E. Y.-X. *Organometallics* **2002**, *21*, 13–15.
- (28) Jin, J.; Wilson, D. R.; Chen, E. Y.-X. *Chem. Commun.* **2002**, 708–709.
- (29) Jin, J.; Chen, E. Y.-X. *Macromol. Chem. Phys.* **2002**, *203*, 2329–2333.
- (30) Bandermann, F.; Ferenz, M.; Sustmann, R.; Sicking, W. *Macromol. Symp.* **2001**, *174*, 247–253.
- (31) Karanikolopoulos, G.; Batis, C.; Pitsikalis, M.; Hadjichristidis, N. *Macromolecules* **2001**, *34*, 4697–4705.
- (32) Bolig, A. D.; Chen, E. Y.-X. *J. Am. Chem. Soc.* **2001**, *123*, 7943–7944.

- 
- (33) Frauenrath, H.; Keul, H.; Höcker, H. *Macromolecules* **2001**, *34*, 14–19.
- (34) Nguyen, H.; Jarvis, A. P.; Lesley, M. J. G.; Kelly, W. M.; Reddy, S. S.; Taylor, N. J.; Collins, S. *Macromolecules* **2000**, *33*, 1508–1510.
- (35) Bandermann, F.; Ferenz, M.; Sustmann, R.; Sicking, W. *Macromol. Symp.* **2000**, *161*, 127–134.
- (36) Cameron, P. A.; Gibson, V.; Graham, A. J. *Macromolecules* **2000**, *33*, 4329–4335.
- (37) Stuhldreier, T.; Keul, H.; Höcker, H. *Macromol. Rapid Commun.* **2000**, *21*, 1093–1098.
- (38) Chen, E. Y.-X.; Metz, M. V.; Li, L.; Stern, C. L.; Marks, T. J. *J. Am. Chem. Soc.* **1998**, *120*, 6287–6305.
- (39) Shiono, T.; Saito, T.; Saegusa, N.; Hagihara, H.; Ikeda, T.; Deng, H.; Soga, K. *Macromol. Chem. Phys.* **1998**, *199*, 1573–1579.
- (40) Hong, E.; Kim, Y.; Do, Y. *Organometallics* **1998**, *17*, 2933–2935.
- (41) Li, Y.; Ward, D. G.; Reddy, S. S.; Collins, S. *Macromolecules* **1997**, *30*, 1875–1883.
- (42) Deng, H.; Shiono, T.; Soga, K. *Macromol. Chem. Phys.* **1995**, *196*, 1971–1980.
- (43) Deng, H.; Shiono, T.; Soga, K. *Macromolecules* **1995**, *28*, 3067–3073.
- (44) Soga, K.; Deng, H.; Yano, T.; Shiono, T. *Macromolecules* **1994**, *27*, 7938–7940.
- (45) Collins, S.; Ward, D. G.; Suddaby, K. H. *Macromolecules* **1994**, *27*, 7222–7224.
- (46) Collins, S.; Ward, S. G. *J. Am. Chem. Soc.* **1992**, *114*, 5460–5462.
- (47) Lian, B.; Thomas, C. M.; Navarro, C.; Carpentier, J.-F. *Macromolecules* **2007**, *40*, 2293–2294.
- (48) Mariott, W. R.; Rodriguez-Delgado, A.; Chen, E. Y.-X. *Macromolecules* **2006**, *39*, 1318–1327.
- (49) Kostakis, K.; Mourmouris, S.; Pitsikalis, M.; Hadjichristidis, N. *J. Polym. Sci. Part A: Polym. Chem.* **2005**, *43*, 3337–3348.

- 
- (50) Deng, H.; Soga, K. *Macromolecules* **1996**, *29*, 1847–1848.
- (51) Miyake, G. M.; Chen, E. Y.-X. *Macromolecules* **2008**, *41*, 3405–3416.
- (52) Miyake, G. M.; Mariott, W. R.; Chen, E. Y.-X. *J. Am. Chem. Soc.* **2007**, *129*, 6724–6725.
- (53) Mariott, W. R.; Chen, E. Y.-X. *Macromolecules* **2005**, *38*, 6822–6832.
- (54) Mariott, W. R.; Chen, E. Y.-X. *Macromolecules* **2004**, *37*, 4741–4743.
- (55) Spaether, W.; Klaß, K.; Erker, G.; Zippel, F.; Fröhlich, R. *Chem. Eur. J.* **1998**, *4*, 1411–1417.
- (56) Caporaso, L.; Cavallo, L. *Macromolecules* **2008**, *41*, 3439–3445.
- (57) Caporaso, L.; Gracia-Budría, J.; Cavallo, L. *J. Am. Chem. Soc.* **2006**, *128*, 16649–16654.
- (58) Tomasi, S.; Weiss, H.; Ziegler, T. *Organometallics* **2007**, *26*, 2157–2166.
- (59) Tomasi, S.; Weiss, H.; Ziegler, T. *Organometallics* **2006**, *25*, 3619–3630.
- (60) Hölscher, M.; Keul, H.; Höcker, H. *Macromolecules* **2002**, *35*, 8194–8202.
- (61) Hölscher, M.; Keul, H.; Höcker, H. *Chem. Eur. J.* **2001**, *7*, 5419–5426.
- (62) Sustmann, R.; Sicking, W.; Bandermann, F.; Ferez, M. *Macromolecules* **1999**, *32*, 4204–4213.
- (63) (a) Shapiro, P. J.; Cotter, W. D.; Schaefer, W. P.; Labinger, J. A.; Bercaw, J. E. *J. Am. Chem. Soc.* **1994**, *116*, 4623–4640. (b) Okuda, J. *Comments Inorg. Chem.* **1994**, *16*, 185–205. (c) Okuda, J. *Chem. Ber.* **1990**, *123*, 1649–1651. (d) Shapiro, P. J.; Bunel, E.; Schaefer, W. P.; Bercaw, J. E. *Organometallics* **1990**, *9*, 867–869. (e) Piers, W. E.; Shapiro, P. J.; Bunel, E.; Bercaw, J. E. *Synlett.* **1990**, *2*, 74–84.
- (64) (a) Guo, N.; Stern, C. L.; Marks, T. J. *J. Am. Chem. Soc.* **2008**, *130*, 2246–2261. (b) Motta, A.; Fragalà, I. L.; Marks, T. J. *J. Am. Chem. Soc.* **2007**, *129*, 7327–7338. (c) Gibson, V. C.; Spitzmesser, S. K. *Chem. Rev.* **2003**, *103*, 283–315. (d) Chum, P. S.; Kruper, W. J.; Guest, M. J. *Adv. Mater.* **2000**, *12*, 1759–1767. (e) McKnight, A. L.; Waymouth, R. M. *Chem. Rev.* **1998**, *98*, 2587–2598. (f) Stevens, J. C. *Stud. Surf. Sci. Catal.* **1996**, *101*, 11–20; **1994**,

- 
- 89, 277–284. (g) Canich, J. A. Eur. Pat. Appl., EP 0420436 A1, 1991. (h) Stevens, J. C.; Timmers, F. J.; Wilson, D. R.; Schmidt, G. F.; Nickias, P. N.; Rosen, R. K.; Knight, G. W.; Lai, S. Eur. Pat. Appl. EP 0 416815 A2, 1991.
- (65) Allen, R. D.; Long, T. E.; McGrath, J. E. *Polym. Bull.* **1986**, *15*, 127–134.
- (66) Feng, S.; Roof, G. R.; Chen, E. Y.-X. *Organometallics* **2002**, *21*, 832–839.
- (67) (a) Lee, C. H.; Lee, S. J.; Park, J. W.; Kim, K. H.; Lee, B. Y.; Oh, J. S. *J. Mol. Cat., A: Chem.* **1998**, *132*, 231–239. (b) Biagini, P.; Lugli, G.; Abis, L.; Andreussi, P. U.S. Pat. 5,602269, 1997.
- (68) (a) Resconi, L.; Camurati, I.; Grandini, C.; Rinaldi, M.; Mascellani, N.; Traverso, O. *J. Organomet. Chem.* **2002**, *664*, 5–26. (b) Carpentier, J.-F.; Maryin, V. P.; Luci, J.; Jordan, R. F. *J. Am. Chem. Soc.* **2001**, *123*, 898–909.
- (69) Chen, Y.-X.; Marks, T. J. *Organometallics* **1997**, *16*, 3649–3657.
- (70) Kim, Y.-J.; Bernstein, M. P.; Galiano Roth, A. S.; Romesberg, F. E.; Williard, P. G.; Fuller, D. J.; Harrison, A. T.; Collum, D. B. *J. Org. Chem.* **1991**, *56*, 4435–4439.
- (71) Rodriguez-Delgado, A.; Chen, E. Y.-X. *J. Am. Chem. Soc.* **2005**, *127*, 961–974.
- (72) (a) Brar, A. S.; Singh, G.; Shankar, R. *J. Mol. Struct.* **2004**, *703*, 69–81. (b) Bovey, F. A.; Mirau, P. A. *NMR of Polymers*; Academic Press: San Diego, CA, 1996. (c) Kawamura, T.; Toshima, N.; Matsuzaki, K. *Makromol. Chem., Rapid Commun.* **1993**, *14*, 719–724. (d) Chujo, R.; Hatada, K.; Kitamaru, R.; Kitayama, T.; Sato, H.; Tanaka, Y. *Polym. J.* **1987**, *19*, 413–424. (e) Ferguson, R. C.; Ovenall, D. W. *Macromolecules* **1987**, *20*, 1245–1248. (f) Ferguson, R. C.; Ovenall, D. W. *Polym. Prepr.* **1985**, *26*, 182–183. (g) Subramanian, R.; Allen, R. D.; McGrath, J. E.; Ward, T. C. *Polym. Prepr.* **1985**, *26*, 238–240.
- (73) (a) ADF2007, *Theoretical Chemistry, Vrije Universiteit, Amsterdam*, 2007, Users's Manual. (b) Baerends, E. J.; Ellis, D. E.; Ros, P. *Chem. Phys.* **1973**, *2*, 41–51.
- (74) Vosko, S. H.; Wilk, L.; Nusair, M. *Can. J. Phys.* **1980**, *58*, 1200–1211.

- 
- (75) Becke, A. D. *Phys. Rev. A* **1988**, *38*, 3098–3100.
- (76) (a) Perdew, J. P. *Phys. Rev. B* **1986**, *33*, 8822–8824. (b) Perdew, J. P. *Phys. Rev. B* **1986**, *34*, 7406–7406.
- (77) (a) Klamt, A.; Schüürmann, G. *J. Chem. Soc., Perkin Trans.* **1993**, 799–805. (b) Pye, C. C.; Ziegler, T. *Theor. Chem. Acc.* **1999**, *101*, 396–408.
- (78) Ahlrichs, R.; Bar, M.; Haser, M.; Horn, H.; Kolmel, C. *Chem. Phys. Lett.* **1989**, *162*, 165–169.
- (79) Weigend, F.; Ahlrichs, R. *Phys. Chem. Chem. Phys.* **2005**, *7*, 3297–3302.
- (80) (a) Haeusermann, U.; Dolg, M.; Stoll, H.; Preuss, H. *Mol. Phys.* **1993**, *78*, 1211–1224. (b) Kuechle, W.; Dolg, M.; Stoll, H.; Preuss, H. *J. Chem. Phys.* **1994**, *100*, 7535–7542. (c) Leininger, T.; Nicklass, A.; Stoll, H.; Dolg, M.; Schwerdtfeger, P. *J. Chem. Phys.* **1996**, *105*, 1052–1059.
- (81) Chen, M.-C.; Roberts, J. A. S.; Marks, T. J. *J. Am. Chem. Soc.* **2004**, *126*, 4605–4625.
- (82) Ning, Y.; Zhu, H.; Chen, E. Y.-X. *J. Organomet. Chem.* **2007**, *692*, 4535–4544.
- (83) Lohrenz, J. C. W.; Woo, T. K.; Ziegler, T. *J. Am. Chem. Soc.* **1995**, *117*, 12793–12800
- (84) Tomasi, S.; Razavi, A.; Ziegler, T. *Organometallics* **2007**, *26*, 2024–2036

## CHAPTER VII

### Neutral Metallocene Ester Enolate Complexes of Zirconium for Catalytic Ring-Opening Polymerization of Cyclic Esters

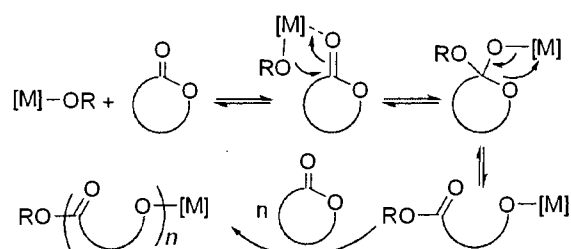
#### Abstract

Several neutral zirconocene bis(ester enolate) complexes have been employed for ring-opening polymerizations and chain transfer polymerizations of L-lactide (L-LA) and  $\epsilon$ -caprolactone ( $\epsilon$ -CL). All  $C_{2v}$ -,  $C_2$ -, and  $C_s$ -ligated neutral zirconocene bis(ester enolate) complexes effectively polymerize  $\epsilon$ -CL at 80 °C with high (>90%) initiator efficiencies. The  $C_s$ -ligated complex  $\text{Ph}_2\text{C}(\text{Cp})(\text{Flu})\text{Zr}[\text{OC}(\text{O}^i\text{Pr})=\text{CMe}_2]_2$  (**1**) also promotes highly efficient polymerization of L-LA and is at least 100 times more reactive than the  $C_{2v}$ - and  $C_2$ -ligated analogues. The L-LA polymerization by **1** exhibits living characteristics, producing PLA with quantitative isotacticity (no sign of monomer epimerization) and controlled molecular weight. This polymerization follows first-order kinetics with respect to both [L-LA] and [**1**], consistent with a monometallic, coordination-anionic propagation mechanism. Zirconocene **1** catalyzes efficient chain transfer polymerization in the presence of  $^i\text{PrOH}$  as a chain transfer reagent (CTR) for the catalytic production of PLA and PCL; and the metallocene system is more robust (in terms of ligand stability and maintaining the polymerization rate) towards excess of a protic CTR than the non-metallocene system.

## Introduction

Ring-opening polymerization (ROP) of heterocyclic monomers via coordination-anionic (also termed coordination-insertion) mechanism<sup>1</sup> is a leading polymerization technique to produce high molecular weight (MW) polymers typical of step-growth products yet through the chain-growth mechanism (Scheme 1). A large number of metal complexes of various types have been extensively investigated as catalysts/initiators for ROP of heterocyclic monomers, particularly cyclic esters (lactides such as L-LA and *rac*-LA; lactones such as  $\epsilon$ -caprolactone,  $\epsilon$ -CL),<sup>2</sup> largely due to the biodegradability and biocompatibility of the resulting lactide and lactone polymers (e.g., poly(lactide), PLA, and poly( $\epsilon$ -CL), PCL).<sup>3</sup> These catalysts/initiators have encompassed organometallic or coordination complexes of main-group elements, transition metals, and lanthanides, for controlled (over tacticity or MW) ROP polymerization of lactides<sup>4</sup> and lactones.<sup>5</sup> Relatively fewer reports have described studies on the catalytic ROP of cyclic esters using metal complexes in the presence of an excess of a chain transfer reagent (CTR).<sup>6</sup>

Scheme 1



Group 4 non-metallocenes (non-Cp complexes) and metallocenes, typically in their cationic forms,<sup>7</sup> are best known for their remarkable success in the production of revolutionary polyolefin materials through their catalyzed homogeneous, single-site, (co)polymerization of nonpolar vinyl monomers ( $\alpha$ -olefins in particular).<sup>8</sup> The polymerization of polar vinyl monomers with such highly electron-deficient group 4 metallocene complexes is less known,<sup>9</sup> despite their established high stereospecificity and degree of control for the polymerization of methacrylates<sup>10</sup> and acrylamides.<sup>11</sup> On the other hand, coordination-anionic ROP of cyclic esters using group 4

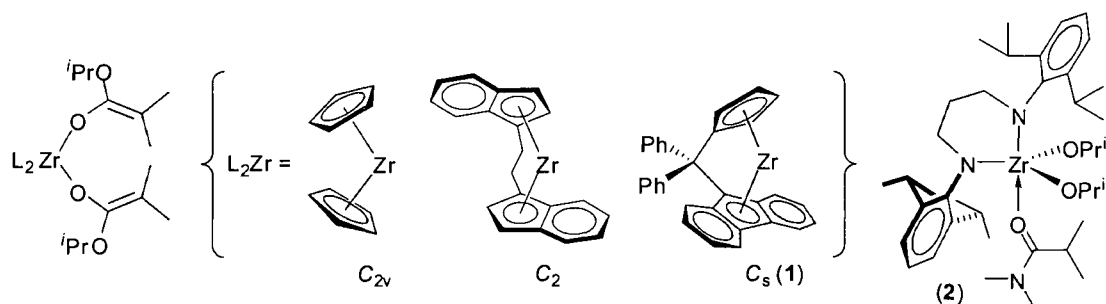
*non-metallocene* complexes is well known thanks to extensive studies in this area (the metal and monomer used in each of the following examples selected for a brief overview are shown in parenthesis for clarity). These catalysts/initiators are typical of those group 4 metal *alkoxides* (as initiating groups) supported by chiral phenoxyimine (Zr; *rac*-LA),<sup>12</sup> tris(phenoxy)amine (Zr, Hf; *rac*-LA),<sup>13</sup> bis( $\beta$ -ketoamidate) (Ti, Zr; *rac*-LA,  $\epsilon$ -CL),<sup>14</sup> bis(iminophenoxide) (“salen”) (Ti; *rac*-LA),<sup>15</sup> *N*-heterocyclic carbene (Ti; *rac*-LA),<sup>16</sup> bis(phenoxy)amine (Ti, Zr, Hf; *rac*-LA, L-LA,  $\epsilon$ -CL),<sup>17</sup> pyrrolylamine (Zr, Hf;  $\epsilon$ -CL),<sup>18</sup> tris(alkoxy or aryloxy) (Ti; *rac*-LA, L-LA),<sup>19</sup> tris(alkoxy or aryloxy)amine (Ti; *rac*-LA, L-LA,  $\epsilon$ -CL),<sup>20</sup> chalcogen-bridged chelating bis(aryloxy) (Ti; L-LA,  $\epsilon$ -CL),<sup>21</sup> and methylene-bridged bis(phenoxy) (Ti;  $\epsilon$ -CL)<sup>22</sup> ligands. In addition to alkoxides, bis(amido)titanium complexes supported by the chelating diaryloxy ligands have also been used for ROP of L-LA and  $\epsilon$ -CL.<sup>23</sup> Other catalysts included homoleptic group 4 alkoxide (Ti, Zr; L-LA,  $\epsilon$ -CL)<sup>24</sup> and acetylacetonate (Zr; L-LA,  $\epsilon$ -CL)<sup>25</sup> complexes as well as the titanium-organic framework derived from Ti(O<sup>*i*</sup>Pr)<sub>4</sub> and 1,4-butanediol (L-LA and  $\epsilon$ -CL).<sup>26</sup>

Fewer reports described polymerization of  $\epsilon$ -CL using group 4 *metallocene* complexes. Titanocene and zirconocene alkyne complexes<sup>27</sup> as well as their bimetallic congeners formed with <sup>*i*</sup>Bu<sub>2</sub>AlH<sup>28</sup> were found active for polymerization of  $\epsilon$ -CL. Titanocene alkoxide species derived from the Cp<sub>2</sub>TiCl-catalyzed radical ROP of epoxides can initiate controlled polymerization of  $\epsilon$ -CL.<sup>29</sup> Half-sandwich (half-metallocene) dichlorotitanium alkoxides have been utilized to mediate controlled polymerization of  $\epsilon$ -CL;<sup>30</sup> substituting the Cp ligand in half-titanocenes with the indenyl ligand resulted in significant (> an order of magnitude)  $\epsilon$ -CL polymerization rate enhancement.<sup>31</sup> Cationic zirconocene complexes such as [Cp<sub>2</sub>ZrMe]<sup>+</sup>[B(C<sub>6</sub>F<sub>5</sub>)<sub>4</sub>]<sup>-</sup> and Cp<sub>2</sub>ZrMe<sup>+</sup>MeB(C<sub>6</sub>F<sub>5</sub>)<sub>3</sub><sup>-</sup>, which are derived from activation of the dimethyl complex with Ph<sub>3</sub>CB(C<sub>6</sub>F<sub>5</sub>)<sub>4</sub> and B(C<sub>6</sub>F<sub>5</sub>)<sub>3</sub>, respectively, are known to promote living polymerization of  $\epsilon$ -CL, however, through a non-coordination, *cationic* mechanism.<sup>32</sup>

The following two points readily become apparent on the basis of the above overview. *First*, there was no report, to the best of our knowledge, on the lactide polymerization using group

4 metallocenes, either their neutral or cationic form. *Second*, as little has been studied on the catalytic ROP of cyclic esters using chain transfer polymerization strategies, there is a need for more research efforts in this field devoted to the catalytic production of polymer chains. To the above two points, we report in this contribution the first efficient lactide polymerization system catalyzed by group 4 metallocenes, especially  $\text{Ph}_2\text{C}(\text{Cp})(\text{Flu})\text{Zr}[\text{OC}(\text{O}^i\text{Pr})=\text{CMe}_2]_2$  (**1**) depicted in Scheme 2 (to point 1) as well as investigation into chain transfer polymerization characteristics of the zirconocene system for the catalytic polymer chain production (to point 2). In addition to addressing the above two fundamentally important points, this study highlights the sharp differences between group 4 metallocene and non-metallocene catalysts in polymerization activity and, especially, converse behavior in their catalyzed chain transfer polymerization upon addition of excess of isopropanol as a CTR.

Scheme 2



## Experimental

**Materials, Reagents, and Methods.** All syntheses and manipulations of air- and moisture-sensitive materials were carried out in flamed Schlenk-type glassware on a dual-manifold Schlenk line, on a high-vacuum line, or in an argon-filled glovebox. NMR-scale reactions (typically in a 0.02 mmol scale) were conducted in Teflon-valve-sealed J. Young-type NMR tubes. HPLC-grade organic solvents were first sparged extensively with nitrogen during filling 20 L solvent reservoirs and then dried by passage through activated alumina (for  $\text{Et}_2\text{O}$ , THF, and  $\text{CH}_2\text{Cl}_2$ ) followed by passage through Q-5 supported copper catalyst (for toluene and hexanes) stainless

steel columns. Benzene- $d_6$  and toluene- $d_8$  were dried over sodium/potassium alloy and vacuum-distilled or filtered, whereas  $CD_2Cl_2$ , and  $CDCl_3$  were dried over activated Davison 4 Å molecular sieves. NMR spectra were recorded on either a Varian Inova 300 (FT 300 MHz,  $^1H$ ; 75 MHz,  $^{13}C$ ; 282 MHz,  $^{19}F$ ) or a Varian Inova 400 spectrometer. Chemical shifts for  $^1H$  and  $^{13}C$  spectra were referenced to internal solvent resonances and are reported as parts per million relative to  $SiMe_4$ , whereas  $^{19}F$  NMR spectra were referenced to external  $CFC_3$ . Elemental analyses were performed by Desert Analytics, Tucson, AZ.

$\epsilon$ -Caprolactone ( $\epsilon$ -CL), L-lactide (L-LA), and butylated hydroxytoluene (BHT-H, 2,6-Di-*tert*-butyl-4-methylphenol) were purchased from Aldrich Chemical Co.  $\epsilon$ -CL was first degassed and dried over  $CaH_2$  overnight, followed by vacuum distillation, while L-LA was purified by sublimation. The purified monomers were stored in brown bottles inside a  $-30$  °C glovebox freezer. BHT-H was recrystallized from hexanes prior to use. Isopropanol and isopropyl isobutyrate were purchased from TCI America and dried over  $CaH_2$ , followed by vacuum distillation. Literature procedures were employed for the preparation of the following ligand and complexes:  $Cp_2Zr[OC(O^iPr)=CMe_2]_2$  ( $Cp = \eta^5$ -cyclopentadienyl),<sup>33</sup> *rac*- $C_2H_4(Ind)_2Zr[OC(O^iPr)=CMe_2]_2$  ( $Ind = \eta^5$ -indenyl),<sup>10c</sup>  $Ph_2C(Cp)(Flu)Zr[OC(O^iPr)=CMe_2]_2$  (**1**,  $Flu = \eta^5$ -fluorenyl),<sup>10a</sup> and  $Cp_2Zr(O^iPr)_2$ .<sup>34</sup>

#### General Procedures for Polymerizations Using Zirconocene Complexes.

Polymerizations were performed either in 25 mL flame-dried Schlenk flasks interfaced to the dual-manifold Schlenk line for runs using external temperature bath, or in 20 mL glass reactors inside the argon-filled glovebox for ambient temperature (*ca.* 25 °C) runs. A predetermined amount of the zirconocene complex such as **1** was first dissolved in 2 mL toluene inside a glovebox, and the polymerization was started by rapid addition of the above solution via gastight syringe to a solution of L-LA (4.5 mmol) or  $\epsilon$ -CL (4.5 mmol) in 3 mL of toluene under vigorous stirring at the pre-equilibrated bath temperature (on a Schlenk line). The amount of the monomers used was the same for all polymerizations, whereas the amount of the zirconocene was adjusted

according to the  $[M]/[Zr]$  ratio specified in the text. For chain transfer polymerizations, a predetermined amount of  $t$ -PrOH was mixed with the monomer in solution before addition of the catalyst. After the measured time interval, a 0.2 mL aliquot was taken from the reaction mixture via syringe and quickly quenched into a 4 mL vial containing 0.6 mL of undried “wet”  $CDCl_3$  stabilized by 250 ppm of BHT-H; the quenched aliquots were later analyzed by  $^1H$  NMR to obtain the monomer conversion data. The polymerization was immediately quenched after the removal of the last aliquot by addition of 1 mL methanol and the solvents were removed in vacuo. The polymer product was precipitated into 50 mL of methanol, stirred for 1 h, filtered, washed with methanol, and dried in a vacuum oven at 50 °C overnight to a constant weight.

**Polymerization Kinetics.** Kinetic experiments were carried out in a stirred glass reactor at ambient temperature ( $\sim 25$  °C) inside the glovebox for  $\epsilon$ -CL polymerization or in flasks at 80 °C on the Schlenk line for L-LA polymerization using stock solutions of the reagents and the procedures described in literature.<sup>10d,35</sup> Specifically, at appropriate time intervals, 0.2 mL aliquots were withdrawn from the reaction mixture using syringe and quickly quenched into 1 mL vials containing 0.6 mL of undried “wet”  $CDCl_3$  mixed with 250 ppm of BHT-H. The quenched aliquots were analyzed by  $^1H$  NMR. For  $\epsilon$ -CL polymerization, the ratio of  $[\epsilon\text{-CL}]_0$  to  $[\epsilon\text{-CL}]_t$  at a given time  $t$ ,  $[CL]_0/[CL]_t$ , was determined by integration of the peaks for  $\epsilon$ -CL (4.2 ppm for the  $OCH_2$  signal) and PCL (4.0 ppm for the  $OCH_2$  signal) according to the equation  $[\epsilon\text{-CL}]_0/[\epsilon\text{-CL}]_t = (A_{4.2} + A_{4.0})/A_{4.2}$ , where  $A_{4.2}$  is the integral for the peak at 4.2 ppm and  $A_{4.0}$  is the integral for the peak at 4.0 ppm. For L-LA polymerization, the  $[L\text{-LA}]_0/[L\text{-LA}]_t$  ratio was determined by integration of the peaks for L-LA (4.8 ppm for the methine proton signal) and PLA (5.4 ppm for the methine proton signal) according to the equation  $[LLA]_0/[LLA]_t = (A_{4.8} + A_{5.4})/A_{4.8}$ . Apparent rate constants ( $k_{app}$ ) were extracted from the slopes of the best fit lines to the plots of  $\ln([M]_0/[M]_t)$  vs. time.

**Polymer Characterizations.** Polymer number-average molecular weight  $M_n$  and polydispersity index ( $PDI = M_w/M_n$ ) were measured by gel permeation chromatography (GPC) analyses carried out at 40 °C and a flow rate of 1.0 mL/min, with  $\text{CHCl}_3$  as the eluent on a Waters University 1500 GPC instrument equipped with one PLgel 5  $\mu\text{m}$  guard and three PLgel 5  $\mu\text{m}$  mixed-C columns (Polymer Laboratories; linear range of molecular weight = 200–2,000,000). The instrument was calibrated with 10 PMMA standards, and chromatograms were processed with Waters Empower software (version 2002).  $^1\text{H}$  NMR spectra for the analysis of PCL and PLA microstructures<sup>36</sup> were recorded in  $\text{CDCl}_3$ .

## Results and Discussion

**Polymerizations of L-LA and  $\epsilon$ -CL by Zirconocene Bis(ester enolate) Complexes.** In this study we chose L-LA over *rac*-LA for a simple reason: high purity (99.9%) L-LA is currently produced on a large industrial scale from L-lactic acid derived from fermentation of biorenewable raw materials such as corn<sup>37</sup> and the prices for L-LA and *rac*-LA are about the same (a rare case where a racemic substance is not any cheaper than its enantiopure isomer), thus possessing no economical advantage for polymerization of *rac*-LA over L-LA as far as the production of isotactic PLA is concerned.

We initially screened the L-LA polymerization using cationic zirconocene alkyl or alkoxy complexes of various ligation, including  $\text{Cp}_2\text{ZrMe}^+\text{MeE}(\text{C}_6\text{F}_5)_3^-$  ( $\text{E} = \text{B}, \text{Al}$ ),  $\text{Cp}_2\text{Zr}(\text{OMe})^+\text{MeB}(\text{C}_6\text{F}_5)_3^-$ , *rac*- $\text{Me}_2\text{Si}(\text{Ind})_2\text{ZrMe}^+\text{MeE}(\text{C}_6\text{F}_5)_3^-$ , and *rac*- $\text{Me}_2\text{Si}(\text{Ind})_2\text{Zr}^{++}[\text{MeAl}(\text{C}_6\text{F}_5)_3^-]_2$ , and found that all were inactive. Next, we turned our attention to *neutral* metallocene *bis(ester enolate)* complexes as we reasoned that the ester enolate ligand, being a strong nucleophile, could initiate the lactide polymerization. Indeed,  $\text{C}_2\text{v}$ -ligated achiral zirconocene bis(ester enolate) complex  $\text{Cp}_2\text{Zr}[\text{OC}(\text{O}^i\text{Pr})=\text{CMe}_2]_2$  exhibits some activity for L-LA polymerization with a  $[\text{L-LA}]/[\text{Zr}]$  ratio of 200 in toluene at 80 °C, although achieving only 7% monomer conversion in 26 h and producing PLA with a low MW of  $M_n = 5.29 \times 10^3$  and narrow

MW distribution (MWD) of PDI = 1.12 (the calculated initiator efficiency,  $I^*$ , is 41%). Similarly,  $C_2$ -ligated chiral  $rac$ - $C_2H_4(Ind)_2Zr[OC(O^iPr)=CMe_2]_2$  is only marginally active for L-LA polymerization ( $[L-LA]/[Zr] = 200$ ) in toluene at 80 °C, achieving only 7% monomer conversion in 18 h; the resulting PLA also has a low MW of  $M_n = 4.38 \times 10^3$  and narrow MWD of PDI = 1.15 ( $I^* = 49\%$ ). Excitingly, the  $C_s$ -ligated complex  $Ph_2C(Cp)(Flu)Zr[OC(O^iPr)=CMe_2]_2$  (**1**) is substantially more active (with >100-fold rate enhancement) under the same conditions (toluene, 80 °C) and can also achieve high monomer conversions. This interesting finding prompted us to investigate the L-LA polymerization by complex **1** in more detail, the results of which were summarized in Table 1.

**Table 1. L-LA Polymerization Results by Zirconocene Bis(ester enolate) **1**<sup>a</sup>**

[Zr] (mmol/L)	[L-LA] <sub>0</sub> / [Zr] <sub>0</sub>	time (min)	conv. (%)	$10^3 M_n^b$ (g/mol)	PDI <sup>b</sup> ( $M_w/M_n$ )	$I^{*c}$ (%)
18.0	50	11	31	2.58	1.18	92
		15	36	2.82	1.21	97
		20	46	3.38	1.22	102
		25	53	3.73	1.23	106
		35	64	4.34	1.23	109
		50	76	5.07	1.24	110
		80	86	5.76	1.24	110
		105	92	5.86	1.25	115
12.9	70	10	19	2.03	1.26	101
		15	27	2.96	1.27	97
		20	34	3.31	1.26	107
		30	45	4.03	1.33	116
		45	58	4.64	1.32	128
		60	68	6.12	1.23	114
		100	83	7.17	1.28	118
		151	91	7.93	1.22	117
9.02	100	15	24	3.07	1.28	117
		20	30	4.21	1.25	106
		35	47	6.38	1.22	108
		45	56	6.51	1.26	126
		65	68	7.95	1.22	125
		90	77	9.14	1.21	123
		130	85	9.90	1.28	125
6.68	135	5	10	2.61	1.21	80
		10	21	4.38	1.25	96
		20	31	5.99	1.26	103
		30	48	9.36	1.23	101
		50	60	9.97	1.21	118
		70	77	12.9	1.21	117

		113	84	14.9	1.18	111
		150	90	15.4	1.15	115
		210	93	16.9	1.12	108
4.51	200	5	5	1.97	1.05	80
		10	8	2.50	1.14	97
		20	17	3.90	1.28	129
		30	24	4.80	1.26	147
		50	49	11.0	1.15	128
		70	61	15.8	1.14	112
		110	71	15.6	1.14	132
		150	75	16.8	1.14	129
		285	84	20.5	1.14	118

<sup>a</sup> All polymerizations were carried out in flame-dried Schlenk flasks (5 mL toluene solution) on a Schlenk line using an external temperature-control bath set at 80 °C. <sup>b</sup> Number-average molecular weight ( $M_n$ ) and polydispersity index (PDI) determined by GPC relative to PMMA standards. <sup>c</sup> Initiator efficiency ( $I^*$ ) =  $M_n(\text{calcd})/M_n(\text{exptl})$ , where  $M_n(\text{calcd}) = \text{MW}(M) \times [\text{M}]/[\text{I}] \times \text{conversion}\% + \text{MW}(\text{chain-end groups})$ .

The polymerization in a low [L-LA]/[Zr] ratio of 50 exhibits living characteristics. A plot of the PLA  $M_n$  vs. monomer conversion gave a linear relationship ( $R^2 = 0.997$ ), whereas MWD remains narrow for all conversions (PDI = 1.18–1.25), Figure 1. The calculated initiator efficiency  $I^*$  values (based on one chain produced per Zr center) range from 92% to 102% for conversions below 46%, implying that only one of the two enolate ligands is used for chain initiation. As monomer conversion gets higher, the  $I^*$  value goes higher (up to 115% at 92% conversion), suggesting either a small degree of chain transfer occurring at the late stage of polymerization or the possibility of a small percentage of initiation by the second enolate ligand at Zr.

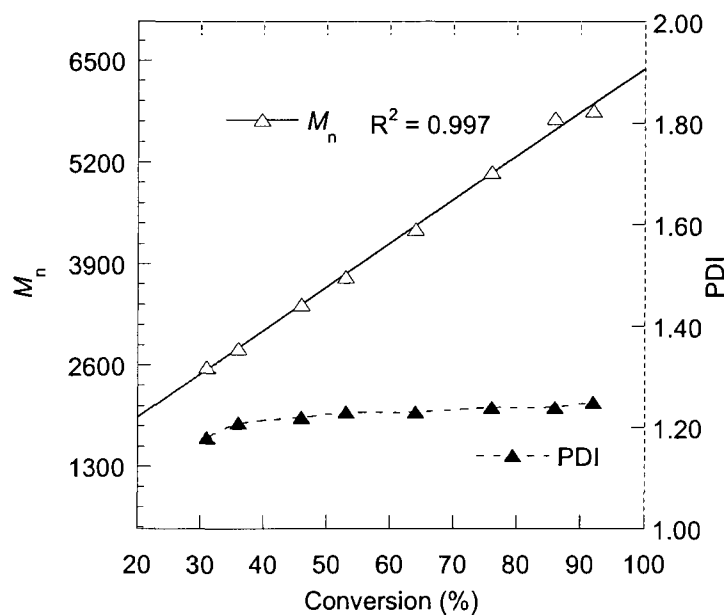


**Figure 1.** Plot of  $M_n$  and PDI of PLA by **1** vs monomer conversion. Conditions:  $[MMA]_0/[1]_0 = 50$ , toluene, 80 °C.

Variations of the  $[L-LA]/[Zr]$  ratio to 70, 100, 135, and 200 still afforded generally well-behaved polymerization (Table 1), although in some cases the  $I^*$  values become somewhat higher due to longer reaction times. The PLA produced from all the  $[L-LA]/[Zr]$  ratios is 100% isotactic (Figure 2), and there is no sign of epimerization at the NMR detection limit.

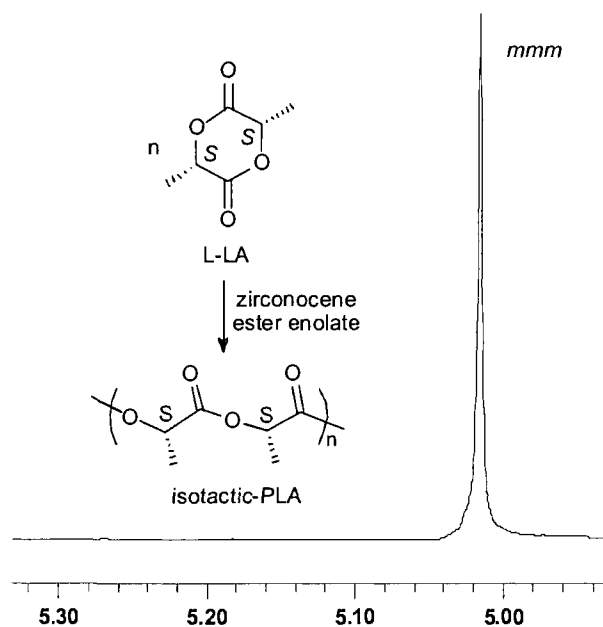


**Figure 2.** Homonuclear decoupled  $^1\text{H}$  NMR of the methine region of isotactic-PLA produced by **1**.

The polymerization by **1** follows strictly first-order kinetics with respect to monomer concentration for all the five  $[\text{L-LA}]/[\text{Zr}]$  ratios investigated (Figure 3). A double logarithm plot (Figure 4) of the apparent rate constants ( $k_{\text{app}}$ ), obtained from the slopes of the best-fit lines to the plots of  $\ln([\text{L-LA}]_0/[\text{L-LA}]_t)$  vs time, as a function of  $\ln[\text{Zr}]$ , was fit to a straight line ( $R^2 = 0.995$ ) of slope = 0.9(1). The kinetic order with respect to  $[\text{Zr}]$ , given by this slope, reveals that propagation is also approximately first order in  $[\text{Zr}]$ , thus consistent with a *monometallic*, coordination-anionic propagation mechanism depicted in Scheme 1.

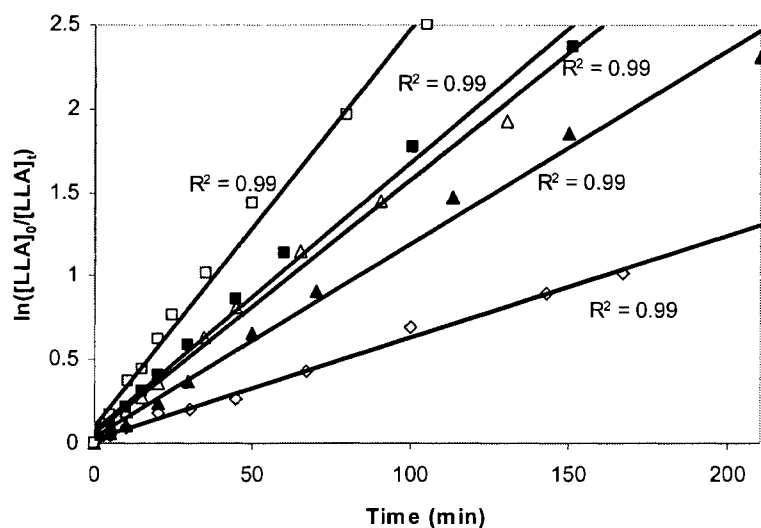


**Figure 3.** Semilogarithmic plots of  $\ln\{[L-LA]_0/[L-LA]_t\}$  vs time for the polymerization of L-LA by **1** in toluene at 80 °C. Conditions:  $[L-LA]_0 = 0.90$  M,  $[1]_0 = 18.0$  mM ( $\square$ ), 12.9 mM ( $\blacksquare$ ); 9.02 mM ( $\Delta$ ), 6.68 mM ( $\blacktriangle$ ), 4.51 mM ( $\diamond$ ).

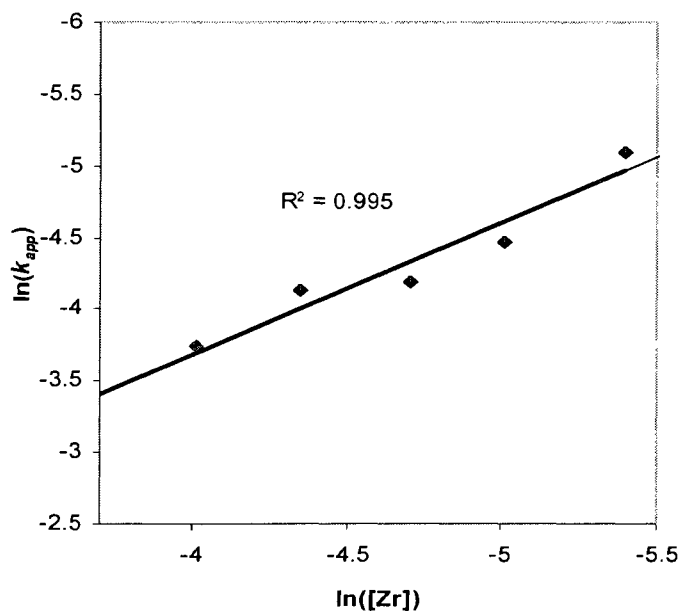


**Figure 4.** Plot of  $\ln(k_{app})$  vs.  $\ln[Zr]$  for the L-LA polymerization by complex **1** in toluene at 80 °C.

We also investigated characteristics of  $\epsilon$ -CL polymerization by these three metallocene bis(ester enolate) complexes, the selected results of which were summarized in Table 2.  $Cp_2Zr[OC(O^iPr)=CMe_2]_2$  exhibits no activity for  $\epsilon$ -CL polymerization in toluene at ambient

temperature, but good activity in toluene at 80 °C with a  $[\epsilon\text{-CL}]/[\text{Zr}]$  ratio of 200, achieving 89% monomer conversion in 8 h and producing PCL with a medium MW of  $M_n = 2.26 \times 10^4$  and PDI = 1.48 (run 2). The calculated  $I^*$  is 91%, suggesting again that only one of the two ester enolate groups was used to initiate the polymerization. The  $C_2$ -ligated chiral *rac*- $C_2H_4(\text{Ind})_2\text{Zr}[\text{OC}(\text{O}^i\text{Pr})=\text{CMe}_2]_2$  is quite active even at ambient temperature, achieving 98% monomer conversion in 9 h with a  $[\epsilon\text{-CL}]/[\text{Zr}]$  ratio of 100. The same polymerization but with a  $[\epsilon\text{-CL}]/[\text{Zr}]$  ratio of 200 in toluene at 80 °C gelled in less than 30 min and gave 100% monomer conversion upon quenching in 7 h ( $M_n = 2.43 \times 10^4$ , PDI = 1.48,  $I^* = 95\%$ , run 4). The  $C_s$ -ligated complex **1** is more active than  $\text{Cp}_2\text{Zr}[\text{OC}(\text{O}^i\text{Pr})=\text{CMe}_2]_2$  but less active than *rac*- $C_2H_4(\text{Ind})_2\text{Zr}[\text{OC}(\text{O}^i\text{Pr})=\text{CMe}_2]_2$ , achieving 88% monomer conversion at ambient temperature after 19 h (run 5 vs. 1 and 3). This activity trend in  $\epsilon\text{-CL}$  polymerization is different than that observed for the L-LA polymerization where the  $C_s$ -ligated complex **1** is at least 100 times more reactive than the other two (vide supra). It is important to note here that all three zirconocene bis(ester enolate) complexes employed for polymerizations here are stable (with no evidence of decomposition by NMR) in toluene solutions at 80 °C up to 20 h.

**Table 2. Selected Results of  $\epsilon\text{-CL}$  Polymerization by Zirconocene Bis(ester enolate) Complexes <sup>a</sup>**

run no.	catalyst (ligand)	$[\epsilon\text{-CL}]/[\text{Zr}]$	temp (°C)	time (h)	conv. (%)	$10^4 M_n$ (g/mol)	PDI ( $M_w/M_n$ )	$I^*$ (%)
1	$\text{Cp}_2$	100	25	8	0			
2	$\text{Cp}_2$	200	80	8	89	2.26	1.48	91
3	<i>rac</i> -EBI	100	25	9	98			
4	<i>rac</i> -EBI	200	80	7	100	2.43	1.48	95
5	$\text{Ph}_2\text{C}(\text{Cp})(\text{Flu})$	200	25	19	88	1.64	1.67	122

<sup>a</sup> Carried out in 5 mL of toluene at indicated temperatures. See footnotes in Table 1 for abbreviation explanations.

**Chain Transfer Polymerization Catalyzed by Zirconocene Complex 1.** To render a catalytic production of polymer chains in the present coordination-anionic polymerization catalyzed by zirconium complexes, a suitable CTR added externally must effectively cleave the growing polymer chain from the active metal center, and the resulting new species containing

nucleophilic part of the CTR moiety (typically in its deprotonated, anionic form) must efficiently reinitiate the polymerization (Scheme 3). The control experiment with  $\text{Cp}_2\text{Zr}(\text{O}^i\text{Pr})_2$ , which showed it exhibits similar activity for L-LA polymerization in toluene at 80 °C to  $\text{Cp}_2\text{Zr}[\text{OC}(\text{O}^i\text{Pr})=\text{CMe}_2]_2$ , suggests that  $^i\text{PrOH}$  be a suitable CTR. Accordingly, to ascertain if  $^i\text{PrOH}$  is indeed a suitable CTR for promoting efficient chain transfer, we varied the  $[^i\text{PrOH}]/[\text{monomer}]$  ratio and examined the changes in polymerization activity and the resulting polymer  $M_n$  for the L-LA polymerization by complex **1** and for the  $\epsilon$ -CL polymerization by complex **2**. Table 3 summarizes the selected results.

### Scheme 3

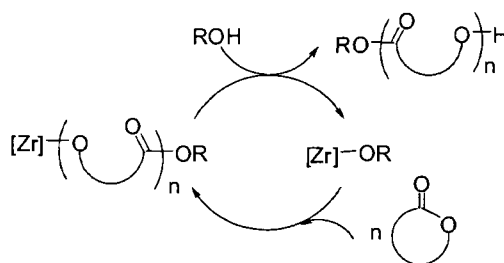


**Table 3.** Chain Transfer Polymerization Results Using  $^i\text{PrOH}$  as a Chain Transfer Reagent <sup>a</sup>

run no.	catalyst (mM)	monomer (M)	$[^i\text{PrOH}]/[\text{Zr}]$	$[^i\text{PrOH}]/[\text{M}]$	time (h)	conv. <sup>b</sup> (%)	$10^3 M_n^c$ (g/mol)	PDI <sup>c</sup> ( $M_w/M_n$ )	$I^*^d$ (%)
1	<b>1</b> (4.51)	L-LA	0	0	5	84	20.5	1.14	118
2	<b>1</b> (4.51)	L-LA	10	0.05	6	100	9.59	1.30	302
3	<b>1</b> (4.51)	L-LA	50	0.25	6	100	3.69	1.30	785

<sup>a</sup> L-LA polymerization were carried out in 5 mL of toluene at 80 °C.  $[\text{M}]/[\text{Zr}] = 200$  for all runs. <sup>b</sup> Monomer conversion determined by  $^1\text{H}$  NMR. <sup>c</sup>  $M_n$  and PDI determined by GPC relative to PMMA standards. <sup>d</sup> Initiator efficiency ( $I^*$ ) as defined in Table 1.

Indeed, addition of  $^i\text{PrOH}$  effected chain transfer polymerization for the polymerization system, as evidenced by a gradual decrease in  $M_n$  (thus increased initiator efficiency of >100% for the catalytic production of polymer chains) as an increase in the amount of  $^i\text{PrOH}$  added (runs 1–3, Table 3). First, for the L-LA polymerization by complex **1**, addition of the CTR did not noticeably affect the polymerization rate (runs 1–3), implying the relative rate constants for propagation ( $k_p$ ) and reinitiation ( $k_{ri}$ ) by the Zr–O $^i\text{Pr}$  moiety (derived from the Zr–PLA chain cleavage by  $^i\text{PrOH}$ ) is about the same ( $k_p \approx k_{ri}$ ); thus, the observed decrease in  $M_n$  while more or

less maintaining the same polymerization rate upon addition of the CTR can be characterized as a “normal chain transfer” polymerization,<sup>38</sup> which is more robust than those non-metallocene system.

A plot of  $1/M_n$  vs the  $[{}^i\text{PrOH}]/[\text{M}]$  ratio gives a linear relationship for the system (Figure 5), the slope of which corresponds to the chain transfer constant ( $C_{tr}$ ), that is, the ratio of rate constants of chain transfer to propagation,  $C_{tr} = k_{tr}/k_p$ .<sup>38</sup> Accordingly,  $C_{tr} (\times 10^4)$  for the L-LA polymerization by complex **1** is estimated to be 8.74 and the ratio of  $k_p/k_{tr}$  is  $1.14 \times 10^3$ , which is less efficient than those non-metallocene system.

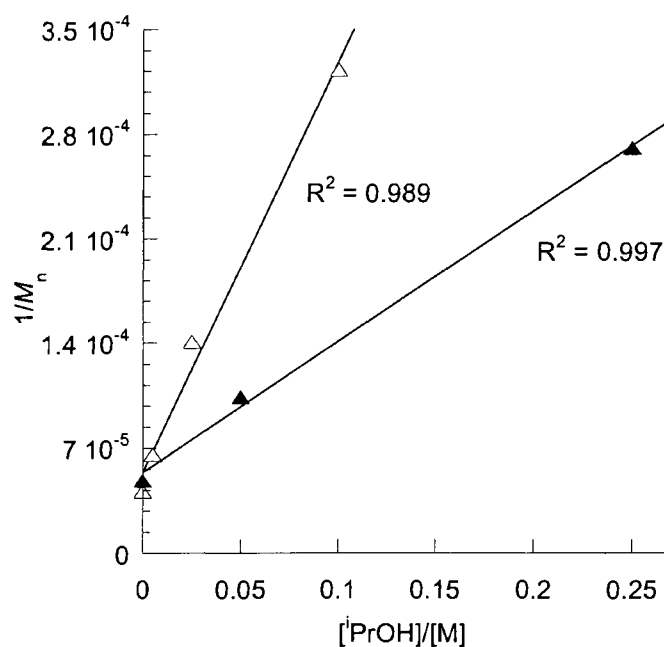


**Figure 5.** Plots of  $1/M_n$  vs  $[{}^i\text{PrOH}]/[\text{M}]$  for chain transfer polymerization of L-LA by complex **1** ( $\blacktriangle$ ).

## Conclusions

Neutral  $C_{2v}$ -,  $C_{2-}$ , and  $C_s$ -ligated zirconocene bis(ester enolate) complexes effectively polymerize  $\epsilon$ -CL in toluene at 80 °C with high initiator efficiencies based on one chain per metal initiation. In the polymerization of L-LA, there exhibit large activity differences among these three types of zirconocenes, with the  $C_s$ -ligated complex **1** exhibiting markedly higher activity (> an order of magnitude) than the  $C_{2v}$ - and  $C_{2-}$ -ligated complexes. Additionally, the L-LA

polymerization by **1** is well behaved and characteristic of living. The PLA produced is 100% isotactic, and there is no sign of epimerization. This polymerization follows first-order kinetics with respect to both monomer and catalyst concentrations. Overall, all evidence obtained from the current study points to a conclusion that the polymerization of L-LA by zirconocene bis(ester enolate) **1** is well-behaved and proceeds with a monometallic, coordination-anionic propagation mechanism.

Zirconocene **1** catalyzes efficient chain transfer polymerization in the presence of *i*PrOH as CTR for the catalytic production of PLA and PCL, but it does exhibit two major differences. First, while complex **1** catalyzes the “normal chain transfer” L-LA polymerization without loss in the polymerization rate upon increasing [CTR], reflecting certain stability of ligand present in complex **1** under the protic reaction conditions. Second, the chain transfer process is less efficient for the L-LA polymerization by **1**, as reflected by the estimated chain transfer constants  $C_{tr}$  ( $\times 10^4$ ) of 8.74.

**Acknowledgment.** This work was supported by the National Science Foundation (NSF-0718061).

## References

---

- (1) Selected reviews: (a) Mecerreyes, D.; Jerome, R.; Dubois, P. *Adv. Polym. Sci.* **1999**, *147*, 1–59. (b) Kuran, W. *Prog. Polym. Sci.* **1998**, *23*, 919–992.
- (2) Recent reviews: (a) Wu, J.; Yu, T.-L.; Chen, C.-T.; Lin, C.-C. *Coord. Chem. Rev.* **2006**, *250*, 602–626. (b) Dechy-Cabaret, O.; Martin-Vaca, B.; Bourissou, D. *Chem. Rev.* **2004**, *104*, 6147–6176. (c) Albertsson, A.-C.; Varma, I. K. *Adv. Polym. Sci.* **2002**, *157*, 1–40. (d) O’Keefe, B. J.; Hillmyer, M. A.; Tolman, W. B. R. *J. Chem. Soc., Dalton Trans.* **2001**, 2215–2224. (e) Yasuda, H. *Prog. Polym. Sci.* **2000**, *25*, 573–626.
- (3) (a) Coulembier, O.; Degée, P.; Hedrick, J. L.; Dubois, P. *Prog. Polym. Sci.* **2006**, *31*, 723–747. (b) Okada, M. *Prog. Polym. Sci.* **2002**, *27*, 87–133. (c) Chiellini, E.; Solaro, R. *Adv. Mater.* **1996**, *8*, 305–313.
- (4) Selected recent examples on lactide polymerization: (a) Douglas, A. F.; Patrick, B. O.; Mehrkhodavandi, P. *Angew. Chem. Int. Ed.* **2008**, *47*, 2290–2293. (b) Chisholm, M. H.; Gallucci, J. C.; Quisenberry, K. T.; Zhou, Z. *Inorg. Chem.* **2008**, *47*, 2613–2624. (c) Pang, X.; Du, H.; Chen, X.; Wang, X.; Jing, X. *Chem. Eur.* **2008**, *14*, 3126–3136. (d) Chmura, A. J.; Chuck, C. J.; Davidson, M. G.; Jones, M. D.; Lunn, M. D.; Bull, S. D.; Mahon, M. F. *Angew. Chem. Int. Ed.* **2007**, *46*, 2280–2283. (e) Nomura, N.; Ishii, R.; Yamamoto, Y.; Kondo, T. *Chem. Eur. J.* **2007**, *13*, 4433–4451. (f) Darensbourg, D. J.; Choi, W.; Richers, C. P. *Macromolecules* **2007**, *40*, 3521–3523. (g) Tang, H.-Y.; Chen, H.-Y.; Huang, J.-H.; Lin, C.-C. *Macromolecules* **2007**, *40*, 8855–8860. (h) Du, H.; Pang, X.; Yu, H.; Zhuang, X.; Chen, X.; Cui, D.; Wang, X.; Jing, X. *Macromolecules* **2007**, *40*, 1904–1913. (i) Platel, R. H.; Hodgson, L. M.; White, A. J. P.; Williams, C. K. *Organometallics* **2007**, *26*, 4955–4963. (j) Huang, C.-A.; Chen, C.-C. *Dalton Trans.* **2007**, 5561–5566. (k) Chisholm, M. H.; Patmore, N. J.; Zhou, Z. *Chem. Commun.* **2005**, 127–129. (l) Hsueh, M.-L.; Huang,

- 
- B.-H.; Wu, J.; Lin, C.-C. *Macromolecules* **2005**, *38*, 9482–9487. (m) Hormnirun, P.; Marshall, E. L.; Gibson, V. C.; White, A. J. P.; Williams, D. J. *J. Am. Chem. Soc.* **2004**, *126*, 2688–2689. (n) Williams, C. K.; Breyfogle, L. E.; Choi, S. K.; Nam, W.; Young, V. G., Jr.; Hillmyer, M. A.; Tolman, W. B. *J. Am. Chem. Soc.* **2003**, *125*, 11350–11359. (o) Cai, C.-X.; Amgoune, A.; Lehmann, C. W.; Carpentier, J.-F. *Chem. Commun.* **2004**, 330–331. (p) Zhong, Z.; Dijkstra, P.; Feijen, J. *J. Am. Chem. Soc.* **2003**, *125*, 11291–11298. (q) Chakraborty, D.; Chen, E. Y.-X. *Organometallics* **2003**, *22*, 769–774. (r) Satoh, Y.; Ikitake, N.; Nakayama, Y.; Okuno, S.; Yasuda, H. *J. Organomet. Chem.* **2003**, *667*, 42–52. (s) Nomura, N.; Ishii, R.; Akakura, M.; Aoi, K. *J. Am. Chem. Soc.* **2002**, *124*, 5938–5939. (t) Ovitt, T. M.; Lobkovsky, E. B.; Coates, G. W. *J. Am. Chem. Soc.* **2002**, *124*, 1316–1326. (u) O’Keefe, B. J.; Monnier, S. M.; Hillmyer, M. A.; Tolman, W. B. *J. Am. Chem. Soc.* **2001**, *123*, 339–340. (v) Jhurry, D.; Bhaw-Luximon, A.; Spassky, N. *Macromol. Symp.* **2001**, *175*, 67–79. (w) Radano, C. R.; Baker, G. L.; Smith, M. R. *J. Am. Chem. Soc.* **2000**, *122*, 1552–1553.
- (5) Selected recent examples on lactone polymerization: (a) Zintl, M.; Molnar, F.; Urban, T.; Bernhart, V.; Preishuber-Pflügl, P.; Rieger, B. *Angew. Chem. Int. Ed.* **2008**, *47*, 3458–3460. (b) Silvernail, C. M.; Yao, L. J.; Hill, L. M. R.; Hillmyer, M. A.; Tolman, W. B. *Inorg. Chem.* **2007**, *46*, 6565–6574. (c) Amgoune, A.; Thomas, C. M.; Ilinca, S.; Roisnel, T.; Carpentier, J.-F. *Angew. Chem. Int. Ed.* **2006**, *45*, 2782–2784. (d) Milione, S.; Grisi, F.; Centore, R.; Tuzi, A. *Organometallics* **2006**, *25*, 266–274. (e) Amgoune, A.; Lavanant, L.; Thomas, C. M.; Chi, Y.; Welter, R.; Dagorne, S.; Carpentier, J.-F. *Organometallics* **2005**, *24*, 6279–6282. (f) Lewiński, J.; Horeglad, P.; Tratkiewicz, E.; Grzenda, W.; Lipkowski, J.; Kolodziejczyk, E. *Macromol. Rapid Commun.* **2004**, *25*, 1939–1942. (g) Chen, C.-T.; Huang, C.-A.; Huang, B.-H. *Macromolecules* **2004**, *37*, 7968–

- 
7973. (h) Sarazin, Y.; Schormann, M.; Bochmann, M. *Organometallics* **2004**, *23*, 3296–3302. (i) Alcazar-Roman, L. M.; O’Keefe, B. J.; Hillmyer, M. A.; Tolman, W. B. *Dalton Trans.* **2003**, 3082–3087. (j) Chakraborty, D.; Chen, E. Y.-X. *Organometallics* **2002**, *21*, 1438–1442. (k) Rieth, L. R.; Moore, D. R.; Lobkovsky, E. B.; Coates, G. W. *J. Am. Chem. Soc.* **2002**, *124*, 15239–15248. (l) O’Keefe, B. J.; Breyfogle, L. E.; Hillmyer, M. A.; Tolman, W. B. *J. Am. Chem. Soc.* **2002**, *124*, 4384–4393. (m) Hsueh, M.-L.; Huang, B.-H.; Lin, C.-C. *Macromolecules* **2002**, *35*, 5763–5768. (n) Yu, R.-C.; Hung, C.-H.; Huang, J.-H.; Lee, H.-Y.; Chen, J.-T. *Inorg. Chem.* **2002**, *41*, 6450–6455. (o) Liu, Y.-C.; Ko, B.-T.; Lin, C.-C. *Macromolecules* **2001**, *34*, 6196–6201.
- (6) Selected examples on chain transfer polymerization: (a) Zhu, H.; Chen, E. Y.-X. *Organometallics* **2007**, *26*, 5395–5405. (b) Amgoune, A.; Thomas, C. M.; Carpentier, J.-F. *Macromol. Rapid Commun.* **2007**, *28*, 693–697. (c) Liao, T.-C.; Huang, Y.-L.; Huang, B.-H.; Lin, C.-C. *Macromol. Chem. Phys.* **2003**, *204*, 885–892. (d) Aida, T.; Inoue, S. *Acc. Chem. Res.* **1996**, *29*, 39–48. (e) Miola-Delaite, C.; Hamaide, T.; Spitz, R. *Macromol. Chem. Phys.* **1999**, *200*, 1771–1778.
- (7) Selected recent reviews: (a) Chen, E. Y.-X.; Rodriguez-Delgado, A. in *Comprehensive Organometallic Chemistry III*; Bochmann, M. Vol. Ed.; Mingos, M. P.; Crabtree, R. H. Chief Eds.; Elsevier: Oxford, **2007**; Vol. 4, pp 759–1004. (b) Cuenca, T. in *Comprehensive Organometallic Chemistry III*; Bochmann, M. Vol. Ed.; Mingos, M. P.; Crabtree, R. H. Chief Eds.; Elsevier: Oxford, **2007**; Vol. 4, pp 323–696. (c) Gibson, V. C.; Spitzmesser, S. K. *Chem. Rev.* **2003**, *103*, 283–315.
- (8) Selected recent books, book chapters, or special journal issues: (a) *Stereoselective Polymerization with Single-Site Catalysts*, Baugh, L. S.; Canich, J. A. M., Eds.; CRC Press: Boca Raton, FL, **2008**. (b) Resconi, L.; Chadwick, J. C.; Cavallo, L. in *Comprehensive Organometallic Chemistry III*; Bochmann, M. Vol. Ed.; Mingos, M. P.; Crabtree, R. H.

- 
- Chief Eds.; Elsevier: Oxford, **2007**; Vol. 4, pp 1005–1166. (c) Marks, T. J. Ed. *Proc. Natl. Acad. Sci. U.S.A.* **2006**, *103*, 15288–15354 and contributions therein (issue on “*Polymerization Special Feature*”). (d) Gladysz, J. A., Ed. *Chem. Rev.* **2000**, *100*, 1167–1681 and contributions therein (issue on *Frontiers in Metal-Catalyzed Polymerization*).
- (9) Selected reviews: (a) Chen, E. Y.-X. *J. Polym. Sci. Part A: Polym. Chem.* **2004**, *42*, 3395–3403. (b) Boffa, L. S.; Novak, B. M. *Chem. Rev.* **2000**, *100*, 1479–1493.
- (10) Selected recent examples: (a) Ning, Y.; Chen, E. Y.-X. *J. Am. Chem. Soc.* **2008**, *130*, 2463–2465. (b) Lian, B.; Thomas, C. M.; Navarro, C.; Carpentier, J.-F. *Organometallics* **2007**, *26*, 187–195. (c) Ning, Y.; Chen, E. Y.-X. *Macromolecules* **2006**, *39*, 7204–7215. (d) Rodriguez-Delgado, A.; Chen, E. Y.-X. *Macromolecules* **2005**, *38*, 2587–2594. (e) Bolig, A. D.; Chen, E. Y.-X. *J. Am. Chem. Soc.* **2004**, *126*, 4897–4906. (f) Stojcevic, G.; Kim, H.; Taylor, N. J.; Marder, T. B.; Collins, S. *Angew. Chem. Int. Ed.* **2004**, *43*, 5523–5526.
- (11) (a) Miyake, G. M.; Chen, E. Y.-X. *Macromolecules* **2008**, *41*, 3405–3416. (b) Miyake, G. M.; Mariott, W. R.; Chen, E. Y.-X. *J. Am. Chem. Soc.* **2007**, *129*, 6724–6725. (c) Mariott, W. R.; Chen, E. Y.-X. *Macromolecules* **2005**, *38*, 6822–6832. (d) Mariott, W. R.; Chen, E. Y.-X. *Macromolecules* **2004**, *37*, 4741–4743.
- (12) Chmura, A. J.; Cousins, D. M.; Davidson, M. G.; Jones, M. D.; Lunn, M. D.; Mahon, M. F. *Dalton Trans.* **2008**, 1437–1443.
- (13) Chmura, A. J.; Davidson, M. G.; Frankis, C. J.; Jones, M. D.; Lunn, M. D. *Chem. Commun.* **2008**, 1293–1295.
- (14) Gornshtein, F.; Kapon, M.; Botoshansky, M.; Eisen, M. *Organometallics* **2007**, *26*, 497–507.

- 
- (15) (a) Atkinson, R. C. J.; Gerry, K.; Gibson, V. C.; Long, N. J.; Marshall, E. L.; West, L. J. *Organometallics* **2007**, *26*, 316–320. (b) Gregson, C. K. A.; Blackmore, I. J.; Gibson, V. C.; Long, N. J.; Marshall, E. L.; White, A. J. P. *Dalton Trans.* **2006**, 3134–3140.
- (16) Patel, D.; Liddle, S. T.; Mungur, S. A.; Rodden, M.; Blake, A.; Arnold, P. L. *Chem. Commun.* **2006**, 1124–1126.
- (17) (a) Gendler, S.; Segal, S.; Goldberg, I.; Goldschmidt, Z.; Kol, M. *Inorg. Chem.* **2006**, *45*, 4783–4790. (b) Chmura, A. J.; Davidson, M. G.; Jones, M. D.; Lunn, M. D.; Mahon, M. F.; Johnson, A. F.; Khunkamchoo, P.; Roberts, S. L.; Wong, S. S. F. *Macromolecules* **2006**, *39*, 7250–7257. (c) Chmura, A. J.; Davidson, M. G.; Jones, M. D.; Lunn, M. D.; Mahon, M. F. *Dalton Trans.* **2006**, 887–889.
- (18) Hsieh, K.-C.; Lee, W.-Y.; Hsueh, L.-F.; Lee, H. M.; Huang, J.-H. *Eur. J. Inorg. Chem.* **2006**, 2306–2312.
- (19) Russell, S. K.; Gamble, C. L.; Gibbins, K. J.; Juhl, K. C. S.; Mitchell, W. S. III, Tumas, A. J.; Hofmeister, G. E. *Macromolecules* **2005**, *38*, 10336–10340. (b) Kim, Y.; Verkade, J. G. *Macromol. Rapid Commun.* **2002**, *23*, 917–921.
- (20) (a) Kim, Y.; Verkade, J. G. *Macromol. Symp.* **2005**, *224*, 105–117. (b) Kim, Y.; Jnaneshwara, G. K.; Verkade, J. G. *Inorg. Chem.* **2003**, *42*, 1437–1447. (c) Kim, Y.; Verkade, J. G. *Organometallics* **2002**, *21*, 2395–2399.
- (21) Takashima, Y.; Nakayama, Y.; Watanabe, K.; Itono, T.; Ueyama, N.; Nakamura, A.; Yasuda, H.; Harada, A. *Macromolecules* **2002**, *35*, 7538–7544.
- (22) Takeuchi, D.; Nakamura, T.; Aida, T. *Macromolecules* **2000**, *33*, 725–729.
- (23) Takashima, Y.; Nakayama, Y.; Hirao, T.; Yasuda, H.; Harada, A. *J. Organomet. Chem.* **2004**, *689*, 612–619.
- (24) Kricheldorf, H. R.; Berl, M.; Scharnagl, N. *Macromolecules* **1988**, *21*, 286–293.

- 
- (25) Kasperczyk, J.; Hu, Y.; Jaworskam, J.; Dobrzynski, P.; Wei, J.; Li, S. *J. Appl. Polym. Sci.* **2008**, *107*, 3258–3266.
- (26) Chuck, C. J.; Davidson, M. G.; Jones, M. D.; Kociok-Köhn, G.; Lunn, M. D.; Wu, S. *Inorg. Chem.* **2006**, *45*, 6595–6597.
- (27) (a) Thomas, D.; Arndt, P.; Peulecke, N.; Spannenberg, A.; Kempe, R.; Rosenthal, U. *Eur. J. Inorg. Chem.* **1998**, 1351–1357. (b) Arndt, P.; Thomas, D.; Rosenthal, U. *Tetrahedron Lett.* **1997**, *38*, 5467–5468.
- (28) Arndt, P.; Spannenberg, A.; Baumann, W.; Rosenthal, U. *Eur. J. Inorg. Chem.* **2001**, 2885–2890.
- (29) Asandei, A.; Saha, G. *Macromol. Rapid Commun.* **2005**, *26*, 626–631.
- (30) (a) Touris, A.; Kostakis, K.; Mourmouris, S.; Kotzabasakis, V.; Pitsikalis, M.; Hadjichristidis, N. *Macromolecules* **2008**, *41*, 2426–2438. (b) Okuda, J.; Rushkin, I. L. *Macromolecules* **1993**, *26*, 5530–5532.
- (31) (a) Okuda, J.; Kleinhenn, T.; König, P.; Taden, I. *Macromol. Symp.* **1995**, *95*, 195–202. (b) Okuda, J.; König, P.; Rushkin, I. L.; Kang, H.-C.; Massa, W. *J. Organomet. Chem.* **1995**, *501*, 37–39.
- (32) (a) Kostakis, K.; Mourmouris, S.; Karanikolopoulos, G.; Pitsikalis, M.; Hadjichristidis, N. *J. Polym. Sci., Part A: Polym. Chem.* **2007**, *45*, 3524–3537. (b) Hayakawa, M.; Mitani, M.; Yamada, T.; Mukaiyama, T. *Macromol. Chem. Phys.* **1997**, *198*, 1305–1317. (c) Mukaiyama, T.; Hayakawa, M.; Mitani, M.; Yamada, T. *Chem. Lett.* **1995**, 737–738.
- (33) Ning, Y.; Zhu, H.; Chen, E. Y.-X. *J. Organomet. Chem.* **2007**, *692*, 4535–4544
- (34) Gray, D. R.; Brubaker, C. H. Jr. *Inorg. Chem.* **1971**, *10*, 2143–2146.
- (35) Rodriguez-Delgado, A.; Chen, E. Y.-X. *J. Am. Chem. Soc.* **2005**, *127*, 961–974.
- (36) (a) Chisholm, M. H.; Iyer, S. S.; McCollum, D. G.; Pagel, M.; Werner-Zwanziger, U. *Macromolecules* **1999**, *32*, 963–973. (b) Thakur, K. A. M.; Kean, R. T.; Hall, E. S.;

---

Kolstad, J. J.; Lindgren, T. A.; Doscotch, M. A.; Siepman, J. I.; Munson, E. J.  
*Macromolecules* **1997**, *30*, 2422–2428.

(37) (a) Mecking, S. *Angew. Chem. Int. Ed.* **2004**, *43*, 1078–1085. (b) Drumright, R. E.; Gruber, P. R.; Henton, D. E. *Adv. Mater.* **2000**, *12*, 1841–1846.

(38) Odian, G. *Principles of Polymerization*; John Wiley & Sons, Inc.: Hoboken, NJ. 4th ed.: 2004; pp 238–255.

## CHAPTER VIII

### SUMMARY

The work described within this dissertation has focused on the polymerization of functionalized alkenes and cyclic esters catalyzed by group 4 transition metallocene complexes. These complexes, owing to the catalyst structure diversity and tunability when used in a suitable initiating form, typically exhibit a high degree of control over polymerization, especially the stereochemistry of polymerization of methacrylates and acrylamides. In return, this dissertation work has also provided several advanced and potentially useful polymeric materials: quantitatively isotactic poly(L-lactide), isotactic-b-syndiotactic stereomultiblock, and highly syndiotactic poly(methacrylates), poly(acrylamides).

In addition, this work has focused on the kinetic and mechanistic aspects of polymerization by the highly active, electron-deficient group 4 metallocene catalysts.

## CHAPTER IX

### APPENDIX

#### LIST OF REFEREED PUBLICATIONS BY YALAN NING

1. Ning, Y.; Zhang, Y.; Rodriguez-Delgado, A.; Chen, E. Y.-X.\* "Neutral Metallocene Ester Enolate and Non-Metallocene Alkoxy Complexes for Catalytic Ring-Opening Polymerization of Cyclic Esters", *Organometallics*. **2008**, *27*, 5632-5640.
2. Ning, Y.; Caporaso, L.; Correa, A.; Gustafson, L.; Cavallo, L.\*; Chen, E. Y.-X.\* "Syndioselective MMA Polymerization by Group 4 Constrained Geometry Catalysts: A Combined Experimental and Theoretical Study", *Macromolecules*. **2008**, *41*, 6910-6919.
3. Ning, Y.; Chen, E. Y.-X.\* "Metallocene-Catalyzed Polymerization of Methacrylates to Highly Syndiotactic Polymers at High Temperatures", *J. Am. Chem. Soc.* **2008**, *130*, 2463 -2465.
4. Ning, Y.; Zhu, H.; Chen, E. Y.-X.\* "Remarkable Lewis Acid Effects on Polymerization of Functionalized Alkenes by Metallocene and Lithium Ester Enolates", *J. Organomet. Chem.* **2007**, *692*, 4535-4544.
5. Ning, Y.; Chen, E. Y.-X.\* "Diastereospecific Ion-Pairing Polymerization of Functionalized Alkenes by Metallocene/Lewis Acid Hybrid Catalysts", *Macromolecules* **2006**, *39*, 7204-7215.
6. Ning, Y.; Cooney, M. J.; Chen, E. Y.-X.\* "Polymerization of MMA by Oscillating Zirconocene Catalysts, Diastereomeric Zirconocene Mixtures, and Diastereospecific Metallocene Pairs", *J. Organomet. Chem.* **2005**, *690*, 6263-6270.
7. More manuscripts are still in **progress**.